DETERMINANTS OF LEAF WATER USE EFFICIENCY IN THE C_4 CROP *SORGHUM BICOLOR*

Yazen Mohanad Mohammed AL-SALMAN

A thesis submitted in fulfilment of the requirements for the degree of Doctor of Philosophy

December 2021

WESTERN SYDNEY UNIVERSITY

Hawkesbury Institute for the Environment

To

Mohammed Obaid & Sabeeh Abdulkareem

ACKNOWLEDGEMENTS

First and foremost, I am grateful for my supervisor, A/Prof. Oula Ghannoum for her fascinating insights into the data and elegant elucidations of scientific concepts. Most importantly, I would like to thank her for her patience and pro-activeness in making this PhD project smooth and very enjoyable. Similarly, I would like to thank my co-supervisor Dr. Francisco Javier Cano for always making this project more novel and impactful, and for being key to designing the experiments.

Next, I would like to thank several contributors from outside Western Sydney University who were vital to this thesis' success. Dr. Emma Mace, Prof. David Jordan and Mr. Alan Cruickshank at the University of Queensland and the Queensland Alliance for Agriculture for their help in propagating and selecting the Sorghum genetic material in this thesis. Dr. Michael Groszmann at the Research School of Biology, Australian National University, for his integral contribution to Chapter 4 of this thesis and his wide-ranging advice.

This project would not have been accomplished without the immense help of several members of the Hawkesbury Institute for the Environment, Western Sydney University. Dr. Andrew Gherlenda for tolerating my endless glasshouse related requests; Dr. Markus Klein, Dr. Pushpinder Matta and Dr. Dominica Wojtalewicz for their help in the lab; Dr. Craig Barton for his crucial help with everything gas exchange related; Miss Serina Majewski and Mr. Gavin Mackenzie for being the first in line for any request and whenever anything goes wrong. Dr. David Harland, Mrs. Patricia Hellier and Mrs. Jenny Harvey for making all the daunting administrative manoeuvring so light and quick for PhD students. I would like to thank Dr. Agnieska Wujeska-Klause, Miss Zineb Choury, Miss Nicole Dunn, Mr. Claudio Cortellazzi and most importantly the much-missed Miss Fiona Koller for their help during data collection.

I would like to acknowledge Prof. David Ellsworth, Dr. Brendan Choat, Dr. Alexander Watson-Lazowski, Dr. Clemence Henry for their engaging discussions at different stages of the thesis; Prof. Paul Milham for proofreading the thesis, and A/Prof. Markus Riegler for always looking out for the students at the hardest of times. Finally, I would like to thank the PhD cohort of the Hawkesbury Institute and the ARC Centre of Excellence for Translational Photosynthesis for being the best possible companions along this journey.

STATEMENT OF AUTHENTICATION

The work presented in this thesis is, to the best of my knowledge and belief, original except as acknowledged in the text. I hereby declare that I have not submitted this material, either in full or in part, for a degree at this or any other institution.

THESIS ABSTRACT

Intrinsic water use efficiency (*iWUE*) is an important leaf trait that can influence crop productivity. This PhD project aimed to identify leaf morphological and functional traits that correlate with high *iWUE* in a key C_4 crop. In the first two experimental chapters, a small number (6-10) *Sorghum bicolor* genotypes were grown under different growth temperatures (Chapter 2) or under changing diurnal light conditions (Chapter 3), and leaf gas exchange was correlated with leaf anatomy and stomatal kinetic responses. In the third experimental chapter (Chapter 4), a large number (89) of Sorghum genotypes with different aquaporin alleles were grown under wet and dry conditions. All experiments were carried out in potted plants grown either in the glasshouse (Chapters 2 and 4) or growth cabinets (Chapter 3).

In chapter 2, the importance of leaf width in determining stomatal conductance and *iWUE* was elucidated. Narrow leaves were generally thinner, with smaller guard, mesophyll and bundle sheath cells and airspace compartments. This compact arrangement likely allowed for more efficient gas exchange and thermoregulation under high temperatures. In chapter 3, the regulation of morning and midday *iWUE* was correlated to morning and midday stomatal conductance, while afternoon conductance had little effect on afternoon *iWUE* as well as integrated diurnal *iWUE*. Tight control on the stomatal aperture was the key factor in reducing conductance and increase diurnal *iWUE*, not strictly stomatal structural features. High diurnal *iWUE* was associated with speedy stomatal closure and water conservation under photosynthetically unfavourable conditions. In chapter 4, the onset of water stress in a large set of genotypes revealed the changing relationship between stomatal conductance and carbon assimilation, exposing the differential contributions of both components to *iWUE* under different conditions. The extent of genetic variation in gas exchange and hydraulic traits was assessed. In chapter 5, I discuss those different findings and attempt to integrate them via exploring how carbon assimilation and stomatal conductance vary under different conditions and explaining the impact of vapour pressure deficit in determining anatomical control on stomatal conductance.

The findings of this thesis are put into the context of global change and the need for improved agricultural productivity. Suggestions are made on the possible agronomic

impact of traits found beneficial in this thesis, their possible trade-offs, and how these findings can be taken further in future research.

TABLE OF CONTENTS

ABBREVIATIONS

% aperture	:	% of operational stomatal aperture to maximum aperture
% C	:	% leaf carbon content
% N	:	% leaf nitrogen content
a_{max}	:	Maximum stomatal aperture
A_n	:	Carbon assimilation rate
a_{op}	:	Operational stomatal aperture
AQP	:	Aquaporins
BS/BSC	:	Bundle sheath / Bundle sheath cell
BSC_{area}	:	Area of a bundle sheath cell
BS_{si}	:	Bundle sheath area per interveinal distance
CA	:	Carbonic anhydrase
CCM	:	Carbon concentrating mechanism
C_i	:	Substomatal (or intercellular) carbon dioxide concentration
$C_i : C_a$	:	Ratio of C_i to ambient CO_2 concentration
dWUE	:	Integrated diurnal *iWUE*
ES	:	Epidermis cell
Excess g_s	:	Excess g_s due to slow stomatal closure
Forgone A	:	Forgone A_n due to slow stomatal opening
Fruc	:	Fructose concentration in the leaf
GCV	:	Genotypic coefficient of variation
Gluc	:	Glucose concentration in the leaf
g_s	:	Stomatal conductance
g_{smax}	:	Maximum theoretical stomatal conductance
H_b	:	Broad-sense heritability
HI	:	Harvest index
IAS	:	Intercellular airspace
IAS_{si}	:	Intercellular airspace area per interveinal distance
IVD	:	Interveinal distance
iWUE	:	Intrinsic water use efficiency
$\Delta iWUE_{gs}$	:	Variation in *iWUE* based on variation in g_s
$\Delta iWUE_{pc}$	:	Variation in *iWUE* based on variation in A_n
k_{cl}	:	Closing time constant of the stomatal pore
K_{leaf}	:	Leaf hydraulic conductivity
k_{op}	:	Opening time constant of the stomatal pore
K_{plant}	:	Soil-to-leaf hydraulic conductivity
LA	:	Leaf area
LL	:	Leaf length
LMA	:	Leaf mass per area
LN	:	Number of leaves
LT	:	Leaf thickness
LW	:	Leaf width
M / BS	:	Mesophyll to bundle sheath ratio
M/MC	:	Mesophyll / Mesophyll cell
MC_{area}	:	Area of a mesophyll cell

MC_{length}	:	Length of a mesophyll cell
M_{si}	:	Mesophyll area per interveinal distance
NAD-ME	:	NAD malic enzyme
NADP-ME	:	NADP malic enzyme
NRP	:	Non-recurrent parent
PCV	:	Phenotypic coefficient of variation
PEPC	:	Phosphoenolpyruvate carboxylase
PEP-CK	:	Phosphoenolpyruvate carboxykinase
PGA	:	3-Phosphoglycerate
PH	:	Plant height
R_{dark}	:	Dark respiration
R_n	:	Night respiration
RP	:	Recurrent parent
RuBP	:	Ribulose-bisphosphate
Rubsico	:	Ribulose-1, 5-bisphosphate Carboxylase Oxygenase
SD	:	Stomatal density
SI	:	Stomatal index
SPAD	:	Special products analysis division
SS	:	Stomatal size
Suc	:	Sucrose concentration in the leaf
TE	:	Transpiration efficiency
TLA	:	Total leaf area
TLV	:	Total number of longitudinal veins
VB_{si}	:	Vascular bundle area per interveinal distance
VD	:	Vein density
VPD	:	Vapour pressure deficit
WU	:	Water Use
WUE	:	Water Use Efficiency
WUE_{cl}	:	Integrated *iWUE* during stomatal closure
WUE_{op}	:	Integrated *iWUE* during stomatal opening
Y	:	Yield
$\Delta^{13}C$	:	Leaf carbon isotope discrimination
Ψ_{leaf}	:	Leaf water potential

LIST OF FIGURES

Chapter 1

Chapter 2

Chapter 3

Chapter 4

Chapter 5

LIST OF TABLES

Blank Page

Chapter 1

GENERAL INTRODUCTION

1.1 RESEARCH CASE

Global environmental change is impacting agricultural systems worldwide, with increasing temperatures and drought events imposing a challenge to increase agricultural production to meet rising demand. Moreover, shortage of arable lands due to increasing world populations imposes further strain on maintaining, let alone increasing, agricultural production. Hence, there is a pressing need to breed crops with higher resource (water, nutrients, radiation) use efficiency that can withstand weather extremes and water stress while also maintaining agricultural productivity. Water use efficiency (*WUE*) is one of the main desirable crop traits, which describes the efficiency of water use by the plant to produce yield, such as grain or biomass. Breeding for *WUE* is challenging, because *WUE* is a complex trait with many contributing physiological processes. At the leaf level, *WUE* is estimated as the ratio of carbon assimilation (A_n) to stomatal conductance, g_s (*iWUE*). Achieving high *iWUE* requires maximizing A_n, reducing g_s, or both. Reduced g_s can be due to genetic factors and may occur under conditions of stress; however, this decreases CO_2 diffusion into the leaf and consequently reduces A_n and biomass accumulation. In an agricultural context, low g_s may be disadvantageous as it would limit crop ability to exploit all the available soil water during the growing seasons. Therefore, while it is desirable to achieve high *iWUE*, it must not come at the expense of yield. In C_4 species, the carbon concentrating mechanism (CCM) enables the achievement of high A_n at low g_s, resulting in C_4 crops, like Maize, Sugarcane and Sorghum having higher *iWUE* relative to C_3 crops. Excessive reduction of g_s ultimately impacts A_n, and hence productivity, even in C_4 crops. Therefore, it is critical to find alternate ways to improve *iWUE* in C_4 crops without compromising photosynthesis or CCM efficiency. Discovering new traits for improving *iWUE* in C_4 crops will not only further our knowledge in this area but will also be useful in breeding programs. This PhD project centres on how the determinants of g_s vary in the model C_4 crop Sorghum (*Sorghum bicolor*) and how that variation impacts *iWUE*.

1.2 CHALLENGES TO AGRICUTLURE AND GLOBAL CHANGE

The rising world populations, expected to reach 10 billion by 2050, imposes a strain on agricultural production worldwide (Rosenzweig and Parry, 1994; Challinor *et al.*, 2014; Long *et al.*, 2015; Rippke *et al.*, 2016; Teuling, 2018). Increased population requires increased agricultural output. Finding new ways to manipulate crops to increase productivity and efficiency has become a key area in the plant sciences. To satisfy increased demands for food production, breeders, farmers and scientists are looking to find new ways to increase crop yields. Current projections show that there is a gap between projected yields of some of the world's main crops and future demand (**Fig.1.1**; Ray et al., 2013). However, increasing crop yields is not the only target for improved plant performance.

Since the Industrial Revolution, increased carbon dioxide (CO_2) emissions have contributed to and accelerated the greenhouse effect (the phenomenon by which radiation from the sun is trapped inside the atmosphere). The greenhouse effect is increasing global temperatures, altering rainfall patterns and intensifying droughts (Alexander et al., 2006). The impact of these climatic changes is extensive and affects all world ecosystems, including agricultural systems. Most of the freshwater used by humanity is directed towards agricultural irrigation (Morison et al., 2008), and thus global change, especially predicted frequency of drought events, will only exacerbate water shortages (Elliott *et al.*, 2014), presenting a further obstacle to improving plant performance. Several projections (Sinclair *et al.*, 2005; Ray *et al.*, 2013; Mueller *et al.*, 2016; Rippke *et al.*, 2016) have indicated that future climate change will adversely impact food production systems, with water availability being the main contributor to stunted yield increases into the future. Hence, a key challenge of our Century is to breed crops with improved productivity while using less resources, particularly precious water, and being more tolerant of extreme weather events.

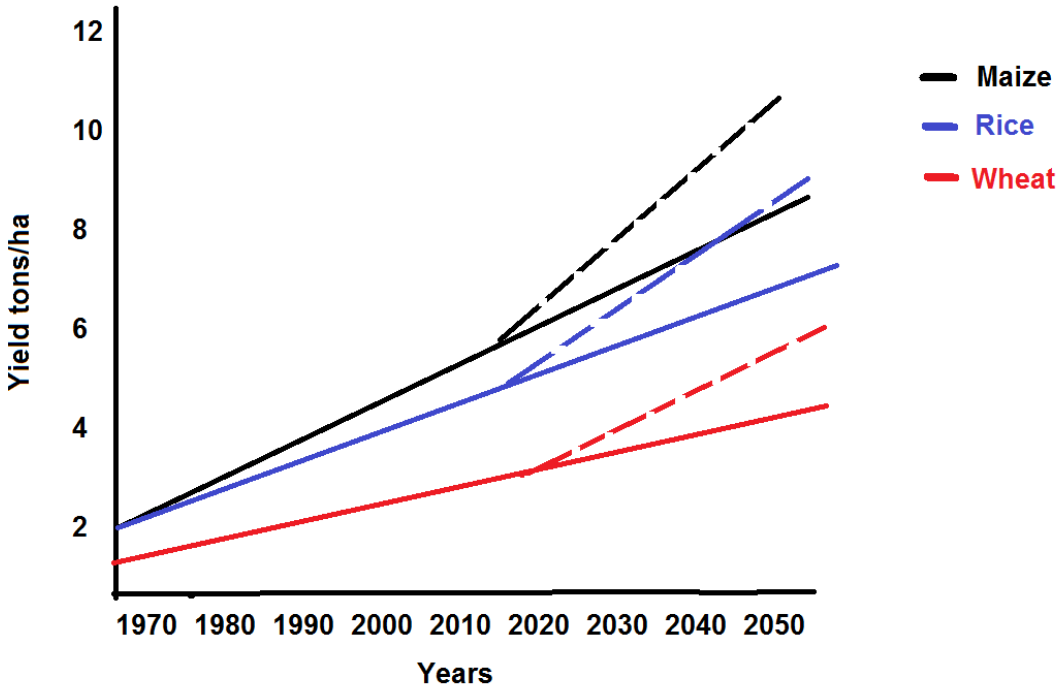

Fig.1.1 The yield gap. Yield projections of four major crops over the next few decades show that expected yield (solid line post 2010) does not match the required yield for rising world populations (dashed line post 2010) (Ray *et al.*, 2013).

1.3 C_3 PHOTOSYNTHESIS

Most terrestrial plants assimilate atmospheric CO_2 via the C_3 photosynthetic pathway. Photosynthesis utilise sunlight energy to produce sugars for growth. During C_3 photosynthesis, atmospheric CO_2 diffuses through the stomata into the intercellular airspaces then through the mesophyll cell wall and plasma membrane, mesophyll cytoplasm and into mesophyll chloroplasts where it is fixed by the Calvin-Benson (C_3) cycle. The light-dependent reactions of photosynthesis are located in the thylakoid membrane. Absorbed light energy excites the reaction centres (P680 and P700) at Photosystems II and I, initiating the electron transport chain. Protons and electrons generated from the split water (H_2O) molecules at PSII and cycled through Cytochrome b_6f are used to produce NADPH and ATP to power the Calvin cycle. The light-independent (dark) reactions of photosynthesis occur in the chloroplast stroma, where CO_2 molecules are fixed onto ribulose bisphosphate (RuBP) via the enzyme Rubisco (ribulose-1, 5-bisphosphate carboxylase/oxygenase) to produce two molecules of 3-phosphoglycerate (PGA). PGA is then converted into glyceraldehyde 3-phosphate (triose phosphates) using energy from NADPH and ATP. Some of the triose phosphates remain in the chloroplasts for RuBP regeneration or starch biosynthesis. Remaining triose phosphates are exported into the cytosol where they are converted into hexoses to form sucrose (or other oligosaccharides), and exported from the source leaves to support plant growth and metabolism (Ghannoum *et al.*, 2017).

Oxygen, a by-product of light-dependent reactions of photosynthesis, is released into the atmosphere. Hence, plants perform important ecological roles by being (1) the primary producers on Earth via harnessing sunlight energy to produce sugars and (2) the producers of oxygen that is used for respiration by many other organisms. However, Rubisco is a bi-functional enzyme, which fixes CO_2 as well as O_2. Due to complex evolutionary and chemical properties, Rubisco has a poor specificity for CO_2 relative to O_2, a low affinity for CO_2 and low catalytic turnover rate relative to other biological catalysts (Bathellier *et al.*, 2018). The oxygenation of Rubisco leads to the production of 2-phosphoglycolate which is further metabolised through the photorespiratory cycle. Photorespiration consumes energy and wastes carbon and nitrogen by the evolution of CO_2 and NH_4^+(Ghannoum *et al.*, 2017). When the CO_2 concentration ($[CO_2]$) is high near Rubisco's active sites, more efficient carboxylation occurs. At low $[CO_2]$ (due to diffusional

resistances or reduced atmospheric [CO_2]), oxygenation increases, dominating the consumption of light energy. With increasing temperature, the rate of oxygenation increases faster than that of carboxylation (Jordan and Ogren, 1984). In C_3 plants, photorespiration increases relative to photosynthesis under low [CO_2], water stress and high temperatures (Betti *et al.*, 2016).

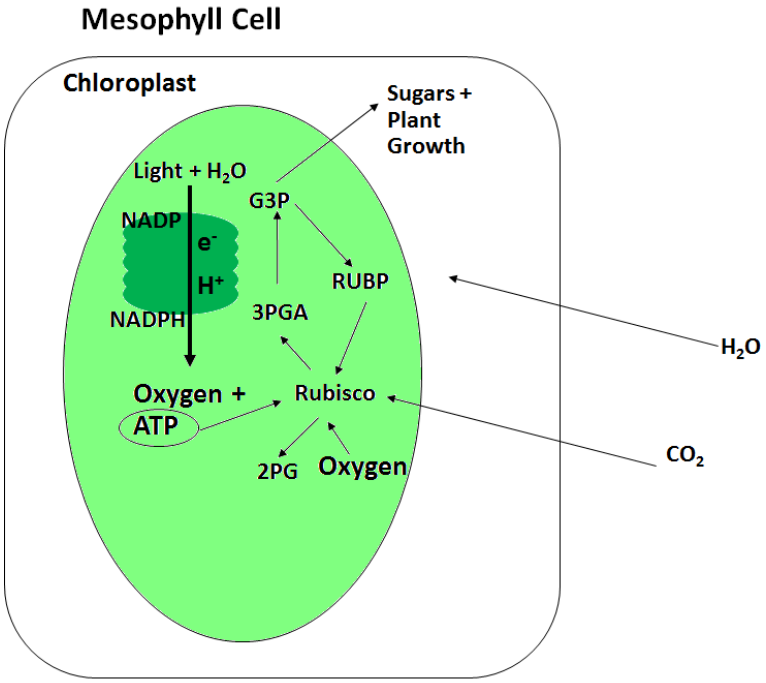

Fig.1.2 A simplified illustration of photosynthesis. (Sharwood *et al.*, 2016)

1.4 C_4 PHOTOSYNTHESIS

During the Miocene and early Pliocene (15-5 million years ago), [CO_2] in the atmosphere plummeted, putting extra strain on the ability of Rubisco to fix CO_2 in the Calvin cycle (Edwards *et al.*, 2010). In addition, aridity forces stomatal closure to conserve water, reducing [CO_2] at the sites of Rubisco. Warm temperatures increase O_2 solubility more than CO_2 and encourages oxygenation more than carboxylation (Jordan and Ogren, 1984). The combination of these factors (low CO_2, aridity and warm temperatures at low latitudes) have been suggested as the main drivers for the evolution of "C_4" photosynthesis (Sage, 2001, 2004; Edwards *et al.*, 2010; Osborne and Sack, 2012).

C_4 photosynthesis refers to a number of anatomical and biochemical alterations from the ancestral C_3 pathway (Hatch, 1987). The main anatomical innovation during C_4 evolution among terrestrial plants is the development of 'Kranz anatomy'. In C_3 leaves, the vessels (veins) are surrounded by bundle sheath cells (BSCs) devoid of chloroplasts, while palisade and spongy mesophyll cells (MCs), are arranged away from the veins (**Fig.1.3**). In C_4 leaves, MCs form an outer layer around the inner BSCs, which form concentric layers of tightly packed, wreath-like (Kranz) cells around the veins (**Fig.1.3**). Relative to C_3, C_4 leaves have larger, more numerous BSCs with more abundant chloroplasts, while MCs have a larger surface area and are in contact with intercellular airspaces and BSCs (Brown and Hattersley, 1989).

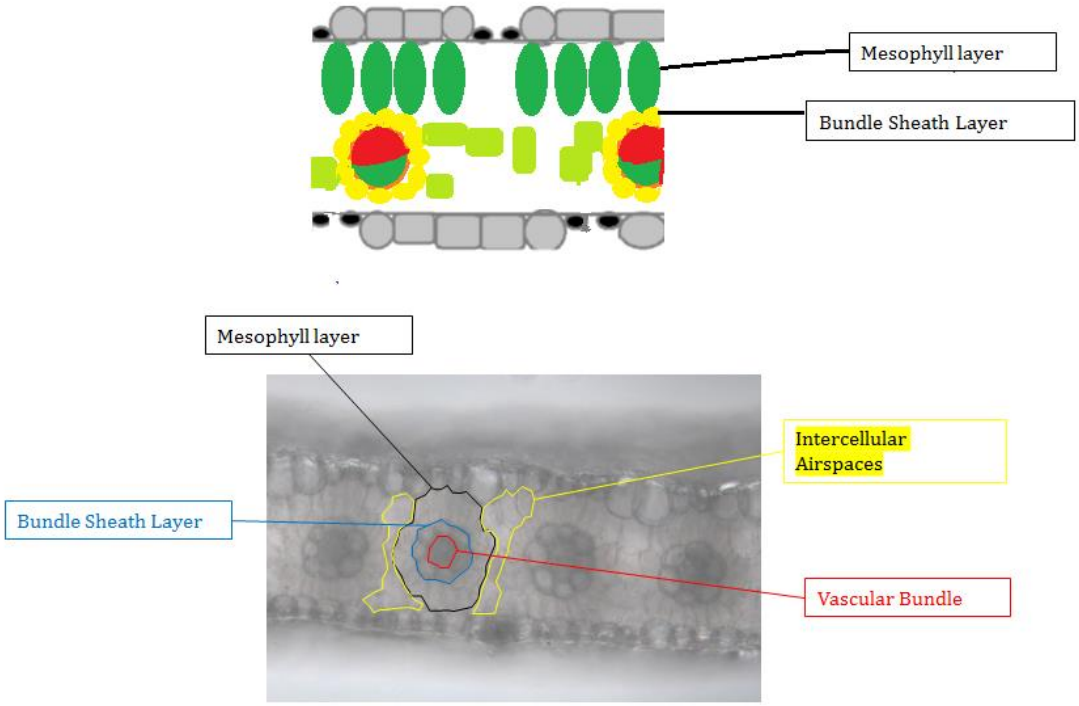

Fig.1.3 Illustration of the differences in anatomy between C_3 and C_4 plant leaves. Notice the wreath like arrangement around the vascular bundle in the C_4 leaf (Sage and McKown, 2006). (Image: Yazen Al-Salman, PhD Thesis 2021).

Biochemically, C_4 photosynthesis is characterised by the operation of a CO_2 concentrating mechanism (CCM) across the MC and BSC, which serves to elevated CO_2 around Rubisco, thus increasing photosynthesis and reducing photorespiration (Hatch, 1987). During C_4 photosynthesis, atmospheric CO_2 diffuses into the mesophyll cytoplasm where it is hydrated by carbonic anhydrase (CA) to produce a carbonate that is fixed by phosphoenolpyruvate carboxylase (PEPC) into a 4-carbon acid (oxaloacetate), hence the name "C_4 photosynthesis". Oxaloacetate is converted into malate or aspartate, transported to the BSCs, and decarboxylated to release CO_2 that can be fixed by Rubisco. In this pathway, Rubisco levels in the MC are suppressed, with BSCs having the majority of Rubisco amounts in C_4 leaves. PEPC has a higher specificity to CO_2 and a higher catalytic rate than Rubisco (Sharwood *et al.*, 2016). Hence, the high rate of PEPC activity leads to a high rate of CO_2 fixation and hence a high [CO_2] near the site of Rubisco. Higher [CO_2] in BSCs increases leaf carbon assimilation rates and plant productivity, giving C_4 plants a competitive advantage over C_3 counterparts. This advantage was seized on by humans at

the dawn of agriculture, especially in tropical regions where C4 crops dominate agricultural systems to this day (Brown, 1999). Maize (*Zea mays*), for example, was domesticated in the Americas, most likely Mexico, around 5000-8000 years ago (Brown, 1999), highlighting how long C_4 crops have been an important fixture of agriculture.

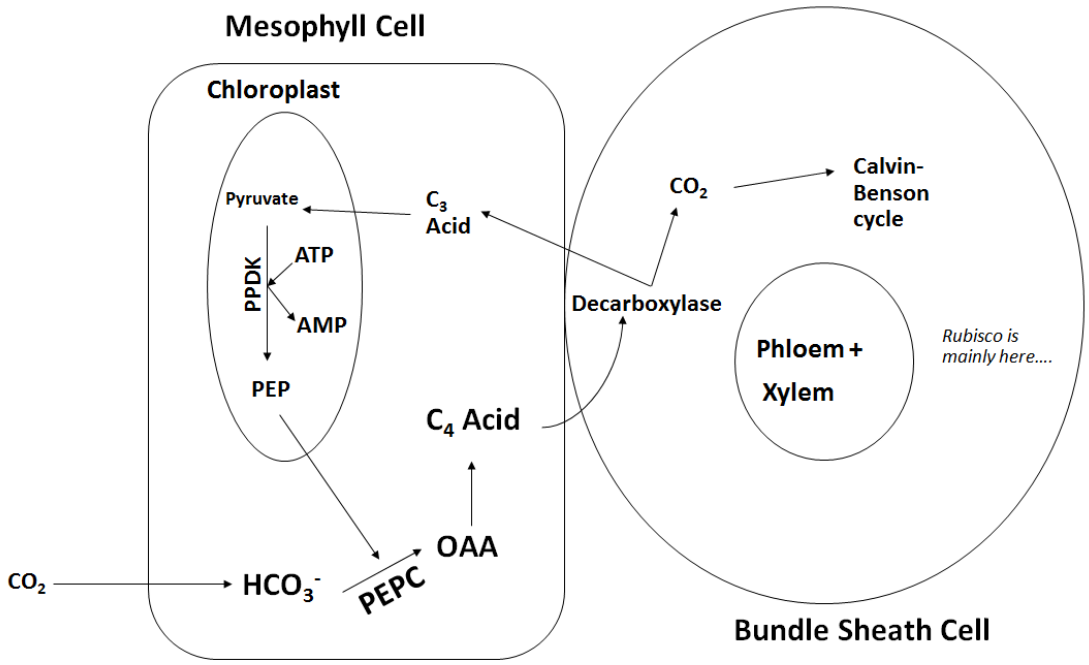

Fig.1.4 The mechanism of CO_2 concentration in C_4 tissues during photosynthetic carbon dioxide assimilation (Sage and McKown, 2006).

Among terrestrial plants, C_4 photosynthesis independently evolved >60 times among angiosperms. The grass family has more than 18 independent C_4 origins (Sage *et al.*, 2011). The identity of the main enzyme that decarboxylates the C_4 acid in the BSC is used as a basis to divide the C_4 lineages into three subtypes: NADP-malic enzyme (NADP-ME subtype), NAD-malic enzyme (NAD-ME subtype) and phosphoenolpyruvate carboxykinase (PEP-CK subtype). The genetic and biochemical basis for these subtypes is now well understood (Christin and Osborne, 2013; Christin *et al.*, 2013; Weissmann *et*

al., 2015; Watson-Lazowski *et al.*, 2018). However, it is becoming increasingly obvious that most C_4 plants operate a secondary decarboxylase, whilst the feasibility of a pure PEP-CK subtype remains a matter of debate (Wang *et al.*, 2014; Yin and Struik, 2021). Most of the major C_4 crops, such as Maize, Sugarcane (*Saccharum* spp.) and Sorghum have the NADP-ME pathway. Several physiological and functional differences have been found between these three subtypes (Leegood and Walker, 1999; Ghannoum *et al.*, 2002; Ghannoum, 2009; Pinto *et al.*, 2016; Sonawane *et al.*, 2017).

The CCM confers ecological and physiological advantages onto C_4 plants: they generally have higher productivity and resource (water, nitrogen and light) use efficiency than C_3 plants (Ehleringer *et al.*, 1997; Long, 1999; Ghannoum *et al.*, 2011). In particular, the saturation of C_4 photosynthesis at low [CO_2] (**Fig.1.5**) allows C_4 leaves to operate with lower stomatal conductance (Taylor *et al.*, 2010, 2012; Pinto *et al.*, 2014). This leads to higher leaf- and plant-level water use efficiency (*WUE*) in C_4 relative to C_3 plants (Long, 1999; Ghannoum *et al.*, 2011).

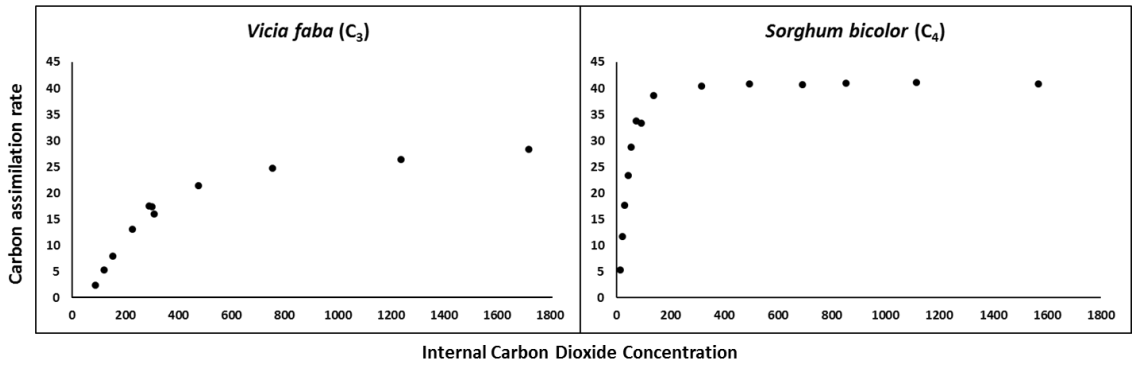

Fig.1.5 CO_2 response curves of a C_3 species (fava bean, *Vicia faba*) and a C_4 species (Sorghum) showing the saturation of photosynthetic assimilation for C_4 species at lower CO_2 concentration and at higher rates of assimilation (Al-Salman, unpublished).

1.5 STOMATA AND CO_2 FIXATION

Prior to fixation in the mesophyll (by Rubisco in the C_3 pathway or CA/PEPC in the C_4 pathway), CO_2 diffuses into the leaf through the stomata. Stomata are microscopic pores on the leaf surface (usually on both sides of the leaf). Through these pores, CO_2 diffuses into the sub-stomatal cavity, the intercellular airspaces and into the mesophyll cells. The stomatal pores present a resistance to CO_2 diffusion, regulating the exchange between the atmosphere and the leaf. The stomatal pore is formed by two "guard" cells, which control the aperture of the stomatal pore. In grasses, guard cells are flanked by subsidiary cells (Cai *et al.*, 2017), which facilitate rapid movement. An open pore leads to greater uptake of CO_2.

In the opposite direction to CO_2 diffusing into the leaf, water vapour diffuses out of the leaf. Liquid water moves through the xylem vessels into BSCs and MCs, where it evaporates into the intercellular airspaces and out of the stomata to the atmosphere (**Fig.1.6**). To maximize CO_2 intake, the leaf must open its stomata, which increases water loss. The leaf alters the opening and closing of the stomata through changing the turgor pressure of the guard cells (Franks and Farquhar, 2001, 2007; Mott and Franks, 2001; Buckley *et al.*, 2003). During opening, turgor pressure in guard cells increases due to changes in ion fluxes, causing the cells to swell and expand into neighbouring cells, opening the stomatal pore. Conversely, ions flux out of the guard cells reduces turgor pressure, and causing guard cells to become flaccid and closing the pore (Jezek and Blatt, 2017).

The opening and closing of the stomata depend on several environmental factors. Increase in ambient [CO_2] induces stomatal closure (Mott, 1988), as a mean of reducing water loss in the face of increasing CO_2 availability. Hence, stomatal closure under high [CO_2] produces net benefit to the leaf. Conversely, reduced atmospheric [CO_2] induces stomatal opening in order to allow more CO_2 into the leaf, increasing water loss through the pore. Drought and low air humidity also induce stomatal closure to restrict water loss (Mott and Parkhurst, 1991; Mott *et al.*, 1997; Mott and Peak, 2010). Light stimulates stomatal opening to maximize CO_2 intake under photosynthetically favourable conditions (Mott and Franks, 2001; Mott *et al.*, 2008).

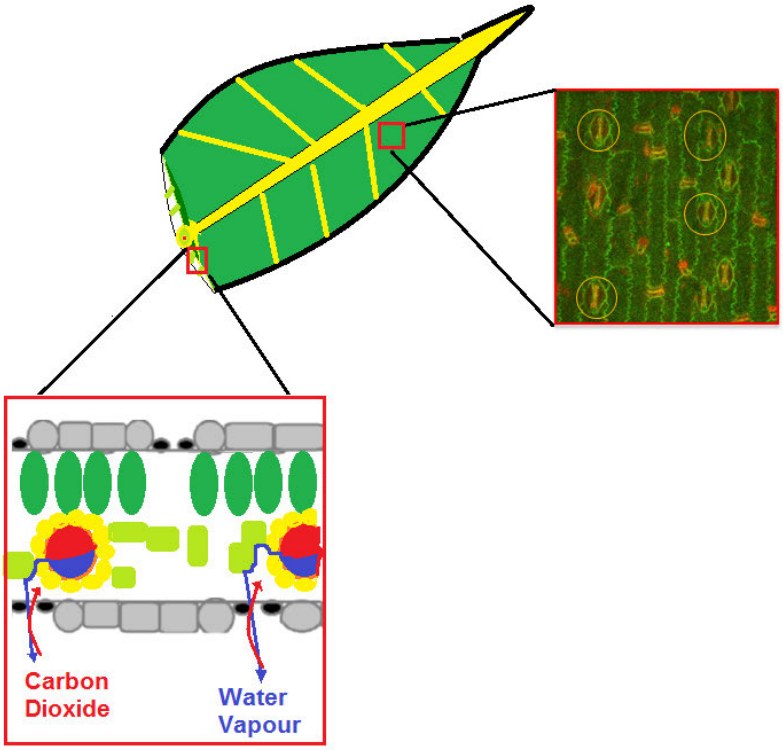

Fig.1.6 Simplified illustration of CO_2 and H_2O path in the leaf (Scoffoni *et al.*, 2016). (image: Yazen Al-Salman, PhD Thesis 2021).

1.6 LEAF LEVEL WATER USE EFFICIENCY

Water use efficiency (*WUE*) is a physiological trait that is quantified as the ratio of carbon gain per unit of water investment. Furthermore, WUE is quantified on different scales from the field to leaf level (Condon et al., 2004; Medrano et al., 2015) (**Fig.1.7**). At the leaf level, the unit of *WUE* is usually termed transpiration efficiency (*TE*), and is estimated by the ratio of carbon assimilated to water lost through transpiration:

$$TE = \frac{A}{E} = \frac{g_{sc}(C_a - C_i)}{g_{sw}\,(W_i - W_a)} \qquad (1.1)$$

Where A_n is carbon assimilation rate; E is transpiration rate; g_{sc} is stomatal conductance to CO_2 and g_{sw} is stomatal conductance to water vapour; C_a and C_i are ambient and intercellular CO_2 concentrations respectively; W_a and W_i are ambient and intercellular water vapour concentrations respectively. The rate of water vapour diffusion is 1.6 faster than CO_2 (g_{sw} = 1.6 g_{sc}). Hence:

$$TE = \frac{(C_a - C_i)}{1.6\,(W_i - W_a)} \qquad (1.2)$$

Increased *TE* can be achieved by increasing ($C_a - C_i$) and/or decreasing ($W_i - W_a$). The CO_2 drawdown ($C_a - C_i$) depends on A_n, which is mainly a biochemical limitation, but variation in g_s also influence C_i. The term ($W_i - W_a$) depends on both g_s and leaf-to-air vapour pressure deficit (VPD), which in turn depends on physical parameters such as ambient temperature and humidity (Farquhar and Sharkey, 1982). Hence, a more appropriate expression of *TE* (Ghannoum, 2016) that indicates genetic differences independent of VPD is the intrinsic WUE (*iWUE*) which relates A_n (biochemical factor) to g_s (diffusive factor):

$$iWUE = \frac{A}{g_s} \qquad (1.3)$$

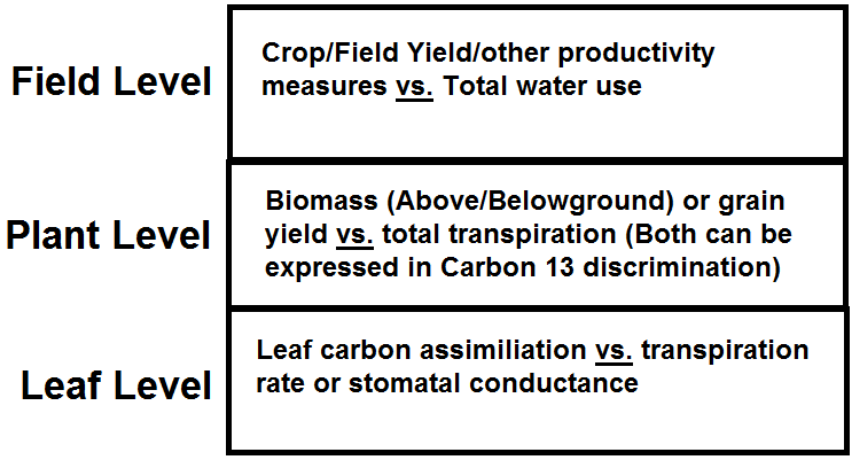

Fig.1.7 Different levels of water use efficiency (Medrano *et al.*, 2015).

1.7 WATER USE EFFICIENCY AS A CROP TRAIT

Most of the world's freshwater resources are used for irrigation in agriculture (Condon et al., 2004). With increased food demand, demand for more water allocation for agriculture is inevitable. Furthermore, rising temperatures due to global climate change will increase crop water use as well increasing variability in rainfall (Alexander *et al.*, 2006). Hence, attempting to find and breed crops that maximise production for less or similar demand is crucial. More importantly, this increases the need to not just improve the *WUE* of crops, but to understand drivers of *WUE* and its impact on other agronomic traits (Leakey *et al.*, 2019). Passioura (1977) expressed *WUE* relative to crop yield as follows:

$$Y = WUE \times Water\ Use \times HI \qquad (1.4)$$

Where *Y* is crop yield; *Water Use* is irrigation water used; and *HI* is harvest index, which is the proportion of grain yield to standing biomass. This expression has widely used and it establishes *WUE* (and its proxies such as *iWUE*) as key components of increasing yield.

C_3 crop varieties that exhibit higher *iWUE* have higher yields (Rebetzke et al., 2002; Condon et al., 2004; Passioura, 2006). Measuring *iWUE* using leaf gas exchange analysers (which measure A_n and g_s) is time consuming and gives a snap shot of a leaf's capacity to balance carbon gain and water loss (Passioura, 2006). While *iWUE* provides instantaneous estimation of *WUE*, it does not integrate the different timescales of variations in *WUE* that occur diurnally, seasonally or in response to changes in water availability and climatic factors (Leakey *et al.*, 2019). Plant-level *WUE* (ratio of biomass produced per whole plant water use) or grain *WUE* (ratio of grain produced per whole plant water use) are not suited for quick phenotyping. The stable carbon isotope composition of the leaf, specifically the ratio of ^{13}C relative to ^{12}C ($\delta^{13}C$), can be a good proxy for *iWUE* in C_3 plants (Farquhar and Richards, 1984). During photosynthesis, ^{13}C is discriminated against with plants containing a smaller ration of ^{13}C relative to ^{12}C when compared to ambient air. In addition, ^{13}C is discriminated against during diffusion from the air into the leaf, which is largely controlled by the stomata. Carbon isotope

discrimination ($\Delta^{13}C$) correlates with the ratio of C_i to C_a, which is an important indicator of *iWUE* (Condon *et al.*, 2004). Hence, isotopic analysis of leaf samples has become a powerful method of obtaining a time-integrated measure of *iWUE*, as it takes into account gas fluxes occurring throughout the leaf lifespan (Leakey *et al.*, 2019).

However, $\Delta^{13}C$ has not shown a consistent relationship with yield (Condon *et al.*, 2004), and more importantly for this thesis, $\Delta^{13}C$ is more difficult to estimate in C_4 crops (see details below). Also, $\Delta^{13}C$, and by extension *iWUE*, have tended to correlate with more conservative crop growth (Condon *et al.*, 2004), which can be disadvantageous for crops when water is available. Higher *iWUE* usually means a reduction in g_s, which results in lower C_i and consequently lower A_n, reducing plant productivity. In the expression from Passioura (1977) (**Eq.1.4**), *Water Use* is a component of *Y*, and hence reducing transpiration and water uptake under favourable conditions can be disadvantageous. Moreover, under drought conditions, high *WUE* (and conservative growth) is not correlated with the development of deeper root systems that can access stored soil moisture (Blum, 2009; Chaves *et al.*, 2016). There is also evidence that reduced g_s (and increased *iWUE*) under high temperatures can minimize evaporative cooling, potentially causing heat damage (Chaves *et al.*, 2016; Drake *et al.*, 2018; Caine *et al.*, 2019). Synchronizing plant growth cycle and grain filling (for seed crops) with predicted seasonal moisture supply is often the first step in breeding for water-limited environments (Blum, 2009). A crop with higher *WUE* is potentially able to make the most of water limiting environments by maximizing gain for water available, while also relieving the impact of water stress later in the growth cycle by additional conservation of soil moisture (Jackson *et al.*, 2016), as the latter stages of growth, especially the reproductive stage, are the most vulnerable to drought (Blum, 2009), and of course for seed crops it is the stage that makes those crops valuable. The vulnerability to drought during the seed formation and filling is especially conspicuous for rainfed crops (Blum, 2009), such as Sorghum (see below). Ultimately, *WUE* (and *iWUE*) remains an important trait in preserving soil moisture for rainfed crops especially since irrigation will need to be reduced due to the factors discussed earlier regarding water shortages and global climate change.

1.8 *iWUE* IN C_4 CROPS

Due to the operation of a carbon concentrating mechanism (CCM) in the leaves, C_4 plants generally exhibit higher *iWUE* than C_3 species (Wand et al., 1999; Taylor et al., 2011; Pinto et al., 2014; Way et al., 2014). The high A_n of C_4 species allows C_4 species to reduce their stomatal apertures during times of high evapotranspirative demand (Knapp, 1993; Ward et al., 1999; Huxman and Monson, 2003; Osborne and Sack, 2012), reducing their g_s compared to C_3 species. The CCM of C_4 species allows for high A_n even under low CO_2 intake as a result of stomatal closure, gaining high *iWUE* even under stress conditions (Steduto *et al.*, 1997; Ghannoum *et al.*, 2001, 2002; Vogan and Sage, 2011; Ghannoum, 2016). Most past studies investigating *iWUE* in C_4 crops have focussed on measuring leaf gas exchange (i.e., A_n and g_s), as the relationship between $\Delta^{13}C$ and *iWUE* is weak and less consistent in C_4 plants (Henderson *et al.*, 1992; Ellsworth and Cousins, 2016). This is due to multiple complicated processes involved in C_4 photosynthesis, and therefore cannot reliably be used for screening of C_4 populations (Feldman *et al.*, 2018). The components of isotopic fractionation of ^{13}C as it moves through the leaves are more diverse in C_4 leaves, as different sites of CO_2 fixation (by PEPC and then by Rubisco) makes apportioning discrimination events to certain enzymes or processes much trickier. Another important factor that determines $\Delta^{13}C$ in C_4 leaves is bundle sheath leakiness, which represents the fraction of PEPC-fixed CO_2 that passively leaks from bundle sheath cells back to the mesophyll (von Caemmerer *et al.*, 2014). In addition, improving *iWUE* in C_4 crops was met with early setbacks when early studies reported low genetic variability for whole-plant *WUE* (Hammer *et al.*, 1997).

All the above, combined with naturally high *iWUE* of C_4 crops compared to C_3, has resulted in less focus and available information about what drives high *iWUE* in C_4 crops and the impact of high *iWUE* on C_4 crop productivity. C_4 crops dominate tropical and sub-tropical agricultural systems, with crops such as Maize, Sorghum and Sugarcane being key crops in these agro-ecosystems (Leakey, 2009). These warm regions (such as sub-Saharan Africa) are 1) projected to experience the greatest shift in climatic variability with the onset of climate change and its impact on agriculture and 2) are experiencing the fastest rise in population as well as being among the world's poorest populations (Foley *et al.*, 2011; Borrell, Mullet, *et al.*, 2014). Hence, there is an imperative to undertake detailed studies of the variations in *iWUE* among C_4 crops, determine the physiological and genetic

basis of these variations, and establish whether better *iWUE* translates into tangible agronomic traits, such as yield.

1.9 STOMATAL FORM AND FUNCTION IN RELATION TO *iWUE* IN C_4 GRASSES

Stomatal conductance is determined by the size and number of the stomata on leaf surfaces. Small stomatal size (*SS*) and higher stomatal density (*SD*) have been shown to yield higher g_s in species across the plant kingdom (Salisbury, 1928; Hetherington and Woodward, 2003; Franks and Beerling, 2009; Franks *et al.*, 2009; Monda *et al.*, 2016; Sack and Buckley, 2016). Smaller stomata generally mean reduced pore depth and thus a shorter distance for CO_2 diffusion, whilst overcoming space limitation that limits production of more stomata (Franks and Farquhar, 2007). Increasing *iWUE* tends to correspond with lower g_s as a result of smaller and fewer stomata (Miller-Rushing *et al.*, 2009; Doheny-Adams *et al.*, 2012; Drake *et al.*, 2013; Tanaka *et al.*, 2013; Franks *et al.*, 2015; Hentschel *et al.*, 2016). Therefore, variations in stomatal characteristics can constitute important anatomical feature that can underpin higher *iWUE* in C_4 crops (Way, 2012; Taylor *et al.*, 2014; Way *et al.*, 2014). C_4 grasses generally have lower *SD* compared to C_3 counterparts (Malone *et al.*, 1993; Taylor *et al.*, 2012), leading to lower g_s values that are further encouraged due to the CCM and high assimilation capacity of C_4 grasses. Taylor et al. (2012) also highlighted the negative *SD* vs *SS* relationship in C_4 grasses (**Fig.1.8**), with this relationship becoming weaker under dry conditions. This suggests that the control of g_s by altering stomatal traits is prominent in C_4 species.

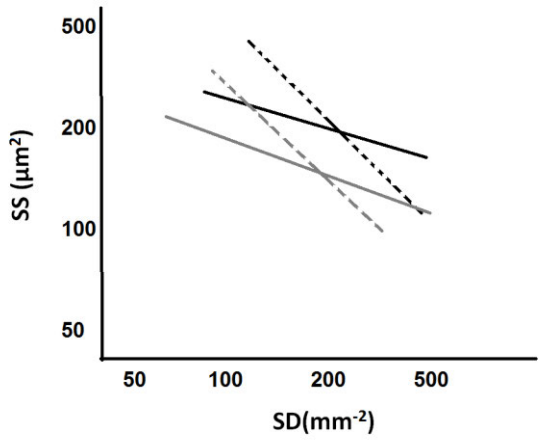

Fig.1.8 Relationship between stomatal density, D_s (mm^{-2}) and stomatal size, S_s (μm^{-2}) in a collections of C_3 (black symbols) and C_4 (white symbols) grasses (Taylor *et al.*, 2012), Solid lines represent data from dry environments, while dashed lines represent data from wet habitats.

Another important aspect of C_4 stomatal morphology is the "dumb-bell" shape of C_4 grass stomata, compared to the "kidney-shaped" guard cells of most C_3 taxa. The dumb-bell shape of grass stomatal gives them a mechanical advantage that enables them to respond much more quickly to transient changes in environmental conditions (Franks and Farquhar, 2007). Single measurements of *iWUE* depend on steady state values of g_s and A_n. However, this measurement requires controlled environmental conditions inside the leaf gas exchange chamber, which is not representative of the natural environmental fluctuations, such as the variation of light intensity during the day period. While the photosynthetic apparatus can respond quickly to environmental changes, the stomatal aperture "lags" behind in its response (Kirschbaum *et al.*, 1988; Tinoco-Ojanguren and Pearcy, 1993a, 1993b; von Caemmerer *et al.*, 2004; Mott *et al.*, 2008; Lawson and Blatt, 2014), leading to a mismatch between A_n and g_s (**Fig.1.9**). This lag can limit the attainment of high A_n under favourable conditions and causes excessive water loss under unfavourable conditions. These inefficiencies in stomatal behaviour result in lower *iWUE*, making the optimisation of stomatal behaviour a key component of achieving higher *iWUE* (Lawson and Blatt, 2014), especially when it comes to scaling *iWUE* over longer timescales where responses to environmental variability can be a strong determining factor of *iWUE*.

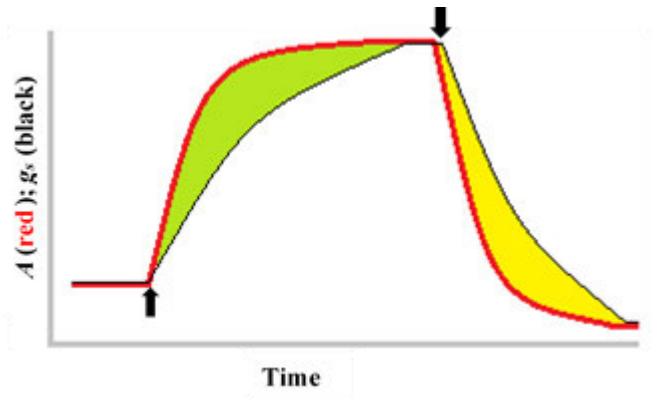

Fig.1.9 Response of stomatal conductance (g_s, black) and carbon assimilation (A_n, red) to a step change in light. The green shaded area represents g_s limitation on A_n due to slow stomatal opening after an increase in light intensity. The yellow shaded area represents excess water loss due to slow stomatal closure after light intensity decreases (black arrows represent light intensity increase and decrease).

1.10 MORPHOLOGY OF C_4 GRASSES IN RELATION TO *iWUE*

The anatomical arrangement of C_4 species contributes greatly to the ability of C_4 crops to achieve high A_n as explained earlier. The development of Kranz anatomy starts after vein formation, where the M and BS start developing and are arranged around the veins (Dengler *et al.*, 1986; Bergmann, 2004). Changes in leaf size (especially width) ultimately impacts the expansion of M and BS cells and also vein size, changing the volume and total size of M and BS along the leaf (Mckown and Dengler, 2007). Changes in M and BS size can lead to an increase in photosynthetic enzyme concentration and increasing A_n (Feldman *et al.*, 2017; Reeves *et al.*, 2018), and hence increasing *iWUE*. The anatomical arrangement of C_4 leaves can have a significant impact on i*WUE* at multiple scales in various ways. First, environmental conditions can influence leaf anatomical development by changing the rates of cell expansion and division (Lafarge *et al.*, 1998). Hence, the interaction of leaf morphological changes combined with physiological leaf responses to environmental change will influence the resulting *iWUE*. For example, having smaller leaves reduces the evaporative surface area, reducing the total amount of water lose from the leaf and that is required to be taken in by the plant. Also, smaller leaves lead to smaller boundary layers, and hence lowered resistance. This lowered resistance can lead to an increase in transpiration rate, but the total transpiration will be mitigated by reduced leaf size as well as reduced stomatal pore due to reducedboundary layer resistance, mitigating any increase in transpiration andlowering total plant transpiration compared to larger leaves (Jarvis and McNaughton, 1986; Schuepp, 1993). Secondly, in C_4 grasses, the development of stomata is dependent on vein development, with stomata forming in specified cell files adjacent to the veins (Rudall *et al.*, 2017). Changes in vein characteristics in C_4 leaves change the distribution, size and density of stomata (Ueno *et al.*, 2006; Reeves *et al.*, 2018). In addition, morphological changes affect the transport path lengths inside the leaves, as well as the size of intercellular airspaces, possibly imposing more resistance on diffusive conductance and the rates of CO_2 and H_2O transport (Rockwell *et al.*, 2014; Fiorin *et al.*, 2016; Buckley *et al.*, 2017). Hence, morphological changes in C_4 leaves will likely have a large impact on *iWUE* due to a combination of interactions, with morphological changes likely to have genetic basis that would be useful for breeders when targeting improvement in *iWUE*.

1.11 AQUAPORIN PROTEINS AND LEAF PHYSIOLOGY

Aquaporin channels are integral membrane proteins, found embedded in the lipid bilayer that envelopes plant and animal cells. The term "aqua"-porin was applied to these proteins as they facilitate the rapid and selective transport of water and other nutrients (Chaumont *et al.*, 2001; Reddy *et al.*, 2015). Aquaporins (AQPs) are involved in several key leaf process. Up-regulation of AQPs in some species increased hydraulic conductivity (Lopez *et al.*, 2013; Prado and Maurel, 2013; Prado *et al.*, 2013), including in Maize (Caldeira *et al.*, 2014), a key C_4 crop. AQP control of hydraulic flow in the leaf affects stomatal function. Guard cells that control the opening and closing of the stomatal aperture require ion and water influx to swell or shrink and change the pore size. AQP expression in the guard cells impacts membrane permeability to water (Heinen *et al.*, 2014). This is necessary for guard cells as their plasmodesmata cease to function at maturity, and hence they will require hydraulic signals from the sub-stomatal cavity or neighbouring mesophyll cells through their plasma membrane. Recent evidence showed that increased guard cell permeability is dependent on AQPs to facilitate abscisic acid (ABA) mediated closure of stomata (Grondin *et al.*, 2015). This links AQPs with faster stomatal closure in response to environmental stimuli, a trait that is becoming increasing appreciated for determining crop *iWUE* (Lawson and Blatt, 2014; McAusland *et al.*, 2016). CO_2-permeable AQPs bring into light their impact on mesophyll conductance (g_m), the physiological trait that describes the rate of CO_2 diffusion from the sub-stomatal airspaces to the initial sites of carboxylation. The role of g_m as limiting factor to photosynthetic carbon assimilation is now established (Evans, 2020), and hence highlighting possible contributors to the rate of g_m, such CO_2-permeable AQPs, can lead to improvements in leaf resource use efficiency and increased productivity. Several AQP proteins have been shown to increase g_m in key crops such as Barley, *Hordeum vulgare* (Hanba *et al.*, 2004) and Rice, *Oryza sativa* (Ding *et al.*, 2016). Differences in AQP diversity between C_3 and C_4 species is a nascent area of research, and plenty of overlap has already been observed in the function of certain AQPs in C_3 and C_4 species (Groszmann *et al.*, 2017). AQPs present another possible genetically robust avenue to explore controls on *iWUE* in C_4 leaves, with the ability of AQPs to control H_2O and CO_2 fluxes likely playing a very important role in regulating *iWUE* in C_4 leaves.

1.12 Sorghum bicolor

Sorghum bicolor evolved in Africa after splitting with rice 50–70 million years ago and is an important global crop grown for food, feed, fibre, and fuel (Borrell, Mullet, *et al.*, 2014). It is a C_4 crop of the NADP-ME subtype, like Maize. Cultivated Sorghum is part of the species *Sorghum bicolor* subsp. *bicolor*. Those varieties are annual, 3-5 m in height and have thick culms (Dillon *et al.*, 2007). Cultivated Sorghum is divided into 5 basic races, differing in grain shape, glumes and panicles. These 5 races also differ in some of their physiological adaptations and geographic origins (**Fig.1.10**). The traits of these races would have developed over time due to human breeding for productivity and due to human-influenced dispersal. The races are:

- **Bicolor**: Open inflorescence with pendulous branches; long, clasping glumes; elliptic grain.
- **Guinea**: Large, open inflorescences with open branches; long, separated glumes that expose grains; twisted grains.
- **Caudatum**: Compact inflorescences; grains with one side flat and other curves; shorter glumes that expose grains.
- **Kafir**: Compact, cylindrical inflorescences; elliptic spikelets; tightly clasping, long glumes.
- **Durra**: Compact inflorescences; flat, ovate shaped sessile spikelets; middle-creased lower glume; distinct texture on tip of lower glume.

Sorghum is diploid (2n=20) and genetically diverse thanks to a number of factors, including its sexual compatibility with many of its wild and weedy relatives. A comprehensive analysis of genetic diversity in sorghum landraces and core collections based on race, latitude of origin, photoperiod, seed quality, agronomic traits and DNA markers has demonstrated that sorghum has considerable polymorphism that has been poorly exploited in terms of crop improvement (Dillon *et al.*, 2007; Mace *et al.*, 2019). However, this genetic diversity is now being probed for beneficial crop traits, with a major advance in Sorghum being the stay-green characteristic (Borrell, Mullet, *et al.*, 2014).

Sorghum is a staple in tropical agricultural ecosystems, especially in sub-Saharan Africa. In Australia it is the main summer crop of the rain-fed agricultural production systems of north-eastern Australia, where it is an important rotational crop supplying feed grain to the livestock industry (George-Jaeggli *et al.*, 2017). Variability in rainfall means crops growing in such areas are mainly dependant on stored soil moisture, and hence having high *iWUE* can be very beneficial in conserving soil moisture in the field with usually high atmospheric VPD that leads to high transpiration rates, and so traits that limit transpiration are important in Sorghum.

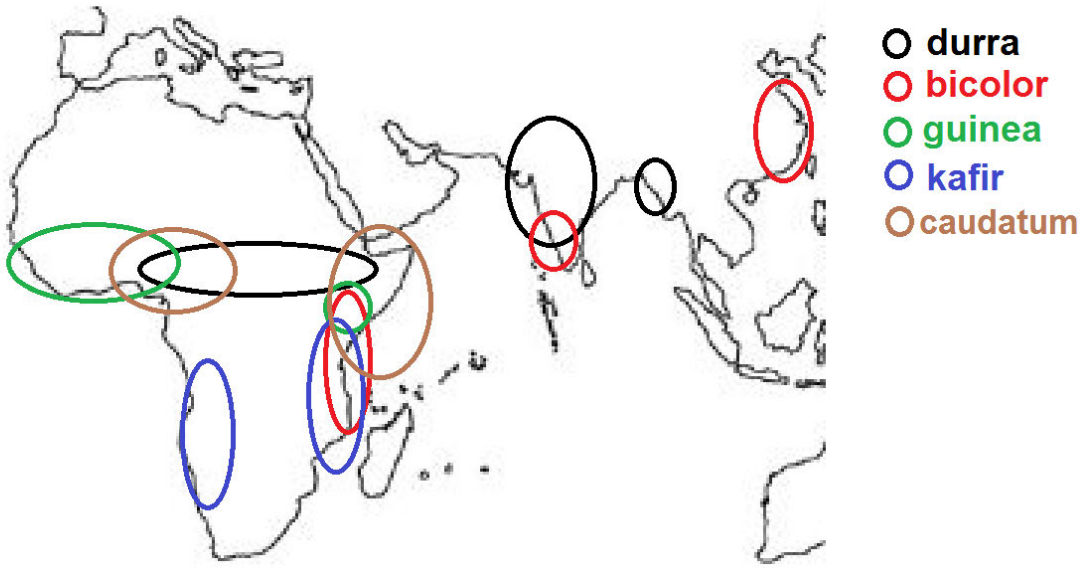

Fig.1.10 Historical geographic distribution of the 5 Sorghum races (OECD, 2017).

1.13 KNOWLEDGE GAPS

The traits that enable the achievement of high *iWUE* in C_4 species are the focus of this thesis. In particular, factors other than the CCM that influence *iWUE* in C_4 species, especially crops, have rarely been explored (Vadez *et al.*, 2014; Ellsworth and Cousins, 2016; Reeves *et al.*, 2018). Maximizing *iWUE* requires the coordination of several leaf anatomical and functional traits and exploring this coordination in Sorghum would provide insight into which traits limit the achievement of high *iWUE* in a C_4 crop. Most past studies investigating leaf-level *iWUE* in C_4 crops have focussed on measuring leaf gas exchange (ie, A_n and g_s). Certain anatomical characters have been shown to relate to *iWUE* (Doheny-Adams et al., 2012; Franks et al., 2015), but these relationships have not been elucidated fully, especially within C_4 species. Anatomical variables related to the stomata and veins impact leaf processes. In addition, the anatomical sophistication of C_4 leaves suggests a significant role for anatomical structures in influencing *iWUE*. Recently, (Cano *et al.*, 2019) reported a positive correlation between leaf width (*LW*) and g_s across C_4 grasses, with wide leaves having lower *iWUE*. This finding opens a promising avenue to explore the impact of leaf anatomy on *iWUE* in C_4 crop species, especially since unpublished data from our group (Pan *et al.*, 2021) confirmed this association between *LW* and *iWUE* using a large number of field-grown Sorghum genotypes.

Leaf gas exchange processes have been shown to be diurnally and seasonally coordinated under different conditions with a strong circadian influence (Taylor *et al.*, 2014; Resco de Dios, 2017; Matthews *et al.*, 2018). This, in addition to the variation in *iWUE* across different timescales (minutes, hours, days, etc.), highlights a need to further investigate the diurnal variation in *iWUE*, especially now it is known that leaf anatomy can be an important determinant gas exchange rates. Furthermore, the light environment is highly variable under field conditions, and plant responses to transient changes in the environment can be important in determining *iWUE* over longer periods (Zur and Jones, 1984; Vialet-Chabrand *et al.*, 2016; Resco de Dios *et al.*, 2020). If not captured, these dynamic responses can invalidate the scaling of *iWUE* to field level, the comparison with other measures of *WUE*.

Finally, a trade-off has been reported between hydraulic efficiency and drought tolerance or *iWUE*, including in Sorghum (Holloway-Phillips and Brodribb, 2011b; Choudhary and

Sinclair, 2014). This raises questions about how consistent or beneficial *iWUE* can be under different water availabilities (as discussed earlier), and whether restricting g_s to achieve higher *iWUE* can be detrimental for higher yields. Along with these possible trade-offs, aquaporins have long been hypothesized to play an important role in all aspects of leaf physiology. A recent discovery of AQP genes in Sorghum (Groszmann et al., unpublished) provides the template to test drought response of Sorghum lines that express different AQP genes. Because AQPs are influential in determining stomatal response to the environment and to CO_2 flux into the mesophyll, they are likely to influence both A_n and g_s, and consequently *iWUE*. Based on all the above, the project was designed to address the following knowledge gaps:

1. Elucidate the covariation of leaf anatomical variables, and how these anatomical associations influence *iWUE* in a key C_4 crop (*S.bicolor*) grown under different temperatures (**Chapter 2**).

2. Determine the physiological drivers of diurnal *iWUE* in Sorghum leaves, including sugar accumulation and responses of stomatal kinetics to light transients (**Chapter 3**).

3. Explore the extent of genetic control on *iWUE* and highlight the differential contribution of A_n and g_s to *iWUE* in Sorghum under well-watered and water stress conditions (**Chapter 4**).

1.14 OBJECTIVES & POTENTIAL OUTCOMES

This project focussed mainly on various genotypes of the C_4 crop *S.bicolor*. Sorghum is an ideal genetic and genomic model, whereby extensive genetic maps and enviable germplasm diversity exist domestically because Australia is one of the key Sorghum breeding centres in the world. Sorghum can also be genetically modified. Therefore, discoveries in Sorghum can be translated by genetic modification or marker-assisted breeding. In this project, measurements of *iWUE* were performed together with less commonly measured traits, including:

i. leaf structure, particularly stomata, vein and Kranz anatomical traits;
ii. diurnal patterns of leaf gas exchange and sugar accumulation;
iii. responses of stomatal kinetics to light transients;
iv. leaf water status, leaf hydraulics and plant morphology under well-watered and water-stressed conditions;
v. quantifying the genetic heritability and relationships of *iWUE* components.

1. **The specific objective of Chapter 2** was to investigate how growth temperature affects the relationship between *LW* and *iWUE*, and what anatomical features that mediate this relationship under the various growth temperatures.

2. **The specific objective of Chapter 3** was to investigate how *gs* diurnally regulates *iWUE*, and how this regulation is constrained by sugar accumulation, stomatal anatomy or stomatal responses to light transients.

3. **The specific objective of Chapter 4** was to partition components of *iWUE* (one controlled by A_n variation and the other by g_s variation) and to investigate possible trade-offs between *iWUE* and drought tolerance. The extent of genetic control on these traits was assessed in a large set of Sorghum genotypes with different Aquaporin alleles.

Expected outcomes

This project aims to discover alternative traits for breeding *Sorghum bicolor* with high *iWUE*. In particular, the project seeks to identify leaf anatomical traits with strong genetic basis and high heritability that directly influence *iWUE* in C_4 crops, or indirectly by influencing the dynamic responses of g_s and/or A_n. Ultimately, factors controlling variation in *iWUE* under various environmental factors and different temporal scales will be revealed. Another outcome is to elucidate whether Sorghum, as a C_4 crop known for its drought resistance, exhibits any trade-offs between drought tolerance and high *iWUE*, and what traits underpin this.

1.15 THESIS STRUCTURE

Research undertaken during my PhD project is presented herein as a series of three experimental chapters submitted or prepared for submission to peer-reviewed journals. The thesis is comprised of five chapters. Three chapters (2, 3 and 4) describe three separate experiments whilst Chapters 1 and 5 were prepared as a general Introduction and Discussion for the whole Thesis.

Chapters	Title
Chapter 1	General introduction
Chapter 2	Smaller stomata and cell size is associated with higher water use efficiency in Sorghum genotypes grown under different temperatures
Chapter 3	Diurnal regulation of water use efficiency is influenced by morning stomatal conductance and stomatal pore size, and is linked to efficient stomatal response to transient light
Chapter 4	The influence of water stress on the relative contribution of photosynthesis and stomatal conductance on intrinsic water use efficiency in a large selection of Sorghum genotypes differing in Aquaporin alleles
Chapter 5	General Discussion

Chapter 2

Smaller stomata and cell size is associated with higher water use efficiency in Sorghum genotypes grown under different temperatures

2.1 ABSTRACT

Intrinsic water use efficiency (*iWUE*) is an important trait that influences crop productivity. Building on our recent work that highlighted a strong correlation between *iWUE* and leaf width (*LW*), I aimed to identify leaf morphological traits that correlate with high *iWUE* in a key C_4 crop. Ten *Sorghum bicolor* genotypes with varying *LW* were grown under three temperatures and measured leaf gas exchange as well as leaf surface and internal anatomy. Stomatal conductance (g_s) and *LW* correlated negatively with *iWUE* across genotypes and growth temperatures. Smaller stomatal size (*SS*) and operational aperture (a_{op}) led to lower g_s in narrow leaves. Narrow leaves were characterised by higher vein density (*VD*), smaller epidermal, mesophyll and bundle sheath cell sizes, lower cross-sectional surface area of intercellular airspaces per interveinal distance (IAS_{si}) and were generally thinner. Increasing growth temperature increased assimilation rate, g_s, *LW*, maximum stomatal aperture (a_{max}) and IAS_{si}, and reduced *iWUE*. In conclusion, narrow leaves achieve higher *iWUE* in a key C_4 crop under warm temperatures due to smaller stomatal size and aperture which reduce water loss, and greater intercellular path length, cell size and vein density which ensure efficient hydraulic supply under evaporative conditions.

2.2 INTRODUCTION

Growing population requires increased agricultural production which is threatened by climate change (Rosenzweig and Parry, 1994; Ray *et al.*, 2013; Challinor *et al.*, 2014; Valin *et al.*, 2014; Rippke *et al.*, 2016). Given the majority of available freshwater is utilised for agriculture (Postel *et al.*, 1996), it is critical to breed new crop varieties that more efficiently use available water since this level of consumption is not sustainable (Condon *et al.*, 2004). Climate change is expected to alter rainfall and drought patterns and lead to increased air temperature, heat stress and evaporative demand (Alexander *et al.*, 2006). Leaf-level water use efficiency (*WUE*) is expressed as the ratio of net carbon assimilation rate (A_n) to transpiration rate (E). E is strongly dependent on vapour pressure deficit, which is determined by ambient temperature and humidity (Jones, 2013). Therefore, intrinsic *WUE* (*iWUE*), defined as the ratio of A_n to stomatal conductance (g_s), better reflects the genetic controls on leaf *WUE* (Chaves *et al.*, 2016).

Crops that utilise the C_4 photosynthetic pathway are vital to the global food supply (Leakey, 2009). C_4 plants dominate tropical and subtropical regions (Edwards *et al.*, 2010), where agricultural yield is particularly vulnerable due to climatic change (Challinor *et al.*, 2014), and where C_4 crops are key to the well-being of the population (Leakey, 2009). There has already been extensive selection for higher yields and carbon assimilation, and so it is uncertain how much more capacity remain for solely manipulating carbon gains in crops (Leakey *et al.*, 2019), especially in C_4 crops due to their carbon concentrating mechanism (CCM). However, by increasing *iWUE*, crops might be able to extend the availability of soil water, especially in crops that are dependent on rainfall such as *Sorghum bicolor* (Ghannoum, 2016; George-Jaeggli *et al.*, 2017) potentially extending water availability until grain filling, thereby limiting the impact of water stress later in the growth cycle (Jackson *et al.*, 2016). Consequently, selection for traits that improve *iWUE* is still highly desirable (Hall and Richards, 2013). However, breeding for physiologically complex processes like *iWUE* is difficult for a number of reasons including low heritability, environmental factors and the lack of genetic variability for whole plant *WUE* (Hammer *et al.*, 1997; Ghannoum, 2016). Hence, a better understanding of the physiological processes that underpin observed differences in *iWUE* is key to developing robust selection criteria (Hall and Richards, 2013). For breeding

purposes, traits underpinning high *iWUE* must be easy and inexpensive to measure and be highly heritable (Richards, 2006).

Recently, Cano *et al.* (2019) demonstrated that leaf width (*LW*) correlated negatively with *iWUE* in diverse C_4 grasses, mainly due to a positive association between *LW* and g_s. They hypothesized that wide leaves operate at higher g_s to offset the impact of the boundary layer (BL) on leaf temperature. The BL is a thick layer of still air that surrounds the leaf and imposes a diffusion resistance on water leaving (and CO_2 entering) the stomatal pores. The thickness of the BL scales with the leaf dimension exposed to the wind (Schuepp, 1993). Since convective heat loss in leaves occurs mainly via transpiration through the stomata (Gates, 1968), an increased BL thickness leads to leaves requiring bigger stomatal apertures to enable higher transpiration rates to cool (Jarvis and McNaughton, 1986; Leigh *et al.*, 2017).

High heritability in *LW* in Sorghum populations is established (Liang *et al.*, 1973, 1975). The trends between *LW*, g_s and *iWUE* found in Cano *et al.* (2019) among diverse C_4 grasses were replicated in research by Pan *et al.* (2021) within 48 Sorghum genotypes. Pan *et al.* (2021) also found that some stomatal and vein traits correlated with *LW* (and consequently *iWUE*). The current study builds on the findings of Cano *et al.* (2019) and Pan *et al.* (2021) by identifying the leaf surface and internal anatomical traits that change with *LW* among a selection of Sorghum genotypes grown under different temperatures.

The value of g_s on an area basis, under constant environmental conditions, is controlled by the numbers and dimensions of the stomatal complexes (Hetherington and Woodward, 2003; Franks and Beerling, 2009). Most angiosperms maximize g_s per surface area by increasing stomatal density (*SD*) and reducing stomatal size (*SS*) for two main reasons. Firstly, smaller stomata reduce the distance gas molecules traverse as they diffuse through the pore (Franks and Farquhar, 2007; Franks and Beerling, 2009). Secondly, smaller stomata increase surface area in contact with neighbouring cells, which facilitates the exchange of ions and osmolytes and enable fast stomatal kinetic responses (Dow *et al.*, 2014; Lawson and Blatt, 2014). Manipulating *SD* and/or *SS* influences *iWUE*, but the combined responses of *SS* and *SD* that lead to higher *iWUE* are species specific (Bertolino, Caine and Gray, 2019). For example, there is evidence that genetically reducing *SD* leads to higher *iWUE* without impacting yield in a number of graminoid C_3

crops (Hughes *et al.*, 2017; Caine *et al.*, 2019; Dunn *et al.*, 2019). The impact of reduced *SS* on *iWUE* seems more prominent under stress (Franks and Farquhar, 2001; Doheny-Adams *et al.*, 2012; Zhao *et al.*, 2015), but there are studies showing *SS* is genetically linked to *iWUE* in *Arabidopsis* ecotypes (Dittberner *et al.*, 2018). The requirement for larger leaves to have higher transpiration rates in order to maintain leaf temperature (Leigh *et al.*, 2017) means that there is likely an association between *LW* and stomatal anatomy.

Variation in stomatal anatomy is generally concurrent with changes in vein anatomy (Boyce *et al.*, 2009; Brodribb and Feild, 2010; Zhang *et al.*, 2012; Fiorin *et al.*, 2016). In C_4 grasses, stomatal development starts axially at the leaf base, with stomatal complexes (guard and subsidiary cells) being formed in specified cell files adjacent to veins (Rudall *et al.*, 2017; Hepworth *et al.*, 2018). Hence, changes in the vein density (*VD*) of longitudinal veins influences the distribution and density of stomata in different grasses (Ueno *et al.*, 2006; Way, 2012; Xiong *et al.*, 2017; Reeves *et al.*, 2018; Schuler *et al.*, 2018; Pathare *et al.*, 2020). In grasses, including C_4 species, there is a negative association between *LW* (and leaf size in general) and *VD* (Sage, 2001; McKown and Dengler, 2009; Smillie, Pyke and Murchie, 2012; Griffiths et al., 2013; Ruwanthi Nayananjalee et al., 2017). High *VD* in mutated rice plants correlated with narrow leaves (Feldman *et al.*, 2014). These plants had low interveinal distance (*IVD*), mesophyll : bundle sheath ratio (*M:BS*) and leaf thickness (*LT*), and hence end up with a higher Rubisco concentration, leading to higher A_n without affecting transpiration (Feldman *et al.*, 2017). In accessions of C_4 *Gynandropsis gynandra*, the opposite was observed, with increase in *VD*, *SD* and BS cell size (BSC_{area}) being negatively correlated with *iWUE* (Reeves *et al.*, 2018). Generally, *VD* is an important determinant of C_4 photosynthesis (Ogle, 2003; Mckown and Dengler, 2007) through its effects on the size and spacing of M and BS cells between cellular tissues (Mckown and Dengler, 2007; Rizal *et al.*, 2015). In C_4 grasses, photosynthetic tissues develop from the meristem around the vasculature (Dengler *et al.*, 1985, 1986, 1994; Langdale *et al.*, 1989; Dengler and Nelson, 1999). Hence, it is likely that the development of stomata, veins and C_4 Kranz anatomy are interlinked, and the combined effect can lead to variations in *iWUE*.

The enzymes of C_4 photosynthesis function optimally at warm temperatures (Sage, 2002, 2004), improving A_n. High temperatures also increase VPD and consequently evaporative demand. These responses exert opposite effects on *iWUE*. Moreover, the rates of cell

division and expansion increase with temperature in C_4 crops (Ben-Haj-Salah and Tardieu, 1995; Lafarge *et al.*, 1998), likely affecting leaf anatomy.

This study aims to investigate how variations in *LW* influence the leaf anatomy and gas exchange, ultimately determining *iWUE*. In the C_4 crop *Sorghum bicolor*, I hypothesized that: 1) an increase in growth temperature will increase *LW*, A_n and g_s, and reduce *iWUE*; 2) narrower leaves will have lower g_s and higher *iWUE*; 3) *SS* will be the main indicator of g_s and will correlate with *LW*; 4) wide leaves will have higher *IVD* and low *VD*; and 5) increase in *IVD* will increase the size of M, BS and intercellular airspace (IAS). To test these hypotheses, ten *Sorghum bicolor* genotypes that vary in *LW* were grown in the glasshouse under three different temperatures.

2.3 MATERIALS & METHODS

Plant material

Ten *Sorghum bicolor* (L.) Moench genotypes (**Table 2.1**) were selected from more than 500 accessions of the Sorghum conversion program (SCP) to address two criteria: low tillering and high variation in *LW*. The SCP is a backcross breeding scheme in which genomic regions conferring early maturity and dwarfing from an elite donor were introgressed into approximately 800 exotic Sorghum accessions representing the breadth of genetic diversity in Sorghum. The ten genotypes were selected to represent a wide range of *LW* (measured on the 10th leaf in order of appearance) during a field trail at Gatton, Queensland, Australia (-27.563593, 152.279396).

Plant culture

Seeds were germinated in trays of 3 cm depth filled with soil and kept under controlled conditions of 25 °C, 60% humidity, and constant darkness. Four days after germination plants were initially transplanted into 10 cm long pots and moved to a naturally lit glasshouse at 22°C. After one week, 3 homogeneous groups of plants of similar size were selected for growth at three air temperatures and were transplanted into 7.5 L cylindrical pots of 40 cm depth to allow the development of a deep root system. The soil substrate used throughout the experiment was a blend of soil, sand and organic material such as decomposed bark. The particle size promoted good drainage and aeration and avoided water pooling around plant roots. I added 18.5 g of fertilizer (Osmocote Plus Organic All Purpose) per. Fertilizer was mixed along pot height, leaving higher amounts in the lower half of pot, where roots will grow more densely by the end of experiment. Pots were randomly distributed within the glasshouse and rotated every week to minimize microclimate effect.

There were three temperature treatments in three adjacent rooms (8m long x 3m wide x 5m tall) in a naturally lit, controlled environment greenhouse (Plexiglas Alltop SDP 16; Evonik Performance Materials, Darmstadt, Germany) at the Hawkesbury Institute for the Environment, Western Sydney University, Richmond, New South Wales, Australia (-33.612032, 150.749098). The temperature treatments were designed to promote differences in leaf anatomy generated by the combination of temperature and vapour

pressure deficit (VPD) and cover the entire range of average summer temperatures experienced by sorghum crops in its different areas of production (Hammer *et al.*, 2016; Ciampitti *et al.*, 2019). The mean daily temperatures for the three treatments averaged 19..8°C for the low temperature (LT or cool), 25.6°C for medium temperature (MT or warm = LT + 6°C) and 30.3°C in the high temperature treatment (HT or hot = MT + 7°C), including mean daily temperatures during the light period of **22°C**, **28°C** and **35°C**, respectively. A typical diurnal range of ~11°C was maintained in all treatments by heating and cooling throughout the day-night cycle (Automated Logic WebCTRL Building Management System; Braemar Th320 Natural gas heater; Dunnair PHS25 Air Conditioner, using Vaisala HMP110 Humidity/Temperature probes and HMT130 Transmitters). Relative humidity was kept close to 60% in the three glasshouse chambers (Carel Humidisk 65 humidifier), leading to maximum VPD of 1.3, 1.8 and 2.7 kPa in LT, MT and HT, respectively. The photosynthetic photon flux density (PPFD) at canopy height (Apogee quantum sensor, USA) varied with prevailing weather conditions but was equivalent across rooms. Daytime maximum PPFD was often ~1500 µmol m^{-2} s^{-1}.

Leaf gas exchange

Leaf level gas exchange was measured using the LI-6400XT infra-red gas analyser, or IRGA (LiCor Biosciences, Lincoln, Nebraska) with the 2 cm^2 fluorescence chamber (64—40 leaf chamber fluorometer). The 12th, 13th or 14th fully expanded leaf (depending on genotype growth rate) was selected for measurement. Gas exchange measurements were done 40-50 days after emergence when plants were at the vegetative stage and before head formation. The flat area of the leaf lamina, i.e. where illumination is highest, was used for the LI-6400XT cuvette and two days after harvested for analysis of leaf anatomy and width. Conditions inside the LI-6400XT chamber were 400 ppm of CO_2; 2000 µmol m^{-2} s^{-1} of light intensity (10% blue light); and the block temperature was set to match the respective growth temperature. Measurements of net carbon assimilation rate (A_n) and stomatal conductance to water vapour (g_s) were obtained once gas exchange was stabilised within the cuvette. Intrinsic water use efficiency (*iWUE*) was calculated as the ratio $A_n : g_s$. Gas exchange was measured only during sunny days and between 10:00 and 13:00 h, local time.

Leaf anatomy and leaf mass per area

A 1 cm long section, spanning the width of the leaf, was cut at the middle of the leaf, the same position previously used for gas exchange. The leaf sections were fixed in a mixture of formaldehyde, acetic acid and 70% ethanol in 5: 5: 90 proportions respectively for 24h. Subsequently they were kept in 70% ethanol and in darkness at room temperature. This section was used for stomatal, vein and inner leaf trait measurements. Below this 1 cm section, 4 leaf discs (1 cm^2) were sampled and dried in a 70 °C oven for 48 hrs. The dried leaf material was weighed. Leaf mass (g) was divided by disc area (cm^2) to get leaf mass per area (*LMA*, g cm^{-2}).

Stomatal traits

For stomatal measurements, two small leaf sections between the 2nd and 3rd major veins were cut, one to each side of the midrib. Confocal microscopy (Leica TCS SP5, Leica Microsystems) was used to image the adaxial and abaxial surfaces off both sections, producing 4 images per leaf at x10 magnification. Images from the microscope were analysed using Image J (Schneider *et al.*, 2012). Stomata in between two minor longitudinal veins were identified to cover a significant portion of the image, and the rectangular area between them was calculated. The stomata in this area were counted. Stomatal density (*SD*) was calculated as the number of stomata per unit area. The mean *SD* of both sides is the data presented in the results as mm^{-2}. Within each area where *SD* was calculated, ten stomata were randomly selected to measure the following variables. Stomatal size (*SS*) was calculated by multiplying stomatal width (W_s, including two guard cells and two subsidiary cells) by guard cell length (L_s) and expressed in μm^2. Epidermal cell size (*ES*) was calculated by dividing the area of the epidermal layer (minus the stomata) by the number of epidermal cells in that area and expressed in μm^2. Maximum pore aperture (a_{max}) was calculated as:

$$a_{max} = W_{gc} \times L_a \qquad (2.1)$$

where W_{gc} = width of the guard cell complex of closed stomata and L_a = is the length of the pore; a_{max} is expressed in μm^2. This formulation was used because the shape of the fully open stomatal pore in grasses geometrically fits a rectangular shape (Franks and

Farquhar, 2007; Franks *et al.*, 2014). Further details of stomatal measurements are in **Fig.2.S1**. Theoretical maximum conductance (g_{smax}) was calculated as follows:

$$g_{smax} = \frac{d}{v}\left((SD \times a_{max})/(l + \frac{\pi}{2}\sqrt{\frac{a_{max}}{\pi}})\right) \qquad (2.2)$$

where d = diffusivity of water vapor in air; v = molar volume of air; l = stomatal pore depth which is assumed to be equivalent to W_{gc} / 2. The model assumes that the stomatal aperture is at its maximum and that all stomata are open. To correct for leaf and growth temperature and atmospheric pressure at the site of measurement, d and v were recalculated before being entered into equation (2.2). The equation for d was based on Marrero & Mason (1972):

$$l\,n(Pd) = ln(A) + sln(T) - \frac{S}{T} \qquad (2.3)$$

where A, s and S are empirical constants for the diffusion of water vapour in air with A = 0.00000187 (atm cm^2 s^{-1} (K)$^{-s}$); s = 2.072; S = 0 (K), T is the temperature in Kelvin degrees (K) and P is atmospheric pressure at our site (102610 Pa). Using equation 2.3 and the value for constants reported before, the units of d are in cm^2 s^{-1}, and to be used in equation 2.2, d needs to be transformed to m^2 s^{-1} by dividing by 10000. The calculation for v was based on the molar volume of an ideal gas:

$$v = \frac{RT}{P} \qquad (2.4)$$

where R is the ideal gas constant = 8.314462618 J mol^{-1} K^{-1}. Finally, the operational stomatal pore (a_{op}) that matches the corresponding measured g_s can be calculated using the following formula (Pan et al., 2021). Equation 2.2 can be modified to estimate a_{op}, with the terms rearranged and g_{smax} replaced with measured g_s, but keeping the same theoretical framework. Basically, a_{op} is the replacement term for a_{max}. The resulting equation is:

$$a_{op} = \frac{\left(g_s^2 v^2 \frac{\pi}{4} + 2dSDg_s vl\right) + \sqrt{g_s^4 v^4 \frac{\pi^2}{16} + g_s^3 v^3\, \pi dSDl}}{2d^2SD^2} \qquad (2.5)$$

The ratio of the operational stomatal pore area (a_{op}) to a_{max} is expressed as a percentage, % stomatal aperture *(% aperture*).

Vein traits

A 2-3 mm long section from the same 1 cm long section fixed earlier was cut and put through the clearing and staining protocol. This was achieved following the protocol of Berlyn and Myschke (1976) as laid out by Sack and Scoffoni (http://prometheuswiki.org/tiki-index.php?page=Quantifying+leaf+vein+traits). In brief, the leaf is immersed in 3% Sodium Hydroxide (NaOH) until cleared. The leaf is then rinsed with water and excess pigment removed with 4% Sodium hypochlorite (Bleach), then put through an ethanol series (20% → 100%), 5 minutes at each level. The leaf was stained with Safranin (1%) followed by fast green (1%) for 3-5 minutes at each pigment. A reverse ethanol series (100% → 20%) was then applied to the leaf, also for 5 minutes at each level, before being rinsed with water and mounted on microscope slides. Leaves were imaged under x10 magnification using a light microscope (Axio Scope.A1, Carl Zeiss Microscopy GmbH, Jena, Germany), and images were analysed using image J. Analysis was carried out on the area of the leaf between the 2nd and 3rd major veins, just above or below the area where stomatal traits were calculated. Vein density (*VD*) was calculated as vein length per area (mm mm^{-2}) including transverse veins; inter-veinal distance (*IVD*), was defined as the average distance between longitudinal veins, calculated by dividing distance between the veins at the edge of the image over the number of inter-veinal areas. The *IVD* was expressed in µm after dividing measurements by 1000. Further details of vein measurements are in **Fig.2.S2**.

Internal leaf anatomy traits

From the same 1 cm long leaf section that was fixed and preserved, a ≥1 mm transverse cross section of the leaf was hand cut using a razor blade. The cut leaf section spanned the leaf width. The section was cleared following the protocol mentioned earlier. The section was rinsed with water and mounted on a microscope slide. Leaves were imaged under x10 magnification in a light microscope (see above), and images were analysed using Image J. A region between the 2nd and 3rd major veins was selected for analysis, and up to 3 images were taken spanning that region. In each image, 2 separate regions were

identified, each spanning from the middle of the vascular bundle of one vein to the middle of the vascular bundle of the neighbouring vein, with the combination of these 2 regions comprising two full veins (half vein – vein – half vein; **Fig.2.S3** for full details). In each region, measurements of total cross-section area of mesophyll (M), bundle sheath (BS), intercellular airspace (IAS), vascular bundle (VB) and both epidermal layers were obtained. Interveinal distance (IVD_c) was calculated as the distance between two midveins. M cell length (MC_{length}) was the average of the vertical and horizontal mesophyll extension length. Leaf thickness (LT) measurements with and without the epidermis were carried out at different points of the region to adjust for changes in epidermis thickness and leaf topology. The thickness presented in the results is the mesophyll thickness, without the epidermis, and that is what LT refers to in this manuscript (this is mainly to avoid bulliform cells that interfere with LT measurements and secondly it is more related to path length.). The areas of single M (MC_{area}) and BS (BSC_{area}) cells were calculated by diving total M or BS area by the number of M or BS cells. The ratio of total M surface area to total BS surface area is *M:BS*. Finally, the proportion of M, BS, IAS and VB in each region was normalized by dividing the total area of each component by the IVD_c, to obtain the cross-sectional surface area of each anatomical component per IVD_c (i.e. per interveinal distance: M_{si}, BS_{si}, IAS_{si}, VB_{si}). Finally, the two regions in each image were average for all those variables, and the resulting values from the 3 images were averaged as well to get the mean per biological replicate (n=3).

Statistical Analysis

Figures and statistical analysis were conducted using R software (R Core Team (2020). R: A language and environment for statistical computing. R Foundation for Statistical Computing, Vienna, Austria. URL https://www.R-project.org/). Normality was checked by fitting a generalized linear model and inspecting residual plots. Analysis of variance was carried out via a linear mixed-effects model (packages lme4 and nlme). Variance within groups was performed using a *post hoc* Tukey test. Regression analysis was carried in R using linear modelling (lm). The model was formulated to predict the significance of a linear relationship between the two variables in the form of:

$$y = mx + c$$

where *y* (predicted) and *x* (predictor) are the y-axis and x-axis variables, respectively, *m* is the slope of the relationship, and *c* is the y-axis intercept. *m* represents the direction of the relationship (negative or positive). A Pearson product moment correlation analysis was performed to test statistical significance of relationships and obtain correlation coefficients. To streamline the dimensionality of the large number of variables, a Principal Component Analysis (PCA) was performed using the FactoMineR package (Le *et al.*, 2008) in R. PCA reduces data by geometrically projecting them onto lower dimensions called principal components (PCs), with the goal of finding the best summary of the data using a limited number of PCs (Lever *et al.*, 2017).

2.4 RESULTS

Temperature effects on leaf gas exchange and anatomy

Leaf gas exchange parameters varied significantly (p<0.001) with growth temperature. CO_2 assimilation rate (A_n) increased less than stomatal conductance (g_s) with each temperature (**Fig.2.1 a**, **b**), leading to a decrease in intrinsic water use efficiency (*iWUE*) (**Fig.2.1 c**). Leaf mass per area (*LMA*) also increased (p<0.001) with increasing temperature (**Fig.2.1 d**). Leaf width (*LW*) and total number of longitudinal veins (*TLV*) were significantly higher (p<0.05) at the hotter treatments (**Fig.2.1 e**, **f**). Vein density (*VD*) was highest (p<0.05) and the interveinal distance (*IVD*) was lowest at the warm (28°C) treatment (**Fig.2.1 g**, **h**). Epidermal cell size (*ES*), stomatal density (*SD*) and stomatal size (*SS*) did not vary significantly with growth temperature (**Fig.2.1 i**, **j** and **k,** respectively), but maximum pore aperture (a_{max}) increased (p<0.05) between the cool (22°C) and hot (35°C) treatments (**Fig.2.1 l**). Leaf mesophyll thickness (*LT*) differed significantly (p<0.05) between the warm and hot treatments only (**Fig.2.1 m**), while cross-sectional surface area of intercellular airspaces per *IVD* (IAS_{si}) was higher (p<0.05) at the hotter treatment (**Fig.2.1 n**). Finally, mesophyll to bundle sheath surface area ratio (*M:BS*) increased (p<0.05) between cool and hot treatments (**Fig.2.1 o**). The interactions of Temperature and *LW* were tested in **Table 2.4**, to highlight the significant impact of *LW* on those variables that overrides temperature effects. These interactions are pivotal for the correlation analysis results (see also **Table 2.S3**).

Relationship between *LW* and gas exchange

There was a positive relationship (r=0.92, p<0.001) between A_n and g_s across temperatures (**Fig.2.2 a; Table 2.S3**). Overall, there was a negative association between A_n and *iWUE* (r=-0.65, p<0.001; **Fig.2.2 b**). However, this relationship disappeared within each temperature(**Table 2.S3**), indicating the overall relationship was mainly a result of the strong increase of A_n with temperature. In contrast, there was a strong (r=-0.88, p<0.001), consistent negative relationship between g_s and *iWUE* (**Fig.2.2 c**). This was reflected in a strong (r=0.87, p<0.001) positive correlation between *LW* and g_s, and a negative one (r=-0.87, p<0.001) between *LW* and *iWUE* (**Fig.2.3 b**, **c**) (**Table 2.S3)**. These results suggest that g_s was the main determinant of *iWUE* among the Sorghum genotypes.

Anatomical determinants of g_s

There was no relationship between *SD* and g_s (**Fig.2.4 a; Table 2.S3**). In contrast, there were positive associations between g_s and *SS* (r=0.57, p<0.05; **Fig.2.4 b and Table 2.S3**), a_{max} (r=0.64, p<0.001; **Fig.2.4 c**), the operational stomatal pore area (a_{op}) (r=0.81, p<0.001; **Fig.2.4 e**), and the percentage of a_{op} to a_{max} (*% aperture*) (r=0.64, p<0.001; **Fig.2.4 f**). Theoretical maximum conductance (g_{smax}) was positively (r=0.49, p<0.05) correlated with g_s, but this correlation was very weak within each temperature (**Fig.2.4 c**). There was a negative relationship between *SD* and *SS* (r=-0.41, p<0.05; **Fig.2.4 g**), and between SD and ES (r=-0.63, p<0.005; **Fig.2.4 h**). Cell and aperture size related features (*SS*, *ES*, a_{max}, a_{op} etc..) all showed positive correlations with *LW* (**Table 2.S1**), indicating that wider leaves achieved higher g_s due larger and more open stomatal pores. This was especially true at the two higher temperature treatments (**Table 2.S3**).

Variation of vein anatomy with *LW*

No clear (p>0.1) relationships were found between vein anatomical variables and *LW* at the 22°C treatment (**Fig.2.5 a**, **c; Table 2.S3**). However, among the warm and hot treatments, *LW* was negatively correlated (r=-0.57, p<0.05) with *VD* and positively with *IVD* (r=0.45, p<0.07) (**Fig.2.5 a**, **c; Table 2.S3**). A positive relationship (r=0.57, p<0.05) was also found between *VD* and *SD* across all three temperatures (**Fig.2.5 d**), but it was significant at the 22°C and 35°C temperatures only (**Table 2.S3**)

Variation of leaf anatomy with *IVD* and *LW*

A positive relationship between *LT* and *LW* (r=0.5, p<0.05), and *LT* and *IVD* (r=0.55, p<0.05) was observed (**Fig.2.6 a**, **b**). Cross-sectional mesophyll surface area per *IVD* (M_{si}) did not vary with *LW* at any temperature(p>0.1; **Fig.2.6 c; Table.2.S4**), but cross-sectional bundle sheath surface area per *IVD* (BS_{si}) and IAS_{si} were positively correlated with *LW* especially at higher temperatures (r=0.51 and r=0.59, p<0.05; **Fig.2.6 e**, **g; Table.2.S3**). Furthermore, *IVD* was positively correlated with mesophyll cell length (MC_{length}), mesophyll cell area (MC_{area}) and bundle sheath cell area (BSC_{area}) (r=0.59, r=0.47 and r=0.69 respectively, p<0.05; **Fig.2.6 d**, **f** and **h** respectively).

Impact of *LW* and temperature

Generally, *LW* was more determinant of variation in anatomical characters than temperature after conducting an ANCOVA (**Table 2.4**). Larger genotypic variation in *LW* at the higher temperature (35°C) (Tables **2.1**, **2.2** and **2.3**) likely resulted in the significant correlations observed in the 35°C treatment between parameters (**Table 2.S3**). This is discussed further below.

2.5 DISCUSSION

During crop breeding, it is desirable to select for traits that are easily phenotyped, heritable and with simple underlying genetics (Hall and Richards, 2013). Water use efficiency (*WUE*) is underpinned by complex physiological processes, which has hindered the development of simple selection traits for higher *WUE*. Stable carbon isotope composition has been successfully utilised as a proxy for breeding high *WUE* in C_3 crops (Rebetzke *et al.*, 2002); however the application of this tool to C_4 crops has yielded limited success so far (Henderson *et al.*, 1998; Ellsworth and Cousins, 2016; Feldman *et al.*, 2018; Ellsworth *et al.*, 2020) for complex reasons (von Caemmerer *et al.*, 2014). Recent reports (Cano *et al.*, 2019; Pan et al., 2021) negatively linked leaf width (*LW*), a heritable trait in Sorghum (Liang *et al.*, 1973), and intrinsic *WUE* (*iWUE*) in diverse C_4 grasses. The current study exploited the genetic differences in *LW* among genotypes from a diversity panel to identify traits associated with high *iWUE* under different growth temperatures.

Wider leaves have larger stomata which increases stomatal conductance and reduces *iWUE*

The positive relationship between *LW* and stomatal conductance (g_s) reported here (**Fig.2.3 b**) is in line with previous findings (Baldocchi *et al.*, 1985; Cano *et al.*, 2019; Pan et al., 2021). Wider leaves are characterised by an enlarged stomatal complex (*SS*) and functional aperture (a_{op}) especially at higher temperatures (**Table 2.S3**). Hence, increased g_s was mediated by larger aperture size, rather than stomatal density (*SD*). This is consistent with a recent study using various C_4 grasses (Israel, 2020), where *SS* and a_{op} negatively correlated with *iWUE*. Producing and operating more stomata has a high energetic cost (Franks and Beerling, 2009). But when CO_2 supply is not limiting for photosynthesis, as is the case in C_4 species, leaves select for lower *SD* (Taylor *et al.*, 2012)—in contrast, C_3 plants take on the energetic cost because they need the higher conductance rate to maintain high C_i levels. The operational limits on stomata are set during leaf development (Franks and Casson, 2014). In C_4 grasses, signalling from the veins limit production of stomata to specific cell files in the leaf epidermis, such that most stomata are arranged in files next to the veins (Raissig *et al.*, 2017; Way, 2012; McKown and Bergmann, 2018). Furthermore, leaves maintain a coordination between liquid (veins) and vapour (stomata) phases of hydraulic transport (Brodribb *et al.*, 2017), such

that *SD* and vein density (*VD*) scale together, as reported here (**Fig.2.5 d**). Wider leaves had greater interveinal distances (*IVD*) at the warm (28°C) and hot (35°C) temperatures (**Fig.2.5 c**; **Table 2.S3**), leading to the negative relationship between *IVD* and *SD*: *i.e.*, wider leaves had more widely spaced veins and stomatal files (**Table 2.S1**). Hence the stomata of wide leaves compensated by having larger *SS* and a_{op} (**Table 2.S1**) which increases the diffusive area across the pore to sustain the higher transpiration demand, especially at warmer temperatures (Assouline *et al.*, 2010). A positive link between *IVD* and *SS* was also found in Maize, another C_4 crop (Miranda *et al.*, 1981). Brodribb, Jordan and Carpenter (2013) reported that expansion of epidermal cells pushes stomata apart, reducing *SD* and increasing *SS*, as confirmed here (**Fig.2.4 h** and **Table 2.S1**). In our study, the relationship between *SD* and *LW* was not significant; however, the relationship tended to be negative, particularly if only warm and hot treatments were considered. Further, the study of Pan *et al.* (2021) reported a weak negative relationship between *LW* and *SD* among a greater number of sorghum lines.

Increasing *IVD* in wider leaves enlarges cells and airspaces

Wide leaves in Sorghum had more longitudinal veins (**Table 2.S1**), as reported in Rice (Schuler *et al.* 2018). Similar to our study (**Fig 2.6**), Schuler *et al.* (2018) found that increasing *LW* leads to bigger bundle sheath cells (BSC_{area}), *IVD*, and leaf thickness (*LT*). Their findings however were not all statistically significant, and they did not find any change in *VD* with *LW*. In Sorghum, a negative association was observed between *VD* and *LW* at the warm and hot temperatures (**Fig.2.5 a**; **Table 2.S3**). Development of major (1^{st} order) veins increases with *LW* (Dengler *et al.*, 1985), increasing the *IVD* between major veins. This increases the space that can be filled with minor veins, but fewer minor veins may develop by full leaf expansion, especially with the high energetic cost of producing lignin (Sage, 2004), presumably reducing total *VD*. In this study, measurement of *VD* depended mostly on minor and transverse veins, with available evidence suggesting changes in *VD* in C_4 plants occurs mainly through changes in minor and transverse veins (Ueno *et al.*, 2006). A trend towards reduced minor *VD* with leaf expansion has been observed in tropical *Ochnaceae* species (Schneider *et al.*, 2017). In contrast, reduced leaf expansion has been shown to increase *VD* in C_4 *Flaveria* (McKown and Dengler, 2009). Higher *VD* improves hydraulic supply of leaves (Sack and Frole, 2006), and married with reduced *LT* (**Table 2.S1, 2.S3**), which reduces the path length from veins to sites of

evaporation, hydraulic resistance is reduced as water moves slowly in living cells (Sack and Holbrook, 2006; Fiorin *et al.*, 2016). Hence, movement of water from vascular bundles to sites of evaporation occurs faster in narrower leaves, which can cool themselves more efficiently via latent cooling, allowing them to have better thermal, and ultimately stomatal, control. Interestingly, there was a positive relationship between *LW*, *SS* and cross-sectional vascular bundle surface area per *IVD* (VB_{si}) (**Table 2.S1, 2.S3**). Size of vasculature and *LW* has been shown to correlate in Sugarcane and Maize, two NADP-ME crops (Colbert and Evert, 1982; Russell and Evert, 1985). Similarly, in a survey of almost 500 globally distributed species, Sack *et al.* (2012) found vein diameter and leaf size correlated positively with each other and negatively with *VD*. This indicates that the coordination between veins and stomata (liquid and vapour phase transport) can occur by varying cell size and expansion as opposed to cell differentiation, as modification of cell size provides a rapid way for plants to adapt to growth conditions (Brodribb *et al.*, 2013, 2017). In a number of angiosperm lineages, leaf expansion and with it differential cell expansion, especially of epidermal cells, lead to 'dilution' of *SD* and *VD* (Carins Murphy *et al.*, 2012, 2016; Brodribb *et al.*, 2013, 2017; Zhang *et al.*, 2018).

Wider leaves had more intercellular airspaces, IAS, at the higher growth temperatures (**Fig.2.6 g, Table 2.S3**). In C_4 grasses, M and BS cells develop after vein formation (Dengler *et al.*, 1986; McKown and Dengler, 2009). Hence, leaf expansion leads to the expansion of M and BS cells, as well as IAS, to fill the space between the more distant veins (i.e., higher *IVD*) in wider leaves (**Fig.2. 6 d**, **f** and **h**). This is a similar process to that linking *IVD*, *SD* and *SS* outlined above that is regulated by epidermal cell expansion (Brodribb *et al.*, 2013, 2017; Carins Murphy *et al.*, 2016). In C_4 *Flaveria* spp., BS size is controlled by cell expansion (Mckown and Dengler, 2007), which might explain the positive relationship between cross-sectional BS surface area per *IVD* (BS_{si}) with *IVD* and *LW* (**Fig.2. 6** and **Table 2.S1**). The size of M tissue increases due to increased cell expansion and *VD* in C_4 *Flaveria* (Mckown and Dengler, 2007), which may explain the lack of relationship between cross-sectional M surface area per *IVD* (M_{si}) and *LW*; however M cell size (MC_{area}) was still positively correlated with *IVD*. Previous studies have also found that *LT* can influence M and BS size positively, with thinner—and in our case, narrower (**Fig.2.6 a**)—leaves thought to have better control on carbon and water fluxes between cells (Schneider *et al.*, 2017) and to have a lower rate of CO_2 leakiness (Dengler *et al.*,

1994). Lower *IVD* can also mean that CO_2 escaping from one BS cell can be captured by a neighbouring BS cell, possibly contributing to the higher *iWUE* of narrow leaves. Rizal *et al.* (2015) analysed two Sorghum mutants with lower *VD* compared to parental lines and found that reduced *VD* is associated with thicker leaves, bigger MC_{area} and BSC_{area}, and shorter plants, confirming most of our findings here.

C_4 Leaf anatomy and water use efficiency

To link leaf anatomy and *iWUE*, it is important to understand how anatomical traits influence transpirational fluxes and stomatal behaviour. In our study, greater *SS* is associated with increased IAS area, M and BS cell sizes and *LT*, while *SD* shows the opposite association (**Table 2.S1**). Firstly, there is evidence in *Arabidopsis* that manipulating the stomatal patterning on the leaf epidermis affects M development and IAS area (Masle *et al.*, 2005; Dow *et al.*, 2017). Water in the liquid phase moves through the M and BS, before evaporating in the IAS and the substomatal cavity. Greater cell expansion, and hence cell size, increases the liquid phase path length, which is more thermally conductive than the vapour phase (Rockwell *et al.*, 2014), likely leading to an increase in leaf temperature and requiring larger stomatal aperture for efficient evaporative cooling. Furthermore, increasing IAS and cell size encourages vapour phase conductance through latent heat transfer as the water evaporates from the mesophyll (Buckley *et al.*, 2017), as rate of diffusion is quicker in vapour than liquid phase (Miranda *et al.*, 1981; Parkhurst, 1994) and there is more surface area contact between IAS and M due to bigger M and IAS areas. Since stomata open in response to increased vapour pressure in the sub-epidermal layer (Lange *et al.*, 1971; Shope *et al.*, 2008), the increase in evaporation from M due to higher thermal conductance will increase vapour pressure in the IAS and cause the stomata to open (Pieruschka *et al.*, 2010). This fits with our observations because: 1) plants in our experiment were well watered, hence wide leaves are able to conduct water to supply the evaporation rate; and 2) our results show that increased sizes of M, BS and IAS correlate with higher *SS* and lower *SD,* similar to a trend found in some temperate deciduous trees (Aasamaa *et al.*, 2001). However, only cross-sectional IAS surface area per *IVD* (IAS_{si}) had a strong correlation with g_s. Buckley *et al.* (2017) highlighted that IAS and/or increased exposure of M cells to IAS is more important than cell size in driving inner leaf evaporation. The relationship between increased MC_{area}, *LT* and IAS_{si} has been observed in *Arabidopsis* (Lehmeier *et al.*, 2017) and Wheat

(Lundgren *et al.*, 2019). The latter study found that increased presence of functional stomata came with more sub-stomatal airspaces, higher g_s and hence, lower *iWUE*. The one-cell-spacing rule of stomatal distribution requires each stomatal complex to be accompanied by large sub-stomatal airspaces to allow for vapour phase gaseous diffusion (Harrison *et al.*, 2020), which might explain the positive relationship between IAS_{si}, *SS* and g_s.

Effect of growth temperature and vapour pressure deficit on leaf physiology and anatomy

Net CO_2 assimilation rate (A_n), g_s, and *LW* increased with each growth temperature. The Pearson correlation analyses showed no significant relationships between anatomical parameters and A_n (**Table 2.S1**), and the relationship of A_n and *LW* disappears within temperature treatments. Hence, the overall relationship of A_n and *LW* was likely caused by the impact of temperature on enzyme kinetics of C_4 photosynthesis (**Fig.2.1 a**). C_4 grasses generally dominate grasslands of low latitudes and altitudes, and thrive at higher temperatures (Edwards *et al.*, 2010). The optimum temperature for A_n in Sorghum is close to 38°C (Sonawane *et al.*, 2017), with PEP carboxylase, the enzyme that initially fixes CO_2 in the mesophyll, thought to function best above 30°C (Chaves *et al.*, 2016). Increased g_s with temperature is attributed to the increase in evaporative demand due to evaporative cooling and the increase in VPD at higher temperatures. In Maize, increasing temperatures increase the rate of leaf and cell expansion (Ben-Haj-Salah and Tardieu, 1995; Reymond *et al.*, 2003), and leaf elongation in Maize (Tardieu *et al.*, 2000) and Sorghum (Lafarge *et al.*, 1998). Leaf extension and appearance rates in some C_4 plants are highest around 35°C (Virmani and Sivakumar, 1984; Kim *et al.*, 2007). This can explain the significant increase in *LW* with increasing temperature (**Fig.2.1 f**). However, there was no significant trend observed for most of the anatomical traits measured, whether stomatal, vein or inner layer. Cell division rate also increases with temperature (Granier and Tardieu, 1998); hence, combined small increments in cell size and/or number in response to warmer temperature might cause any effect of temperature to be less noticeable. Ultimately, I found that the response of anatomical variables to growth temperature was genotype specific (**Table 2.2**; **Table 2.3**). This is similar to what Stamp *et al.* (1985) found in Maize genotypes grown under four different temperature treatments. An examination of the literature reveals no conclusive patterns about the

response of leaf anatomical features to temperature. Temperature caused a decrease in *SD* (Kemp and Cunningham, 1981; Reddy *et al.*, 1998; Luomala *et al.*, 2005), an increase in *SD* (Ferris *et al.*, 1996), or had no effect (Apple *et al.*, 2000; Djanaguiraman *et al.*, 2011; Sadras *et al.*, 2012). Similarly, some studies showed guard cell length and *SS* decreased with temperature (Ferris *et al.*, 1996; Djanaguiraman *et al.*, 2011), but Sadras *et al.* (2012) found that rising growth temperatures stimulated g_s via increasing *SS* and operating stomatal aperture (a_{op}). While in our study *SS* did not change with temperature, the hotter temperature treatments had a significantly greater maximum aperture (a_{max}) (**Fig.2.1 l**) and a_{op} (**Table 2.2**). Generally, cool climates promote thicker leaves (Luomala *et al.*, 2005), but in our study *LT* correlated positively with *LW*, and *LW* increased at hotter temperatures. Response of *LT* to temperature seems mainly species specific (Kemp and Cunningham, 1981; Ferris *et al.*, 1996; Aasamaa *et al.*, 2005; Luomala *et al.*, 2005; Djanaguiraman *et al.*, 2011; Zhou *et al.*, 2011). Thicker leaves would have also contributed to higher g_s because thicker leaves (with bigger cells and IAS) have a higher *LMA* and require a higher transpiration rate to cool off to maintain metabolism. To summarise, the response of leaf morphology to growth temperature was mostly evident through increased *LW* and its consequences leaf and stomatal traits, as discussed for the genotypic variations in *LW* (**Fig.2.4**, **Fig.2.5** and **Fig.2.6**). Ultimately, faster development at high temperature means that leaves of similar insertion reach different sizes under different temperatures when sampled at the same time as we have done here. Thus, larger variation in *LW* under 35°C explains why most anatomical correlations were more significant at that temperature, and why *LW* had a bigger impact than temperature.

Increasing growth temperature also alters vapour pressure deficit (VPD) (**Fig.2.S10**). I investigated the impact of changing VPD on g_s and stomatal anatomy in more detail in chapter 5. High VPD, especially in the 35°C treatment, means that g_s needs to be minimized as under those conditions evaporative demand is high, but A_n has already reached a maximum, partly due to the increase in g_s but also because of above-discussed impact of high temperature on C_4 enzymes. Leaf-level VPD (VPD_L) was plotted against *SS* and *LW*, and it clearly shows (**Fig.5.3**) that the control of *SS* on g_s is most significant at VPD of more than 2 kPA. This is a key piece of information, as it potentially shows the combined effect of VPD and temperature and means that high temperatures do not

necessarily lead to excess water loss through g_s. This is discussed in more detail in Chapter 5 where the results of different chapters contribute to the conclusions.

Conclusion

In the C_4 crop Sorghum, narrow leaves had lower g_s and higher *iWUE* relative to wider leaves, whether *LW* differed due to genotypes or growth temperature. Changes in *LW* did not alter A_n within each treatment, presenting the opportunity to select for lower g_s to improve *iWUE* in Sorghum. Our study elucidated how narrow leaves achieve lower *gs* and higher *iWUE* in Sorghum at warm temperatures, due to smaller stomatal size and aperture to reduce water loss, and shorter intercellular path length and greater vein density to ensure efficient hydraulic supply under evaporative conditions. Narrower leaves may also allow more light penetration through the canopy, increasing light capture and carbon assimilation by the plant (Cano *et al.*, 2019). It remains to be determined how additional stress (such as water limitation) might affect the response of *iWUE* in narrow leaves, and whether these anatomical arrangements are beneficial then and in the field.

Table 2.1. Mean (±SE) of leaf gas exchange, leaf mass per area and leaf width parameters for each Sorghum genotype at the corresponding temperature treatment. The table shows the results of the post hoc Tukey's test for analysis of variance between genotypes per treatments and between treatments in the last column. Mean values that share similar symbols (none, a or b) have no significant difference ($p<0.05$) between them (n=3).

Unique Genotype ID		FF_SC842-14E	FF_SC449-14E	LR9198	FF_SC1201-6-3	FF_SC56-14E	QL12	R931945-2-2	SC1079-11Ebk	FF_SC906-14E	FF_SC500-9	**Treatment Mean**
A_n (µmol m^{-2} s^{-1})	22°C	38.9 (1.7)	39.0 (0.9)	32.3 (1.7)	38.5 (3.3)	32.9 (1.7)	40.8 (0 6)	37.8 (1.2)	36.7 (0.2)	39.7 (2 9)	32.6 (1.9)	36.9 (0.9)
	28°C	38.3 (0.7)a	47.0 (0.3)bc	41.9 (2 2)ac	48.9 (0.3)c	43.1 (1.4)ac	48.7 (1 2)c	43.3 (1.9)ac	41.1 (0.9)ab	43.8 (0.4)ac	42.6 (2.0)ac	43.9 (1.0)a
	35°C	45.8 (0.9)ab	50.2 (1.1)bc	43.9 (1 9)a	51.9 (0.6)c	51.2 (0.9)bc	50.5 (0 2)bc	49.1 (0.6)ac	45.9 (0.5)ab	44.2 (0 9)a	48.3 (1.8)ac	48.1 (0.9)b
g_s (mol m^{-2} s^{-1})	22°C	0 24 (0)ab	0.23 (0.01)ab	0.19 (0 01)a	0 27 (0.03)ab	0.2 (0.02)a	0.26 (0 01)ab	0 24 (0.01)ab	0.24 (0.01)ab	0.28 (0 02)b	0 20 (0.01)a	0.24 (0.01)
	28°C	0 25 (0.01)a	0.31 (0)ac	0.29 (0 03)ac	0 35 (0.01)c	0.31 (0.01)ac	0.31 (0 01)ac	0 31 (0.01)ac	0.31 (0.01)ac	0.33 (0 01)bc	0 27 (0.01)ab	0.31 (0.01)a
	35°C	0 32 (0.01)a	0.34 (0.01)ab	0.33 (0 01)a	0.43 (0.04)b	0.39 (0.01)ab	0.35 (0)ab	0 39 (0.02)ab	0.37 (0.01)ab	0.34 (0 01)a	0 35 (0.02)ab	0.36 (0.01)b
iWUE (µmol CO_2 mol^{-1} H_2O)	22°C	163 8 (5 3)	166.9 (1.9)	169.0 (6.8)	146 6 (6.7)	167.4 (9.8)	159.6 (3.0)	154 9 (2 3)	150.9 (3.8)	139.7 (2.2)	162 6 (11.2)	158.2 (2.9)
	28°C	150 8 (2.1)	150.2 (1.0)	143.9 (15.9)	139 9 (2 9)	137.3 (1.8)	159.9 (2.5)	140 9 (5.4)	132.4 (4.1)	131.1 (3.0)	158.1 (1 5)	144.5 (3.0)a
	35°C	142.7 (3 5)	147.0 (5.7)	135.0 (5.0)	125 3 (13.5)	128.3 (3.4)	145.9 (1.1)	124.1 (4 9)	124.3 (1.8)	131.1 (3.6)	136 8 (1 6)	134.1 (2.7)b
Leaf mass per area (g m^{-2})	22°C	20.6 (0.5)a	18.6 (2.2)	23.2 (0 8)	22.4 (0.6)	20.9 (0.5)	25.0 (0.1)	20.8 (2.1)	22.3 (0.9)	23.2 (1.4)a	22.7 (0.9)	21.9 (0.5)
	28°C	22.1 (0.7)ab	29.7 (0.1)e	21.5 (0 5)a	27.1 (0.8)de	22.5 (1.1)ac	26.9 (0.7)de	25.8 (0.7)bce	24.5 (0.3)acd	26.5 (1 2)ce	24.5 (1.00acd	25.1 (0.8)a
	35°C	23.6 (0.2)a	26.9 (0.7)ab	23.7 (1 2)a	31.4 (0.8)c	26.9 (1.1)ab	30.3 (0)bc	31.3 (0.4)c	29.7 (1.2)bc	27.9 (0 6)bc	31.4 (0.3)c	28.3 (0.9)b
Leaf Width (cm)	22°C	2.4 (0 2)a	2.9 (0.4)ab	2.7 (0.3)a	4 6 (0 2)c	2.8 (0.3)a	3.4 (0.1)ac	3.4 (0.4)ac	4.4 (0.3)bc	4.7 (0.3)c	2 6 (0.3)a	3.4 (0.3)
	28°C	3.4 (0 03)a	5.5 (0.2)bd	5.2 (0.4)bc	6 6 (0.1)d	5.5 (0.2)bd	4.5 (0.3)ab	5.4 (0 2)bd	5.7 (0.4)bd	6.2 (0.2)cd	4 8 (0.2)b	5.3 (0.3)a
	35°C	3 2 (0.1)a	5.2 (0.2)b	5.0 (0.2)b	8.1 (0.1)e	6.2 (0.2)c	5.2 (0.02)b	6 5 (0.1)c	7.3 (0.2)de	6.6 (0.3)cd	6.4 (0.1)c	5.9 (0.4)b

A_n: carbon assimilation rate; *g_s*: stomatal conductance; *iWUE*: Intrinsic water use efficiency.

Table 2.2. Mean (±SE) of leaf stomatal and vein parameters for each Sorghum genotype at the corresponding temperature treatment. The table shows the results of the post hoc Tukey's test for analysis of variance between genotypes per treatments and between treatments in the last column. Mean values that share similar symbols (none, a or b) have no significant difference ($p<0.05$) between them (n=3). Epidermal cell size was measured on seven selected genotypes as this measurement occurred later in the analysis period where time was of constraint.

Unique Genotype ID		FF_SC842-14E	FF_SC449-14E	LR9198	FF_SC1201-6-3	FF_SC56-14E	QL12	R931945-2-2	SC1079-11Ebk	FF_SC906-14E	FF_SC500-9	**Treatment Mean**
SD (mm^{-2})	22°C	184.1 (9 2)abc	189.7 (9.9)ad	149.2 (7.3)a	220 2 (6 9)cd	234.4 (11.5)d	197 5 (10.5)bd	198.2 (6.1)bd	151.2 (1.6)a	169.0 (8.9)ab	172.8 (5.2)ab	186.7 (8.3)
	28°C	192 9 (9 2)	199.7 (15.2)	157.4 (6.6)	183 8 (3 2)	209.7 (20.9)	208 9 (35.4)	189.9 (20.7)	174.1 (24.7)	164.9 (7.5)	189.9 (17.9)	187 (5.3)
	35°C	191.1 (15.3)ac	228 3 (5.1)c	161.1 (6.2)ab	144 3 (2 6)a	196 6 (17.7)ac	209 8 (8.7)bc	185.8 (8.9)ac	145.6 (12.3)a	190.0 (12.1)ac	233.7 (4.4)c	188.6 (9.3)
SS (μm^2)	22°C	741 6 (61)ab	724 3 (33)a	1213 (18)d	1004 (27)cd	1051 (49)cd	888 3 (56)ac	959.0 (15)bc	1012 (57)cd	978.1 (14)c	1045 (48)cd	961.6 (43.9)
	28°C	723.7 (16)a	1077 (107)b	1049 (24)b	996 9 (23)ab	959 5 (20)ab	900.7 (54)ab	1009 (9.4)b	991.1 (83)ab	1111 (56)b	983.4 (19)ab	980 (32.4)
	35°C	695 (23)a	969 (37)bc	1002 (51)bc	1052 (7.6)bc	1057 (45)bc	957 (19)bc	1147 (46)cd	1265 (23)d	1041 (52)bc	922 (33)b	1010.7 (44 8)
a_{max} (μm^2)	22°C	142 9 (3.1)a	144.1 (12.6)a	214.9 (4.4)a	215.7 (5.1)	215 6 (1 6)	163 9 (15)	190.2 (4.2)	188.7 (3.6)	184.8 (1.3)	228.7 (15)	188.9 (9.2)a
	28°C	179 2 (6 5)b	211.1 (18)b	198.6 (9.5)ab	222.7 (4.1)	214.4 (4 2)	173 2 (12)	195.4 (9.2)	206.3 (14)	202.9 (9.3)	200.1 (4.6)	200.4 (4.6)ab
	35°C	155 6 (8.7)ab	195 9 (5.3)ab	181.1 (7.6)b	212.4 (3 6)	224 5 (17)	181 8 (0.9)	228.6 (13)a	245.6 (1.9)a	205.8 (6.3)	197.6 (3.5)	202.9 (7.9)b
Epidermal cell size (μm^2)	22°C	2830 (665 3)	2275.8 (191.4)	-	2130.4 (84.5)	-	2113 (24 5)	1912 (22 3)	3003.4 (253)	2446.3 (61 2)	-	2387.3 (139.9)
	28°C	2497.9 (31.9)ab	2593.8 (341)ab	-	2385.8 (236)ab	-	2255.2 (237.7)ab	1831.6 (123.1)a	2806.4 (364.8)av	3283.5 (64.7)b	-	2522 (158.6)
	35°C	1848.1 (86.3)a	2175.2 (214.7)ab	-	2623.6 (39.2)ab	-	2366.3 (106 2)ab	2384.2 (149.5)ab	2945.8 (262)b	2742.8 (82.1)ab	-	2440.8 (128.6)
Operational aperture (μm^2)	22°C	12.5 (0 2)ab	12.7 (0.7)ab	15.7 (1.1)ab	14.9 (2.4)ab	10.4 (1 9)a	14.7 (1 3)ab	14.7 (0 2)ab	18 2 (0 5)ab	19.7 (2 3)b	14 8 (1.7)ab	14 8 (0 8)
	28°C	14.7 (1 5)	19 5 (2 0)	24.4 (4 6)	24.5 (0.6)	19.2 (1 9)	17 8 (2 8)	20 5 (1 8)	23.7 (4.1)	24 5 (0.7)	17 6 (1.0)	20 6 (1 0)a
	35°C	19 (1 6)a	17 8 (0 6)a	25 3 (2 3)ab	42.2 (5.8)c	26.9 (2 9)ab	18.7 (1 2)a	27 8 (3 3)ab	35 3 (3 0)bc	20 9 (1 8)a	18 2 (1.2)a	25 2 (2 5)a
% stomatal aperture	22°C	8.7 (0.2)ac	8.9 (0.3)ac	7.3 (0.5)ac	7.0 (1.2)ac	4.8 (0.9)a	9.2 (1.3)bc	7.7 (0.3)ac	9.7 (0.1)bc	10 6 (1 3)c	6.4 (0.4)ab	8.03 (0 5)a
	28°C	8.2 (0.9)	9.2 (0.2)	12.1 (1.7)	11.0 (0.2)	9.0 (0.9)	10.1 (1 3)	10 5 (1 0)	11 2 (1 3)	12.1 (0 3)	8.8 (0 5)	10 2 (0.4)ab
	35°C	12.1 (0 5)	9.1 (0.4)	13 9 (0.7)	19.8 (2.4)a	11.9 (0.4)	10 3 (0.7)	12 0 (0 8)	14.4 (1.1)	10.1 (0.7)	9.2 (0 5)	12 3 (0 9)b
Interveinal Distance (µm)	22°C	127.1 (2 8)ab	116.7 (2.7)a	127.2 (2.8)ab	117.4 (9.7)ab	124.1 (5.4)ab	133 9 (8.3)ab	127.3 (3.9)ab	134.0 (4.6)ab	149.9 (6.6)b	134.2 (9.7)ab	129.2 (2.3)a
	28°C	131 2 (1 3)	119.4 (3.1)	120.1 (6.3)	110 8 (8 8)	102.7 (0.1)	120 6 (7.8)	114.1 (3.2)	119.4 (5.8)	126.8 (10.2)	124.2 (3.7)	119 (2.5)b
	35°C	116 6 (4 6)ab	109 5 (5.7)a	114.4 (2.9)a	127 8 (5 9)ab	123.7 (4.4)ab	120.4 (6.9)ab	144.9 (5.9)b	129.1 (7.7)ab	124.5 (4.5)ab	124.9 (3.8)ab	123.6 (2.9)ab
VD ($mm\ mm^{-2}$)	22°C	10.5 (0.1)	11.1 (0 3)	10 8 (0.1)	11.8 (0.7)	11.5 (0.4)	11 3 (0 5)	11 2 (0 3)	10.4 (0 2)	9.8 (0.4)	10 2 (0.5)	10 9 (0 2)a
	28°C	10.5 (0 3)	11 6 (0 2)	11 3 (0 6)	11.7 (0.7)	12.7 (0 02)	11.7 (0 5)	11 6 (0 2)	11.1 (0 5)	11 3 (0 6)a	11 6 (0.3)	11 5 (0 2)b
	35°C	11.5 (0.4)ab	12 5 (0.4)b	11 8 (0.1)ab	10.6 (0.60)ab	11.1 (0.4)ab	11 9 (0 6)ab	10.1 (0 3)a	10 9 (0 3)ab	11 5 (0.4)ab	11 6 (0.3)ab	11 3 (0 2)ab
Total Number of Longitudinal Veins	22°C	156.4 (1 8)a	195 8 (25.8)ab	423.3 (16.6)e	423.7 (9 3)e	369 5 (13.9)de	319 8 (24.1)cd	326 (11.5)cd	291.6 (15.3)cd	254.9 (28.7)bc	334.2 (0)ce	309.5 (26.5)
	28°C	247.1 (21.5)a	419 5 (27.9)b	432.6 (33)b	416 8 (16.4)b	375 3 (8 8)ab	364 8 (14.6)ab	311.1 (6.6)ab	419 (42.6)b	422.7 (0)b	393.4 (0)ab	380.2 (17.8)a
	35°C	230 3 (3.7)a	428 8 (17.2)bcd	478.9 (16.5)cd	-	433.7 (4 6)bcd	357 5 (7.5)ac	437.7 (20.6)bcd	503.3 (36.1)d	449.1 (29.1)cd	304.8 (3.3)ab	402.7 (27.7)a
g_{smax} ($mol\ m^{-2}\ s^{-1}$)	22°C	1.6 (0.1)a	1.6 (0.04)a	1.5 (0.1)a	2.2 (0.1)bc	2.4 (0.1)c	1.7 (0.1)a	1.9 (0.1)ab	1.5 (0.02)a	1.6 (0.1)a	1.8 (0 02)a	1.8 (0.1)
	28°C	1.8 (0.1)	2.0 (0.1)	1.6 (0.04)	1.9 (0.1)	2.2 (0.2)	1.9 (0.3)	1.9 (0.2)	1.8 (0.2)	1.7 (0.1)	1.9 (0 2)	1.9 (1.0)
	35°C	1.7 (0.1)abc	2.3 (0.04)d	1.5 (0.03)a	1.5 (0.02)a	2.1 (0.1)d	2.1 (0.1)cd	2.1 (0.03)bd	1.7 (0.1)ab	2.0 (0.1)bd	2.3 (0 04)d	1.9 (0.1)

SD : Stomatal Density; *SS* : Stomatal Size; a_{max} : maximum stomatal aperture; g_{smax} : theoritical anatomical conductance; *VD* : Vein density.

Table 2.3. Mean (±SE) of measured inner leaf anatomical parameters for each Sorghum genotype at the corresponding temperature treatment. The table shows the results of the post hoc Tukey's test for analysis of variance between genotypes per treatments and between treatments in the last column. Mean values that share similar symbols (none, a or b) have no significant difference ($p<0.05$) between them (n=3)

Unique Genotype ID		FF_SC842-14E	FF_SC449-14E	LR9198	FF_SC1201-6-3	FF_SC56-14E	QL12	R931945-2-2	SC1079-11Ebk	FF_SC906-14E	FF_SC500-9	**Treatment Mean**
LT (µm)	22°C	100.4 (2.0)ab	97.1 (2.6)a	122.0 (8.6)bc	110 6 (0)ac	97.3 (8.4)ab	97.5 (5.7)abd	118.8 (5.5)ac	129.1 (5.5)c	131.6 (1 2)c	131.1 (4.1)dc	113.6 (4.4)ab
	28°C	91.3 (2.5)abc	126.4 (4.3)cd	118.1 (5.5)ad	94.9 (1.2)abc	82.3 (7.9)a	118.1 (0.7)ad	88 9 (6.8)ab	118 9 (9.1)bd	132.5 (6 8)d	103 9 (7.3)ad	107.5 (5 2)a
	35°C	91.3 (0)a	107 0 (3.3)a	-	115 9 (0.3)a	124.4 (7.9)a	112 9 (4.1)a	136.4 (2.5)ab	160.7 (3.6)b	127.3 (4 3)a	108 2 (8.5)a	120.5 (8 3)b
M / BS ratio	22°C	2.5 (0.2)ab	2.9 (0.3)b	2.5 (0.1)ab	2.5 (0.1)ab	1.9 (0.1)a	1.9 (0.2)a	2.2 (0.2)ab	2.4 (0.1)ab	2.1 (0)a	2.1 (0.1)ab	2.3 (0.1)
	28°C	3.1 (0.1)d	3.5 (0.1)d	2.9 (0.1)cd	2.2 (0.2)ac	1.7 (0.2)ab	2.3 (0.1)bc	1.6 (0.1)a	2.2 (0.1)ac	2.1 (0.1)ab	2.1 (0.1)ac	2.4 (0.2)
	35°C	2.9 (0)ab	3.5 (0.1)b	-	2.9 (0.7)ab	2.5 (0.1)ab	2.5 (0.1)ab	2.3 (0.1)a	2.3 (0.1)a	2.4 (0.1)a	1.8 (0.1)a	2.6 (0.2)
M_{si} ($\mu m^2\ \mu m^{-1}$)	22°C	53.5 (2.2)bc	55.2 (2.9)ac	61.8 (3.2)c	55.4 (1.3)bc	43.2 (4.4)ab	38.0 (0.6)b	52 9 (3.1)bc	61.7 (3.4)c	58.4 (0.4)c	53.4 (0.4)bc	53.4 (2.3)
	28°C	50.4 (0.8)bc	74.5 (0.3)d	61.4 (4.5)cd	45.8 (0.5)ac	32.8 (4.3)a	52.8 (1.7)bc	36.7 (5.2)ab	54.4 (4.6)c	55 9 (0.5)cd	42.1 (0.9)ac	50.7 (3.7)
	35°C	53.1 (0)ab	64.9 (2.9)b	-	50.8 (7.0)ab	52.7 (0.8)ab	50.9 (2.7)ab	59.7 (0.9)b	67.2 (1.2)b	55 6 (2.1)ab	38.8 (3.9)a	54 9 (2.7)
BS_{si} ($\mu m^2\ \mu m^{-1}$)	22°C	21.7 (1.1)ab	19.2 (1.3)a	24.8 (0.7)ac	22.1 (0.5)ac	21.7 (1.8)ab	20.2 (1.7)ab	24.4 (2.2)ac	26.5 (0.2)bc	28.4 (0.7)c	25.3 (0.8)ac	23.4 (0.9)
	28°C	16.5 (0.4)a	21.5 (0 6)ac	21.4 (1.0)ac	21.5 (1.1)ab	19.0 (0.5)ab	22.8 (0.1)bc	22 8 (1.2)bc	24.4 (1.1)abc	26 9 (1.2)c	20.2 (1.7)ab	21.7 (0.9)
	35°C	18.6 (0)ab	18.8 (0.4)b	-	18.9 (1.0)b	21.7 (1.2)ab	20.7 (0.6)ab	25 8 (0.9)ac	29.9 (1.0)c	23.4 (0.7)ab	22.1 (1.3)ab	22 2 (1.2)
VB_{si} ($\mu m^2\ \mu m^{-1}$)	22°C	4.7 (0.4)ab	4.3 (0.6)a	7.2 (0.3)b	5.5 (0.7)ab	5.7 (0.6)ab	5.3 (0.3)ab	6.9 (0.7)b	5.4 (0.4)ab	5.9 (0.6)ab	6.1 (0.6)ab	5.7 (0.3)
	28°C	4.7 (0.5)	6.8 (0.3)b	6.8 (1.0)	4.6 (0.2)	4.9 (0.5)	5.5 (0.2)	5.7 (0.5)a	5.1 (0.7)	5.8 (0.3)	6.3 (0.4)	5.6 (0.3)
	35°C	3.9 (0)	5.4 (0.3)	-	4.9 (0.1)	6.3 (0.6)	4.7 (0.4)	7.6 (0.5)	7.4 (0.3)	6.0 (0.4)	7.8 (1.4)	6.0 (0.4)
IAS_{si} ($\mu m^2\ \mu m^{-1}$)	22°C	17.3 (0.6)ab	13.8 (0.4)a	27.3 (8.3)ac	23.9 (0.7)ac	24.1 (1.2)ac	31.3 (4.2)bc	26 8 (1.0)ac	29.1 (1.7)ac	31.4 (0.4)bc	42.6 (4.8)c	26 8 (2.4)
	28°C	14.9 (1.0)a	16.8 (2.5)a	26.5 (0.7)ab	19.1 (0.5)a	23.9 (4.5)ab	34.8 (3.5)ab	21 9 (1.7)ab	30.7 (2.9)ab	40.4 (7.9)b	29.1 (4.5)ab	25 8 (2.4)
	35°C	11.9 (0)a	17.8 (1.4)a	-	33.6 (2.9)ab	39.1 (7.8)ab	31.9 (1.4)ab	34.4 (2.0)ab	51.5 (2.6)b	38.1 (1.9)ab	35.3 (2.7)ab	32 6 (3.7)a
M cell length (µm)	22°C	21.8 (0.8)ab	21.7 (0.8)ab	20.8 (1.6)ab	20.7 (1.2)ab	17.4 (1.6)a	17.6 (0.1)a	21 6 (0.4)ab	24.2 (1.6)b	24.4 (0.4)b	21.2 (0.6)ab	21.1 (0.7)
	28°C	19.5 (0.7)bcd	23.9 (0.8)d	21 (0.4)bcd	17.4 (0.3)ac	13.6 (1.1)a	20.8 (0)bcd	16 2 (1.2)ab	20.9 (1.8)bcd	21.4 (0.7)cd	18.4 (0.2)ad	19 3 (0.9)a
	35°C	19.4 (0)ab	21.0 (0.7)ab	-	19.6 (0.9)ab	20.3 (0.4)ab	20.7 (0.6)ab	25.1 (0.5)cd	26.3 (0.8)d	22.1 (0.5)bc	17.3 (0.7)a	21 3 (0.9)
M cell area (μm^2)	22°C	330.2 (9.3)ab	283.1 (16.4)ab	323.3 (19.3)ab	334 6 (26 9)ab	208.9 (41.4)a	195.1 (4.3)a	257.4 (14.8)ab	380.7 (37 0)b	347.8 (6.7)b	311 6 (24 5)ab	297.3 (18.1)
	28°C	262.9 (1.7)bc	339 6 (26 2)b	364.6 (0)b	229 8 (8.2)ab	146.7 (20)a	279 3 (5.8)bc	169.1 (30)ac	294 5 (38 2)bc	318.5 (14.9)b	231 6 (13.4)ab	262.8 (17.9)
	35°C	241.7 (0)ab	280 9 (12.1)ab	-	290 2 (45.4)ab	267.9 (12.8)ab	268 6 (13 3)ab	335.9 (3.5)bc	413 6 (3.5)c	310.2 (12.9)ac	215 5 (23 5)a	291.6 (18.2)
BS cell area (μm^2)	22°C	365.5 (36.1)ab	301 9 (38.1)a	377.3 (13.2)ab	346.7 (17.7)ab	284.7 (42.8)a	312 6 (28 6)a	375.3 (50.6)ab	485 2 (20 5)bc	603.1 (12.3)c	428.4 (10 2)ab	388.1 (28.9)
	28°C	248.6 (10.7)a	338.7 (21.1)ab	313.8 (35.5)a	321 2 (20 0)a	225.9 (6.5)a	380 8 (5.2)ab	299.9 (23.9)a	382 2 (50 8)ab	492.3 (32.2)b	361.1 (50.4)ab	336.5 (22.6)
	35°C	294.5 (0)ac	265 3 (6.8)a	-	291 9 (4.6)ab	312.6 (28.6)ab	307.7 (2.3)ab	444.8 (17.3)cd	530 3 (20 9)d	398.8 (22.4)bc	383 3 (33 0)ac	358.8 (27.5)
Interveinal Distance (µm)	22°C	135.4 (5.4)ab	126.4 (6.7)a	132.4 (6.7)a	139 3 (4.1)ab	116.2 (6.5)a	126.1 (0.6)a	129.6 (8.3)a	141 (6.4)ab	157.9 (1.7)b	137 6 (2.7)ab	134.2 (3.4)a
	28°C	125.2 (3.2)ab	128 5 (11 3)ab	132 (8 5)ab	123 8 (3.1)ab	102.5 (2.6)a	131 3 (1.9)ab	116.2 (4.5)ab	117 2 (10.7)ab	142.5 (3.7)b	143 3 (6.9)b	126.2 (3.7)b
	35°C	123.8 (0)ab	114 8 (2.6)a	-	135 9 (3.5)ab	127.4 (8.1)ab	116 9 (3.7)a	145.6 (2.1)b	143 8 (2.7)b	136.2 (2 9)ab	138 8 (4.1)ab	131.5 (3 5)
Hydraulic Distance (µm)	22°C	90.15 (1.42)ab	87.7 (1.92)a	100.82 (3.7)ab	91.65 (0.26)ab	87.41 (1.13)a	86.26 (3.65)ac	100.51 (1.59)ab	107 3 (0.88)b	106.22 (0.51)bc	105 98 (1 92)ab	96.4 (2.72)
	28°C	85.24 (0.55)a	102 89 (1.78)ab	95.39 (1.32)ab	84.11 (0.7)a	77.77 (2.93)a	96.59 (2.42)ab	80 63 (2.56)a	99.94 (0.65)ab	115.75 (2.92)b	86.2 (2.26)a	92 5 (3.73)
	35°C	85.26 (0)a	91.83 (0.39)a	-	104 23 (6.16)ab	102.15 (3.78)a	94.78 (1.54)a	112.56 (0.94)ab	127 54 (0 23)b	107.46 (1.64)ab	95.99 (2.45)a	102.4 (3 98)a

M: Mesophyll; *BS*: Bundle Sheath; *LT*: Leaf Mesophyll Thickness; M_{si}: Mesophyll surface area per interveinal distance; BS_{si}: Bundle sheath surface area per interveinal distance; VB_{si}: Vascular bundle surface area per interveinal distance; IAS_{si}: Intercellular airspace surface area per interveinal distance

Table 2.4. Statistical output from a full-factorial mixed effects ANCOVA with leaf width as the covariate. Ths table also presents all the parameters measured with their abbreviations.

Variables	df	Temperature	Leaf Width	Temperature * Leaf Width
Net carbon assimilation rate (A_n)	1,2	<0 0001	0 015	0.6728
Stomatal conductance (g_s)	1,2	<0 0001	<0 0001	0.6951
Intrinsic water use efficiency (*iWUE*)	1,2	<0 0001	<0 0001	0.8761
Leaf mass per area (*LMA*)	1,2	<0 0001	<0 0001	0 965
Leaf wid h (*LW*)	1,2	<0 0001	-	-
Stomatal density (*SD*)	1,2	0.9722	0.0556	0.6106
Stomatal size (*SS*)	1,2	0.3408	<0 0001	0.1193
Calculated maximum stomatal pore aperture (a_{max})	1,2	0.0791	<0 0001	0.1753
Epidermal cell area (*ES*)	1,2	0.7261	0.0557	0 335
Operational stomatal aperture (a_{op})	1,2	<0 0001	<0 0001	0.1067
% stomatal aperture (*% aperture*)	1,2	<0 0001	0.0013	0.6903
Theoritical maximum stomatal conductance (g_{smax})	1,2	0.2315	0.8749	0.8904
Interveinal distance measured from leaf lateral sections (*IVD*)	1,2	0.0227	0.0725	0.1963
Vein density (*VD*)	1,2	0.0407	0.1175	0 216
Total number of longitudinal veins (*TLV*)	1,2	<0 0001	<0 0001	0.3525
Leaf mesophyll thickness (*LT*)	1,2	0.0045	0.0002	0.4272
Mesophyll to bundle sheath ratio (*MBS*)	1,2	0.3882	0.0163	0.6215
Mesophyll surface area per IVD_c (M_{si})	1,2	0.1531	0.4433	0.9278
Bundle sheath surface area per IVD_c (BS_{si})	1,2	0.1526	<0 0001	0.8784
Vascular bundle surface area per IVD_c (VB_{si})	1,2	0.1361	0.0309	0.4685
Intercellular airspace surface area per IVD_c (IAS_{si})	1,2	0.0023	0.0001	0.1924
Average mesophyll cell length, vertical or horizontal (MC_{length})	1,2	0.0083	0.1298	0.3755
Mesophyll cell area (MC_{area})	1,2	0.0569	0.0366	0.3584
Bundle sheath cell area (BSC_{area})	1,2	0.0817	0.0001	0.4755
Interveinal distance measured from leaf cross-sections (IVD_c)	1,2	0.0458	0.0016	0.0312
Hydraulic Distance ($Dist_H$)	1,2	0.0027	0.0001	0.2735

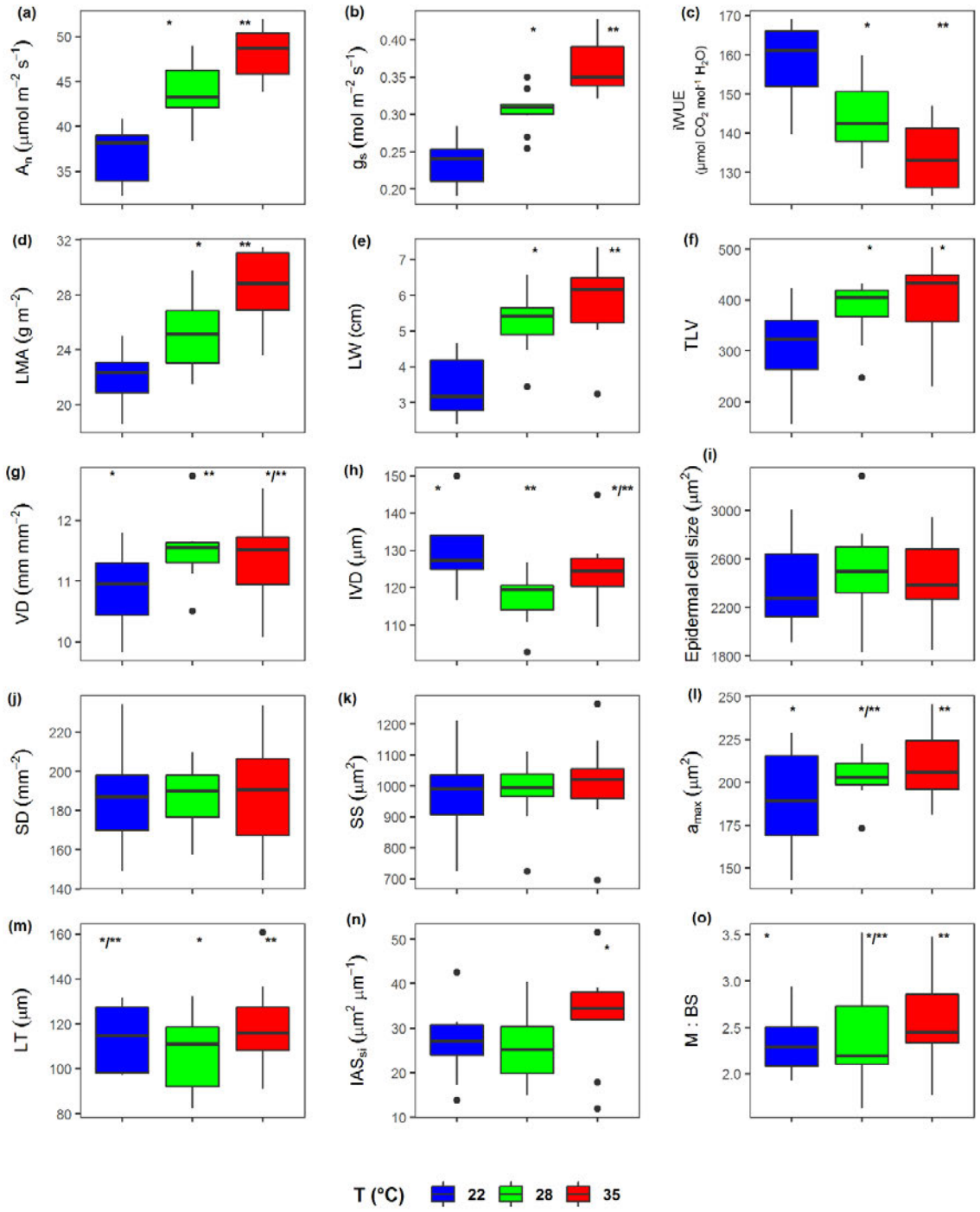

Fig.2.1 The distribution of trait values among the three separate temperature treatments. The distribution is summarized by boxplots for each treatment. The values in each boxplot compromise all measurements per replicate (n=3) across the ten genotypes, yielding *n=30* for most of the individual boxplots shown. Each box encompasses the 25th and 75th percentiles, with whiskers extending to show the extreme values of the measured variable. Statistically significant difference is represented at the top of each boxplot, with boxplots that share the same symbol (none, * or **) having no difference between them. Different treatment growth temperatures are represented by the different fill colour of the boxplot: blue=22°C, green=28°C, red=35°C. **(a)** Net carbon assimilation rate (*A_n*); **(b)** Stomatal conductance (*g_s*); **(c)** Intrinsic water use efficiency (*iWUE*); **(d)** Leaf mass per area (*LMA*); **(e)** Leaf width (*LW*); **(f)** Total number of longitudinal veins (*TLV*); **(g)** Vein density (*VD*); **(h)** Interveinal distance (*IVD*); **(i)** Epidermal cell size; **(j)** Stomatal density (*SD*); **(k)** Stomatal size (*SS*); **(l)** maximum stomatal pore aperture (*a_{max}*); **(m)** Leaf mesophyll thickness (*LT*); **(n)** Cross-sectional intercellular airspace surface area per *IVD* (*IAS_{si}*); **(o)** Mesophyll to bundle sheath ratio (*M : BS*).

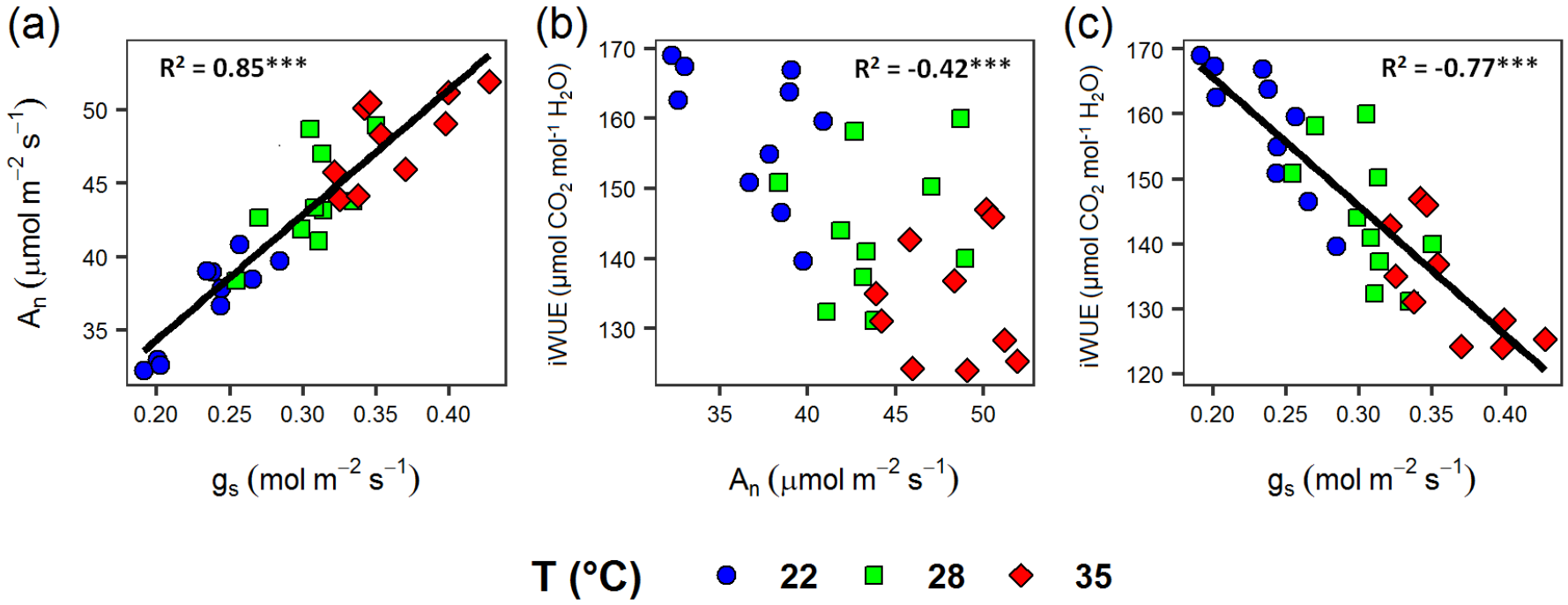

Fig.2.2 The relationship between the key gas exchange parameters. Data was collected on the youngest fully expanded leaf and measured at corresponding growth temperature and saturating light levels. Each point in the scatter plot represents the mean value of the variable per genotype, per treatment (n=3). Standard error bars were removed to ensure clearer presentation (Table 2.1). The black line represents the line of best fit for the data, with the corresponding R^2 value represented that is deduced from a Pearson product-moment correlation analysis (Table 2.S1). Different treatment growth temperatures are represented by the different fill colour of the scatter points: blue=22°C, green=28°C, red=35°C. Degrees of statistical significance are represented as: $p<0.001$ (***), $p<0.05$ (**), $p<0.1$ (*). (a) Net carbon assimilation rate (A_n) vs. stomatal conductance (g_s); **(b)** Intrinsic water use efficiency ($iWUE$) vs. net carbon assimilation rate (A_n); **(c)** Intrinsic water use efficiency ($iWUE$) vs. stomatal conductance (g_s).

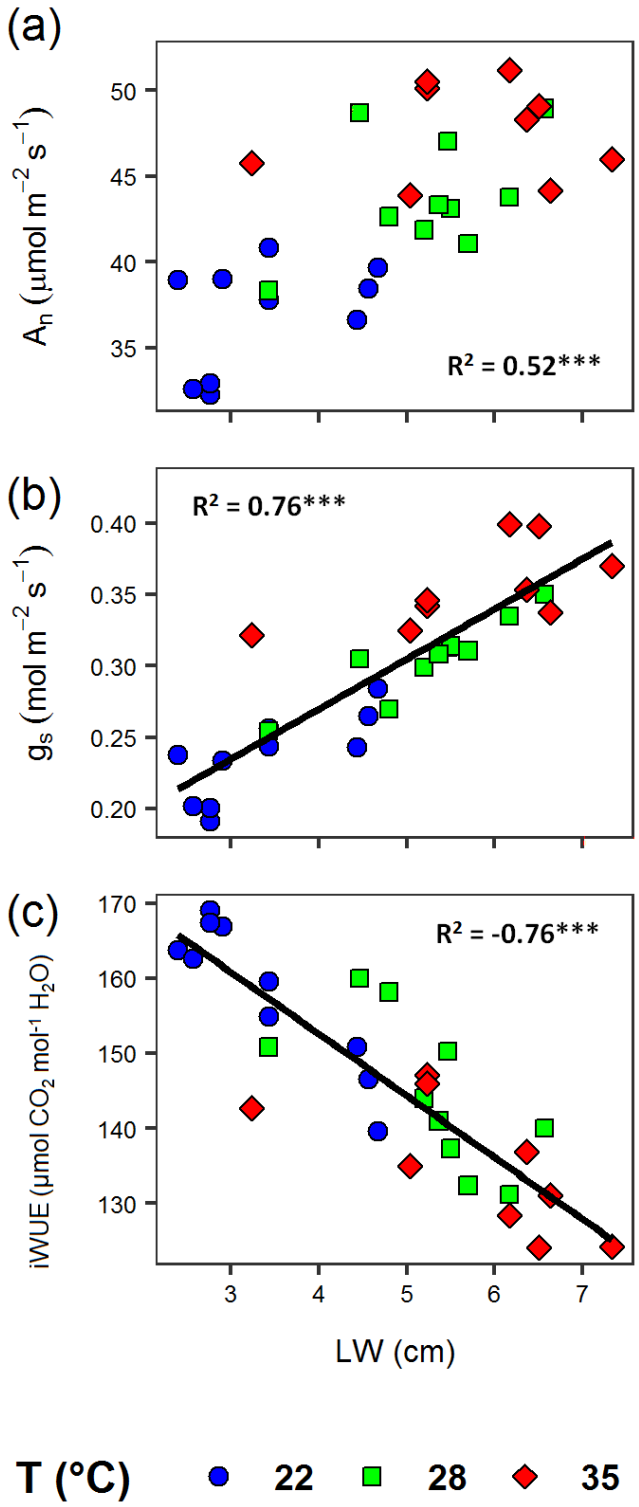

Fig.2.3 The relationship between gas exchange parameters and leaf width. Gas exchange data was collected on the youngest fully expanded leaf and measured at corresponding growth temperature and saturating light levels. The same leaf was measured at its midpoint laterally to obtain leaf width measurements. Each point in the scatter plot represents the mean value of the variable per genotype, per treatment (n=3). Standard error bars were removed to ensure clearer presentation (Table 2.1). The black line represents the line of best fit for the data, with the corresponding R^2 value represented that is deduced from a Pearson product-moment correlation analysis (Table 2.S1). Different treatment growth temperatures are represented by the different fill colour of the scatter points: blue=22°C, green=28°C, red=35°C. Degrees of statistical significance are represented as: p<0.001 (***), p<0.05 (**), p<0.1 (*). (a) Net carbon assimilation rate (A_n) vs. leaf width (LW); **(b)** stomatal conductance (g_s) vs. leaf width (LW); **(c)** Intrinsic water use efficiency ($iWUE$) vs. leaf width (LW).

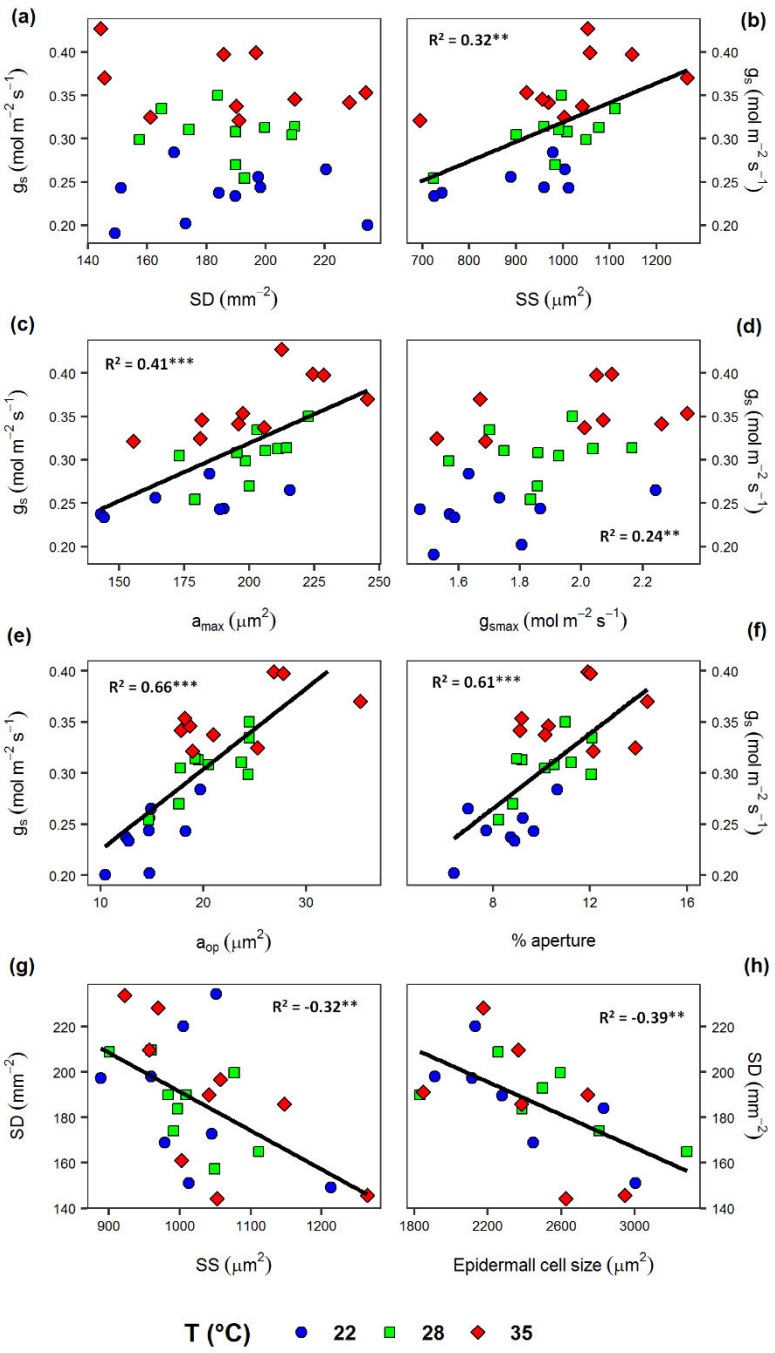

Fig.2.4 The relationship between stomatal conductance and stomatal anatomical traits. Stomatal conductance was measured on the youngest fully expanded leaf and measured at corresponding growth temperature and saturating light levels. The same leaf was then sampled, and the area at between 2nd and 3rd major veins from the midrib halfway up the leaf was analysed for stomatal traits. Each point in the scatter plot represents the mean value of the variable per genotype, per treatment (n=3). Standard error bars were removed to ensure clearer presentation (Table 2.1 for stomatal conductance; Table 2.2 for stomatal anatomical traits). The black line represents the line of best fit for the data, with the corresponding R^2 value represented that is deduced from a Pearson product-moment correlation analysis (Table 2.S1). Different treatment growth temperatures are represented by the different fill colour of the scatter points: blue=22°C, green=28°C, red=35°C. Degrees of statistical significance are represented as: p<0.001 (***), p<0.05 (**), p<0.1 (*). Measurements conducted on genotypes LR9198, FF_SSC56-14E, and FF_SC500-9 at 22°C were considered influential outliers for plots **(b)** and **(d)**. Stomatal conductance (g_s) vs. (a) Stomatal density (*SD*), **(b)** Stomatal size (*SS*),), **(c)** Calculated maximum pore aperture (a_{max}), **(d)** Calculated theoretical maximum conductance (g_{smax}), **(e)** Operational pore aperture (a_{op}), **(f)** Percentage ratio of a_{op} to a_{max} *(% aperture*); **(g)** Stomatal density (*SD*) vs. Stomatal size (*SS*); **(h)** Stomatal density (*SD*) vs. Epidermal cell size.

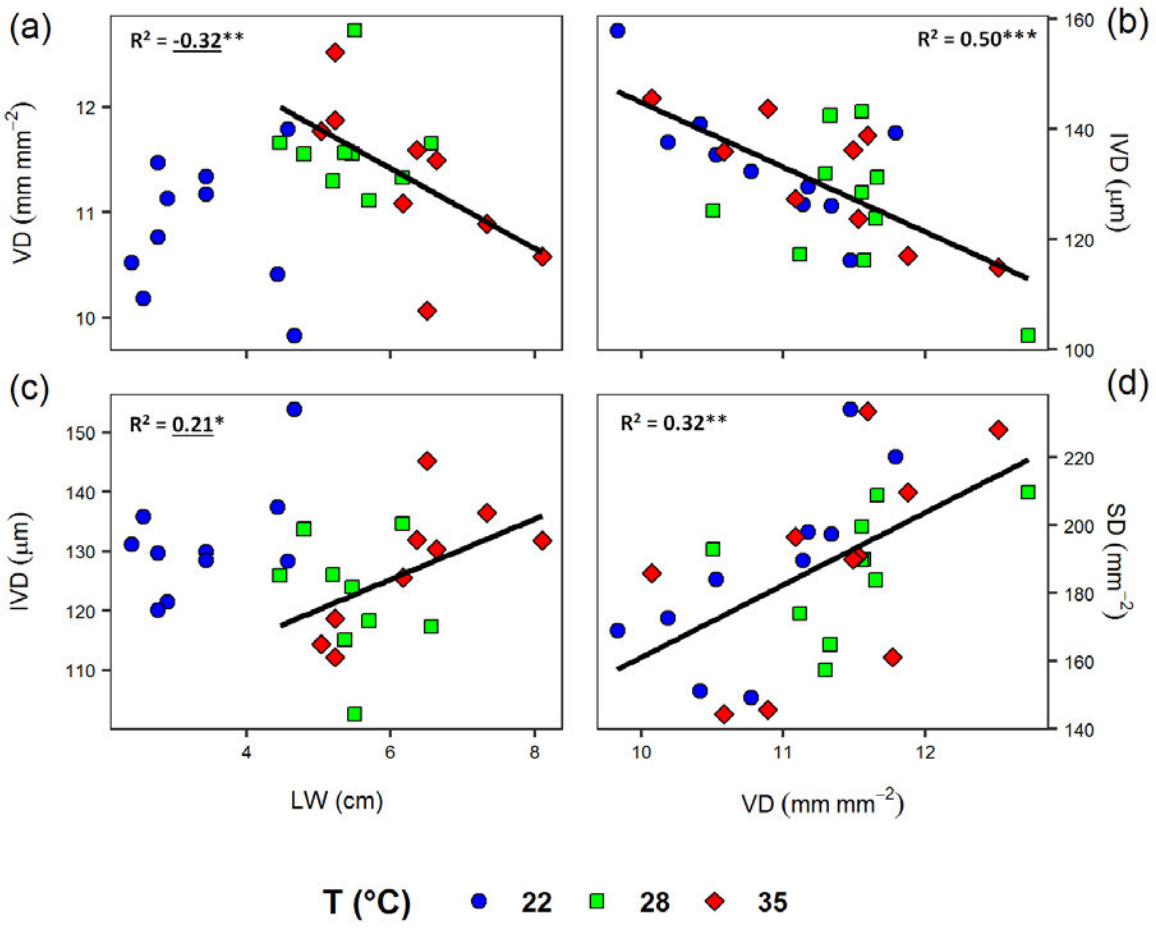

Fig.2.5 The relationship between vein anatomy and leaf width and stomatal density. Leaf width was measured on the portion sampled from the middle of the youngest fully expanded leaf. The same portion was used for measurement of vein of stomatal traits by analysing the area between 2nd and 3rd major veins from the midrib. Each point in the scatter plot represents the mean value of the variable per genotype, per treatment (n=3). Standard error bars were removed to ensure clearer presentation (Table 2.1 for leaf width; Table 2.2 for stomatal and vein anatomical traits). The black line represents the line of best fit for the data, with the corresponding R^2 value represented that is deduced from a Pearson product-moment correlation analysis (Table 2.S1). Different treatment growth temperatures are represented by the different fill colour of the scatter points: blue=22°C, green=28°C, red=35°C. Degrees of statistical significance are represented as: $p<0.001$ (***), $p<0.05$ (**), $p<0.1$ (*). Fig.2.5 a and Fig.2.5 c only showed a significant relationship after excluding measurements from 22°C from the analysis. Measurements conducted on genotype FF_SC842-14E were considered influential outliers for plots **(a)** and **(c)**. The interveinal distance (*IVD*) values in Fig.2.5 c are the average of *IVD* values measured from leaf paradermal sections and values measured from leaf cross-sections. The values of *IVD* in Fig.25 d are the values measured from leaf cross-sections. Leaf width (*LW*) vs. **(a)** Vein density (*VD*), **(b)** Interveinal distance (*IVD*); **(c)** Interveinal distance (*IVD*) vs. vein density (*VD*); **(d)** Stomatal density (*SD*) vs. vein density (*VD*).

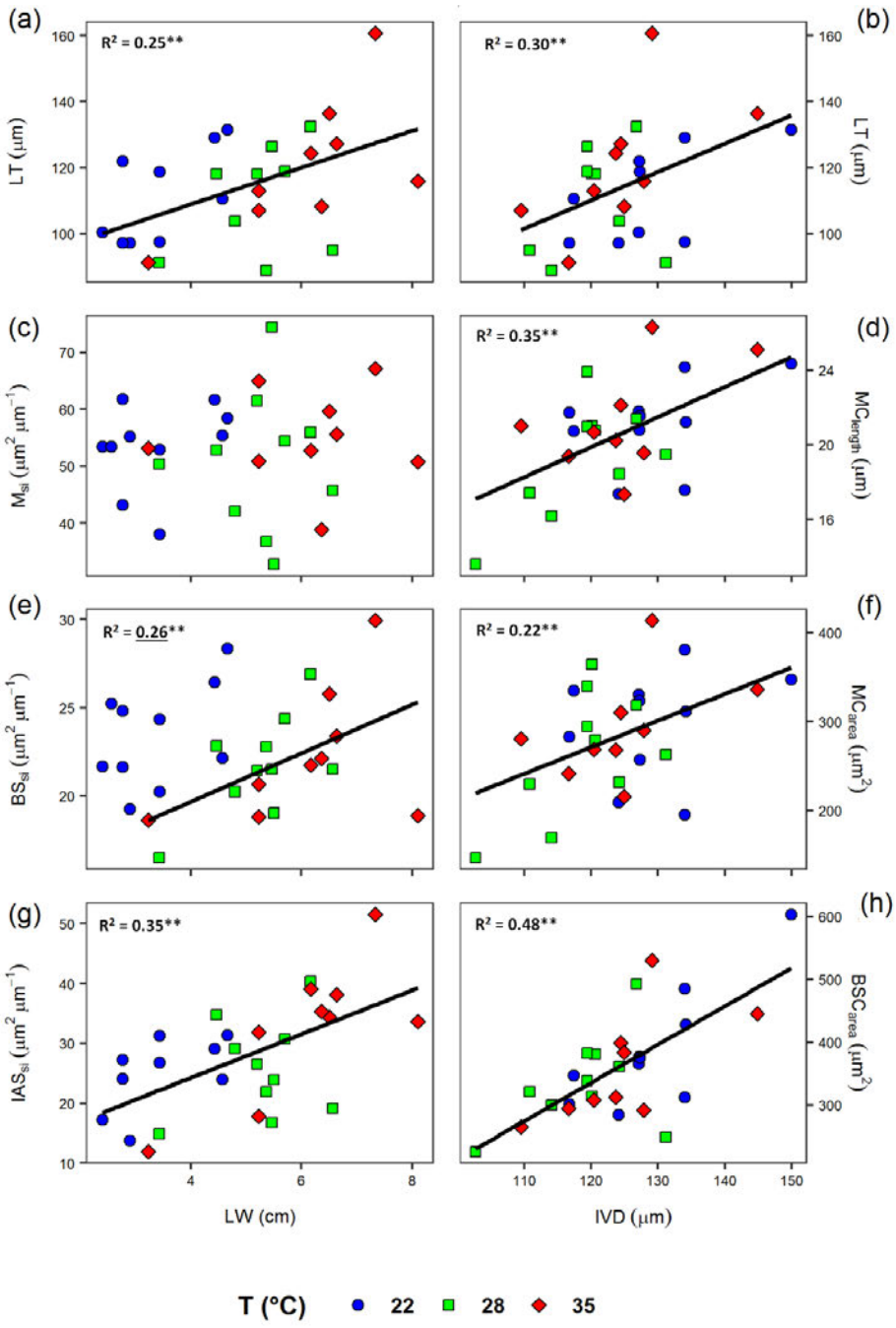

Fig.2.6 The relationship between leaf width and interveinal distance with inner leaf anatomy. Leaf width was measured on the portion sampled from the middle of the youngest fully expanded leaf. The same portion was used for measurement of vein and inner anatomy traits by analysing the area between 2nd and 3rd major veins from the midrib. Each point in the scatter plot represents the mean value of the variable per genotype, per treatment (n=3). Standard error bars were removed to ensure clearer presentation (Table 2.1 for leaf width; Table 2.2 for vein anatomical traits; Table 2.3 for inner leaf anatomy). The black line represents the line of best fit for the data, with the corresponding R^2 value represented that is deduced from a Pearson product-moment correlation analysis (Table 2.S1). Different treatment growth temperatures are represented by the different fill colour of the scatter points: blue=22°C, green=28°C, red=35°C. Degrees of statistical significance are represented as: $p<0.001$ (***), $p<0.05$ (**), $p<0.1$ (*). Fig.2.6 e only showed a significant relationship after excluding measurements from 22°C from the analysis. Measurements conducted on genotype FF_SC500-9 at 22°C were considered influential outliers for plots **(a)**, **(b)** and **(g)**. No data was collected for genotype LR9198 at the 35°C (Table 2.3 legend). Leaf width (*LW*) is plotted with **(a)** Leaf thickness (*LT*), **(c)** Cross-sectional mesophyll surface area per *IVD* (M_{si}), **(e)** Cross-sectional bundle sheath surface area per *IVD* (BS_{si}), **(g)** Cross-sectional intercellular airspace surface area per *IVD* (IAS_{si}); Interveinal distance (*IVD*) is plotted with **(b)** leaf thickness (*LT*), **(d)** Average mesophyll cell length (MC_{length}), **(f)** Mesophyll cell area (MC_{area}), **(h)** Bundle sheath cell area (BSC_{area}). Interveinal distance values presented in this Fig. are measured from leaf paradermal sections.

2.6 SUPPLEMENTARY

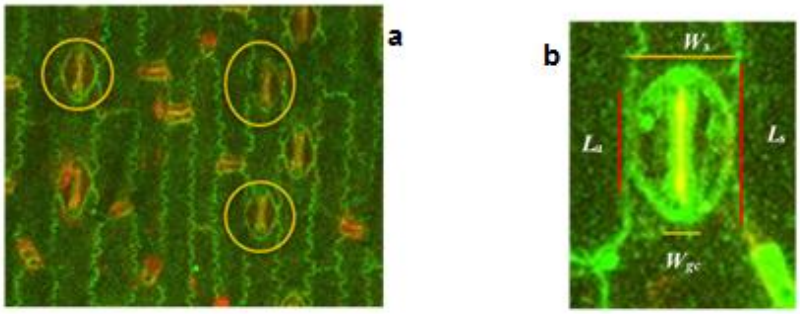

Fig.2.S1 Confocal images to illustrate sampling of stomatal features. **(a)** shows stomata identified for *SD* measurement. **(b)** shows stomatal dimensions: Width of stomata (W_s) (with subsidiary cells), width of guard cells (W_{gc}), length of stomata (L_s), and length of aperture (L_a).

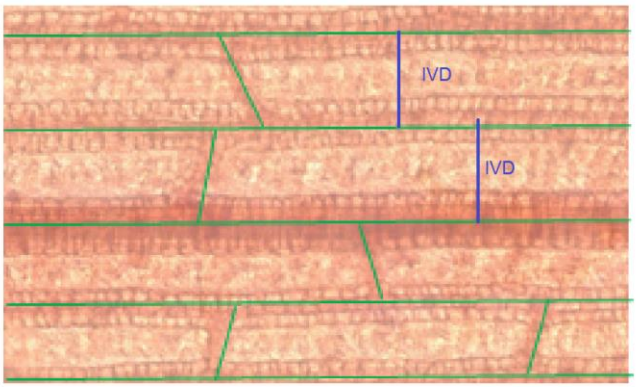

Fig.2.S2 Light microscopy image of a cleared and stained leaf showing the veins in green lines. Full length of the green lines per area compromised vein density (*VD*). interveinal distance (*IVD*) is also highlighted.

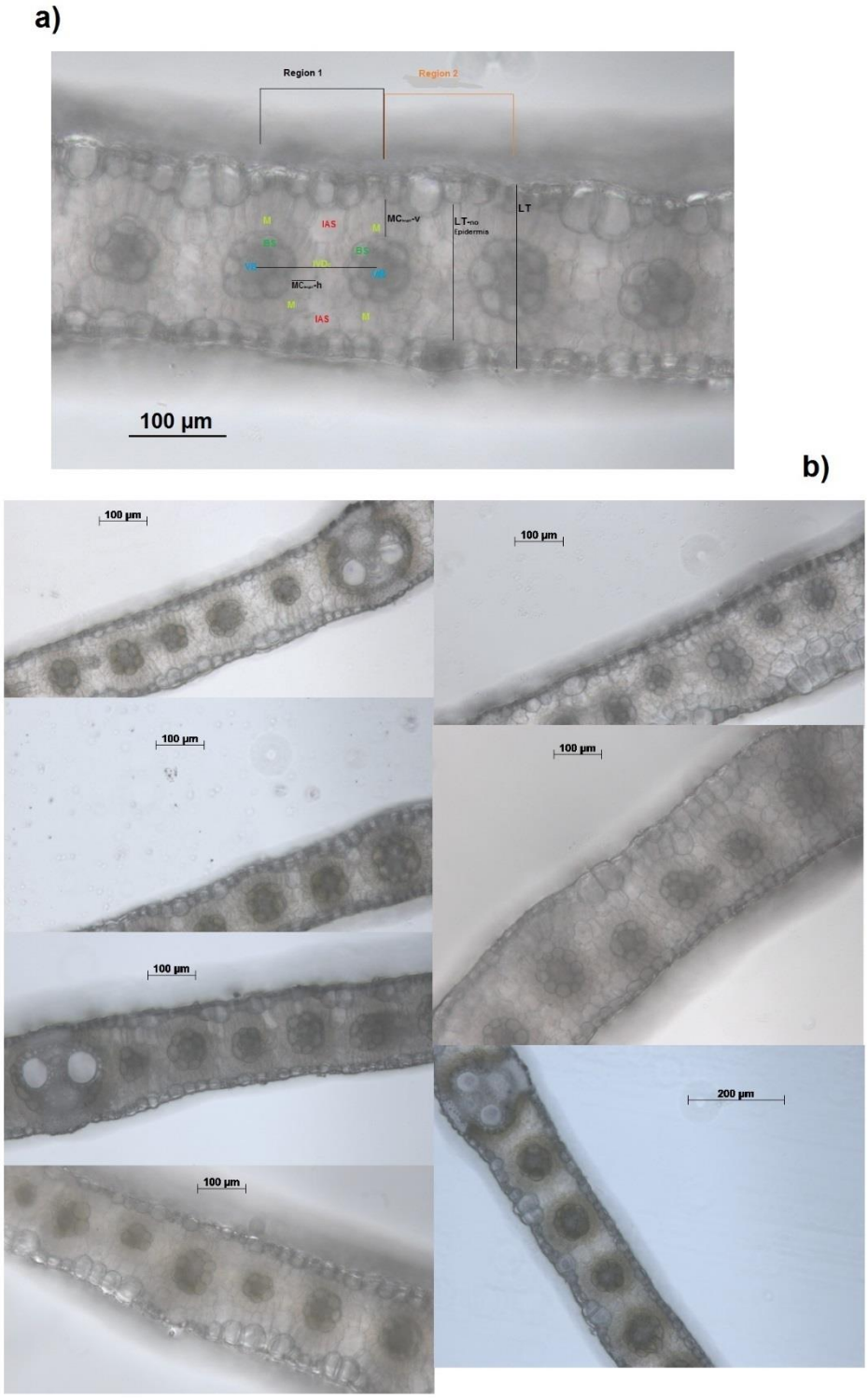

Fig.2.S3 Light microscopy image of a cleared transverse leaf cross-section showing the main anatomical components that were measured. IAS: Intercellular air spaces, M: Mesophyll cells; BS: Bundle sheath cells; VB: Vascular bundle; IVD_C: Interveinal distance; *LT*: Leaf Thickness; *LT*-no epidermis: Leaf Mesophyll Thickness; MC_{length}-h: length of horizontal mesophyll cells; MC_{length}-v: length of vertical mesophyll cells.

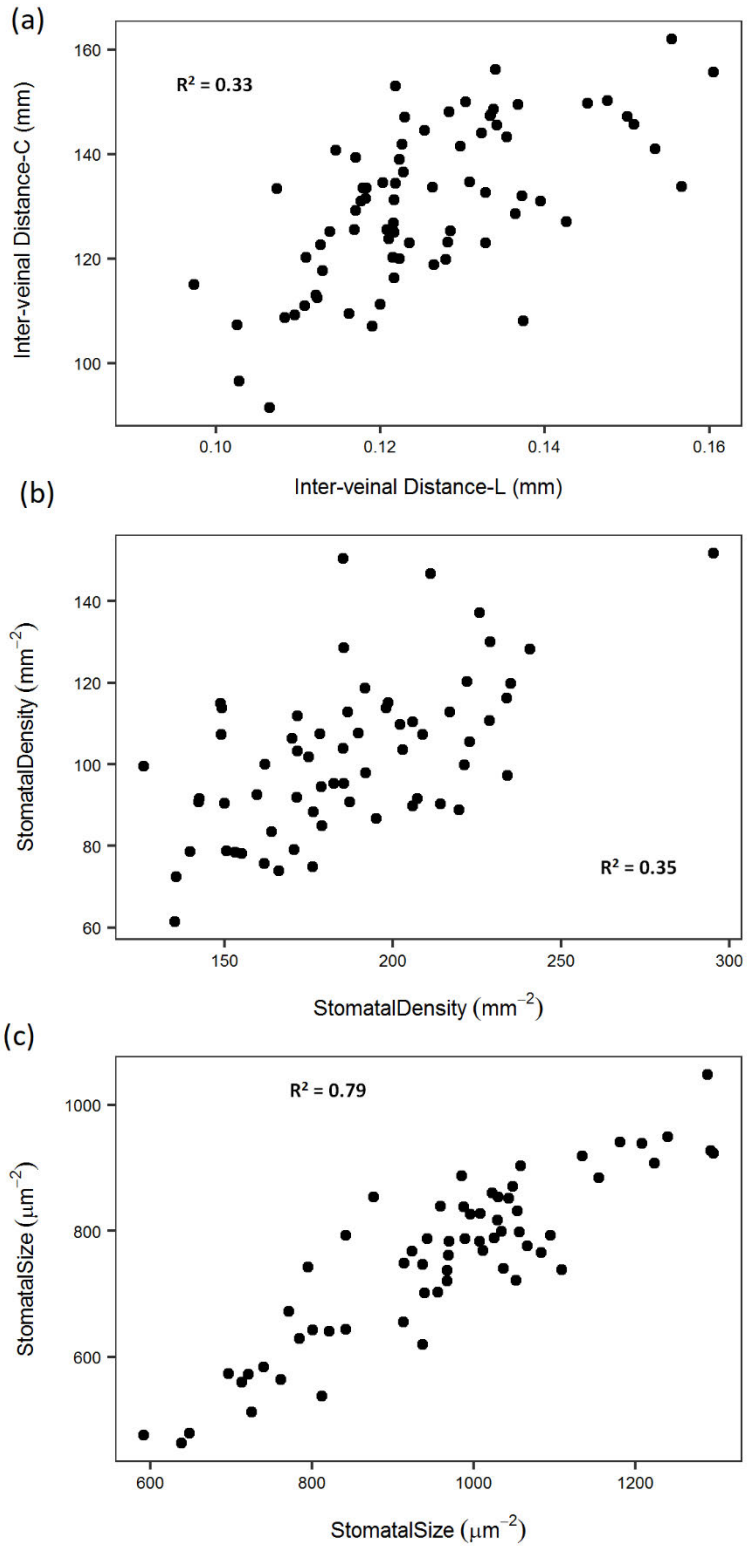

Fig.2.S4 Plots of data points of **(a)** Interveinal distance measured from cross-sections (y-axis) vs. Interveinal distance measured from paradermal sections (x-axis). **(b)** Stomatal density measured during first stage of analysis (x-axis) vs. Stomatal density measured later when analysing for epidermal cell size (y-axis). **(c)** Similar to (b) but for stomatal size. This figure was constructed to show consistency of measurements.

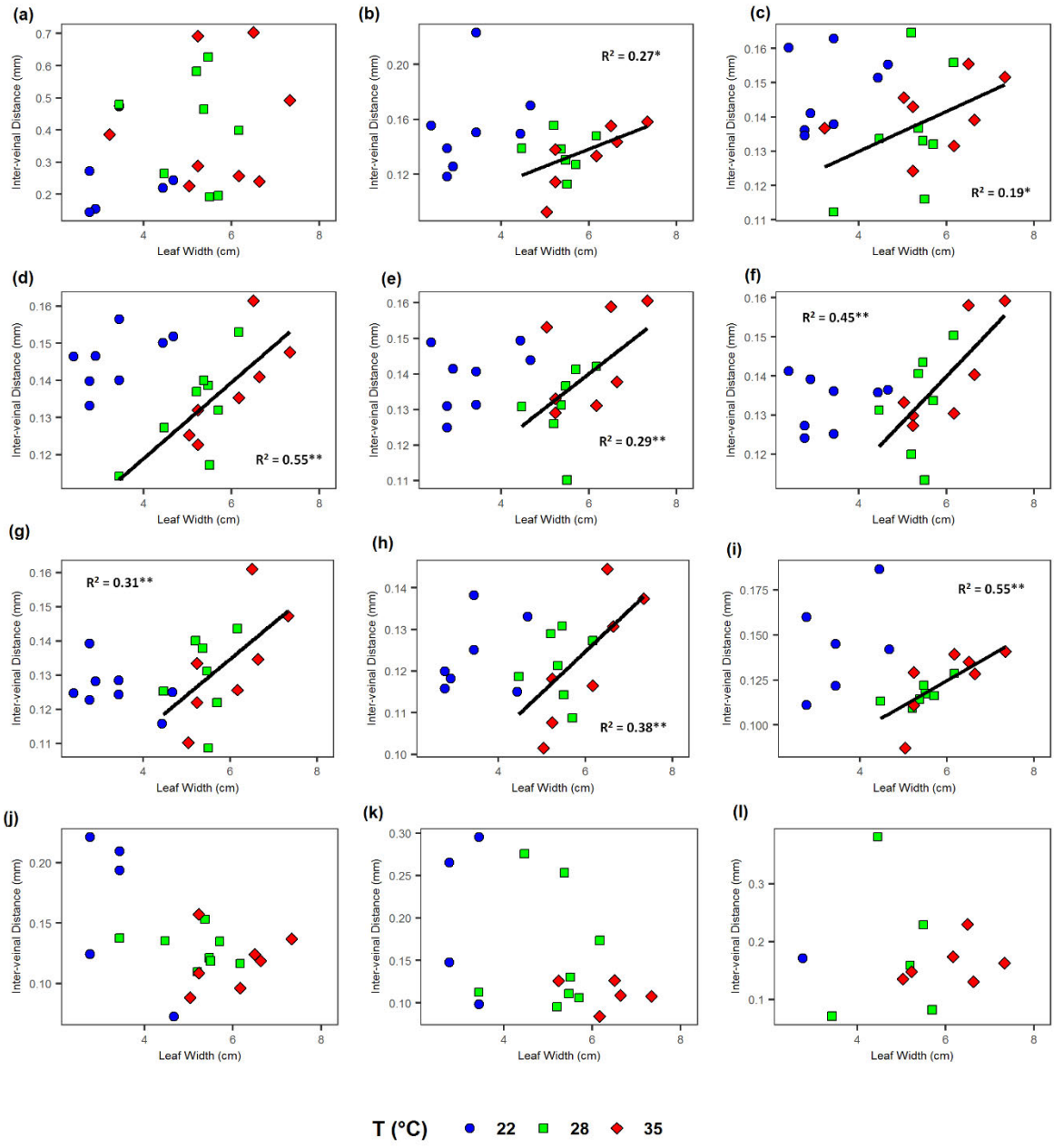

Fig.2.S5 Regression plots of leaf width (x-axis) vs. Interveinal distance measured from scanned leaf sections (y-axis). Figures **(a)** to **(l)** each represent a different section of the leaf across the leaf width (midrib to leaf edge). Each plot represents the average interveinal distance between two major veins, with **(a)** is the average interveinal distance between the midrib and 1st major vein, **(b)** is the average interveinal distance between 1st and 2nd major veins…and so on. Each point is the average (n=3) for each genotype at each temperature treatment.

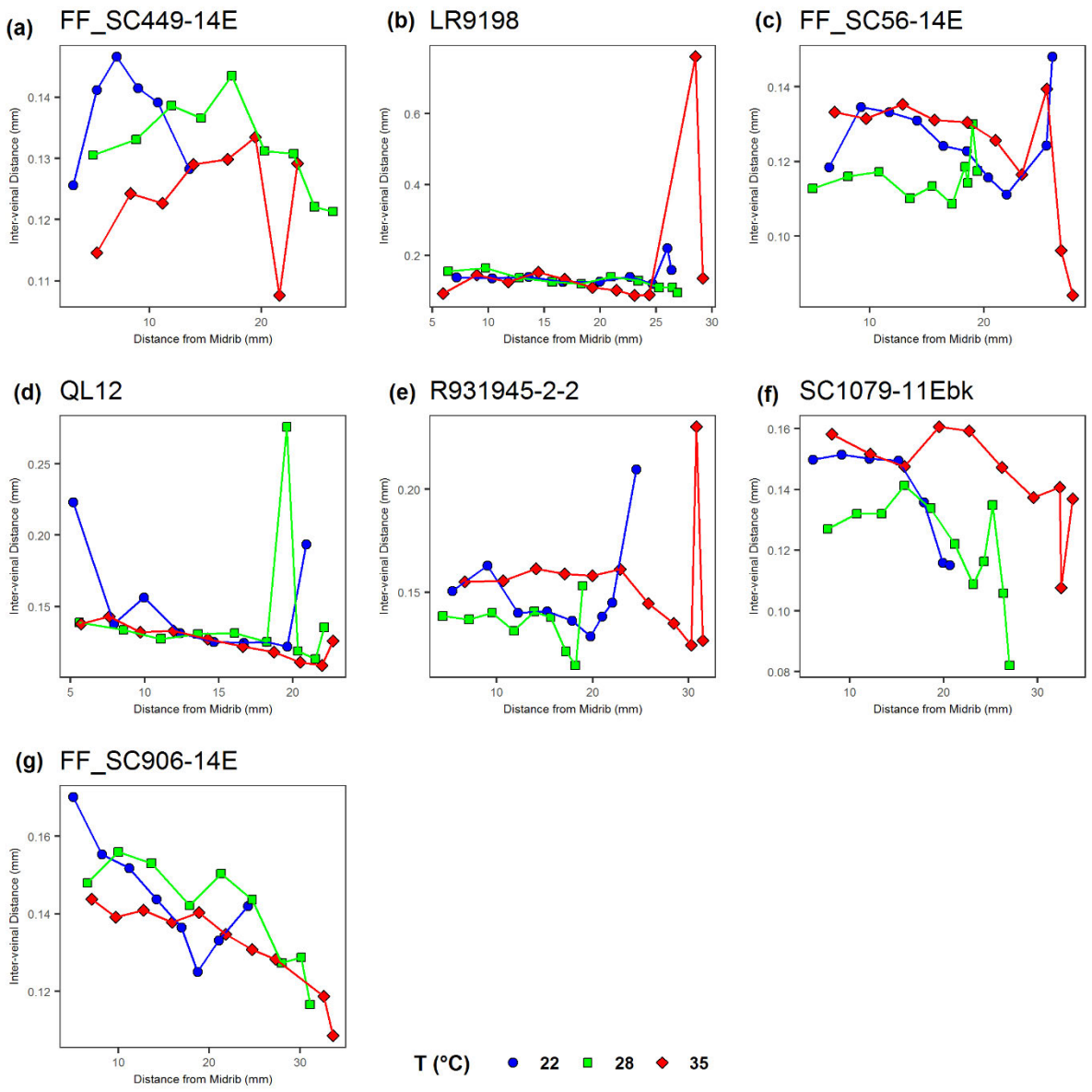

Fig.2.S6 Plots showing the change in interveinal distance at each leaf section (see Fig.2.S5 for description of sections) along the leaf width for 7 different genotypes of varying leaf width (see Table 2.1 for leaf width of each genotype). The x-axis shows the distance of each section from the midrib (distance from midrib to the major vein that starts each sections). For example, the first point is of the interveinal distance vs. the distance from midrib to 1st major vein; second point represents distance from midrib to 2nd major vein….and so on.

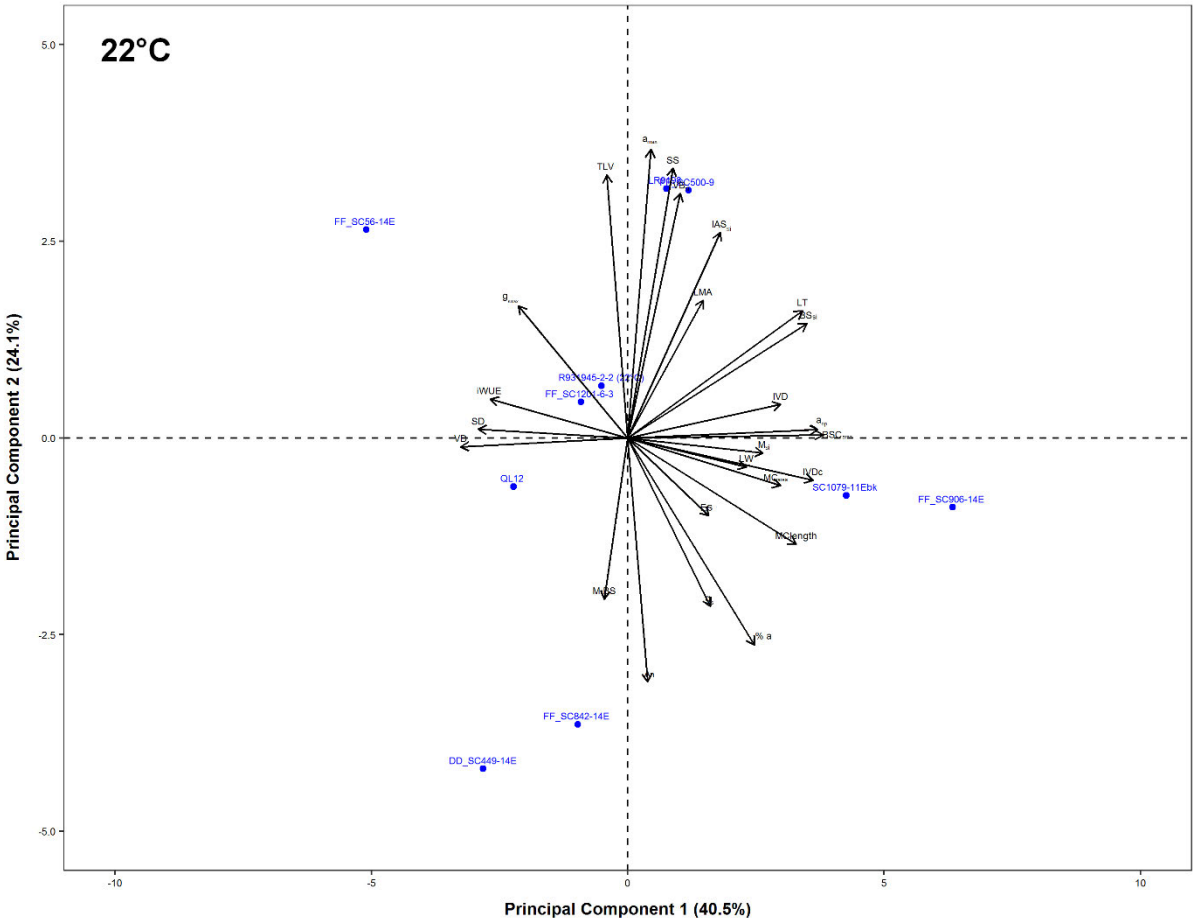

Fig.2.S7 Principal component analyses biplots of the variables measured at 22°C (PC1 and PC2 explain 64.6%). The analyses yielded five components with eigenvalues >1 (Table 2.S2) for each separate analysis. Plot below shows the two main components that explain most of the variation. The data points analysed represented the mean value of the variable per species (standard error values are presented in Table 2.1, Table 2.2 and Table 2.3). Blue circles represent the position of different genotypes. *LT*: leaf mesophyll thickness (µm); IVD_c: interveinal distance measured from leaf cross-sections (µm); *M:BS*: mesophyll to bundle sheath ratio; MC_{length}: length of mesophyll cell; MC_{area}: area of single mesophyll cell (µm²); BSC_{area}: area of single bundle sheath cell (µm²); M_{si}: mesophyll surface area per interveinal distance (µm² µm^{-1}); BS_{si}: bundle sheath surface area per interveinal distance (µm² µm^{-1}); VB_{si}: vascular bundle surface area per interveinal distance (µm² µm^{-1}); IAS_{si}: intercellular airspace surface area per interveinal distance (µm² µm^{-1}); *SD*: stomatal density (mm^{-2}); SS: stomatal size (µm²); a_{max}: maximum stomatal pore aperture (µm²); a_{op}: operation stomatal aperture (µm²); *% aperture*: percentage of a_{op} to a_{max}; g_{smax}: maximum theoretical stomatal conductance (mol m^{-2} s^{-1}); *IVD*: inter-veinal distance (mm); *DV*: vein density (mm mm^{-2}); *TLV*: Total Number of longitudinal veins; $\delta^{13}C$: carbon isotopic composition (‰); *LMA*: leaf mass per area (g m^{-2}); A_n: carbon assimilation rate (µmol m^{-2} s^{-1}); g_s: stomatal conductance (mol m^{-2} s^{-1}); *iWUE*: intrinsic water use efficiency (µmol CO_2 mol^{-1} H_2O); *LW*: leaf width (cm); *ES*: Epidermal cell size (µm²).

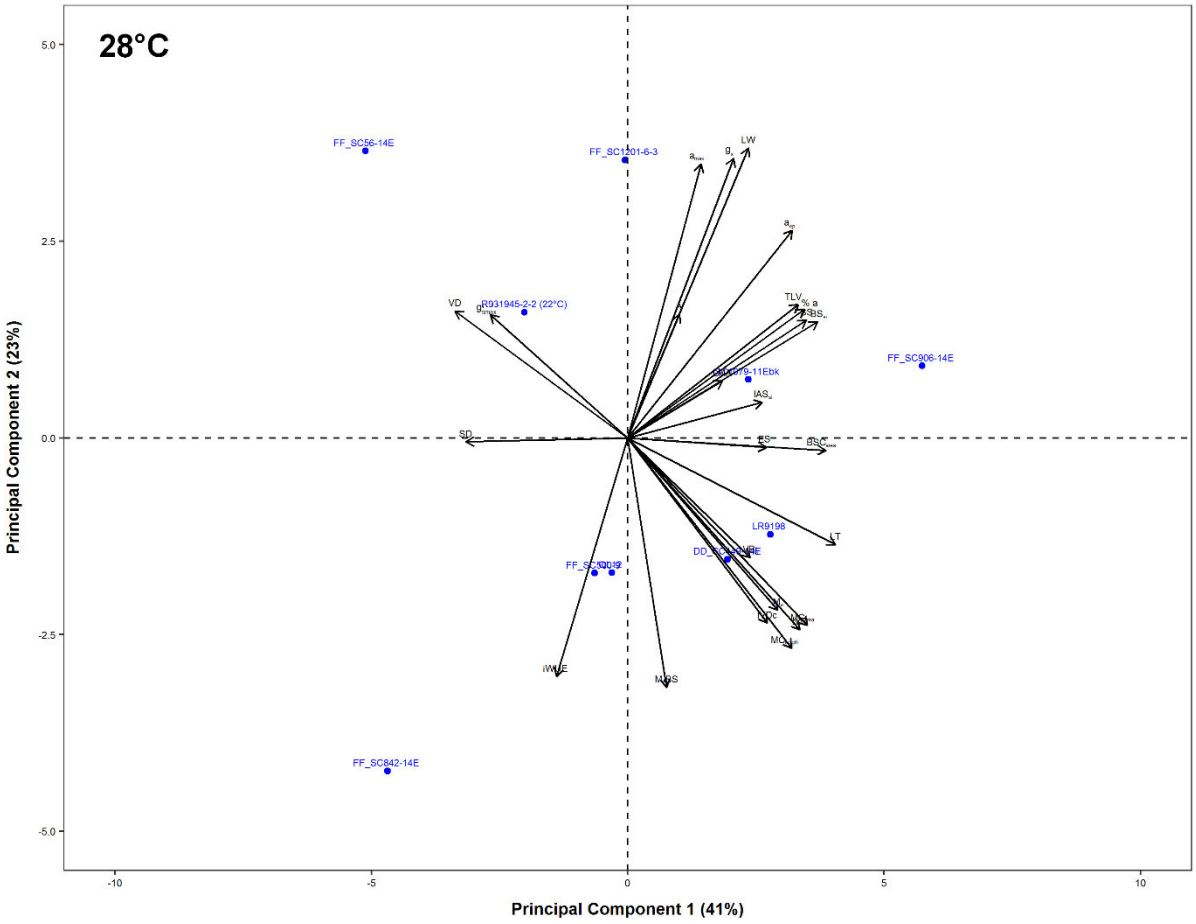

Fig.2.S8 Principal component analyses biplots of the variables measured at 28°C (PC1 and PC2 explain 64%). The analyses yielded five components with eigenvalues >1 (Table 2.S2) for each separate analysis. Plot below shows the two main components that explain most of the variation. The data points analysed represented the mean value of the variable per species (standard error values are presented in Table 2.1, Table 2.2 and Table 2.3). Blue circles represent the position of different genotypes. *LT*: leaf mesophyll thickness (µm); IVD_c: interveinal distance measured from leaf cross-sections (µm); *M:BS*: mesophyll to bundle sheath ratio; MC_{length}: length of mesophyll cell; MC_{area}: area of single mesophyll cell (µm²); BSC_{area}: area of single bundle sheath cell (µm²); M_{si}: mesophyll surface area per interveinal distance (µm² µm^{-1}); BS_{si}: bundle sheath surface area per interveinal distance (µm² µm^{-1}); VB_{si}: vascular bundle surface area per interveinal distance (µm² µm^{-1}); IAS_{si}: intercellular airspace surface area per interveinal distance (µm² µm^{-1}); *SD*: stomatal density (mm^{-2}); SS: stomatal size (µm²); a_{max}: maximum stomatal pore aperture (µm²); a_{op}: operation stomatal aperture (µm²); *% aperture*: percentage of a_{op} to a_{max}; g_{smax}: maximum theoretical stomatal conductance (mol m^{-2} s^{-1}); *IVD*: inter-veinal distance (mm); *DV*: vein density (mm mm^{-2}); *TLV*: Total Number of longitudinal veins; $\delta^{13}C$: carbon isotopic composition (‰); *LMA*: leaf mass per area (g m^{-2}); A_n: carbon assimilation rate (µmol m^{-2} s^{-1}); g_s: stomatal conductance (mol m^{-2} s^{-1}); *iWUE*: intrinsic water use efficiency (µmol CO_2 mol^{-1} H_2O); *LW*: leaf width (cm); *ES*: Epidermal cell size (µm²).

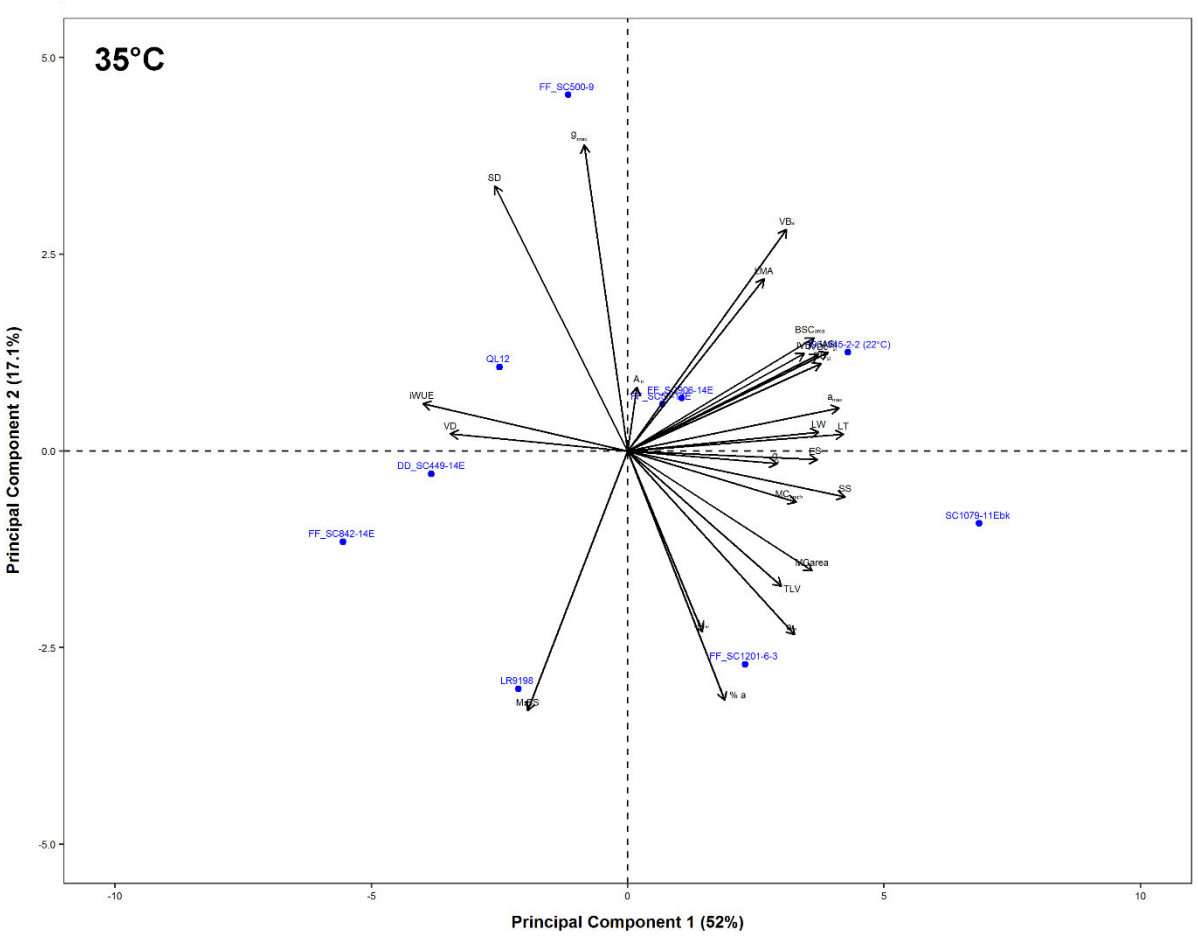

Fig.2.S9 Principal component analyses biplots of the variables measured at 35°C (PC1 and PC2 explain 69.1%). The analyses yielded five components with eigenvalues >1 (Table 2.S2) for each separate analysis. Plot below shows the two main components that explain most of the variation. The data points analysed represented the mean value of the variable per species (standard error values are presented in Table 2.1, Table 2.2 and Table 2.3). Blue circles represent the position of different genotypes. *LT*: leaf mesophyll thickness (µm); IVD_c: interveinal distance measured from leaf cross-sections (µm); *M:BS*: mesophyll to bundle sheath ratio; MC_{length}: length of mesophyll cell; MC_{area}: area of single mesophyll cell (µm²); BSC_{area}: area of single bundle sheath cell (µm²); M_{si}: mesophyll surface area per interveinal distance (µm² µm⁻¹); BS_{si}: bundle sheath surface area per interveinal distance (µm² µm⁻¹); VB_{si}: vascular bundle surface area per interveinal distance (µm² µm⁻¹); IAS_{si}: intercellular airspace surface area per interveinal distance (µm² µm⁻¹); *SD*: stomatal density (mm⁻²); SS: stomatal size (µm²); a_{max}: maximum stomatal pore aperture (µm²); a_{op}: operation stomatal aperture (µm²); *% aperture*: percentage of a_{op} to a_{max}; g_{smax}: maximum theoretical stomatal conductance (mol m⁻² s⁻¹); *IVD*: inter-veinal distance (mm); *DV*: vein density (mm mm⁻²); *TLV*: Total Number of longitudinal veins; $\delta^{13}C$: carbon isotopic composition (‰); *LMA*: leaf mass per area (g m⁻²); A_n: carbon assimilation rate (µmol m⁻² s⁻¹); g_s: stomatal conductance (mol m⁻² s⁻¹); *iWUE*: intrinsic water use efficiency (µmol CO_2 mol⁻¹ H_2O); *LW*: leaf width (cm); *ES*: Epidermal cell size (µm²).

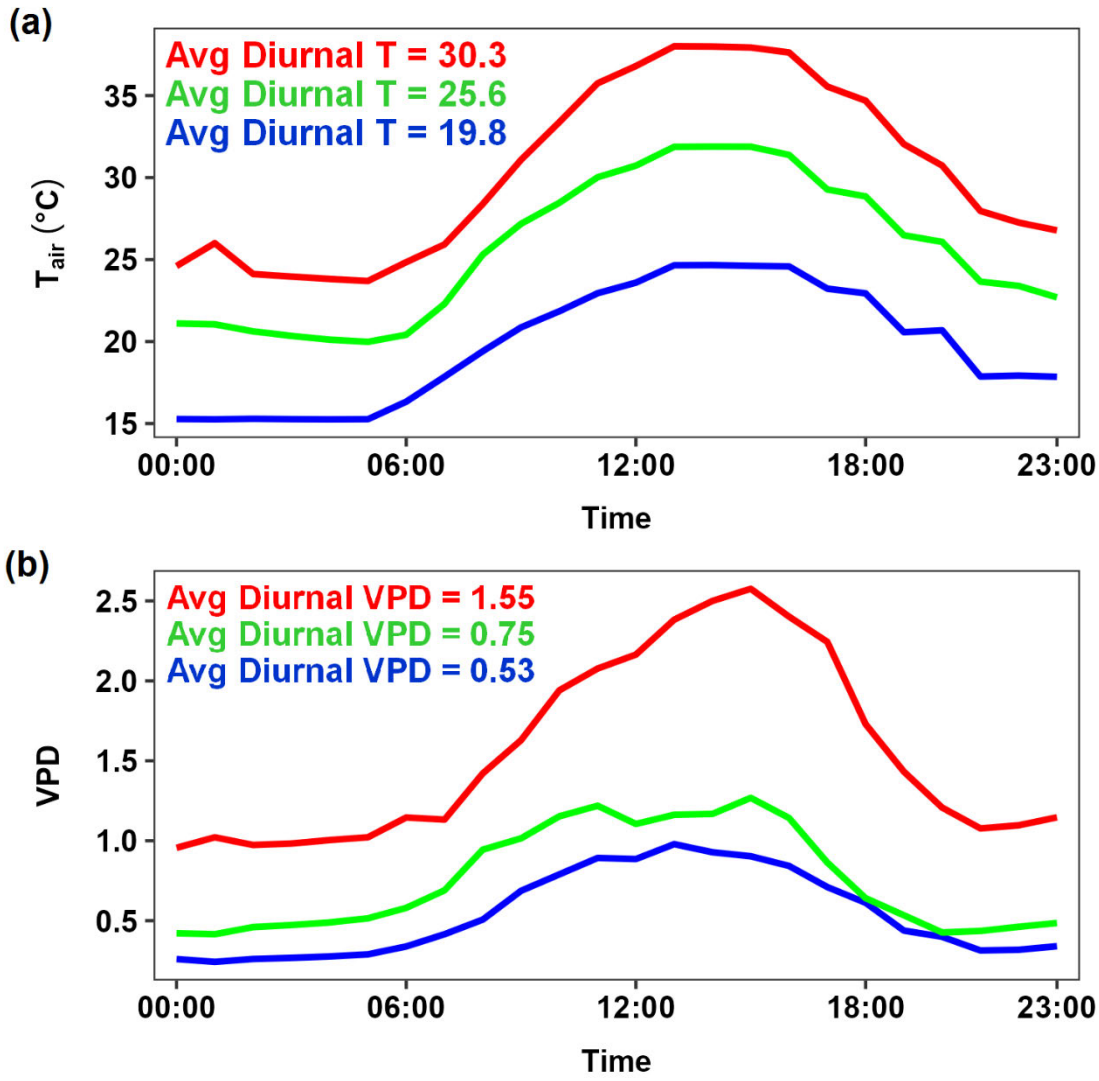

Fig.2.S10 Environmental growth conditions of the plants at the three treatments.

Table 2.S1. Pearson product-moment correlation analysis results for the relationships between the measured variables. The *r* coefficient and the statistical significance were determined using the mean value per species, per treatment for each variable. Statistical significance was judged as: $p<0.001$ (***), $p<0.05$ (**), $p<0.1$ (*), $p>0.1$ (ns). Underlined coefficients show the correlation between the variables was significant after excluding the 22°C treatment.

	IVD_c	M/BS	MC_{length}	MC_{area}	BSC_{area}	M_{si}	BS_{si}
LT	0.66***	ns	0.83***	0.8***	0.79***	0.68***	0.8***
IVD_c	-	ns	0.64***	0.64***	0.82***	0.39**	0.61***
M/BS	-	-	0.39**	ns	ns	0.68***	-0.4**
MC_{length}	-	-	-	0.93***	0.7***	0.87***	0.62***
MC_{area}	-	-	-	-	0.7***	0.86***	0.67***
BSC_{area}	-	-	-	-	-	0.41**	0.91***
M_{si}	-	-	-	-	-	-	0.39**
BS_{si}	-	-	-	-	-	-	-
VB_{si}	-	-	-	-	-	-	-
IAS_{si}	-	-	-	-	-	-	-
SD	-	-	-	-	-	-	-
SS	-	-	-	-	-	-	-
a_{max}	-	-	-	-	-	-	-
ES	-	-	-	-	-	-	-
a_{op}	-	-	-	-	-	-	-
$\%\ a$	-	-	-	-	-	-	-
g_{smax}	-	-	-	-	-	-	-
IVD	-	-	-	-	-	-	-
VD	-	-	-	-	-	-	-
TLV	-	-	-	-	-	-	-
LMA	-	-	-	-	-	-	-
A_n	-	-	-	-	-	-	-
g_s	-	-	-	-	-	-	-
$iWUE$	-	-	-	-	-	-	-

Table 2.S1 continued…..

	VB_{si}	IAS_{si}	SD	SS	a_{max}	ES	a_{op}
LT	0.62***	0.75***	-0.51**	0.69***	0.49**	0.59**	0.46**
IVD_c	0.46**	0.47**	-0.45**	0.52**	ns	0.44**	ns
M / BS	ns	ns	ns	ns	ns	ns	ns
MC_{length}	0.34*	ns	-0.45**	0.51**	ns	0.51**	ns
MC_{area}	ns	ns	-0.59**	0.41**	ns	0.68***	0.48*
BSC_{area}	0.44**	0.6***	-0.48**	0.43**	ns	0.53**	ns
M_{si}	ns	ns	-0.39**	0.33*	ns	0.43*	ns
BS_{si}	0.55**	0.66***	-0.47**	0.64***	0.41**	0.46**	0.4*
VB_{si}	-	0.54**	ns	0.69***	0.65**	ns	ns
IAS_{si}	-	-	ns	0.65***	0.55**	0.49**	0.49**
SD	-	-	-	-0.41**	ns	-0.63**	-0.55**
SS	-	-	-	-	0.85***	0.56**	0.5**
a_{max}	-	-	-	-	-	ns	0.48**
ES	-	-	-	-	-	-	ns
a_{op}	-	-	-	-	-	-	-
$\% a$	-	-	-	-	-	-	-
g_{smax}	-	-	-	-	-	-	-
IVD	-	-	-	-	-	-	-
VD	-	-	-	-	-	-	-
TLV	-	-	-	-	-	-	-
LMA	-	-	-	-	-	-	-
A_n	-	-	-	-	-	-	-
g_s	-	-	-	-	-	-	-
$iWUE$	-	-	-	-	-	-	-

Table 2.S1 continued.....

	% a	g_{smax}	IVD	VD	TLV	LMA	A_n	g_s	iWUE	LW
LT	0.39*	ns	0.55**	-0.48**	0.49**	0 37**	ns	0.46**	-0 23**	0.5**
IVD_c	ns	-0.36*	0.48***	-0.71***	ns	ns	ns	ns	ns	ns
M / BS	ns	ns	ns	ns	ns	ns	ns	ns	ns	ns
MC_{length}	ns	-0.36*	0.59**	-0.6**	0.54**	ns	ns	ns	ns	ns
MC_{area}	ns	-0.44**	0.47**	-0.57**	0.56**	ns	ns	ns	ns	ns
BSC_{area}	ns	-0.34*	0.69**	-0.59***	0.53**	ns	ns	ns	ns	ns
M_{si}	ns	ns	ns	ns	0.49**	ns	ns	ns	ns	ns
BS_{si}	ns	ns	0.54**	-0.48**	0.64**	ns	ns	ns	-0 51**	0.51**
VB_{si}	ns	ns	0.38**	-0.46*	0.52**	0 35*	ns	ns	ns	0.43*
IAS_{si}	0.39*	ns	0.43**	-0.41**	0.51**	0.46**	ns	0.49**	-0.43**	0.59***
SD	-0 56**	0.88***	-0.35*	0.57**	-0.47**	ns	ns	ns	0.48**	ns
SS	ns	ns	0.56**	-0.63**	0.57**	0.43**	ns	0 57**	-0.44**	0.57**
a_{max}	ns	-0.34*	ns	-0.47**	0.73***	0.42**	ns	0 64***	-0.48**	0.5**
ES	ns	-0.38*	ns	ns	ns	ns	ns	ns	-0.48*	0.38*
a_{op}	0.93***	ns	ns	-0.68**	0.64***	0 63***	0 62***	0 81***	-0 82***	0.84***
% a	-	-0.42*	ns	-0.59**	0.34*	0 53**	0 65***	0.78***	-0.74***	0.71***
g_{smax}	-	-	ns	0.52**	ns	ns	ns	0.49**	-0 36*	0.49**
IVD	-	-	-	-0.87***	ns	0 59**	ns	0.48**	0.42*	0.45*
VD	-	-	-	-	ns	0.44*	ns	-0 54**	0.54**	-0.57**
TLV	-	-	-	-	-	0.46**	0 32*	0.47**	-0.49**	0.65***
LMA	-	-	-	-	-	-	0.79***	0 8***	-0 62***	0.75***
A_n	-	-	-	-	-	-	-	0 92***	-0 65***	0.72***
g_s	-	-	-	-	-	-	-	-	-0 88***	0.87***
iWUE	-	-	-	-	-	-	-	-	-	-0.87***

LT: leaf mesophyll thickness (µm); IVD_c: interveinal Distance measured from leaf cross-sections (µm); *M : BS*: mesophyll to bundle sheath ratio; MC_{length}: length of mesophyll cell (µm); MC_{area}: area of single mesophyll cell (µm^2); BSC_{area}: area of single bundle sheath cell (µm^2); M_{si}: mesophyll surface area per IVD_c (µm^2 µm^{-1}); BS_{si}: bundle sheath surface area per IVD_c (µm^2 µm^{-1}); VB_{si}: vascular bundle surface area per IVD_c (µm^2 µm^{-1}); IAS_{si}: intercellular airspace surface area per IVD_c (µm^2 µm^{-1}); *SD*: stomatal density (mm^{-2}); *SS*: stomatal size (µm^2); a_{max}: maximum stomatal pore aperture (µm^2); *ES*: Epidermal cell size (µm^2); a_{op}: operation stomatal aperture (µm^2); *% a*: percentage of a_{op} to a_{max}; g_{max}: maximum theoritical stomatal conductance (mol m^{-2} s^{-1}); *IVD*: inter-veinal distance (mm); *DV*: total vein density (mm mm^{-2}); *TLV*: Total Number of longitudinal veins; $\delta^{13}C$: carbon isotopic composition (‰); *LMA*: leaf mass per area (g m^{-2}); A_n: net carbon assimilation rate (µmol m^{-2} s^{-1}); g_s: stomatal conductance (mol m^{-2} s^{-1}); *iWUE*: intrinsic water use efficiency (µmol CO_2 mol^{-1} H_2O); *LW*: leaf width (cm).

Table 2.S2. Component loadings and total variance of principal components from a principal component analysis (PCA) of the measured variables. Input data into the PCA analysis constituted the mean value of the variable per species, per treatment. Components with eigenvalues >1 are retained and are shown in the table, along with the absolute component loading for each retained dimension

	All Temperatures					22°C					28°C					35°C				
Principal Components & Variables	**PC1**	**PC2**	**PC3**	**PC4**	**PC5**	**PC1**	**PC2**	**PC3**	**PC4**	**PC5**	**PC1**	**PC2**	**PC3**	**PC4**	**PC5**	**PC1**	**PC2**	**PC3**	**PC4**	**PC5**
Eigenvalue	9.4	5.7	3.1	2.1	1.6	10.1	6.02	3.8	2.3	1.1	10.3	5.7	3.2	2.1	1.2	12.9	4.3	3.3	1.9	1.2
(%) Variance Explaioned	37.6	22.6	12.5	8.4	6.5	40.5	24.1	15.2	9.2	4.6	41.04	22.9	12.6	8.3	4.8	51.9	17.1	13.3	7.8	4.9
Leaf mesophyll thickness (LT)	0.93	-0.21	0.07	0.2	0.08	0.87	0.41	-0.13	0.07	-0.03	0.9	-0.3	0.18	0.05	0.18	0.94	0.05	0.29	0.11	0
Stomatal size (SS)	0.76	0.08	0.3	0.3	-0.4	0.22	0.87	-0.26	0.17	0.15	0.78	0.33	0.1	-0.23	-0.15	0.94	-0.13	0.2	0.2	0
Operational stomatal aperture (a_{op})	0.7	0.57	-0.28	-0.2	-0.18	0.94	0.03	0.19	0.06	0.22	0.71	0.59	-0.21	-0.23	-0.13	0.73	-0.52	-0.43	0.01	-0.04
Intercellular airspace surface area per IVD_c (IAS_{si})	0.74	0.05	0.44	-0.2	-0.04	0.46	0.67	0.25	-0.36	-0.06	0.58	0.1	-0.27	0.65	0.2	0.87	0.28	0.01	0.06	-0.3
Bundle sheath surface area per IVD_c (BS_{si})	0.76	-0.41	0.34	-0.08	-0.03	0.89	0.37	-0.04	0.01	-0.15	0.82	0.33	-0.04	0.34	0.02	0.84	0.25	0.43	-0.14	0.05
Bundle sheath cell area (BSC_{area})	0.75	-0.48	0.18	-0.19	0.19	0.97	0.01	0.07	-0.05	-0.18	0.86	-0.04	0	0.46	0.17	0.81	0.32	0.36	-0.27	0.06
Leaf width (LW)	0.6	0.75	0.01	-0.09	0.02	0.59	-0.09	0.56	0.48	0.03	0.52	0.82	0.13	-0.12	-0.03	0.83	0.05	-0.34	0.24	-0.3
Mesophyll cell area (MC_{area})	0.74	-0.42	-0.34	0.31	0.07	0.76	-0.15	-0.41	0.37	-0.11	0.78	-0.53	0.12	-0.23	0.11	0.8	-0.34	0.45	0.07	0.1
Average mesophyll cell length, vertical or horizontal (MC_{length})	0.71	-0.42	-0.3	0.3	0.29	0.84	-0.34	-0.28	0.24	-0.1	0.71	-0.59	0.26	-0.16	0.13	0.73	-0.14	0.53	0.08	0.36
Interveinal distance measured from leaf cross-sections (IVD_c)	0.67	-0.45	0.02	-0.19	0.32	0.92	-0.14	0.13	0.15	-0.1	0.6	-0.52	0.03	0.32	-0.13	0.83	0.27	-0.13	-0.39	0.07
Calculated maximum stomatal pore aperture (a_{max})	0.59	0.3	0.53	0.27	-0.33	0.11	0.93	0	0.27	-0.15	0.32	0.77	0.24	-0.29	-0.07	0.92	0.12	0.01	0.33	-0.02
Leaf mass per area (LMA)	0.53	0.64	0.11	0	0.34	0.37	0.45	0.5	-0.33	0.33	0.41	0.16	0.79	0.22	-0.03	0.59	0.49	-0.4	0.21	0
Total number of longitudinal veins (TLV)	0.54	0.52	0.19	0.4	-0.37	-0.1	0.85	0.18	0.36	0.26	0.74	0.38	0.21	-0.14	-0.01	0.67	-0.38	0.24	0.43	-0.24
Vascular bundle surface area per IVD_c (VB_{si})	0.58	-0.08	0.54	0.24	0.11	0.26	0.79	-0.04	0.06	0.3	0.53	-0.34	0.22	-0.13	-0.43	0.69	0.63	0.1	0.03	0
Epidermal cell area (EpS)	0.57	-0.11	-0.1	-0.01	-0.26	0.4	-0.25	-0.48	-0.2	-0.4	0.6	-0.03	-0.19	-0.09	0.7	0.82	-0.02	0.09	0.09	-0.54
% stomatal aperture ($\%\ aperture$)	0.53	0.53	-0.53	-0.35	-0.08	0.63	-0.67	0.18	-0.18	0.28	0.77	0.36	-0.34	-0.01	-0.19	0.42	-0.71	-0.53	-0.14	-0.05
Stomatal conductance (g_s)	0.46	0.82	-0.17	-0.13	0.24	0.41	-0.54	0.69	0.23	0.02	0.46	0.79	0.27	-0.02	0.06	0.65	-0.04	-0.67	0.27	0.2
Interveinal distance measured from leaf lateral sections (IVD)	0.6	-0.53	0.15	-0.31	0.31	0.76	0.11	0.31	-0.52	-0.13	0.75	-0.54	-0.07	0.32	-0.06	0.77	0.28	-0.23	-0.27	0.4
Mesophyll surface area per IVD_c (M_{si})	0.56	-0.27	-0.46	0.61	0.1	0.67	-0.05	-0.57	0.45	0.09	0.65	-0.49	0.36	-0.41	0.12	0.32	-0.51	0.64	0.33	0.32
Net carbon assimilation rate (A_n)	0.24	0.82	-0.2	-0.05	0.4	0.1	-0.79	0.57	0.04	0.18	0.22	0.35	0.78	0.27	-0.16	0.04	0.18	-0.66	0.63	0.27
Mesophyll to bundle sheath ratio (M:BS)	-0.02	0.07	-0.75	0.6	0.13	-0.12	-0.52	-0.63	0.48	0.24	0.17	-0.71	0.34	-0.57	0.12	-0.44	-0.73	0.05	0.42	0.19
Theoritical maximum stomatal conductance (g_{smax})	-0.26	0.43	0.64	0.37	0.37	-0.54	0.43	0.44	0.4	-0.41	-0.6	0.35	0.67	0.04	0.24	-0.19	0.87	0.12	0.42	0.09
Stomatal density (SD)	-0.6	0.25	0.46	0.27	0.51	-0.74	0.03	0.5	0.28	-0.34	-0.7	-0.01	0.6	0.27	0.17	-0.58	0.75	0.1	0.28	0.08
Vein density (VD)	-0.61	0.57	0.06	0.32	-0.08	-0.83	-0.03	0.25	0.4	0.19	-0.75	0.36	0.21	0	0.25	-0.77	0.05	0.39	0.31	-0.36
Intrinsic water use efficiency ($iWUE$)	-0.58	-0.65	0.08	0.2	-0.03	-0.68	0.13	-0.6	-0.37	0.14	-0.31	-0.67	0.44	0.3	-0.29	-0.89	0.13	0.22	0.2	0

Table 2.S3. Pearson producted-moment correlation analysis results for within treatment interactions.

		IVD_c			M/BS			MC_{length}			MC_{area}			BSC_{area}			M_{si}			BS_{si}			VB_{si}			IAS_{si}			$Dist_H$			SD		
		22	28	35	22	28	35	22	28	35	22	28	35	22	28	35	22	28	35	22	28	35	22	28	35	22	28	35	22	28	35	22	28	35
	22	0.72**	-	-	ns	-	-	0.68**	-	-	0.65**	-	-	0.84**	-	-	0.67**	-	-	0.94***	-	-	0.58*	-	-	0.6*	-	-	0.98***	-	-	-0.66**	-	-
LT	28	-	0.63**	-	-	ns	-	-	0.89***	-	-	0.87**	-	-	0.82**	-	-	0.82**	-	-	0.68**	-	-	0.58*	-	-	0.56*	-	-	0.98***	-	-	ns	-
	35	-	-	0.66*	-	-	ns	-	-	0.85**	-	-	0.91***	-	-	0.85**	-	-	ns	-	-	0.92***	-	-	0.65*	-	-	0.87**	-	-	0.98***	-	-	ns
	22	-	-	-	ns	-	-	0.81**	-	-	0.77**	-	-	0.91***	-	-	0.62*	-	-	0.75**	-	-	ns	-	-	ns	-	-	0.69**	-	-	ns	-	-
IVD_c	28	-	-	-	-	ns	-	-	0.62*	-	-	0.6*	-	-	0.69**	-	-	ns	-	-	ns	-	-	ns	-	-	ns	-	-	0.58*	-	-	ns	-
	35	-	-	-	-	-	-0.62*	-	-	ns	-	-	ns	-	-	0.81***	-	-	ns	-	-	0.73**	-	-	0.74**	-	-	0.66*	-	-	0.76**	-	-	ns
	22	-	-	-	-	-	-	ns	-	-	ns	-	-	ns	-	-	ns	-	-	ns	-	-	ns	-	-	-0.78**	-	-	ns	-	-	ns	-	-
M/BS	28	-	-	-	-	-	-	-	0.74**	-	-	0.71**	-	-	ns	-	-	0.83**	-	-	ns	-	-	ns	-	-	ns	-	-	ns	-	-	ns	-
	35	-	-	-	-	-	-	-	-	ns	-	-	ns	-	-	-0.63*	-	-	ns	-	-	ns	-	-	-0.68**	-	-	-0.63*	-	-	ns	-	-	ns
	22	-	-	-	-	-	-	-	-	-	0.87**	-	-	0.8**	-	-	0.84**	-	-	0.67**	-	-	ns	-	-	ns	-	-	0.72**	-	-	-0.66**	-	-
MC_{length}	28	-	-	-	-	-	-	-	-	-	-	0.93***	-	-	0.58*	-	-	0.94***	-	-	ns	-	-	ns	-	-	ns	-	-	0.83**	-	-	ns	-
	35	-	-	-	-	-	-	-	-	-	-	-	0.95***	-	-	0.74**	-	-	0.81**	-	-	0.81**	-	-	ns	-	-	ns	-	-	0.81**	-	-	ns
	22	-	-	-	-	-	-	-	-	-	-	-	-	0.68**	-	-	0.90***	-	-	0.61*	-	-	0.98**	-	-	ns	-	-	0.65**	-	-	-0.65**	-	-
MC_{area}	28	-	-	-	-	-	-	-	-	-	-	-	-	-	ns	-	-	0.93***	-	-	ns	-	-	0.55*	-	-	ns	-	-	0.79**	-	-	-0.56*	-
	35	-	-	-	-	-	-	-	-	-	-	-	-	-	-	0.75**	-	-	0.79**	-	-	0.81**	-	-	ns	-	-	0.62*	-	-	0.9***	-	-	-0.67*
	22	-	-	-	-	-	-	-	-	-	-	-	-	-	-	-	0.58*	-	-	0.91***	-	-	ns	-	-	ns	-	-	0.84**	-	-	-0.62*	-	-
BSC_{area}	28	-	-	-	-	-	-	-	-	-	-	-	-	-	-	-	-	ns	-	-	0.86**	-	-	ns	-	-	0.79**	-	-	0.85**	-	-	ns	-
	35	-	-	-	-	-	-	-	-	-	-	-	-	-	-	-	-	-	ns	-	-	0.97***	-	-	0.75**	-	-	0.74**	-	-	0.86**	-	-	ns
	22	-	-	-	-	-	-	-	-	-	-	-	-	-	-	-	-	-	-	0.6*	-	-	ns	-	-	ns	-	-	0.68**	-	-	-0.69**	-	-
M_{si}	28	-	-	-	-	-	-	-	-	-	-	-	-	-	-	-	-	-	-	-	ns	-	-	0.56*	-	-	ns	-	-	0.74**	-	-	ns	-
	35	-	-	-	-	-	-	-	-	-	-	-	-	-	-	-	-	-	-	-	-	ns	-	-	ns	-	-	ns	-	-	ns	-	-	ns
	22	-	-	-	-	-	-	-	-	-	-	-	-	-	-	-	-	-	-	-	-	-	0.57*	-	-	0.64*	-	-	0.94***	-	-	-0.6*	-	-
BS_{si}	28	-	-	-	-	-	-	-	-	-	-	-	-	-	-	-	-	-	-	-	-	-	-	ns	-	-	0.74**	-	-	0.72**	-	-	ns	-
	35	-	-	-	-	-	-	-	-	-	-	-	-	-	-	-	-	-	-	-	-	-	-	-	0.75**	-	-	0.79**	-	-	0.9***	-	-	ns
	22	-	-	-	-	-	-	-	-	-	-	-	-	-	-	-	-	-	-	-	-	-	-	-	-	ns	-	-	0.55*	-	-	ns	-	-
VB_{si}	28	-	-	-	-	-	-	-	-	-	-	-	-	-	-	-	-	-	-	-	-	-	-	-	-	-	ns	-	-	ns	-	-	ns	-
	35	-	-	-	-	-	-	-	-	-	-	-	-	-	-	-	-	-	-	-	-	-	-	-	-	-	-	0.68**	-	-	0.65*	-	-	ns
	22	-	-	-	-	-	-	-	-	-	-	-	-	-	-	-	-	-	-	-	-	-	-	-	-	-	-	-	0.59*	-	-	ns	-	-
IAS_{si}	28	-	-	-	-	-	-	-	-	-	-	-	-	-	-	-	-	-	-	-	-	-	-	-	-	-	-	-	-	0.59*	-	-	ns	-
	35	-	-	-	-	-	-	-	-	-	-	-	-	-	-	-	-	-	-	-	-	-	-	-	-	-	-	-	-	-	0.87**	-	-	ns
	22	-	-	-	-	-	-	-	-	-	-	-	-	-	-	-	-	-	-	-	-	-	-	-	-	-	-	-	-	-	-	-0.71**	-	-
$Dist_H$	28	-	-	-	-	-	-	-	-	-	-	-	-	-	-	-	-	-	-	-	-	-	-	-	-	-	-	-	-	-	-	-	ns	-
	35	-	-	-	-	-	-	-	-	-	-	-	-	-	-	-	-	-	-	-	-	-	-	-	-	-	-	-	-	-	-	-	-	-0.66*
	22	-	-	-	-	-	-	-	-	-	-	-	-	-	-	-	-	-	-	-	-	-	-	-	-	-	-	-	-	-	-	-	-	-
SD	28	-	-	-	-	-	-	-	-	-	-	-	-	-	-	-	-	-	-	-	-	-	-	-	-	-	-	-	-	-	-	-	-	-
	35	-	-	-	-	-	-	-	-	-	-	-	-	-	-	-	-	-	-	-	-	-	-	-	-	-	-	-	-	-	-	-	-	-
	22	-	-	-	-	-	-	-	-	-	-	-	-	-	-	-	-	-	-	-	-	-	-	-	-	-	-	-	-	-	-	-	-	-
SS	28	-	-	-	-	-	-	-	-	-	-	-	-	-	-	-	-	-	-	-	-	-	-	-	-	-	-	-	-	-	-	-	-	-
	35	-	-	-	-	-	-	-	-	-	-	-	-	-	-	-	-	-	-	-	-	-	-	-	-	-	-	-	-	-	-	-	-	-
	22	-	-	-	-	-	-	-	-	-	-	-	-	-	-	-	-	-	-	-	-	-	-	-	-	-	-	-	-	-	-	-	-	-
a_{max}	28	-	-	-	-	-	-	-	-	-	-	-	-	-	-	-	-	-	-	-	-	-	-	-	-	-	-	-	-	-	-	-	-	-
	35	-	-	-	-	-	-	-	-	-	-	-	-	-	-	-	-	-	-	-	-	-	-	-	-	-	-	-	-	-	-	-	-	-

Table 2.S3. continued

		IVD_c			M / BS			MC_{length}			MC_{area}			BSC_{area}			M_{si}			BS_{si}			VB_{si}			IAS_{si}			$Dist_H$			SD		
		22	28	35	22	28	35	22	28	35	22	28	35	22	28	35	22	28	35	22	28	35	22	28	35	22	28	35	22	28	35	22	28	35
ES	22	-	-	-	-	-	-	-	-	-	-	-	-	-	-	-	-	-	-	-	-	-	-	-	-	-	-	-	-	-	-	-	-	-
	28	-	-	-	-	-	-	-	-	-	-	-	-	-	-	-	-	-	-	-	-	-	-	-	-	-	-	-	-	-	-	-	-	-
	35	-	-	-	-	-	-	-	-	-	-	-	-	-	-	-	-	-	-	-	-	-	-	-	-	-	-	-	-	-	-	-	-	-
a_{op}	22	-	-	-	-	-	-	-	-	-	-	-	-	-	-	-	-	-	-	-	-	-	-	-	-	-	-	-	-	-	-	-	-	-
	28	-	-	-	-	-	-	-	-	-	-	-	-	-	-	-	-	-	-	-	-	-	-	-	-	-	-	-	-	-	-	-	-	-
	35	-	-	-	-	-	-	-	-	-	-	-	-	-	-	-	-	-	-	-	-	-	-	-	-	-	-	-	-	-	-	-	-	-
% a	22	-	-	-	-	-	-	-	-	-	-	-	-	-	-	-	-	-	-	-	-	-	-	-	-	-	-	-	-	-	-	-	-	-
	28	-	-	-	-	-	-	-	-	-	-	-	-	-	-	-	-	-	-	-	-	-	-	-	-	-	-	-	-	-	-	-	-	-
	35	-	-	-	-	-	-	-	-	-	-	-	-	-	-	-	-	-	-	-	-	-	-	-	-	-	-	-	-	-	-	-	-	-
g_{smax}	22	-	-	-	-	-	-	-	-	-	-	-	-	-	-	-	-	-	-	-	-	-	-	-	-	-	-	-	-	-	-	-	-	-
	28	-	-	-	-	-	-	-	-	-	-	-	-	-	-	-	-	-	-	-	-	-	-	-	-	-	-	-	-	-	-	-	-	-
	35	-	-	-	-	-	-	-	-	-	-	-	-	-	-	-	-	-	-	-	-	-	-	-	-	-	-	-	-	-	-	-	-	-
IVD	22	-	-	-	-	-	-	-	-	-	-	-	-	-	-	-	-	-	-	-	-	-	-	-	-	-	-	-	-	-	-	-	-	-
	28	-	-	-	-	-	-	-	-	-	-	-	-	-	-	-	-	-	-	-	-	-	-	-	-	-	-	-	-	-	-	-	-	-
	35	-	-	-	-	-	-	-	-	-	-	-	-	-	-	-	-	-	-	-	-	-	-	-	-	-	-	-	-	-	-	-	-	-
VD	22	-	-	-	-	-	-	-	-	-	-	-	-	-	-	-	-	-	-	-	-	-	-	-	-	-	-	-	-	-	-	-	-	-
	28	-	-	-	-	-	-	-	-	-	-	-	-	-	-	-	-	-	-	-	-	-	-	-	-	-	-	-	-	-	-	-	-	-
	35	-	-	-	-	-	-	-	-	-	-	-	-	-	-	-	-	-	-	-	-	-	-	-	-	-	-	-	-	-	-	-	-	-
TLV	22	-	-	-	-	-	-	-	-	-	-	-	-	-	-	-	-	-	-	-	-	-	-	-	-	-	-	-	-	-	-	-	-	-
	28	-	-	-	-	-	-	-	-	-	-	-	-	-	-	-	-	-	-	-	-	-	-	-	-	-	-	-	-	-	-	-	-	-
	35	-	-	-	-	-	-	-	-	-	-	-	-	-	-	-	-	-	-	-	-	-	-	-	-	-	-	-	-	-	-	-	-	-
LMA	22	-	-	-	-	-	-	-	-	-	-	-	-	-	-	-	-	-	-	-	-	-	-	-	-	-	-	-	-	-	-	-	-	-
	28	-	-	-	-	-	-	-	-	-	-	-	-	-	-	-	-	-	-	-	-	-	-	-	-	-	-	-	-	-	-	-	-	-
	35	-	-	-	-	-	-	-	-	-	-	-	-	-	-	-	-	-	-	-	-	-	-	-	-	-	-	-	-	-	-	-	-	-
A_n	22	-	-	-	-	-	-	-	-	-	-	-	-	-	-	-	-	-	-	-	-	-	-	-	-	-	-	-	-	-	-	-	-	-
	28	-	-	-	-	-	-	-	-	-	-	-	-	-	-	-	-	-	-	-	-	-	-	-	-	-	-	-	-	-	-	-	-	-
	35	-	-	-	-	-	-	-	-	-	-	-	-	-	-	-	-	-	-	-	-	-	-	-	-	-	-	-	-	-	-	-	-	-
g_s	22	-	-	-	-	-	-	-	-	-	-	-	-	-	-	-	-	-	-	-	-	-	-	-	-	-	-	-	-	-	-	-	-	-
	28	-	-	-	-	-	-	-	-	-	-	-	-	-	-	-	-	-	-	-	-	-	-	-	-	-	-	-	-	-	-	-	-	-
	35	-	-	-	-	-	-	-	-	-	-	-	-	-	-	-	-	-	-	-	-	-	-	-	-	-	-	-	-	-	-	-	-	-
iWUE	22	-	-	-	-	-	-	-	-	-	-	-	-	-	-	-	-	-	-	-	-	-	-	-	-	-	-	-	-	-	-	-	-	-
	28	-	-	-	-	-	-	-	-	-	-	-	-	-	-	-	-	-	-	-	-	-	-	-	-	-	-	-	-	-	-	-	-	-
	35	-	-	-	-	-	-	-	-	-	-	-	-	-	-	-	-	-	-	-	-	-	-	-	-	-	-	-	-	-	-	-	-	-

LT: leaf mesophyll thickness (µm); IVD_c: interveinal Distance measured from leaf cross-sections (µm); *M : BS*: mesophyll to bundle sheath ratio; MC_{length}: length of mesophyll cell (µm); MC_{area}: area of single mesophyll cell (µm^2); BSC_{area}: area of single bundle sheath cel l (µm^2); M_{si}: mesophyll surface area per IVD_c (µm^2 µm^{-1}); BS_{si}: bundle sheath surface area per IVD_c (µm^2 µm^{-1}); VB_{si}: vascular bundle surface area per IVD_c (µm^2 µm^{-1}); IAS_{si}: intercellular airspace surface area per IVD_c (µm^2 µm^{-1}); $Dist_H$: Hydrau lic Distance (µm); *SD*: stomatal density (mm^{-2}); *SS*: stomatal size (µm^2); a_{max}: maximum stomatal pore aperture (µm^2); *ES*: Epidermal cel l size (µm^2); a_{op}: operation stomatal aperture (µm^2); *% a*: percentage of a_{op} to a_{max}; g_{max}: maximum theoritical stomatal conductance (mol m^{-2} s^{-1}); *IVD*: inter-veinal distance (mm); *DV*: total vein density (mm mm^{-2}); *TLV*: Total Number of longitudinal veins; $\delta^{13}C$: carbon isotopic composition (‰); *LMA*: leaf mass per area (g m^{-2}); A_n: net carbon assim lation rate (µmol m^{-2} s^{-1}); g_s: stomatal conductance (mol m^{-2} s^{-1}); *iWUE*: intrinsic w ater use efficiency (µmol CO_2 mol^{-1} H_2O); *LW*: leaf w idth (cm).

Table 2.S3. continued

		SS			a_{max}			ES			a_{op}			% a			g_{smax}			IVD			VD			TLV			LMA			A_n			g_s			iWUE			LW		
		22	28	35	22	28	35	22	28	35	22	28	35	22	28	35	22	28	35	22	28	35	22	28	35	22	28	35	22	28	35	22	28	35	22	28	35	22	28	35	22	28	35
LT	22	0.57*	-	-	ns	-	-	ns	-	-	0.79**	-	-	ns	-	-	ns	-	-	0.61*	-	-	-0.7**	-	-	ns	-	-	ns	-	-	ns	-	-	ns	-	-	ns	-	-	ns	-	-
	28	-	ns	-	-	ns	-	-	0.73*	-	-	ns	-	-	ns	-	-	ns	-	-	ns	-	-	ns	-	-	0.61*	-	-	ns	-	-	ns	-	-	ns	-	-	ns	-	-	ns	-
	35	-	-	0.96***	-	-	0.9**	-	-	0.85**	-	-	ns	-	-	ns	-	-	ns	-	-	0.61*	-	-	ns	-	-	0.85**	-	-	ns	-	-	ns	-	-	ns	-	-	ns	-	-	ns
IVD_c	22	ns	-	-	ns	-	-	ns	-	-	0.85**	-	-	0.62*	-	-	ns	-	-	0.66**	-	-	-0.7**	-	-	ns	-	-	ns	-	-	ns	-	-	0.58*	-	-	-0.78**	-	-	0.63*	-	-
	28	-	ns	-	-	ns	-	-	ns	-	-	ns	-	-	ns	-	-	ns	-	-	0.89**	-	-	ns	-	-	ns	-	-	ns	-	-	ns	-	-	ns	-	-	ns	-	-	ns	-
	35	-	-	0.63*	-	-	0.7*	-	-	ns	-	-	ns	-	-	ns	-	-	ns	-	-	0.83**	-	-	-0.8**	-	-	ns	-	-	ns	-	-	ns	-	-	ns	-	-	-0.86**	-	-	0.66*
M / BS	22	ns	-	-	ns	-	-	ns	-	-	ns	-	-	ns	-	-	ns	-	-	-0.62*	-	-	ns	-	-	ns	-	-	-0.65**	-	-	ns	-	-	ns	-	-	ns	-	-	ns	-	-
	28	-	ns	-	-	ns	-	-	ns	-	-	ns	-	-	ns	-	-	ns	-	-	ns	-	-	ns	-	-	ns	-	-	ns	-	-	ns	-	-	ns	-	-	ns	-	-	ns	-
	35	-	-	ns	-	-	ns	-	-	ns	-	-	ns	-	-	ns	-	-	ns	-	-	ns	-	-	ns	-	-	ns	-	-	ns	-	-	ns	-	-	ns	-	-	ns	-	-	ns
MC_{length}	22	ns	-	-	ns	-	-	ns	-	-	0.71**	-	-	0.63**	-	-	-0.59*	-	-	ns	-	-	-0.7**	-	-	ns	-	-	ns	-	-	ns	-	-	ns	-	-	-0.55*	-	-	ns	-	-
	28	-	ns	-	-	ns	-	-	ns	-	-	ns	-	-	ns	-	-	ns	-	-	0.76**	-	-	-0.72**	-	-	ns	-	-	ns	-	-	ns	-	-	ns	-	-	ns	-	-	ns	-
	35	-	-	0.88**	-	-	0.7*	-	-	ns	-	-	ns	-	-	ns	-	-	ns	-	-	ns	-	-	ns	-	-	0.76**	-	-	ns	-	-	ns	-	-	ns	-	-	ns	-	-	ns
MC_{area}	22	ns	-	-	ns	-	-	0.71*	-	-	0.62*	-	-	ns	-	-	ns	-	-	ns	-	-	-0.58*	-	-	ns	-	-	ns	-	-	ns	-	-	ns	-	-	ns	-	-	ns	-	-
	28	-	ns	-	-	ns	-	-	0.78**	-	-	ns	-	-	ns	-	-	-0.61*	-	-	0.7*	-	-	ns	-	-	ns	-	-	ns	-	-	ns	-	-	ns	-	-	ns	-	-	ns	-
	35	-	-	0.94***	-	-	0.76**	-	-	0.8**	-	-	ns	-	-	ns	-	-	ns	-	-	ns	-	-	ns	-	-	0.8**	-	-	ns	-	-	ns	-	-	ns	-	-	-0.6*	-	-	ns
BSC_{area}	22	ns	-	-	ns	-	-	ns	-	-	0.88***	-	-	0.58*	-	-	ns	-	-	0.83**	-	-	-0.83**	-	-	ns	-	-	ns	-	-	ns	-	-	ns	-	-	-0.71**	-	-	0.57*	-	-
	28	-	ns	-	-	ns	-	-	0.7*	-	-	ns	-	-	0.58*	-	-	ns	-	-	0.85**	-	-	ns	-	-	ns	-	-	ns	-	-	ns	-	-	ns	-	-	ns	-	-	ns	-
	35	-	-	0.76**	-	-	0.69*	-	-	0.68*	-	-	ns	-	-	ns	-	-	ns	-	-	0.63*	-	-	ns	-	-	ns	-	-	ns	-	-	ns	-	-	ns	-	-	-0.63*	-	-	ns
M_{si}	22	ns	-	-	ns	-	-	ns	-	-	0.56*	-	-	ns	-	-	ns	-	-	ns	-	-	ns	-	-	ns	-	-	ns	-	-	ns	-	-	ns	-	-	ns	-	-	ns	-	-
	28	-	ns	-	-	ns	-	-	ns	-	-	ns	-	-	ns	-	-	ns	-	-	ns	-	-	ns	-	-	ns	-	-	ns	-	-	ns	-	-	ns	-	-	ns	-	-	ns	-
	35	-	-	0.66*	-	-	ns	-	-	ns	-	-	ns	-	-	ns	-	-	ns	-	-	ns	-	-	ns	-	-	0.67*	-	-	ns	-	-	ns	-	-	ns	-	-	ns	-	-	ns
BS_{si}	22	0.56*	-	-	ns	-	-	ns	-	-	0.8**	-	-	ns	-	-	ns	-	-	0.74**	-	-	-0.81**	-	-	ns	-	-	ns	-	-	ns	-	-	ns	-	-	-0.57*	-	-	ns	-	-
	28	-	0.72**	-	-	ns	-	-	ns	-	-	0.7**	-	-	0.79**	-	-	ns	-	-	ns	-	-	ns	-	-	0.58*	-	-	ns	-	-	ns	-	-	0.64**	-	-	ns	-	-	0.63**	-
	35	-	-	0.78**	-	-	0.76**	-	-	0.69*	-	-	ns	-	-	ns	-	-	ns	-	-	0.63*	-	-	ns	-	-	0.67*	-	-	ns	-	-	ns	-	-	ns	-	-	-0.63*	-	-	0.8**
VB_{si}	22	0.6*	-	-	0.68**	-	-	ns	-	-	ns	-	-	ns	-	-	ns	-	-	ns	-	-	ns	-	-	0.67**	-	-	ns	-	-	ns	-	-	ns	-	-	ns	-	-	ns	-	-
	28	-	0.66*	-	-	ns	-	-	ns	-	-	ns	-	-	ns	-	-	ns	-	-	ns	-	-	ns	-	-	ns	-	-	ns	-	-	ns	-	-	ns	-	-	ns	-	-	ns	-
	35	-	-	ns	-	-	0.74**	-	-	ns	-	-	ns	-	-	ns	-	-	ns	-	-	0.63*	-	-	ns	-	-	ns	-	-	ns	-	-	ns	-	-	ns	-	-	ns	-	-	ns
IAS_{si}	22	0.58*	-	-	0.63*	-	-	ns	-	-	0.66*	-	-	ns	-	-	ns	-	-	0.63*	-	-	ns	-	-	ns	-	-	0.85**	-	-	ns	-	-	ns	-	-	ns	-	-	ns	-	-
	28	-	ns	-	-	ns	-	-	ns	-	-	ns	-	-	ns	-	-	ns	-	-	ns	-	-	ns	-	-	ns	-	-	ns	-	-	ns	-	-	ns	-	-	ns	-	-	ns	-
	35	-	-	0.85**	-	-	0.84**	-	-	0.95***	-	-	ns	-	-	ns	-	-	ns	-	-	ns	-	-	ns	-	-	0.68*	-	-	0.59*	-	-	ns	-	-	ns	-	-	-0.73**	-	-	0.79**
$Dist_H$	22	ns	-	-	ns	-	-	ns	-	-	0.77**	-	-	ns	-	-	ns	-	-	0.62*	-	-	-0.74**	-	-	ns	-	-	ns	-	-	ns	-	-	ns	-	-	ns	-	-	ns	-	-
	28	-	ns	-	-	ns	-	-	0.85**	-	-	ns	-	-	ns	-	-	ns	-	-	ns	-	-	ns	-	-	ns	-	-	ns	-	-	ns	-	-	ns	-	-	ns	-	-	ns	-
	35	-	-	0.93***	-	-	0.9***	-	-	0.88***	-	-	0.65*	-	-	ns	-	-	ns	-	-	0.67*	-	-	-0.63*	-	-	0.8**	-	-	ns	-	-	ns	-	-	ns	-	-	-0.82**	-	-	0.74**
SD	22	ns	-	-	ns	-	-	-0.78**	-	-	-0.67**	-	-	ns	-	-	0.88***	-	-	0.77**	-	-	0.76**	-	-	ns	-	-	ns	-	-	ns	-	-	ns	-	-	ns	-	-	ns	-	-	ns
	28	-	-0.63*	-	-	ns	-	-	ns	-	-	-0.73**	-	-	-0.78**	-	-	0.88***	-	-	0.7**	-	-	ns	-	-	ns	-	-	ns	-	-	ns	-	-	ns	-	-	ns	-	-	ns	-
	35	-	-	-0.68**	-	-	ns	-	-	ns	-	-	-0.85**	-	-	-0.87***	-	-	0.91***	-	-	ns	-	-	0.57*	-	-	ns	-	-	ns	-	-	ns	-	-	ns	-	-	0.67**	-	-	ns
SS	22	-	-	-	0.88***	-	-	ns	-	-	ns	-	-	ns	-	-	ns	-	-	ns	-	-	ns	-	-	ns	-	-	ns	-	-	-0.83**	-	-	ns	-	-	ns	-	-	ns	-	-
	28	-	-	-	-	0.66*	-	-	ns	-	-	0.75**	-	-	0.62*	-	-	ns	-	-	ns	-	-	ns	-	-	ns	-	-	ns	-	-	ns	-	-	0.66**	-	-	ns	-	-	0.8**	-
	35	-	-	-	-	-	0.93***	-	-	0.87**	-	-	0.65*	-	-	-	-	-	ns	-	-	0.59*	-	-	-0.67**	-	-	0.72**	-	-	ns	-	-	ns	-	-	0.55*	-	-	-0.76**	-	-	0.78**

Table 2.S3. continued

		SS			a_{max}			ES			a_{op}			% a			g_{smax}			IVD			VD			TLV			LMA			A_n			g_s			iWUE			LW		
		22	28	35	22	28	35	22	28	35	22	28	35	22	28	35	22	28	35	22	28	35	22	28	35	22	28	35	22	28	35	22	28	35	22	28	35	22	28	35	22	28	35
a_{max}	22	-	-	-	-	-	-	ns	-	-	ns	-	-	-0.65**	-	-	ns	-	-	ns	-	-	ns	-	-	0.85**	-	-	ns	-	-	-0.75**	-	-	ns	-	-	ns	-	-	ns	-	-
	28	-	-	-	-	-	-	-	ns	-	-	ns	-	-	ns	-	-	ns	-	-	ns	-	-	ns	-	-	ns	-	-	ns	-	-	ns	-	-	0.64*	-	-	-0.57*	-	-	0.79**	-
	35	-	-	-	-	-	-	-	-	ns	-	-	0.59*	-	-	ns	-	-	ns	-	-	0.66*	-	-	-0.62*	-	-	ns	-	-	ns	-	-	ns	-	-	0.7**	-	-	-0.79**	-	-	0.69**
ES	22	-	-	-	-	-	-	-	-	-	ns	-	-	ns	-	-	ns	-	-	ns	-	-	ns	-	-	ns	-	-	ns	-	-	ns	-	-	ns	-	-	ns	-	-	ns	-	-
	28	-	-	-	-	-	-	-	-	-	-	ns	-	-	ns	-	-	ns	-	-	0.74*	-	-	ns	-	-	ns	-	-	ns	-	-	ns	-	-	ns	-	-	ns	-	-	ns	-
	35	-	-	-	-	-	-	-	-	-	-	-	ns	-	-	ns	-	-	ns	-	-	ns	-	-	ns	-	-	0.86**	-	-	ns	-	-	ns	-	-	ns	-	-	-0.7*	-	-	0.88**
a_{op}	22	-	-	-	-	-	-	-	-	-	-	-	-	0.67**	-	-	ns	-	-	0.72**	-	-	-0.71**	-	-	ns	-	-	ns	-	-	ns	-	-	ns	-	-	-0.75**	-	-	0.73**	-	-
	28	-	-	-	-	-	-	-	-	-	-	-	-	-	0.91***	-	-	ns	-	-	ns	-	-	ns	-	-	0.75**	-	-	ns	-	-	ns	-	-	0.77**	-	-	-0.72**	-	-	0.85**	-
	35	-	-	-	-	-	-	-	-	-	-	-	-	-	-	0.92***	-	-	-0.65**	-	-	ns	-	-	-0.72**	-	-	0.67**	-	-	ns	-	-	ns	-	-	0.77**	-	-	-0.79**	-	-	0.73***
% a	22	-	-	-	-	-	-	-	-	-	-	-	-	-	-	-	-0.74**	-	-	ns	-	-	ns	-	-	-0.59*	-	-	ns	-	-	0.73**	-	-	0.71**	-	-	ns	-	-	ns	-	-
	28	-	-	-	-	-	-	-	-	-	-	-	-	-	-	-	-	-0.65**	-	-	ns	-	-	ns	-	-	0.59*	-	-	ns	-	-	ns	-	-	0.62*	-	-	-0.58*	-	-	0.63*	-
	35	-	-	-	-	-	-	-	-	-	-	-	-	-	-	-	-	-	-0.83**	-	-	ns	-	-	-0.57*	-	-	ns	-	-	ns	-	-	ns	-	-	0.59*	-	-	-.0.58*	-	-	ns
g_{smax}	22	-	-	-	-	-	-	-	-	-	-	-	-	-	-	-	-	-	-	ns	-	-	0.64*	-	-	ns	-	-	ns	-	-	ns	-	-	ns	-	-	ns	-	-	ns	-	-
	28	-	-	-	-	-	-	-	-	-	-	-	-	-	-	-	-	-	-	-	-0.67*	-	-	0.8**	-	-	ns	-	-	ns	-	-	ns	-	-	ns	-	-	ns	-	-	ns	-
	35	-	-	-	-	-	-	-	-	-	-	-	-	-	-	-	-	-	-	-	-	ns	-	-	ns	-	-	ns	-	-	ns	-	-	ns	-	-	ns	-	-	ns	-	-	ns
IVD	22	-	-	-	-	-	-	-	-	-	-	-	-	-	-	-	-	-	-	-	-	-	-0.8**	-	-	ns	-	-	0.58*	-	-	ns	-	-	ns	-	-	ns	-	-	ns	-	-
	28	-	-	-	-	-	-	-	-	-	-	-	-	-	-	-	-	-	-	-	-	-	-	-0.79**	-	-	ns	-	-	ns	-	-	ns	-	-	ns	-	-	ns	-	-	ns	-
	35	-	-	-	-	-	-	-	-	-	-	-	-	-	-	-	-	-	-	-	-	-	-	-	-0.92***	-	-	ns	-	-	0.66*	-	-	ns	-	-	0.62*	-	-	-0.75**	-	-	0.6*
VD	22	-	-	-	-	-	-	-	-	-	-	-	-	-	-	-	-	-	-	-	-	-	-	-	-	ns	-	-	ns	-	-	ns	-	-	ns	-	-	ns	-	-	ns	-	-
	28	-	-	-	-	-	-	-	-	-	-	-	-	-	-	-	-	-	-	-	-	-	-	-	-	-	ns	-	-	ns	-	-	ns	-	-	ns	-	-	ns	-	-	ns	-
	35	-	-	-	-	-	-	-	-	-	-	-	-	-	-	-	-	-	-	-	-	-	-	-	-	-	-	ns	-	-	ns	-	-	ns	-	-	-0.78**	-	-	0.9***	-	-	-0.72**
TLV	22	-	-	-	-	-	-	-	-	-	-	-	-	-	-	-	-	-	-	-	-	-	-	-	-	-	-	-	ns	-	-	ns	-	-	ns	-	-	ns	-	-	ns	-	-
	28	-	-	-	-	-	-	-	-	-	-	-	-	-	-	-	-	-	-	-	-	-	-	-	-	-	-	-	-	ns	-	-	ns	-	-	0.62*	-	-	ns	-	-	0.74**	-
	35	-	-	-	-	-	-	-	-	-	-	-	-	-	-	-	-	-	-	-	-	-	-	-	-	-	-	-	-	-	ns	-	-	ns	-	-	ns	-	-	ns	-	-	0.66*
LMA	22	-	-	-	-	-	-	-	-	-	-	-	-	-	-	-	-	-	-	-	-	-	-	-	-	-	-	-	-	-	-	ns	-	-	ns	-	-	ns	-	-	ns	-	-
	28	-	-	-	-	-	-	-	-	-	-	-	-	-	-	-	-	-	-	-	-	-	-	-	-	-	-	-	-	-	-	-	0.72**	-	-	ns	-	-	ns	-	-	ns	-
	35	-	-	-	-	-	-	-	-	-	-	-	-	-	-	-	-	-	-	-	-	-	-	-	-	-	-	-	-	-	-	-	-	ns	-	-	0.63*	-	-	ns	-	-	0.75**
A_n	22	-	-	-	-	-	-	-	-	-	-	-	-	-	-	-	-	-	-	-	-	-	-	-	-	-	-	-	-	-	-	-	-	-	0.88***	-	-	ns	-	-	ns	-	-
	28	-	-	-	-	-	-	-	-	-	-	-	-	-	-	-	-	-	-	-	-	-	-	-	-	-	-	-	-	-	-	-	-	-	-	0.66**	-	-	ns	-	-	ns	-
	35	-	-	-	-	-	-	-	-	-	-	-	-	-	-	-	-	-	-	-	-	-	-	-	-	-	-	-	-	-	-	-	-	-	-	-	0.69**	-	-	ns	-	-	ns
g_s	22	-	-	-	-	-	-	-	-	-	-	-	-	-	-	-	-	-	-	-	-	-	-	-	-	-	-	-	-	-	-	-	-	-	-	-	-	-	-0.85**	-	-	0.78**	-	-
	28	-	-	-	-	-	-	-	-	-	-	-	-	-	-	-	-	-	-	-	-	-	-	-	-	-	-	-	-	-	-	-	-	-	-	-	-	-	-	-0.6*	-	-	0.91***	-
	35	-	-	-	-	-	-	-	-	-	-	-	-	-	-	-	-	-	-	-	-	-	-	-	-	-	-	-	-	-	-	-	-	-	-	-	-	-	-	-	-0.71**	-	-	0.75**
iWUE	22	-	-	-	-	-	-	-	-	-	-	-	-	-	-	-	-	-	-	-	-	-	-	-	-	-	-	-	-	-	-	-	-	-	-	-	-	-	-	-	-	-0.92***	-	-
	28	-	-	-	-	-	-	-	-	-	-	-	-	-	-	-	-	-	-	-	-	-	-	-	-	-	-	-	-	-	-	-	-	-	-	-	-	-	-	-	-	-	-0.68**	-
	35	-	-	-	-	-	-	-	-	-	-	-	-	-	-	-	-	-	-	-	-	-	-	-	-	-	-	-	-	-	-	-	-	-	-	-	-	-	-	-	-	-	-	-0.75**

LT leaf mesophyll thickness (µm); IVD_x interveinal Distance measured from leaf cross-sections (µm); *M BS* mesophyll to bundle sheath ratio; $MC_{exp,s}$ length of mesophyll cell (µm); MC_{area} area of single mesophyll cell (µm²); BSC_{area} area of single bundle sheath cell (µm²); M_s mesophyll surface area per IVD_x (µm² µm⁻¹); BS_s bundle sheath surface area per IVD_x (µm² µm⁻¹); VB_x vascular bundle surface area per IVD_x (µm² µm⁻¹); IAS_x intercellular airspace surface area per IVD_x (µm² µm⁻¹); $Dist_H$ Hydraulic Distance (µm); *SD* stomatal density (mm⁻²); *SS* stomatal size (µm²); a_{max} maximum stomatal pore aperture (µm²); *ES* Epidermal cell size (µm²); a_{op} operation stomatal aperture (µm²); % *a* percentage of a_{op} to a_{max}; g_{max} maximum theoretical stomatal conductance (mol m⁻² s⁻¹); *IVD* inter-veinal distance (mm); *DV* total vein density (mm mm⁻²); *TLV* Total Number of longitudinal veins; $\delta^{13}C$ carbon isotopic composition (‰); *LMA* leaf mass per area (g m⁻²); A_n net carbon assimilation rate (µmol m⁻² s⁻¹); g_s stomatal conductance (mol m⁻² s⁻¹); *iWUE* intrinsic water use efficiency (µmol CO_2 mol⁻¹ H_2O); *LW* leaf width (cm).

Chapter 3

Diurnal regulation of water use efficiency is influenced by morning stomatal conductance and stomatal pore size, and is linked to efficient stomatal response to transient light

3.1 ABSTRACT

Most studies measure leaf-level intrinsic (*iWUE*) at midday assuming it is representative of plant function across the day. Stomata, photosynthesis and sugars fluctuate diurnally and in response to changing environments, affecting *iWUE*. I grew six Sorghum genotypes with contrasting stomatal anatomy and *iWUE* under mild environmental conditions to describe how diurnal *iWUE* is regulated. I also investigated stomatal responses to light transients (simulating sun flecks and transient cloud shadows). I found that morning and midday stomatal conductance (g_s) greatly determined diurnal *iWUE*, while afternoon *gs* had little influence. While stomatal density (*SD*) scaled positively with *iWUE*, g_s was mostly regulated by pore size, irrespective of maximum aperture size. The rate of stomatal closure in response to lower light intensity correlated with diurnal *iWUE*, unlike the rate of stomatal opening to increased light intensity. Photosynthetic depression at the end of the light period was not explained by sugar accumulation. In conclusion, single measurements are not sufficient to infer diurnal *iWUE* in the key C_4 crop Sorghum, with time of day needed to take into consideration. However, Sorghum genotypes that conserved water under short-term light transients were also more conservative throughout the day without negatively impacting photosynthesis. That is, the rate of stomatal closure to lower light intensity can be a novel selection trait for improving *iWUE* in C_4 crops.

3.2 INTRODUCTION

Rising global population will increase demand for water, meaning that agricultural production will need to use, if anything, less of the available water (Condon *et al.*, 2004). Water use efficiency (*WUE*) describes the efficiency of water use by the plant to produce yield, usually by comparing bulk water use per unit carbon gained. At leaf level, *WUE* is expressed as the ratio of water use relative to carbon assimilation rate (A_n) to stomatal conductance to water vapour (g_s). Due to their carbon concentrating mechanism (CCM), C_4 crops, such as *Sorghum bicolor*, already achieve higher *iWUE*, and combined with lack of genetic variability and low heritability for *iWUE* associated traits has deterred breeding for *iWUE* in C_4 crops (Balota *et al.*, 2008; Leakey *et al.*, 2019). In the previous study, several anatomical features including leaf width, stomatal features and vein density have been shown to influence *iWUE* under different conditions. Specifically, this study aimed to utilise the variation in stomatal density and size shown in the various sorghum genotypes to further probe control on *iWUE* under non steady-state conditions.

Most studies of leaf *WUE* are performed by measuring instantaneous leaf gas exchange and assuming that *iWUE* is representative of whole-plant *WUE* (Medrano *et al.*, 2015). Similarly, *iWUE* is dependent on steady-state gas exchange measurements, but over the day there are environmental changes on temporal scales that can influence g_s and A_n and hence influencing *iWUE* (Moualeu-Ngangue *et al.*, 2016). Several studies have established that A_n and g_s vary diurnally, with a big contribution from the circadian clock (de Dios *et al.*, 2016; Resco de Dios, 2017; Resco de Dios *et al.*, 2017, 2020; Resco de Dios and Gessler, 2018). Usually, in sunny, clear days, A_n and g_s follow the increase in sunlight over the diurnal period to a maximum at midday, before dropping in the afternoon with decreased light as the sun fades. Under non-limiting conditions and over diurnal periods, g_s is mainly dependent on irradiance (Vialet-Chabrand *et al.*, 2013). One inference from this is that *iWUE* measured at midday, the period of most intense sunlight and highest evaporative demand, is the most representative of the leaf's ability to restrict transpiration relative to carbon gain (Leakey *et al.*, 2019). Cowan and Farquhar (1977) have suggested that leaves optimise carbon gain to water lost by maximizing A_n for a given g_s, possibly signifying that midday measurements of *iWUE* are sufficient to represent leaf performance. However, diurnal changes in light conditions, as well as the effect of circadian rhythm, metabolic factors (such as ABA or sugar accumulation) and hydraulic changes have shown to impact

A_n and g_s values at different times of the day (Mencuccini *et al.*, 2000; Bucci *et al.*, 2003; Bläsing *et al.*, 2005; Haydon *et al.*, 2013; Resco de Dios and Gessler, 2018). This would ultimately lead to different *iWUE* values across the day.

The relative rate of response of A_n and g_s to short-term changes in light conditions are asymmetric (Kirschbaum *et al.*, 1988; Tinoco-Ojanguren and Pearcy, 1993a, 1993b), with the response of A_n usually an order of magnitude faster (McAusland *et al.*, 2016). This lag in the stomatal response creates a temporal disconnect between g_s and A_n (Lawson and Blatt, 2014). This lag can limit the attainment of high A_n under favourable conditions (such as high light) when the leaf suddenly needs to open the stomata. Under photosynthetically unfavourable conditions (such as low light), this lag causes excessive water loss without any gains in carbon capture. These inefficiencies in stomatal behaviour result in lower *iWUE*, making the optimisation of stomatal behaviour a key component of achieving higher *iWUE* (Lawson and Blatt, 2014). Nonetheless, few studies have explored the variation in stomatal response rate and its impact on *iWUE*. In addition, Matthews *et al.* (2018) showed that the rate of g_s response to light is different at different times of the day, corresponding with different steady state values of g_s and *iWUE*. Consequently, selecting for improved stomatal responses to changing environmental conditions can be a way to improve *iWUE*.

Previous research showed that g_s is dependent on stomatal aperture and size in the leaves of Sorghum (Chapter 2; Pan *et. al.*, 2021). Variation in stomatal density (*SD*) and size (*SS*) have also been linked to the rate of stomatal opening and closing (Hetherington and Woodward, 2003). Lower *SS* leads to a greater membrane surface area to volume ratio (Drake *et al.*, 2013), enabling faster exchange of ions and solutes between the guard cells and neighbouring epidermal cells (Lawson and Blatt, 2014), and leading to faster stomatal responses. Because of the negative relationship between *SS* and *SD* found across angiosperms (Franks and Beerling, 2009), increased *SD* has also been related an increase in stomatal opening rate (Drake *et al.*, 2013). In C_4 grasses, the relationship between *SD* and *SS* is less strict (Taylor *et al.*, 2012). Nonetheless, the dumb-bell shaped guard cells unique to graminoid grasses—compared to the kidney shaped guard cells other lineages—gives them an advantage that results in faster stomatal responses due to an increase in volume-to-surface-area ratio between guard cells and subsidiary cells (Franks

and Farquhar, 2007). One of the aims of this study is to probe the impact of stomatal anatomy on the speed of stomatal responses in the model C_4 graminoid, Sorghum.

Lastly, the relationship between diurnal leaf gas exchange and soluble sugar accumulation was investigated in this study. Triose phosphate utilisation post the Calvin cycle and soluble sugar export from the source leaf affect photosynthetic gene expression and ultimately photosynthetic rates (Paul and Pellny, 2003; Paul and Foyer, 2001). In addition, sugars impact circadian regulation of diurnal gene expression (Bläsing *et al.*, 2005; Haydon *et al.*, 2013). Soluble sugars are a key product of photosynthesis, with sucrose, for example, a key transport molecule of carbohydrates and energy sources from the source to sink, whether in leaves or other plant organs. Hence, it has been assumed that the accumulation of those molecules at the end of the light period after sustained photosynthesis throughout the day would cause feedback inhibition of photosynthesis and stomatal conductance (Kelly *et al.*, 2013). However, the mechanisms of these assumed feedback responses are still not fully understood, especially in C_4 species (Henry *et al.*, 2020).

This study aims attempted to explore whether steady state ("spot") measurements of *iWUE* (and its main drivers, g_s and A_n) can be reconciled with measures of *WUE* at longer temporal scales. We also investigated how the extent to which variation in stomatal anatomical features affect influences diurnal g_s and *iWUE*. We attempt to link the achievement of high diurnal *iWUE* with stomatal response to simulate the effect of rapid changes in light intensity, like these those experienced in the field.. This is specifically to test responses to transient, rapid changes in light that occur during the day, i.e., sunflecks or passing cloudy weather, and not necessarily to simulate light levels at different times of day (sunset vs midday for example). Those sunflecks can also occur at different times of the day and affect incident light. My aim was to link those responses to sunflecks to steady state *iWUE*. Finally, I explored whether changes in diurnal sugar concentration explain diurnal changes in A_n and g_s.

Specifically, I selected six Sorghum genotypes from the previous experiment that represented extremes in stomatal anatomy, leaf width and *iWUE* to test the following hypotheses: 1) g_s is negatively correlated with *iWUE* across the day; 2) Low g_s is determined by high *SD*, low *SS*, and/or smaller functional aperture; 3) These anatomical

characters will also enable leaves to open and close stomata faster; 4) Fast kinetic stomatal responses will correlate with high *iWUE* across the day; and 5) Accumulation of sugars towards the end of the day is linked to a decrease in photosynthesis.

3.3 MATERIALS & METHODS

Genotype selection

Sorghum genotypes were selected based on the findings of a previous experiment, where ten sorghum genotypes with different leaf width, were subjected to three different growth temperatures. The previous experiment established a coordination between leaf width, stomatal size, stomatal density and water use efficiency. Hence, six genotypes, each three representing a contrasting combination of the four parameters, were selected for this experiment (**Table 3.1**).

Plant culture

The experiment was conducted in two controlled environment chambers (BioChambers walk-in growth cabinets) at the Hawkesbury Institute for the Environment, Western Sydney University, Richmond, NSW, Australia (-33.612032, 150.749098). Seeds were sown in the 3.5 L pots used throughout the experiment. Pots were well watered and covered with tin foil to keep seeds in the dark until 2-3 days after germination, after which the foil was removed, and seedlings exposed to full chamber conditions. The soil mix used was a standard commercial potting mix with no fertiliser pre-added (Turtle Nursery and Landscape Supplies, Windsor, NSW). Fertiliser mix (Yates Thrive All Purpose Soluble Fertiliser) was supplied to the pots with irrigation water every other day. The conditions inside the growth chambers were maintained at 60% humidity; 12 h day/night cycle; 26 / 20 °C day / night air temperature. Carbon dioxide concentration ([CO_2[) was kept at 400 ppm. The photoperiod was divided into three segments to simulate the natural sun light cycle: 2 h at 400 µmol m^{-2} s^{-1} (8-10 am), followed by 8 h at 1000 µmol m^{-2} s^{-1} (10 am to 6 pm), with the final 2 h of the day (6-8 pm) at 400 µmol m^{-2} s^{-1}.

Leaf gas exchange

A Li-6400XT (LICOR Biosciences, Lincoln, Nebraska) was used to measure rates of leaf gas exchange. Net carbon assimilation rate (A_n) and stomatal conductance g_s were measured at four times during the day to follow the diurnal patters: late night/pre-dawn (6 am – 2 hours before 'dawn'); Early morning (9-10 am – I hour after light); Midday (12-2 pm – 4-5 hours after light); Late afternoon (6 pm – 2 hours before darkness). Environmental conditions inside the LI-6400XT leaf cuvettes are maintained at: 25°C block temperature, 400 ppm CO_2, 400 µmol s^{-1} flow rate, 60% relative humidity. Light intensity was 1000 µmol quanta m^{-2} s^{-1} during the 3 day-time measurements to standardise the conditions and gain a better understanding of changes in photosynthetic capacity and highlight the impact of time of day rather than light intensity (i.e. time of day as the sole variable), and 0 µmol quanta m^{-2} s^{-1} for the pre-dawn measurement to obtain dark respiration rate, R_d). At each time point, 4-5 plants were measured, then immediately sampled for sugar analysis. Measurements were made on the youngest fully expanded leaf (YFEL), which corresponded to the 11^{th}-14^{th} leaf after 2 months of growth. The leaf measured at midday was also used for analysis of stomatal anatomy. Intrinsic water use efficiency (*iWUE*) was calculated as the ratio of A_n : g_s at each time point. Overall, sampling was conducted over 3-4 days total, where all gas exchange, hydraulics and anatomical and sugar samples were collected.

Stomatal traits

For analysis of stomatal traits, two negative impressions using nail varnish were taken of the middle portion of the leaf, one impression each side of the midrib. The impressions were attached to a microscope slide using transparent tape and imaged under a light microscope (Axio Scope.A1, Carl Zeiss Microscopy GmbH, Jena, Germany) at x10 magnification. Photomicrographs analysed using Image J (Schneider *et al.*, 2012). Analysis focussed on the area between the 2^{nd} and 3^{rd} minor longitudinal veins. The area under the microscope was calculated, and the stomata were counted. Stomatal density (*SD*) was calculated as the number of stomata per unit area. Within each area where *SD* was calculated, ten stomata were randomly selected to measure the following variables. Stomatal size (*SS*) was calculated by multiplying stomatal width (W_s, including two guard cells and two subsidiary cells) by guard cell length (L_s) and expressed in μm^2. Epidermal

cell size (*ES*) was calculated by dividing the area of the epidermal layer (minus the stomata) by the number of epidermal cells in that area and expressed in μm^2. Maximum pore aperture (a_{max}) was calculated as:

$$a_{max} = W_{gc} \times L_a \qquad (3.1)$$

where W_{gc} = width of the guard cell complex of closed stomata and L_a = is the length of the pore; a_{max} is expressed in μm^2. This formulation was used because the shape of the fully open stomatal pore in grasses geometrically fits a rectangular shape (Franks and Farquhar, 2007; Franks *et al.*, 2014). Also see section 2.3 for more information. Theoretical maximum conductance (g_{smax}) was calculated as follows:

$$g_{smax} = \frac{d}{v}\left((SD \times a_{max})/(l + \frac{\pi}{2}\sqrt{\frac{a_{max}}{\pi}})\right) \qquad (3.2)$$

where d = diffusivity of water vapor in air; v = molar volume of air; l = stomatal pore depth which is assumed to be equivalent to W_{gc} / 2. The model assumes that the stomatal aperture is at its maximum and that all stomata are open. In order to correct for leaf and growth temperature and atmospheric pressure at the site of measurement, d and v were recalculated before being entered into equation (3.2). The equation of d was calculated based on Marrero & Mason (1972):

$$l\,n(Pd) = ln(A) + sln(T) - \frac{S}{T} \qquad (3.3)$$

where A, s and S are empirical constants for the diffusion of water vapour in air with A = 0.00000187 (atm cm^2 s^{-1} (K)$^{-s}$); s = 2.072; S = 0 (K), T is the temperature in Kelvin degrees (K) and P is the local atmospheric pressure at our site (102610 Pa). Using equation 3.3 and the value for constants reported before, the units of d are in cm^2 s^{-1}, and to be used in equation 3.2, d needs to be transformed to m^2 s^{-1} by dividing by 10000. The calculation for v was based on the molar volume of an ideal gas:

$$v = \frac{RT}{P} \qquad (3.4)$$

where R is the ideal gas constant = 8.314462618 J mol^{-1} K^{-1}. Finally, the operational stomatal pore (a_{op}) that matches the corresponding measured g_s (g_s at each time point of

the day) can be calculated using the following formula (Pan et al., 2021). Equation 3.2 can be modified to estimate a_{op}, with the terms rearranged and g_{smax} replaced with measured g_s, but keeping the same theoretical framework. Basically, a_{op} is the replacement term for a_{max}. The resulting equation is:

:

$$a_{op} = \frac{\left(g_s^2 v^2 \frac{\pi}{4} + 2dSDg_s vl\right) + \sqrt{g_s^4 v^4 \frac{\pi^2}{16} + g_s^3 v^3 \, \pi dSDl}}{2d^2 SD^2} \qquad (3.5)$$

The ratio of the operational stomatal pore area (a_{op}) to a_{max} is expressed as a percentage, % stomatal aperture *(% aperture*).

Leaf width and composition

The area in the middle of leaf (where stomatal impressions were taken) was also used as the standardized area to measure leaf width (*LW*). From the gas exchange area, three leaf discs were sampled, dried at 70 °C oven for 48 h then weighed. Leaf mass (g) was divided by disc area (cm^2) to calculate leaf mass per area (*LMA*, g cm^{-2}). The dried leaf material was also used to measure the percentage content of carbon and nitrogen (% C and % N) was determined on ground samples using a CHN analyser (LECO TruSpec, LECO Corporation, Michigan, USA).

Midday leaf water potential, Ψ_{leaf}

The leaf adjacent to the one used for midday gas exchange was used to measure leaf water potential (Ψ_{leaf}) using a pressure chamber (Model 1000 Pressure Chamber, PMS Instrument Company, Albany, Oregon, USA). The leaf was cut and placed inside a plastic bag with a wet paper towel. The bag was exhaled into before sealing then transported into the lab where Ψ_{leaf} was measured within 1 h of excision.

Stomatal kinetic responses

Four to five replicate plants per genotype were selected for the stomatal kinetic analysis performed in the early part of the day (9 – 12 am). These plants were different from those used for the diurnal measurements. A special light regime program was created in the Li-

6400XT. The light regime was made of several 30-minute phases at (1) 400 µmol quanta m^{-2} s^{-1}, (2) 1000 µmol m^{-2} s^{-1}, (3) 100 µmol m^{-2} s^{-1}, (4) 1000 µmol m^{-2} s^{-1} and finally (5) at 100 µmol m^{-2} s^{-1} for 1 h (**Fig.3.S2**). To calculate stomatal kinetics parameters, the model of McAusland *et al.* (2016) was used:

$$g_s\,(t) = (g_{max} - g_0)e^{-e^{\frac{(\lambda - t)}{k}}} + g_0 \qquad (3.6)$$

where $g_s(t)$ is stomatal conductance at time t; g_{max} is the steady state g_s at the asymptote at the end of the response curve; g_0 is the conductance at the start of the light change; k is the time constant that indicates speed of response; λ is a term that describes the time lag in g_s response after the light change and before the response curve starts (negligible for C_4 stomata). The equation describes a Gompertz like curve with exponential increase in g_s until steady state. Excess conductance due to slow stomatal closing was calculated as the time integrated difference between the initial and final g_s during transition from high light to low light:

$$Excess\ Conductance = \int_0^t (g_0 - g_t)dt \qquad (3.7)$$

where t is the time at the end of the curve where g_s reaches steady state. Forgone photosynthesis due to slow stomatal opening was calculated as the difference between the integral of maximum A_n under the observed curve, and the integral of maximum A_n if maximum A_n is reached instantaneously during transition from low light to high light:

$$Forgone\ Photosynthesis = \int_0^t (A_{max-0} - A_{max-t})dt \qquad (3.8)$$

where A_{max-0} and A_{max-t} are extracted from the A_n response curve if A_{max} is reached at time 0 and t respectively. Because the light regime contains distinct phases of high-to-low or low-to-high light changes, the models above (eq. 3.6-3.8) were separately applied to each phase of the curve, and the averages of similar phases per leaf were used (n=4-5).

A_n-C_i Curves

The same leaves used for the stomatal kinetic responses were also used to measure the response of A_n to changes in CO_2 concentrations using a Li-6400XT. The conditions in Li-6400XT cuvette were similar as the diurnal gas exchange, except that light was kept at a

saturating maximum of 1500 µmol m^{-2} s^{-1}. A program was set up to log gas exchange output after 3-5 minutes at each CO_2 concentration. The series of CO_2 concentrations applied were (in ppm): 400, 50, 100, 150, 200, 250, 300, 400, 600, 800, 1000, 1200, 1500, 2000, 400. A linear regression was fitted through the first 4 points of each A_n-C_i curve to calculate the initial slope.

Sugar Analysis

Leaf discs were immediately collected after each diurnal gas exchange measurement from the same area that was inside the LI-6400XT cuvette. The discs were stored in plastic tubes initially in liquid N_2 then at -80°C. Samples were ground (Qiagen Retsch TissueLyser), after which a solution of 80% methanol was added to the ground sample. The mixture was incubated at 90°C on a heat block shaker (30 min). The sample was then centrifuged, and the supernatant transferred to a fresh tube. This was repeated 2-3 times until the ground pellet turned yellow. The supernatant was concentrated using a vacuum evaporator (Concentrator Plus, Eppendorf, Hamburg, Germany) for >3 hours. The concentrated sample was diluted with water and subjected to a series of enzymatic reactions according to the instructions of a sugar analysis kit (Sucrose, D-Fructose, D-Glucose Assay Kit, Megazyme, Bray, Ireland). The colour change was read using a spectrophotometer (Agilent Technologies, Santa Clara, CA) and sugar concentrations were calculated using a spreadsheet provided together with the kit.

Statistical Analysis

Statistical analysis and data visualisation were performed using R software (R Core Team (2020). R: A language and environment for statistical computing. R Foundation for Statistical Computing, Vienna, Austria. URL https://www.R-project.org/). Normality was checked by plotting a generalized linear model and inspecting residual plots. Analysis of variance was carried out using a linear mixed-effects model (packages lme4 and nlme). Variance between groups was performed using a *post hoc* Tukey test. Regression analysis was carried out in R using linear modelling (lm). The model predicted the significance of a linear relationship between the two variables:

$$y = mx + c$$

where *y* (predicted) and *x* (predictor) are the y-axis and x-axis variables respectively, *m* is the slope of the relationship, and *c* is the y-axis intercept. *m* represents the direction of the relationship (negative or positive). A Pearson product moment correlation analysis was performed to test statistical significance of relationships and obtain correlation coefficients.

3.4 RESULTS

Diurnal patterns of gas exchange and soluble sugar concentrations

Carbon assimilation rate (A_n) and stomatal conductance (g_s) increased significantly (p<0.05; **Fig.3.1 a,b**) from pre-dawn/night-time levels to early morning, with another significant (p<0.05) increase from morning to midday. In the afternoon, both A_n and g_s decreased significantly (p<0.05). Intrinsic water use efficiency (*iWUE*) was lowest at midday and highest in the morning and the afternoon (**Fig.3.1 c**). For total soluble sugars (**Fig.3.1 d**), the concentration increased with time during the light period (p<0.05), with maximum occurring in the afternoon. There were significant differences in gas exchange and soluble sugar concentration between genotypes at the individual time points, illustrated in **Table 3.2** and **Table 3.4**. Diurnal pattern of individual sugars is shown in **Fig.3.S2**. Genotype x Time interaction were significant except for *iWUE* (**Table 3.5**), but for the other five variables, changing time had a significant impact on genotype distribution.

Relationship between gas exchange parameters during the day

There was a significant positive relationship between A_n and g_s (**Fig.3.2 a**) in the morning (r=0.93, p<0.001) and afternoon (r=0.97, p<0.001). At midday, the relationship between A_n and g_s had a high r-value but was not significant (r=0.68, p>0.1). There was a significant negative relationship between *iWUE* and g_s (**Fig.3.2 b**) in the morning (r=-0.85, p<0.05) and midday (r=-0.92, p<0.001), but not in the afternoon. There was no correlation between A_n and *iWUE* at any time of the day (**Fig.3.2 c**).

The influence of stomatal anatomy on diurnal g_s

In the morning and midday, g_s was significantly negatively correlated with both adaxial stomatal density (SD_{adax}) (morning r=-0.82, midday r=-0.76, p<0.1; **Fig.3.3 a**) and abaxial stomatal density (SD_{abax}) (morning r=-0.75, midday r=-0.83, p<0.1; **Fig.3.3 b**). These relationships were not significant in the afternoon. Generally, stomatal size (*SS*) displayed no significant relationships with g_s except for a negative relationship (r=-0.76, p<0.1) between adaxial *SS* (SS_{adax}) and midday *gs* (**Fig.3.3 c,d**). Stomatal index (*SI*) and g_s were not correlated (**Fig.3.3 e,f**). Adaxial epidermal cell size (ES_{adax}) was positively correlated

with g_s during the morning and midday (r=0.81, p<0.1 and r=0.84, p<0.05 respectively), but no other relationships were significant with ES (**Fig.3.3 g,h**).

Stomatal pore regulation of g_s and *iWUE*

Morning (r=0.88, p<0.05), midday (r=0.86, p<0.05) and afternoon (r=0.75, p<0.1) g_s were positively correlated with calculated operational aperture (a_{op}; **Fig.3.4 a**). There was a positive correlation between g_s (**Fig.3.4 b**) and a_{op} expressed as a percentage of maximum aperture (*% aperture*) in the morning (r=0.85, p<0.05) and midday (r=0.96, p<0.001), but not in the afternoon. Theoretical maximum stomatal conductance ($g_{s\ max}$) had no influence on g_s (**Fig.3.4 c**), but the percentage ratio of g_s to $g_{s\ max}$ (*% conductance*) was positively correlated with g_s at all times (**Table 3.S1**) and negatively correlated with morning (r=-0.759, p<0.1) and midday (r=-0.92, p<0.1), but not afternoon *iWUE* (**Fig.3.4 d**).

Relationship between diurnal *iWUE* and stomatal kinetic responses

The time-constant describing the speed of stomatal opening (k_{op}) did not correlate with *iWUE* (**Fig.3.5 a**). Similarly, the estimated lost photosynthesis due to slow stomatal opening ($Forgone_{photo}$) showed no association with *iWUE* at any time of the day (**Fig.3.5 c**). However, the time constant describing the speed of stomatal closing (k_{cl}) was negatively linked to morning (r=-0.77, p<0.1) and midday (r=-0.8, p<0.1) *iWUE*, but not in the afternoon (**Fig.3.5 b**). Only midday *iWUE* (r=-0.78, p<0.1) was correlated (**Fig.3.5 d**) with calculated excess conductance due to slow stomatal closing ($Excess_{Cond}$).

Influence of stomatal characteristics on k_{cl}

Both SD_{adax} (r=-0.74, p<0.1) and SD_{abax} (r=-0.97, p<0.05) had a negative association with k_{cl} (**Fig.3.6 a**), but SS_{adax} and SS_{abax} had no influence on k_{cl} (**Fig.3.6 b**). A significant positive association was observed for k_{cl} with morning (r=0.84, p<0.05) and midday (r=0.91, p<0.05) a_{op} (**Fig.3.6 c**), but not in the afternoon. The same trend was observed for *% aperture* (**Fig.3.6 d**) which showed a positive relationship with k_{cl} in the morning (r=0.78, p<0.1) and midday (r=0.8, p<0.1) and afternoon (r=0.78, p<0.05). There was a negative relationship (r=0.75, p<0.1) between k_{cl} and $g_{s\ max}$ (**Fig.3.6 e**), and k_{cl} was positively

correlated with *% conductance* at morning and midday (r=0.8 and r=0.81 respectively, p<0.1; **Fig.3.6 f**).

Soluble sugar concentrations and diurnal gas exchange

The relationships between A_n and g_s with glucose, fructose and sucrose concentrations in the leaf are shown in **Fig.3.7**. No discernible pattern of relationships was observed, apart from a positive relationship between sucrose concentration and A_n (r=0.78, p<0.1; **Fig.3.7 c**) and g_s (r=0.77, p<0.1; **Fig.3.7 f**) at midday. The percentage change in gas exchange and sugar concentration at each time point relative to the maximum was calculated and presented in **Fig.3.8**. The percentage change in fructose concentration was positively correlated with the percentage increase in A_n (r=0.77, p<0.001; **Fig .8 b**) and g_s (r=0.78, p<0.001; **Fig.3.8 e**).

3.5 DISCUSSION

Intrinsic water use efficiency (*iWUE*) refers to the ratio of CO_2 assimilation rate (A_n) to stomatal conductance (g_s). It is usually determined from a single gas exchange measurement during midday. Previous studies (Pan *et al.*, 2021; chapter 2) incorporating the same Sorghum genotypes studied here highlighted the anatomical determinants of the *iWUE* vs g_s relationship. The aim of the current study was to investigate diurnal variation in these relationships, and to test whether determinants of *iWUE* at one time point remain influential throughout the diurnal period. This is important to better understand if *iWUE* is regulated differently throughout the day, especially regarding changing irradiance and the possible effect of circadian clock. Accordingly, the diurnal pattern of *iWUE* and its determinants was measured. In addition, stomatal aperture responses to abrupt changes in light intensity were analysed at midday to test if efficient transition between light phases correlates with the genotype's capacity to maintain high *iWUE* over the day. Finally, evidence indicates that sugar accumulation during the day can have negative feedback on photosynthetic capacity, in addition to the role sugars play as circadian signals. Hence, the diurnal concentration of soluble sugars was determined to discern possible links with leaf gas exchange.

Stomatal conductance exerts a greater influence on *iWUE* in the morning and midday relative to the late afternoon

As previously reported for C_4 leaves (Cano *et al.*, 2019), g_s emerged as the main determinant of *iWUE*, while A_n had little effect (**Fig.3.2**). Determining whether single measurements of *iWUE* are representative of leaf or plant *WUE* in crops over long temporal periods is a key question, and one of the foci of the current study (Condon *et al.*, 2004; Medrano *et al.*, 2015). While stable carbon isotope composition has been successfully utilised as a proxy for integrated *WUE* in C_3 crops (Rebetzke *et al.*, 2002), the application of this tool to C_4 crops, such as Sorghum, has yielded limited success so far (Henderson *et al.*, 1998; von Caemmerer *et al.*, 2014; Ellsworth and Cousins, 2016; Feldman *et al.*, 2018; Ellsworth *et al.*, 2020). Hence. calculating the integral of the diurnal *iWUE* curve to estimate diurnal *WUE* (*dWUE*) provided a proxy for diurnal *iWUE* to be compared with spot measurements at different timepoints. Interestingly, *iWUE* did not change significantly across the time points despite significant change in A_n and *gs*,

possibly indicating that *iWUE* is kept constant throughout the day via coordinating A_n and g_s to achieve constant *iWUE*. This can suggest that these genotypes follow the leaf optimisation hypothesis first proposed by Cowan (1978). where leaves aim to extract the highest carbon gain while minimising water loss through transpiration, which is a relationship that is similar in principle to the A_n/g_s used to obtain *iWUE* . This is in contrast to findings in grapevine (Medrano *et al.*, 2012, 2015), where *iWUE* varied significantly throughout the day along with changes in A_n and g_s. However, those studies integrated canopy locations (and with it, intercepted light) and daily measurements when obtaining their diurnal time courses, which was not investigated in this study. Medrano et al., (2012) do highlight that *dWUE* is related to *iWUE* at midday in grapevine, like we show here in Sorghum, but we add that morning *iWUE* is also related to *dWUE* but not afternoon *iWUE*, highlighting the different controls on *dWUE*.

Higher morning and midday *iWUE* resulted in higher *dWUE*, while afternoon *iWUE* was not influential (**Table 3.S1**). Morning and midday g_s were negatively associated with *dWUE* and *iWUE*, while both *dWUE* and *iWUE* had no association with afternoon g_s (**Table 3.S1**). A previous field study with 48 sorghum genotypes (including the ones used in this study) found similar results. Using a larger sorghum collection, they reported strong g_s *vs iWUE* relationships in the morning and midday, and only a weak one in the afternoon (Pan *et al.*, 2021). The larger field trial confirmed the results reported here, indicating that the influence of g_s on *iWUE* is weaker later in the day. Both afternoon A_n and g_s values were similar to those observed in the morning (**Table 3.2**), where *iWUE* vs g_s relationship was observed. However, the study of Pan et al. (2021) was conducted in the field and with the onset of mild water stress, while this chapter presents the results under a controlled chamber conditions that more thoroughly elucidate the impact of changing light levels and time of day, and how differentially they affect diurnal *iWUE* and g_s. There are multiple mechanisms that cause reduction in g_s and A_n late in the day (discussed below), but that should not stop the dependence of *iWUE*, a ratio incorporating A_n and g_s, on either. The only likely explanation is that the combined effect of reduced A_n and g_s in the afternoon influences *iWUE* but with genotypic difference in which of A_n or g_s is more influential later in the day, removing possible linear association between genotype average *iWUE* and g_s (or A_n).

Diurnal g_s is determined by functional pore size rather than anatomical conductance

Stomatal conductance on area basis is determined by the number (stomatal density, *SD*) and size (*SS*) of stomata (Franks and Beerling, 2009). In this study, *SD* was negatively correlated with morning and midday g_s (**Fig.3.3 a,b**). Generally, increasing g_s by increasing *SD* entails high energetic costs and space limitations that impact guard cell function (Franks and Farquhar, 2007). Due to the operation of the CO_2 concentrating mechanism (CCM), C_4 leaves have non-limiting CO_2 supply to photosynthesis, and generally select for lower *SD* (Taylor *et al.*, 2012). Hence, C_4 grasses, including Sorghum, can compensate for their low *SD* by increasing *SS* to facilitate larger pore sizes and ultimately higher g_s, as seen in the previous work with C_4 grasses (Taylor *et al.*, 2012; Chapter 2; Pan *et al.*, 2021; Israel, 2020). There is usually a negative association between *SD* and *SS* in angiosperms (Franks and Beerling, 2009; Taylor *et al.*, 2012), and that might explain the negative association between *SD* and g_s in this study. In the previous studies with these Sorghum genotypes, there was a positive association between *SD* and *iWUE*, replicated here as well (**Table 3.S1**), and thus it can be concluded that high *SD* leads to smaller *SS* and hence lower g_s. This is what the previous studies found, but in this chapter the data turned out differently (**Fig.3.3 c-d**). The lack of relationship between *SS* and g_s in this study can be partially attributed to the lower evaporative demands in the growth cabinets not requiring an active limitation on transpiration (recorded midday temperature of 25°C and relative humidity of 70%). This closely resembles the cool temperature treatment in the previous chapter, which also showed the weakest relationship between *SS* and g_s (Chapter 2). The lack of a relationship between anatomical maximum conductance (g_{smax}, calculated based on anatomical dimensions of the stomata) and g_s highlights the poor anatomical control on g_s in Sorghum leaves (**Table 3.S1**). Also, while g_{smax} is considered a key determinant of g_s, that is at species level (Franks *et al.*, 2014; Murray *et al.*, 2020), within-species consistency in this relationship can be marginal (Ohsumi *et al.*, 2007; Ouyang *et al.*, 2017). Rather, aperture size was the main determinant of g_s in this study (**Fig.3.4**). While a more open operational pore (a_{op}) generally leads to higher g_s, it is the percentage of a_{op} as part of the maximum pore (a_{max}) that highlights the importance of pore responses in determining g_s rather than the anatomical dimensions. This is further confirmed by the positive relationship between g_s

and the ratio g_s:g_{smax} (% conductance) at the different timepoints, indicating that while g_{smax} remains stable between genotypes, different genotypes achieve higher conductance through increasing aperture size. This is similar to findings in other C_4 grasses (Israel, 2020; Pan *et al.*, 2021), and likely because the shape of graminoid guard cells ("dumb-bell"), combined with the presence of subsidiary cells that facilitate ion and solute movements and a high volume-to-surface area ratio, enables stomatal pores to open quickly and reach larger pores (higher % of a_{max}) under optimal conditions, resulting in higher g_s (Franks and Farquhar, 2007; Lawson and Blatt, 2014; Lawson and Matthews, 2020).

In this study, the impact of pore-related and anatomical determinants of g_s waned during the afternoon (**Fig.3.3** and **Fig.3.4**). Reductions in g_s towards the end of the day were previously observed even under constant light conditions (Matthews *et al.*, 2017; Resco de Dios and Gessler, 2018; Resco de Dios *et al.*, 2020). Given that leaf anatomical features are constant, several processes have been implicated in this afternoon depression. Low leaf water potential (Ψ_{leaf}) at the end of the light period causes stomatal closure (Comstock and Mencuccini, 1998; Mencuccini *et al.*, 2000), as well as reductions in leaf hydraulic conductance, K_{leaf} (Meinzer and Grantz, 1990; Meinzer *et al.*, 1995; Zwieniecki and Holbrook, 1998; Bucci *et al.*, 2003). Stomatal pore responses have been shown to be very reliant on hydraulic signals (Mott and Franks, 2001; Buckley *et al.*, 2003; Buckley, 2005; Franks, 2006), and hence, hydraulic changes are one of the main reasons that explain afternoon g_s depression (Resco de Dios, 2017). In this study, plants were watered at the end of the light period. Hence, it is likely that during the afternoon, after a full day of transpiration, the soil is at its driest, putting into effect the sequence of events that lead to stomatal closure in order to preserve hydraulic integrity and avoid xylem cavitation (Brodribb and Holbrook, 2003, 2004; Brodribb *et al.*, 2003). This mechanism is similar to what occurs under field conditions (Hirasawa and Hsiao, 1999). Only midday Ψ_{leaf} was measured, with lower midday Ψ_{leaf} potentially leading to more closed stomata in the afternoon. However, negative midday Ψ_{leaf} correlated with higher afternoon g_s (**Table 3.S1**). This is possibly because Ψ_{leaf} may recover before the end of the light period (Hirasawa and Hsiao, 1999), which might have occurred in this study when afternoon g_s was measured as there was, in some instances, up to 6 hours between the midday and afternoon measurements. Alternatively, midday leaf water status (represented by Ψ_{leaf})

may be the result of sensitivity to g_s earlier in the day (Whitehead, 1998; Buckley, 2005), and in this study higher morning g_s did lead to more negative midday Ψ_{leaf} (**Table 3.S1**), while in the afternoon hydraulic signals and g_s might be disconnected similar to the observed afternoon disconnect in other parameters within this study. Ultimately, because our plants were well watered, the impact of Ψ_{leaf} on g_s might have been minimal, as midday Ψ_{leaf} and g_s did not correlate anyway. Also, other mechanisms that might explain observed afternoon g_s depression include the accumulation of ABA throughout the day (Mencuccini *et al.*, 2000; Blum, 2015), with ABA a known instigator of stomatal closure (Franks and Farquhar, 2001; McAdam and Brodribb, 2014, 2016). Finally, the accumulation of sugars has also been suggested as a possible feedback signal that causes stomatal closure (Outlaw, 2003; Kelly *et al.*, 2013). This study found no conclusive evidence for this hypothesis, with the possible exception of changes in fructose, as discussed below.

Stomatal closing rate is linked to diurnal *iWUE*, and is influenced by stomatal density and pore area

One of the aims of this study is to relate the leaf's ability to regulate diurnal gas exchange with its responses to transient light conditions that leaves experience under field conditions, such as passing clouds (Kirschbaum *et al.*, 1988; Tinoco-Ojanguren and Pearcy, 1993b, 1993a; Lawson and Vialet-Chabrand, 2018; Murchie *et al.*, 2018). Specifically, the aim was to provide more relevant information regarding the speed of stomatal response and the implications this may have for carbon assimilation and *iWUE* (Matthews *et al.*, 2017; Vialet-Chabrand *et al.*, 2017). The time constants for rate of closing and opening (k_{cl} and k_{op}, respectively) measured here are equivalent to previously reported data for Sorghum (McAusland *et al.*, 2016). Asymmetry between opening and closing responses have been reported before (Vico *et al.*, 2011), with stomatal closing being faster than opening, added to the observation that k_{op} and k_{cl} do not correlate (**Table 3.S1**). This can indicate that a preference to reduce water loss as opposed to increasing assimilation as a mechanism to increase *WUE*, and this is what the data indicate (**Fig.3.5**), as k_{cl} correlated negatively with *iWUE* during the morning and midday but not the afternoon, while k_{op} showed no association. Furthermore, *dWUE* also correlated with k_{cl}, rather than k_{op} (**Table 3.S1**), further suggesting that Sorghum prioritises minimising water loss over maximizing carbon gain during diurnal light

transitions as a mechanism to maintain or increase *iWUE* over long temporal periods. Faster stomatal transitions have been shown before to correlate with *dWUE* in cucumber (Moualeu-Ngangue *et al.*, 2016).

There was a significant correlation between k_{cl} and anatomical features such as *SD*, a_{op}, g_{smax}, *% conductance* and *% aperture* (**Fig.3.6**). Several studies have stipulated that smaller *SS* leads to faster kinetic responses (Drake *et al.*, 2013; Raven, 2014) especially in dumb-bell shaped guard cells such as in Sorghum (Hetherington and Woodward, 2003; McAusland *et al.*, 2016). Leaves follow the one-cell spacing rule during stomatal development (Bergmann, 2004; Franks and Casson, 2014), to allow efficient ion and solute transport to guard cells from epidermal cell during pore opening or closing (Dow *et al.*, 2014; Lawson and Blatt, 2014). A lower *SS* would allow greater surface area to volume ratio between guard and epidermal cells, making solute transfer more efficient (Drake *et al.*, 2013) and stomatal kinetics faster. Because *SS* and *SD* are usually negatively associated, it was expected that the negative association between k_{cl} and *SD* would lead to a positive one between *SS* and k_{cl}. However, that was not observed. There could have been less environmental pressure on *SS* due to the lower evaporative demands of the conditions compared to the previous experiment in chapter 2. In *Banksia* spp., Drake *et al.* (2013) found a significant positive influence of *SD* on k_{op}, highlighting the possibility of *SD* influencing stomatal kinetics as well as *SS*. In grasses, especially C_4 lineages, *SD* is reduced compared to other angiosperms, sometimes in conjunction with reduced *SS* (Way, 2012). Despite increased *SD* potentially negatively impacting stomatal kinetics due to reduced space, the low species-specific *SD* of Sorghum compared to other angiosperms (Franks and Beerling, 2009) can mean that genotypic differences in *SD* can still be associated with faster kinetics as epidermal cell sizes measured here are still large compared to other angiosperms (Carins Murphy *et al.*, 2016), and hence those gnetypes can maintain a high volume-to-surface area ratio. However, k_{cl} and anatomical conductance, g_{smax}, were negatively correlated (**Fig.3.6 e**), indicating a level of anatomical control on the speed of stomatal responses persists when considering a parameter (g_{smax}) that combines different anatomical features (*SD*, maximum aperture, pore depth – see Materials & Methods).

The most likely determining factor in terms of guard cell response speed is the presence of a hydro-mechanical feedback response between the subsidiary and guard cells in

grasses (Franks and Farquhar, 2007). The "see-sawing" effect is observed when changes in osmotic and turgor pressure between the two cells allows guard cells to swell into the subsidiary cells when the stomata opens, and shrink (while subsidiary cells swell) when the stomata closes, enabling a quick and efficient manipulation of the stomatal pore size in graminoid grasses (Franks and Farquhar, 2007). This mechanism can also compensate for increase in *SD* that might lead to space limitation, and that genotypic differences in the efficiency of solute transfer and osmotic adjustment can contribute to differences in stomatal kinetics. Fast stomatal kinetic responses are linked to a water conservation strategy in different species, especially those that evolved under low atmospheric CO_2 concentrations (Elliott-Kingston *et al.*, 2016). Low atmospheric CO_2 concentrations was a factor that led to the evolution of C_4 photosynthesis (Edwards *et al.*, 2010), with C_4 species optimal in low latitudes in open grassland and dry conditions compared to other angiosperms, likely contributing to the evolution of more active stomatal responses that promotes higher water use efficiency in species like Sorghum (Way *et al.*, 2014).

Reduced A_n in the afternoon is not linked to soluble sugar accumulation

Afternoon declines in A_n and g_s have been extensively investigated (Resco de Dios, 2017). Sugars accumulate throughout the day and are exported to sink tissue (Bläsing *et al.*, 2005). Excessive accumulation of sugars can trigger a feedback response that leads to the afternoon depression of photosynthesis and conductance (Paul and Foyer, 2001; Outlaw, 2003; Paul and Pellny, 2003; Kelly *et al.*, 2013). Several studies have linked sugar signals such as starch degradation into sucrose (Thalmann *et al.*, 2016; Thalmann and Santelia, 2017) and hexokinase (a sugar-phosphorylating enzyme) expression (Kelly *et al.*, 2013) to stomatal responses. Inhibition of photosynthesis is thought to be mediated by sugar sensors acting as regulators of photosynthetic gene expression (Sheen, 1990; Thompson *et al.*, 2017), as well as the effect of sugars on the circadian clock genes (Bläsing *et al.*, 2005; Haydon *et al.*, 2013). The diurnal patterns of sugars shown here (**Fig.3.1 d**) are similar to those found at different stages of Maize development (Peng *et al.*, 2014), with sucrose increasing along the day to a maximum in the afternoon, while glucose and especially fructose concentrations track changes in A_n (**Fig.3.S1**). The dominance of Sucrose at the end of the day may result from the breakdown of starch into sucrose, coupled with the formation of sucrose molecules from glucose and fructose molecules. The latter point is evident in the rise of sucrose levels in the afternoon coupled with

decrease in glucose and fructose simultaneously. It is likely that high A_n is accompanied by glucose and fructose production, as well as sucrose, until midday, when lower A_n is observed leading to reduction of glucose and fructose production and the depletion of their pool to produce sucrose (Peng *et al.*, 2014). However, correlation analyses of soluble sugar concentrations with gas exchange did not yield any discernible patterns (**Fig.3.7**), and comparing % changes of the measured parameters (**Fig.3.8**) showed that only % changes in fructose tracked % changes in A_n and g_s. This might indicate an association between gas exchange and sugar signals, but the lack of any inhibitory association with changes in sucrose concentration especially in the afternoon suggests no clear evidence for sugar-mediated inhibition of A_n and g_s. There is little direct evidence for photosynthetic inhibition due to sugars in C_4 species like Sorghum (Henry *et al.*, 2020). Monitoring gene expression changes in response to sugar accumulation can shed additional insights on these responses, as well as measuring starch concentrations during the day, which is a future goal of this study.

Conclusion

This study attempted to elucidate how diurnal variation in gas exchange influenced the capacity of Sorghum leaves to maintain *iWUE* along the day, and whether this capacity is related to the leaf's response to transient changes in light like those experienced under field conditions. Data revealed that morning and midday g_s play a significant role in determining diurnal *iWUE*, and that genotypes equipped to maintain high *iWUE* during the day also exhibit fast stomatal closure, reducing excess transpiration, under photosynthetically unfavourable conditions. The rate of g_s was influenced more by functional pore size than anatomical determinants, highlighting the important role of guard cell physiology and kinetic responses in C_4 crops like Sorghum in determining g_s. The study investigated whether the afternoon depression in gas exchange rates was related to soluble sugar accumulation but found unconvincing evidence to support that hypothesis. In conclusion, selecting for Sorghum genotypes that maintain high *iWUE* during the diurnal period can be achieved by selecting for low morning or midday g_s, and by screening for fast stomatal closure, further expanding the possible traits used to select for high *iWUE* in Sorghum and possibly other C_4 crops.

Table 3.1. Mean (±SE) of the four key variables from the results of Chapter 2 of this thesis used for the selection of genotypes used in this study.

Unique Genotype ID		FF_SC449-14E	QL12	R931945-2-2	SC1079-11Ebk	FF_SC906-14E	FF_SC500-9
iWUE	22°C	166.9 (1.9)	159.6 (3.0)	154.9 (2.3)a	150.9 (3.8)	139.7 (2.2)	162.6 (11.2)
(µmol CO_2 mol^{-1}	28°C	150.2 (1.0)a	159.9 (2.5)	140.9 (5.4)ab	132.4 (4.1)a	131.1 (3.0)	158.1 (1.5)
H_2O)	35°C	147.0 (5.7)a	145.9 (1.1)a	124.1 (4.9)b	124.3 (1.8)a	131.1 (3.6)	136.8 (1.6)
	22°C	189.7 (9.9)	197.5 (10.5)	198.2 (6.1)	151.2 (1.6)	169.0 (8.9)	172.8 (5.2)a
SD (mm^{-2})	28°C	199.7 (15.2)	208.9 (35.4)	189.9 (20.7)	174.1 (24.7)	164.9 (7.5)	189.9 (17.9)ab
	35°C	228.3 (5.1)	209.8 (8.7)	185.8 (8.9)	145.6 (12.3)	190.0 (12.1)	233.7 (4.4)b
	22°C	724.3 (33)a	888.3 (56)	959.0 (15)	1012 (57)	978.1 (14)	1045 (48)
SS ($µm^2$)	28°C	1077 (107)b	900.7 (54)	1009 (9.4)	991.1 (83)	1111 (56)	983.4 (19)
	35°C	969 (37)ab	957 (19)	1147 (46)a	1265 (23)a	1041 (52)	922 (33)
	22°C	2.9 (0.4)	3.4 (0.1)	3.4 (0.4)	4.4 (0.3)	4.7 (0.3)	2.6 (0.3)
Leaf Width (cm)	28°C	5.5 (0.2)a	4.5 (0.3)a	5.4 (0.2)a	5.7 (0.4)a	6.2 (0.2)a	4.8 (0.2)a
	35°C	5.2 (0.2)a	5.2 (0.02)b	6.5 (0.1)b	7.3 (0.2)b	6.6 (0.3)a	6.4 (0.1)b

SD: Stomatal Density; SS: Stomatal Siz ; i*WUE* : intrinsic w ater use efficiency

Table 3.2. Mean (±SE) of leaf gas exchange parameters for each Sorghum genotype at the different time points of the diurnal curve, and the parameters that resulted from analysing stomatal kinetic responses to light transitions. The table also shows the results of the *post hoc* Tukey's test for analysis of variance. Mean values that share similar symbols (none, *a, b* or *c*) have no significant difference (p<0.05) between them (n=4-5).

Unique Genotype ID	QL12	SC1079-11Ebk	R931945-2-2	FF_SC906-14E	FF_SC500-9	FF_SC449-14E	**Mean**
R_n (µmol m^{-2} s^{-1})	-1.2 (0.13)	-1.2 (0.14)	-1.31 (0.13)	-1.25 (0.08)	-1.37 (0.08)	-1.33 (0.19)	-1.28 (0.13) a
A_{mor} (µmol m^{-2} s^{-1})	24.62 (0.49)	23.41 (1.03)	24.27 (0.89)	21.37 (0.75)	23.21 (1.31)	16.91 (0.66)a	22.3 (0.86) b
A_{mid} (µmol m^{-2} s^{-1})	27.47 (0.69)	27.1 (0.98)	25.4 (1.33)	27.63 (2.11)	27.4 (0.58)	25.4 (1.38)	26.73 (1.18) c
A_{aft} (µmol m^{-2} s^{-1})	18.8 (1.8)	18.3 (1.58)	22.01 (1.72)	20.03 (1.93)	20.65 (1.72)	10.89 (1.2)a	18.45 (1.66) b
$g_{s\,n}$ (mol m^{-2} s^{-1})	0.01 (0)a	0.01 (0)ab	0.02 (0)ab	0.01 (0)a	0.02 (0)ab	0.02 (0)b	0.01 (0) a
$g_{s\,mor}$ (mol m^{-2} s^{-1})	0.18 (0.03)b	0.17 (0.02)b	0.17 (0.01)b	0.13 (0)ab	0.14 (0.01)ab	0.1 (0.01)a	0.15 (0.01) b
$g_{s\,mid}$ (mol m^{-2} s^{-1})	0.21 (0.02)b	0.19 (0.02)ab	0.17 (0.01)ab	0.19 (0.02)ab	0.17 (0.01)ab	0.16 (0.01)a	0.18 (0.01) c
$g_{s\,aft}$ (mol m^{-2} s^{-1})	0.13 (0.02)ab	0.12 (0.02)ab	0.14 (0.02)b	0.12 (0.02)ab	0.12 (0.01)ab	0.07 (0)a	0.12 (0.02) b
$iWUE_{mor}$ (µmol CO2 mol-1 H2O)	145.71 (13.78)	145.88 (12.1)	142.58 (6.24)	167.73 (6.03)	163.97 (3.99)	162.28 (5.5)	154.69 (7.94)
$iWUE_{mid}$ (µmol CO2 mol-1 H2O)	133.12 (8.17)a	141.33 (7.17)ab	147.14 (3.74)ab	149.95 (3.26)ab	157.25 (4.07)b	157.38 (2.76)b	147.69 (4.86)
$iWUE_{aft}$ (µmol CO2 mol-1 H2O)	153.8 (10.79)	164.61 (13.48)	158.52 (5.54)	165.78 (7.35)	171.72 (4.19)	150.64 (9.53)	160.84 (8.48)

Table 3.2 continued....

A_{wd} (µmol m^{-2})	64.44 (1.13)	62.92 (1.77)	63.65 (1.82)	62.17 (2.26)	64.17 (1.13)	53.18 (2.51)a	61.75 (1.77)
$g_{s\,wd}$ (mol m^{-2})	0.38 (0.05)b	0.35 (0.04)b	0.34 (0.02)ab	0.33 (0.02)ab	0.32 (0.01)ab	0.27 (0.01)a	0.33 (0.03)
dWUE	136.38 (2.01)	141.12 (7.93)	141.99 (2.07)	155.61 (4.02)	157.25 (2.35)	158.15 (3.82)	148.42 (3.7)
Ψ_{leaf} (-MPa)	0.86 (0.15)ab	0.99 (0.21)b	0.93 (0.05)b	0.91 (0.03)ab	0.7 (0.06)ab	0.48 (0.05)a	0.81 (0.09)
k_{cl} (min)	2.49 (0.29)c	2.25 (0.24)bc	1.48 (0.24)ac	0.84 (0.08)a	1.17 (0.2)ab	1.5 (0.25)ac	1.62 (0.22)
Excess Cond (mol m^{-2})	0.75 (0.11)b	0.67 (0.06)ab	0.55 (0.05)ab	0.43 (0.1)ab	0.38 (0.03)a	0.59 (0.07)ab	0.56 (0.07)
WUE_{cl}	68.19 (7.26)ab	71.42 (4.99)ab	59.77 (3.61)a	108.76 (6.36)c	93.18 (6.04)bc	86.4 (5.12)bc	81.29 (5.56)
k_{op} (min)	3.85 (0.37)	2.73 (0.28)	2.31 (0.52)	1.98 (0.37)	2.93 (0.35)	3.7 (0.5)	2.92 (0.4)
Forgone Photo (µmol m^{-2})	74 (7)ab	65.47 (6.03)ab	57.73 (9.73)a	57.86 (7.33)a	64.2 (6.38)a	98.17 (8.27)b	69.57 (7.46)
WUE_{op}	198.31 (15.73)b	164.27 (6.72)a	142.22 (3.67)a	168.45 (2.06)ab	163.31 (1.93)a	143.35 (3.94)a	163.32 (5.68)
slope	0.46 (0.05)	0.42 (0.03)	0.35 (0.02)	0.35 (0.04)	0.41 (0.01)	0.44 (0.03)	0.41 (0.03)
A_{sat} (µmol m^{-2} s^{-1})	38.31 (1.54)	40.17 (1.49)	38.33 (0.36)	29.45 (3.68)	31.96 (1.45)	37.04 (3.23)	38.88 (3.23)

R_n: pre-dawn carbon assimilation rate (night respiration); A_{mor}: carbon assimilation at early morning; A_{mid}: midday carbon assimilation; A_{aft}: afternoon carbon assimilation; $g_{s\,n}$: night-time conductance; $g_{s\,mor}$: stomatal conductance at early morning; $g_{s\,mid}$: midday stomatal conductance; $g_{s\,aft}$: Afternoon stomatal conductance; $iWUE_{mor}$: morning intrinsic water use efficiency; $iWUE_{mid}$: midday intrinsic water use efficiency; $iWUE_{aft}$: afternoon intrinsic water use efficiency; A_{wd}: integrated carbon assimilation rate over the day; gs_{wd}: integrated stomatal conductance over the day; *dWUE*: integrated water use efficiency over the day; Ψ_{leaf}: midday leaf water potential; k_{cl}: closing time of the stomatal pore; *Excess Cond*: excess stomatal conductance due to mismatch of stomatal closing and assimilation rate decrease; WUE_{cl}: integrated water use efficiency during stomatal closure; k_{op}: opening time of the stomatal pore; *Forgone Photo*: lost carbon assimilation due to mismatch of stomatal opening and assimilation rate increase; WUE_{op}: integrated water use efficiency during stomatal opening.

Table 3.3. Mean (±SE) of stomatal anatomical features, leaf compositional features and leaf width for each Sorghum genotype. The data represented was sampled from the midday leaf of the diurnal curve (see Materials & Methods). The table also shows the results of the *post hoc* Tukey's test for analysis of variance. Mean values that share similar symbols (none, *a, b* or *c*) have no significant difference (p<0.05) between them (n=4-5).

Unique Genotype ID	QL12	SC1079-11Ebk	R931945-2-2	FF_SC906-14E	FF_SC500-9	FF_SC449-14E	**Mean**
LW (cm)	4.35 (0.11)ab	4.63 (0.09)ab	4.88 (0.16)ab	4.48 (0.76)a	5.84 (0.69)b	4.6 (0.25)ab	4.79 (0.34)
LMA (g m^{-2})	48 (1.37)ab	41.75 (0.99)ab	47.88 (1.91)ab	42.25 (1.02)ab	50.89 (1.94)b	38.57 (1.3)a	44.89 (1.42)
% N	3.62 (0.2)ab	3.24 (0.15)ab	3.96 (0.48)ab	2.79 (0.38)ab	3.53 (0.18)b	4.33 (0.13)a	3.58 (0.25)
% C	46.01 (0.15)	46.36 (0.07)	46.41 (0.28)	45.53 (0.25)	46.31 (0.14)	48.64 (1.92)	46.54 (0.47)
SD_{adax} (n° mm^{-2})	70.37 (9.34)a	90.43 (3.24)ab	93.87 (4.69)ab	107.65 (6.09)b	89.07 (3.44)ab	108.79 (2.8)b	93.36 (4.93)
SD_{abax} (n° mm^{-2})	95.53 (9.8)a	101.99 (11.85)ab	124.65 (3.93)ac	136.93 (4.6)bc	131.22 (7.03)c	131.73 (3.73)ac	120.34 (6.82)
SS_{adax} (µm^2)	621.42 (31.52)	753.07 (101.21)	847.97 (64.53)	663.93 (27.62)	734.76 (27.32)	804.82 (31.11)	737.66 (47.22)
SS_{abax} (µm^2)	938.33 (73.76)	867.83 (68.68)	1028.47 (35.5)	947.9 (40.86)	1043.24 (38.81)	991.5 (39.78)	969.54 (49.56)
g_{smax} (mol m^{-2} s^{-1})	1.82 (0.2)	2.14 (0.24)	2.47 (0.07)	2.53 (0.09)	2.32 (0.13)	2.78 (0.06)	2.34 (0.12)
SI_{adax} (%)	0.31 (0.01)	0.35 (0.02)	0.32 (0.01)	0.31 (0.02)	0.32 (0.01)	0.31 (0.01)	0.32 (0.01)
SI_{abax} (%)	0.29 (0.01)	0.3 (0.02)	0.3 (0.01)	0.3 (0.01)	0.32 (0.01)	0.28 (0.01)	0.3 (0.01)

Table 3.3 continued...

ES_{adax} (µm^2)	4531.45 (465.31)a	3586.11 (154.77)ab	3189.24 (131.3)b	2714.11 (104.78)b	3396.33 (212.87)b	2605.09 (100.72)b	3337.06 (194.96)
ES_{abax} (µm^2)	1914.87 (104.48)a	1965.75 (89.57)a	2605.91 (114.8)ab	1935.89 (73.47)a	2057.84 (40.31)a	2778.23 (154.94)b	2209.75 (96.26)
$a_{op\text{-}mor}$ (µm^2)	5.86 (1.43)b	4.13 (0.45)ab	3.74 (0.25)ab	2.16 (0.11)a	2.63 (0.26)ab	1.79 (0.13)a	3.38 (0.44)a
$a_{op\text{-}mid}$ (µm^2)	5.97 (0.9)c	5.69 (0.66)bc	4.38 (0.37)ac	3.68 (0.49)ab	3.58 (0.27)a	3.44 (0.24)a	4.46 (0.49)b
$a_{op\text{-}aft}$ (µm^2)	3.9 (0.91)b	2.85 (0.7)ab	2.95 (0.36)ab	2.07 (0.29)ab	2.16 (0.23)ab	1.15 (0.1)a	2.51 (0.43)c
% $aperture_{mor}$	4.12 (1.01)	2.85 (0.41)	2.53 (0.2)	1.82 (0.08)	1.98 (0.2)	1.17 (0.06)	2.41 (0.38)a
% $aperture_{mid}$	4.11 (0.48)	3.84 (0.45)	2.79 (0.19)	2.83 (0.36)	2.71 (0.25)	2.14 (0.14)	3.07 (0.28)b
% $aperture_{aft}$	2.73 (0.63)	2.04 (0.62)	2.02 (0.26)	1.74 (0.14)	1.59 (0.14)	0.74 (0.03)	1.81 (0.24)c
% $conductance_{mor}$	10.48 (1.97)	8.1 (1.02)	7.15 (0.43)	5.54 (0.21)	5.86 (0.48)	3.92 (0.22)	6.84 (0.85)
% $conductance_{mid}$	10.65 (0.89)	10.27 (1.06)	7.72 (0.44)	7.82 (0.83)	7.63 (0.58)	6.4 (0.32)	8.42 (0.62)a
% $conductance_{aft}$	7.57 (1.48)	6.05 (1.52)	5.89 (0.58)	5.3 (0.37)	4.91 (0.37)	2.64 (0.07)	5.39 (0.61)

LW: leaf width; *LMA*: leaf mass per area; *% N*: percentage leaf nitrogen; *% C*: percentage leaf carbon; SD_{adax}: adaxial stomatal density; SD_{abax}: abaxial stomatal density; SS_{adax}: adaxial stomatal size; SS_{abax}: abaxial stomatal size; $g_{s\,max}$: calculated maximum stomatal conductance; SI_{adax}: adaxial stomatal index; SI_{abax}: abaxial stomatal index; ES_{adax}: adaxial epidermal cell size; ES_{abax}: abaxial epidermal cell size; a_{op}: opertational stomatal pore; *% aperture*: operational pore as a percentage of maximum pore; *% conductance*: stomatal condutance as a percentage of maximum conductance.

Table 3.4. Mean (±SE) of soluble sugar concentrations for each Sorghum genotype at the different time points of the diurnal curve. The table also shows the results of the *post hoc* Tukey's test for analysis of variance. Mean values that share similar symbols (none, *a, b* or *c*) have no significant difference (p<0.05) between them (n=4-5).

Unique Genotype ID	QL12	SC1079-11Ebk	R931945-2-2	FF_SC906-14E	FF_SC500-9	FF_SC449-14E
Glucose$_{n}$ (g m^{-2})	0.57 (0.11)	1.08 (0.22)	1.04 (0.13)	1.05 (0.03)	1.99 (0.17)a	0.76 (0.25)
Fructose$_{n}$ (g m^{-2})	0.52 (0.13)ab	1.17 (0.28)b	0.46 (0.08)a	0.46 (0.03)a	0.72 (0.08)ab	0.19 (0.03)a
Sucrose$_{n}$ (g m^{-2}) a	1.1 (0.52)ab	1.05 (0.56)ab	0.5 (0.25)a	1.08 (0.19)a	2.04 (0.25)b	0.8 (0.04)ab
Glucose$_{mor}$ (g m^{-2})	1.06 (0.22)ab	1.45 (0.28)ab	1.79 (0.4)b	0.85 (0.1)ab	1.77 (0.37)b	0.61 (0.12)a
Fructose$_{mor}$ (g m^{-2})	1.27 (0.36)ab	1.96 (0.32)b	0.95 (0.15)a	0.44 (0.07)a	0.63 (0.14)a	0.31 (0.05)a
Sucrose$_{mor}$ (g m^{-2}) *ab*	3.29 (2.09)b	1.23 (0.68)ab	0.95 (0.31)ab	0.86 (0.24)a	1.46 (0.23)ab	0.56 (0.15)a
Glucose$_{mid}$ (g m^{-2})	1.53 (0.29)ab	2.98 (0.43)b	2.59 (0.42)ab	1.29 (0.25)a	1.98 (0.48)ab	1.34 (0.12)a
Fructose$_{mid}$ (g m^{-2})	1.57 (0.3)a	2.83 (0.46)b	0.89 (0.08)a	0.59 (0.14)a	0.87 (0.14)a	0.51 (0.06)a
Sucrose$_{mid}$ (g m^{-2}) *bc*	3.39 (0.84)	3.55 (0.65)	2.19 (0.3)	3.85 (0.34)	2.38 (0.34)	2.03 (0.29)
Glucose$_{aft}$ (g m^{-2})	1.68 (0.3)ac	2.67 (0.26)c	1.44 (0.17)ab	1.37 (0.18)ab	2.22 (0.14)bc	0.96 (0.1)a
Fructose$_{aft}$ (g m^{-2})	1.12 (0.14)ab	2.3 (0.91)b	0.76 (0.06)a	0.54 (0.13)a	0.71 (0.09)a	0.35 (0.05)a
Sucrose$_{aft}$ (g m^{-2}) *c*	6.45 (0.73)b	2.41 (0.52)a	3.46 (0.81)a	4.56 (0.44)ab	3.42 (0.61)a	3.25 (0.38)a

Concentrations of soluble sugars in the leaf at *n* : pre-dawn/end of night; *mor* : early morning; *mid* : midday; *aft* : afternoon.

Table 3.5 Overview of F-statistics from a full factorial mixed effect ANOVA for the diurnal cycle

	df	A_n (µmol m^{-2} s^{-1})	g_s (mol m^{-2} s^{-1})	***iWUE*** (µmol CO_2 mol^{-1} H_2O)	*Glucose* (g m^{-2})	*Fructose* (g m^{-2})	*Sucrose* (g m^{-2})
Genotype	5	16.699***	7.667***	3.337**	9.83204***	22.29861***	7.66682**
Time	3	771.53***	180.5444***	4.7681**	11.56223***	6.19542**	22.84136***
Genotype*Time	15	3.793***	1.652*	0.93	1.78501*	1.12284	1.98491**

A_n: net carbon assimilation; g_s: stomatal conductance; *iWUE*: intrinsic water use efficiency. Concentrations of individual soluble sugars.

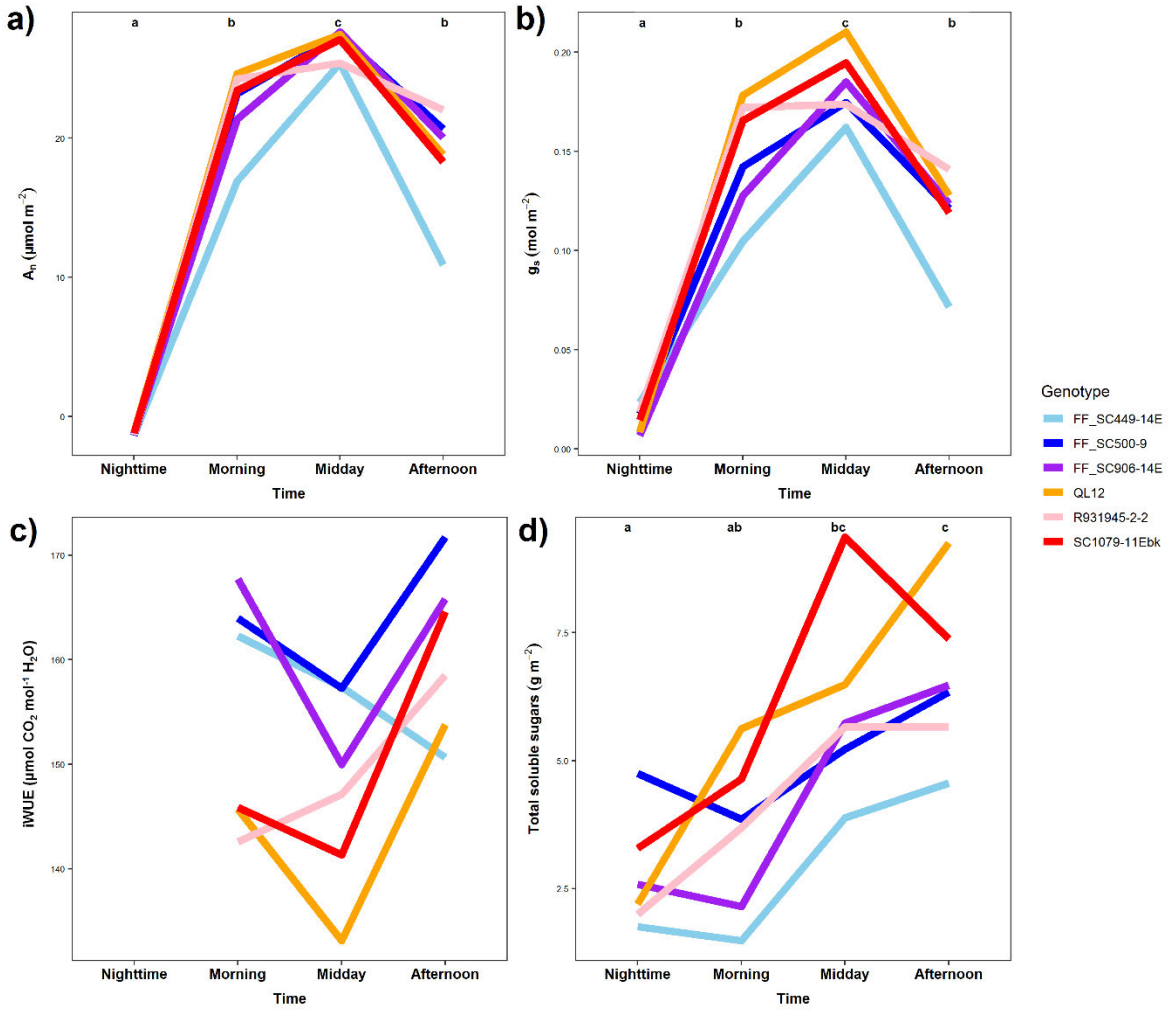

Fig.3.1 Diurnal pattern curves of leaf gas exchange and leaf soluble sugar concentrations. Measurements were taken at four times: end of night-time/pre-dawn, early morning, midday, and late afternoon. The youngest fully expanded leaf was used to measure gas exchange using a LI-6400XT, and the leaf was then quickly excised, and leaf discs taken and stored in liquid nitrogen for sugar analysis later. During the photoperiod, gas exchange was always measured at 1000 µmol m^{-2} s^{-1}, irrespective of incident light in the chamber environment. A different individual plant per genotype was used for each replicate diurnal time point (n=4-5). **(a)** Diurnal pattern of carbon assimilation rate (A_n); **(b)** Diurnal pattern of stomatal conductance (g_s); **(c)** Diurnal pattern of intrinsic water use efficiency (*WUE*); **(d)** Diurnal pattern of soluble sugar concentration in the leaf. The letters (a, b and c) on the plots highlight significant (p<0.05) statistical differences in the parameter between the time points, based on the average genotype values. Post-hoc analysis and standard error values are presented in Table 3.1 and Table 3.3.

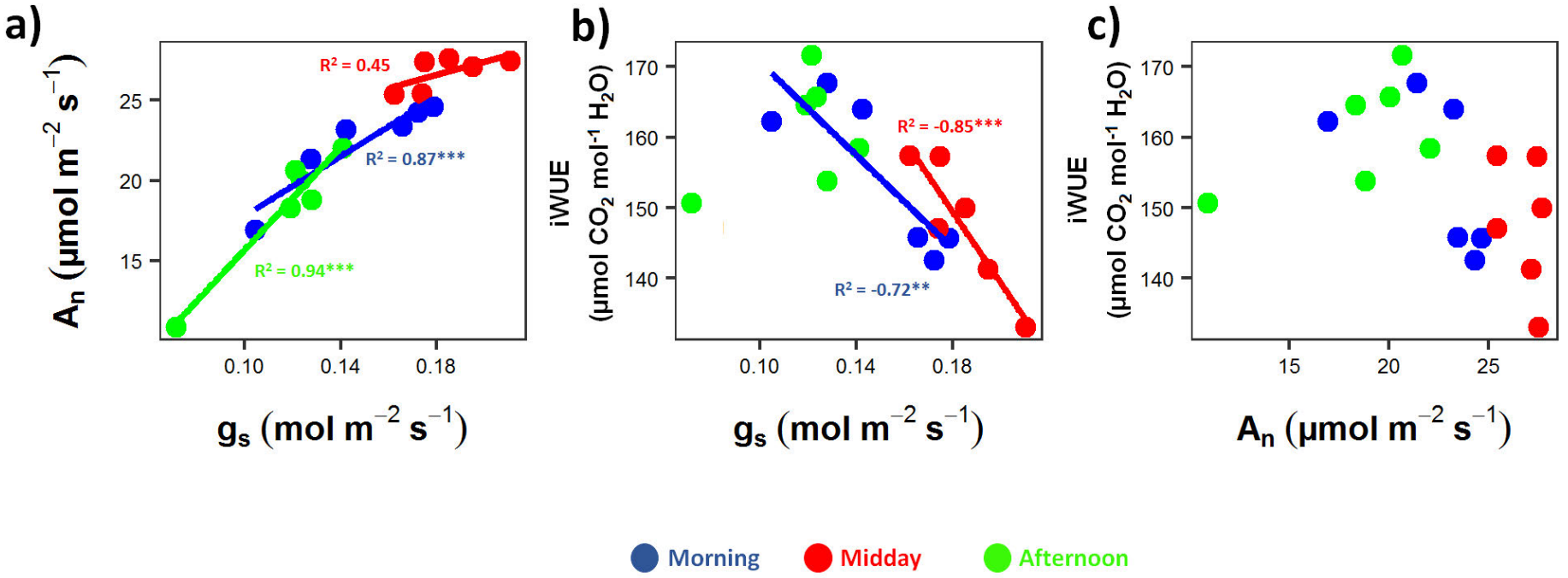

Fig.3.2 Regression analysis between the gas exchange parameters and intrinsic water use efficiency (*WUE*) at each of the three time points of the photoperiod. The youngest fully expanded leaf was used to measure gas exchange using a LI-6400XT at different diurnal timepoints (see Materials & Methods and **Fig. 1**). A different individual plant per genotype was used for each replicate diurnal time point (n=4-5). The resulting gas exchange diurnal curves are presented in **Fig.3.1**. **(a)** Carbon assimilation rate (A_n) vs Stomatal conductance (g_s); **(b)** g_s vs *WUE*; **(c)** A_n vs *WUE*. Each point in the plots represents the mean value of one genotype**.** Standard error values are presented in Table 1. Pearson-product moment analysis was performed on the plots, and analyses that yielded a significant (<0.1) *p*-value are highlighted with a solid correlation line and the corresponding R^2 value, along with the degree of significance (*=p<0.1; **=p<0.05; ***=p<0.001).

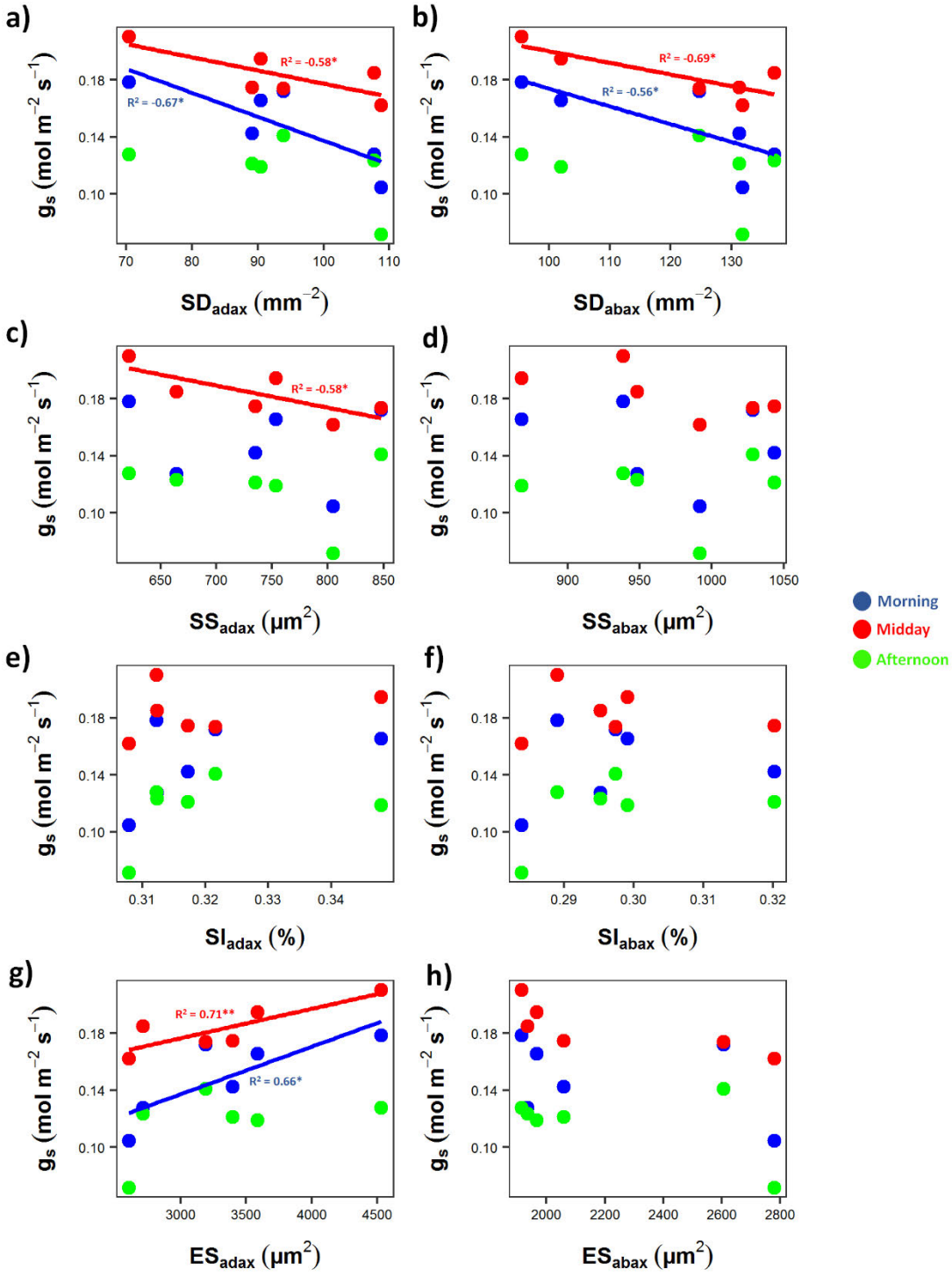

Fig.3.3 Regression analysis between stomatal conductance (g_s) across the photoperiod with leaf stomatal anatomy. The youngest fully expanded leaf was used to measure gas exchange using a LI-6400XT at different diurnal timepoints (see Materials & Methods and **Fig.3.1**), and only the midday was used to obtain genotype average for stomatal anatomy. The leaf was quickly excised, and put into a damp plastic bag, before transporting it to the lab where negative impressions of leaf surface was taken to analyse for stomatal features. A different individual plant per genotype was used for each replicate diurnal time point (n=4-5). The resulting gas exchange diurnal curves are presented in **Fig.3.1**. g_s vs **(a)** Adaxial stomatal density (SD_{adax}); **(b)** Abaxial stomatal density (SD_{abax}); **(c)** Adaxial stomatal size (SS_{adax}); **(d)** Abaxial stomatal size (SS_{abax}); **(e)** Adaxial stomatal index (SI_{adax}); **(f)** Abaxial stomatal index (SI_{abax}); **(g)** Adaxial epidermal cell size (ES_{adax}); **(h)** Abaxial epidermal cell size (ES_{abax}). Each point in the plots represents the mean value of one genotype**.** Standard error values are presented in Table 3.1 and Table 3.2. Pearson-product moment analysis was performed on the plots, and analyses that yielded a significant (<0.1) *p*-value are highlighted with a solid correlation line and the corresponding R^2 value, along with the degree of significance (*=p<0.1; **=p<0.05; ***=p<0.001).

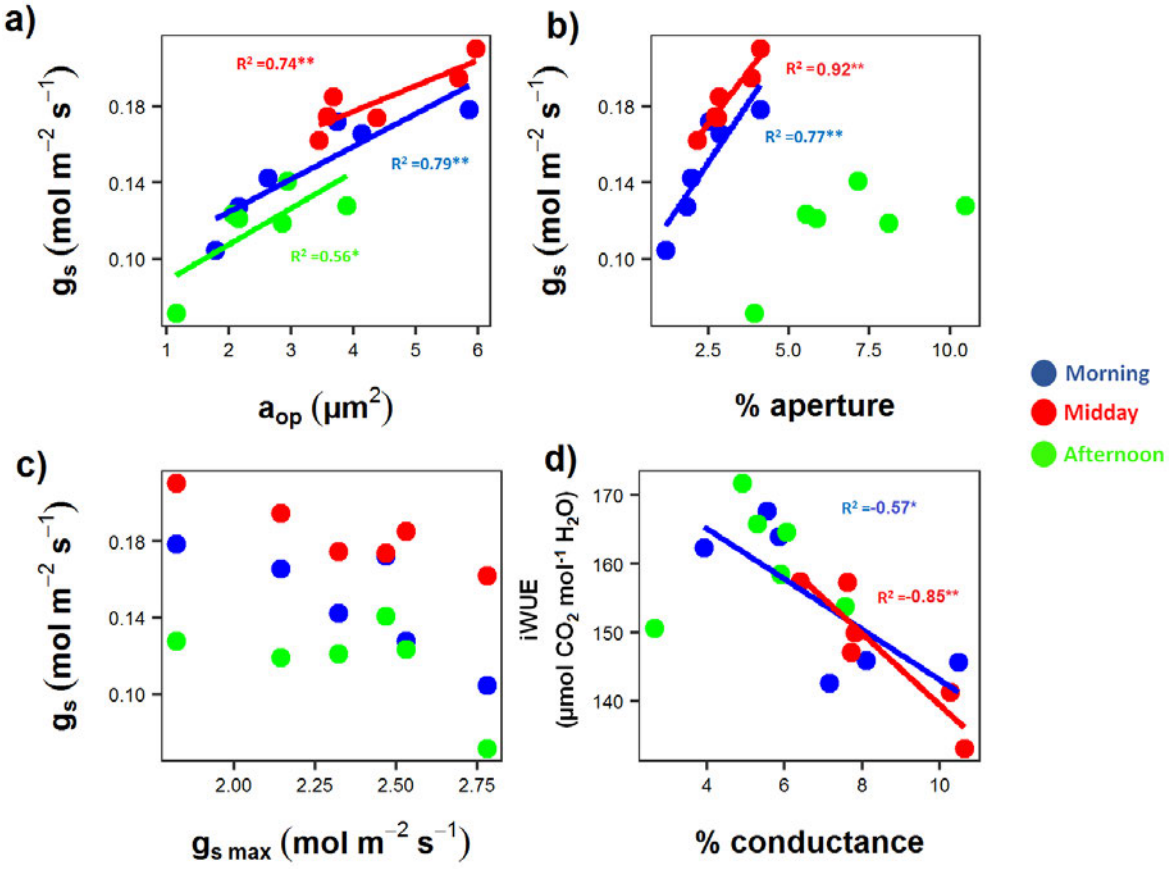

Fig.3.4 Regression analysis between the diurnal values of stomatal conductance (g_s) and calculated stomatal pore features. The youngest fully expanded leaf was used to measure gas exchange using a LI-6400XT at different diurnal time points (see Materials & Methods and **Fig.3.1**), and the midday leaf was then quickly excised, and put into a damp, before transporting it to the lab where negative impressions of leaf surface was taken to analyse for pore features and calculating maximum values (see Materials & Methods). The calculations from the midday leaf was used to calculate genotype averages. A different individual plant per genotype was used for each replicate diurnal time point (n=4-5). The resulting gas exchange diurnal curves are presented in **Fig.3.1**. g_s vs **(a)** Operational stomatal aperture (a_{op}); **(b)** Operational pore as percentage of maximum pore size (*% aperture*); **(c)** Theoritical maximum conductance ($g_{s\,max}$); **(d)** intrinsic water use efficiency (*WUE*) vs Measured stomatal conductance as a percentage of $g_{s\,max}$ (*% conductance*). Each point in the plots represents the mean value of one genotype**.** Standard error values are presented in Table 3.1 and Table 3.2. Pearson-product moment analysis was performed on the plots, and analyses that yielded a significant (<0.1) *p*-value are highlighted with a solid black correlation line and the corresponding R^2 value, along with the degree of significance (*=p<0.1; **=p<0.05; ***=p<0.001).

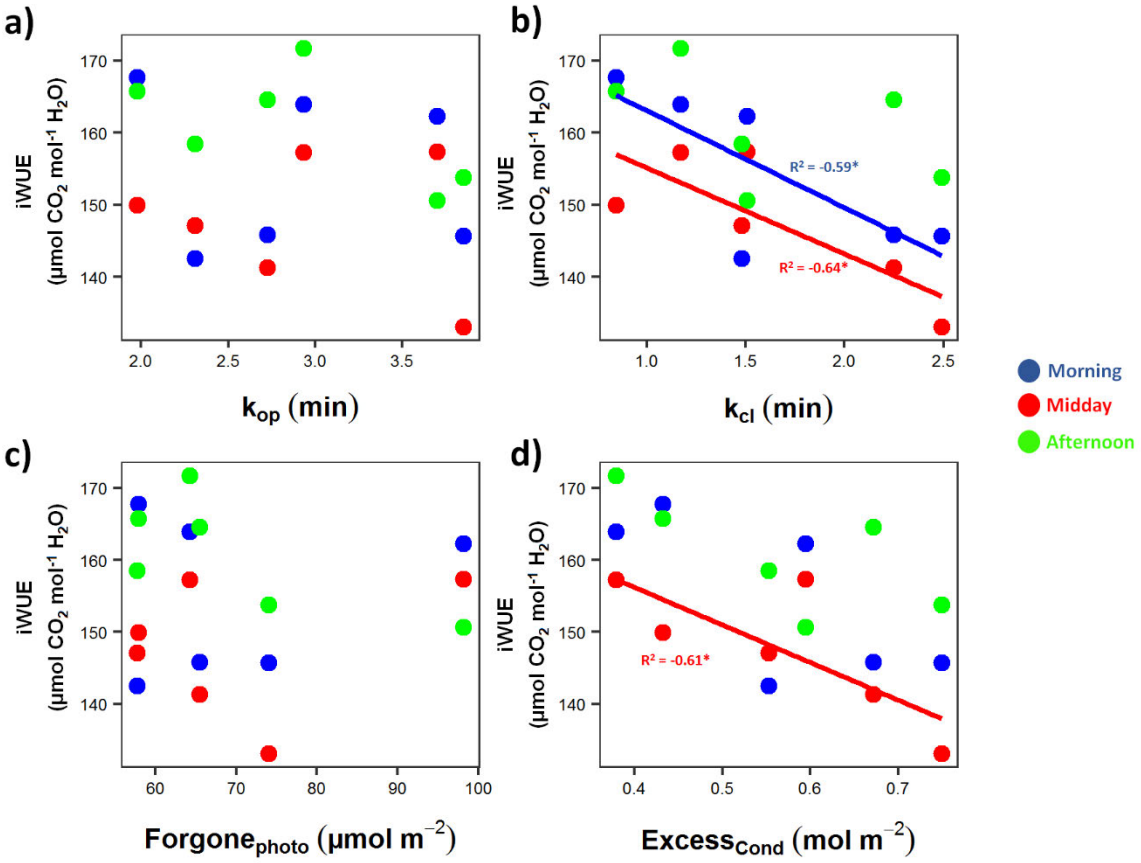

Fig.3.5 Regression analysis between the intrinsic water use efficiency (*iWUE*) and kinetic stomatal features. The youngest fully expanded leaf was used to measure gas exchange using a LI-6400XT at different diurnal time points (see Materials & Methods and **Fig.3.1**). A different individual plant per genotype was used for each replicate diurnal time point (n=4-5). The resulting gas exchange diurnal curves are presented in **Fig.3.1**. Different individuals of the same genotype were used to measure stomatal kinetic responses by using a LI-6400XT to simulate changing light levels in 30-minute segments while measuring gas exchange, and this was used to calculate the different parameters presented (see Materials & Methods). *iWUE* vs **(a)** Opening time constant of the stomatal pore (k_{op}); **(b)** Closing time constant of the stomatal pore (k_{cl}); **(c)** Forgone photosynthesis due to slow stomatal opening; **(d)** Excess conductance due to slow stomatal closing. Each point in the plots represents the mean value of one genotype**.** Standard error values are presented in Table 3.1 and Table 3.2. Pearson-product moment analysis was performed on the plots, and analyses that yielded a significant (<0.1) *p*-value are highlighted with a solid black correlation line and the corresponding R^2 value, along with the degree of significance (*=p<0.1; **=p<0.05; ***=p<0.001).

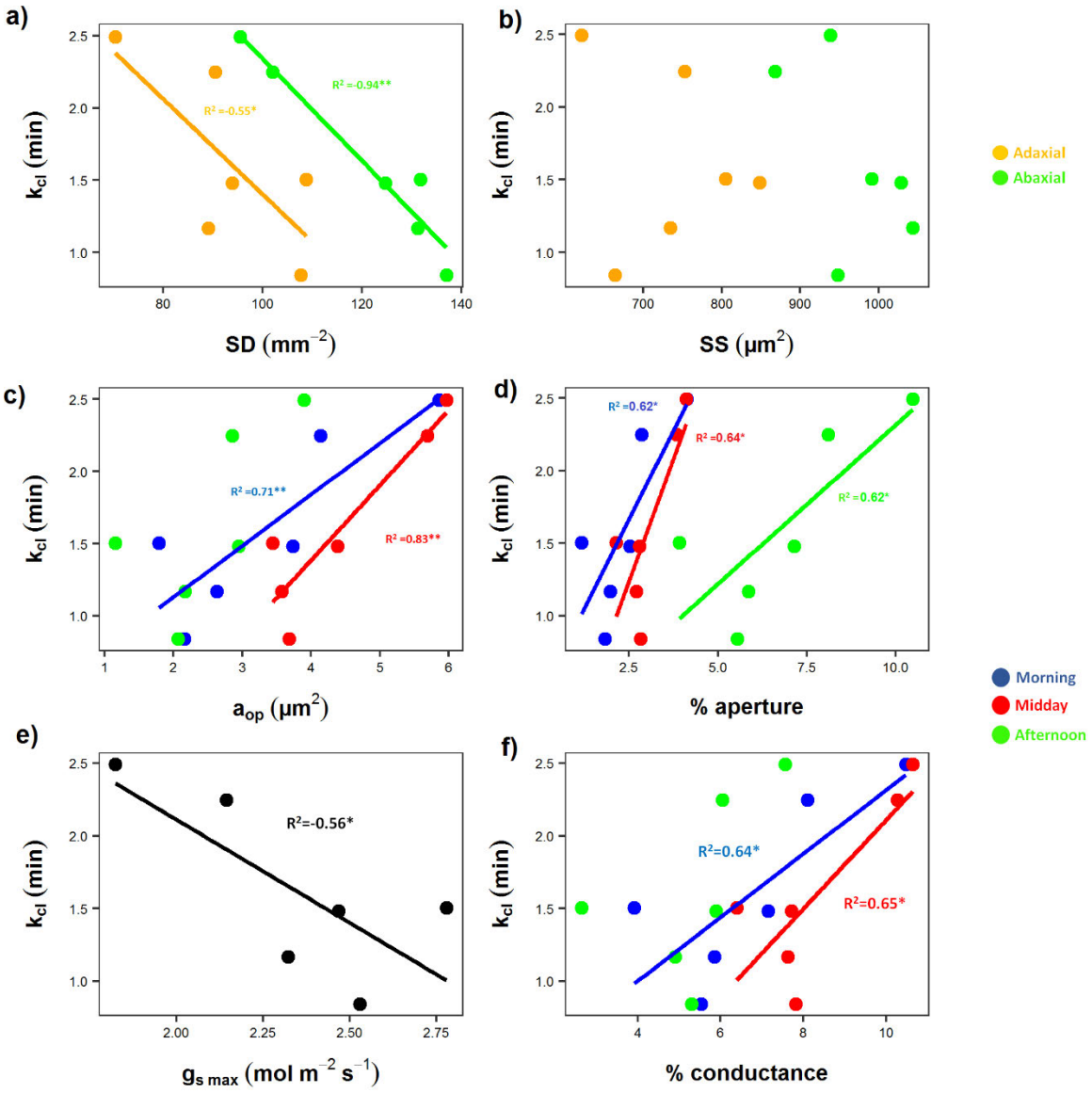

Fig.3.6 Regression analysis between stomatal anatomical and pore features with speed of stomatal closure. The youngest fully expanded leaf was used to measure gas exchange using a LI-6400XT at different diurnal time points (see Materials & Methods and **Fig.3.1**), and the midday leaf was then quickly excised, and put into a damp plastic bag, before transporting it to the lab where negative impressions of leaf surface was taken to analyse for stomatal features. A different individual plant per genotype was used for each replicate diurnal time point (n=4-5). Different individuals of the same genotype were used to measure stomatal kinetic responses by using a LI-6400XT to simulate changing light levels in 30 minute segments while measuring gas exchange, and this was used to calculate time-constant of stomatal closure, k_{cl} (see Materials & Methods). k_{cl} vs **(a)** Stomatal density (*SD*); **(b)** Stomatal size (*SS*); **(c)** Operational stomatal aperture (a_{op}); **(d)** Operational pore as percentage of maximum pore size (*% aperture*) **(e)** Theoretical maximum conductance ($g_{s\ max}$); **(f)** Measured stomatal conductance as a percentage of $g_{s\ max}$ (*% conductance*). Each point in the plots represents the mean value of one genotype**.** Standard error values are presented in Table 3.1 and Table 3.2. Pearson-product moment analysis was performed on the plots, and analyses that yielded a significant (<0.1) *p*-value are highlighted with a solid black correlation line and the corresponding R^2 value, along with the degree of significance (*=p<0.1; **=p<0.05; ***=p<0.001).

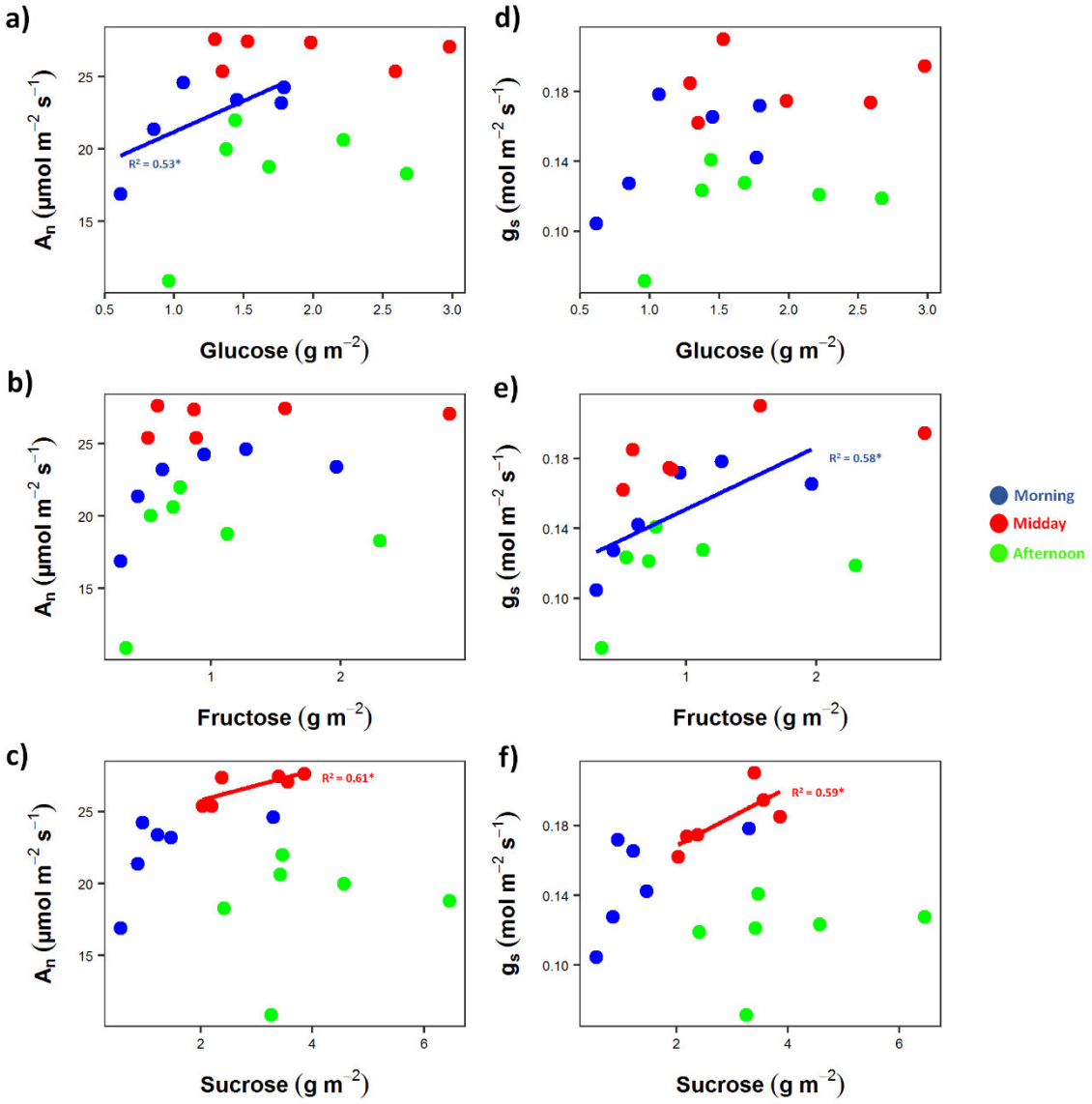

Fig.3.7 Regression analysis between the concentrations of leaf soluble sugars and gas exchange parameters at different diurnal time points. The youngest fully expanded leaf was used to measure gas exchange using a LI-6400XT at different diurnal time points (see Materials & Methods and **Fig.3.1**), and then leaf borers were used to obtain leaf material that was then frozen and later analysed in the lab for the various sugar concentrations. A different individual plant per genotype was used for each replicate diurnal time point (n=4-5). Carbon assimilation rate (A_n) vs **(a)** Glucose concentration; **(b)** Fructose concentration; **(c)** Sucrose concentration; Stomatal conductance (g_s) vs **(d)** Glucose concentration; **(e)** Fructose concentration; **(f)** Sucrose concentration. Each point in the plots represents the mean value of one genotype**.** Standard error values are presented in Table 3.1 and Table 3.3. Pearson-product moment analysis was performed on the plots, and analyses that yielded a significant (<0.1) *p*-value are highlighted with a solid black correlation line and the corresponding R^2 value, along with the degree of significance (*=p<0.1; **=p<0.05; ***=p<0.001).

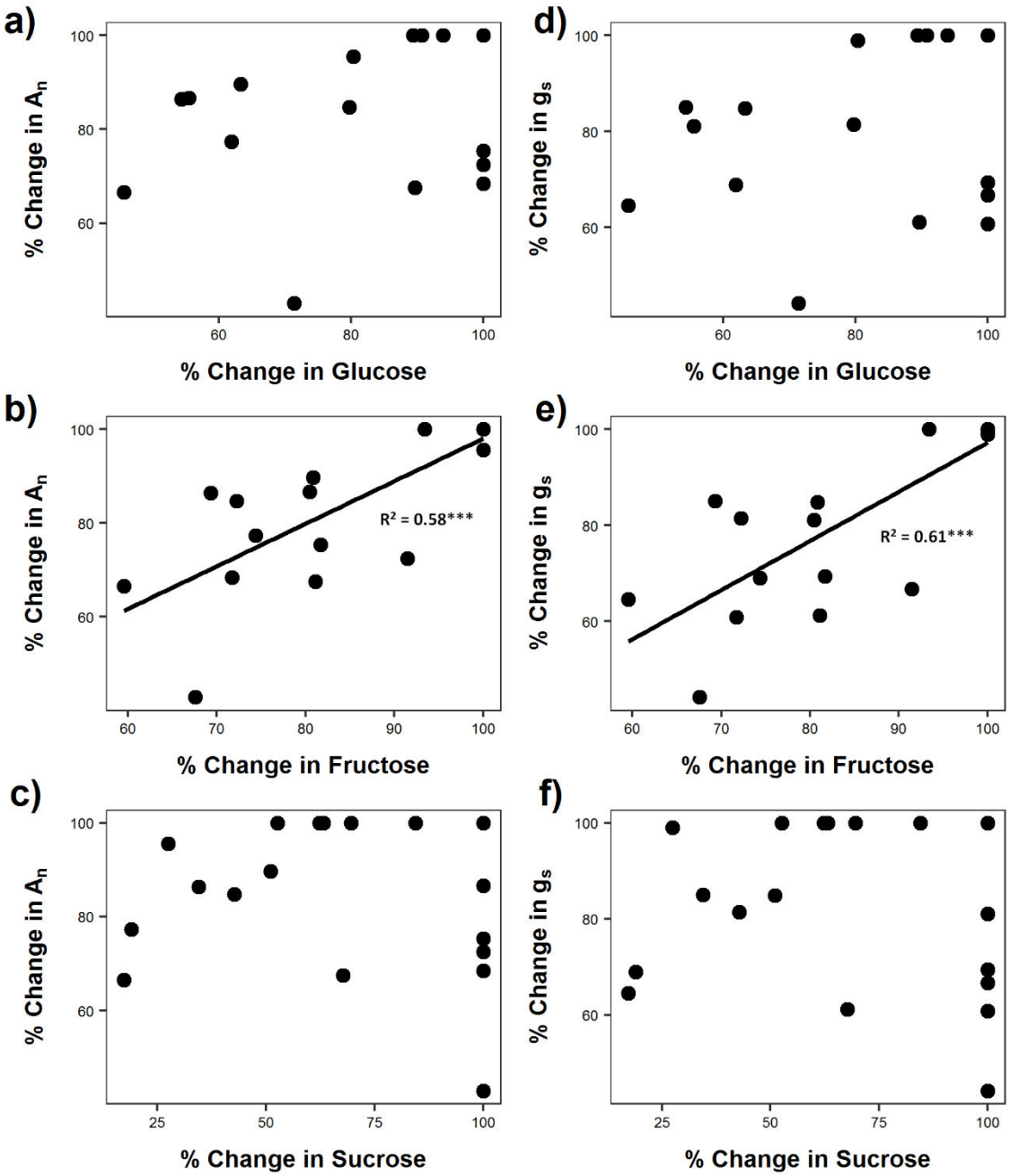

Fig.3.8 Regression analysis of the percentage change in soluble sugar concentration and gas exchange levels. The youngest fully expanded leaf was used to measure gas exchange using a LI-6400XT at different diurnal timepoints (see Materials & Methods and **Fig.3.1**), and then leaf borers were used to obtain leaf material that was then frozen and later analysed in the lab for the various sugar concentrations. A different individual plant per genotype was used for each replicate diurnal time point (n=4-5). The percentage difference between the maximum and each time point was calculated for each gas exchange parameter and each sugar. Percentage change in A_n vs Percentage change in **(a)** Glucose; **(b)** Fructose; **(c)** Sucrose; Percentage change in stomatal conductance (g_s) vs. Percentage change in **(d)** Glucose; **(e)** Fructose; **(f)** Sucrose. Each point in the plots is extracted from the mean value of one genotype**.** Standard error values for mean values of parameters are presented in Table 3.1 and Table 3.3. Pearson-product moment analysis was performed on the plots, and analyses that yielded a significant (<0.1) *p*-value are highlighted with a solid black correlation line and the corresponding R^2 value, along with the degree of significance (*=p<0.1; **=p<0.05; ***=p<0.001).

3.6 SUPPLEMENTARY

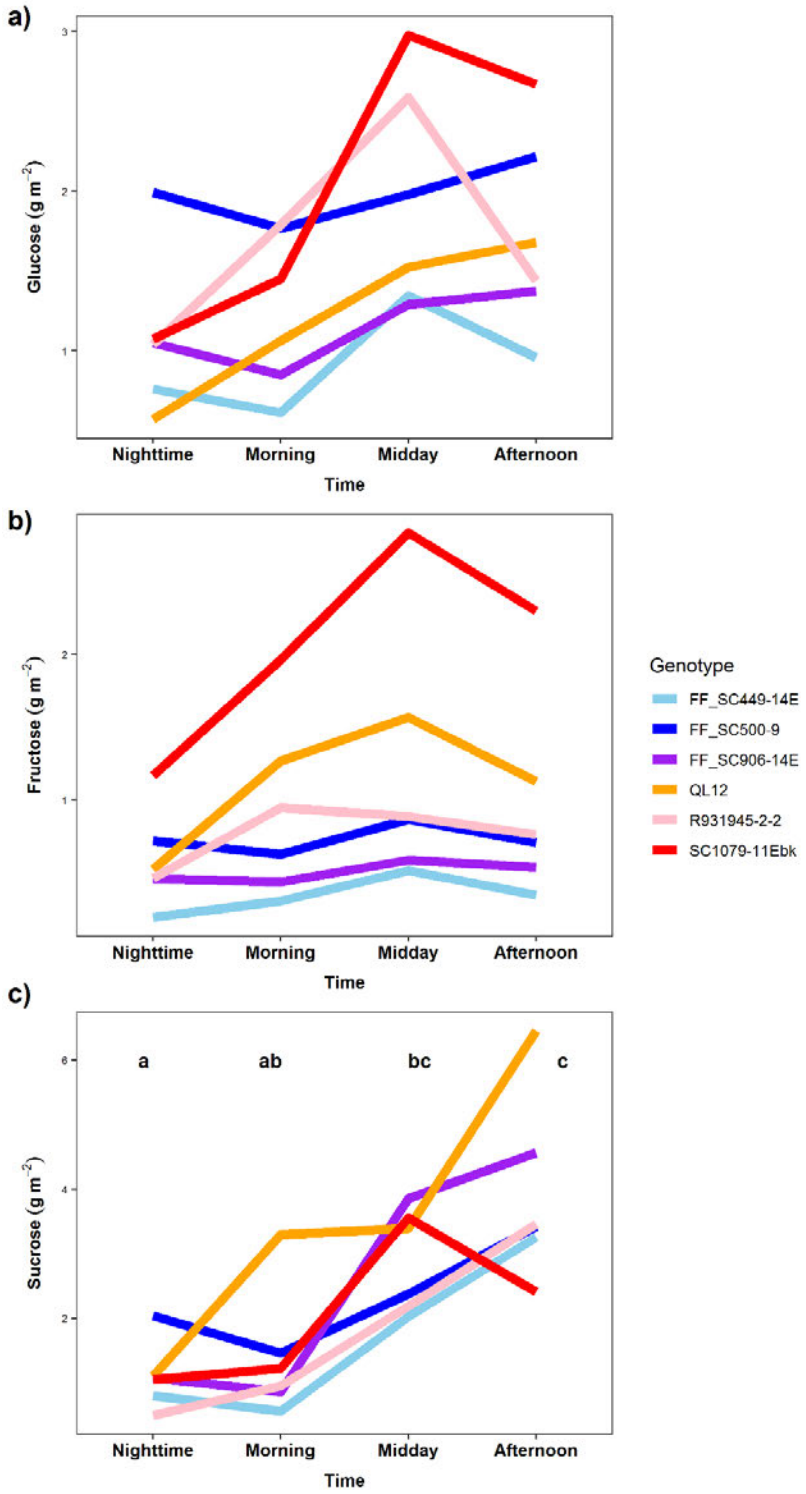

Fig.3.S1 The diurnal pattern of different soluble sugars in the leaves of *Sorghum bicolor* genotypes. **(a)** Glucose concentration; **(b)** Fructose concentration; **(c)** Sucrose concentration. Letters on the plot (none, a, b or c) represent statistically significant difference between the timepoints in soluble sugar concentration, with time points sharing a letter having no significant concentration between them. n=4-5.

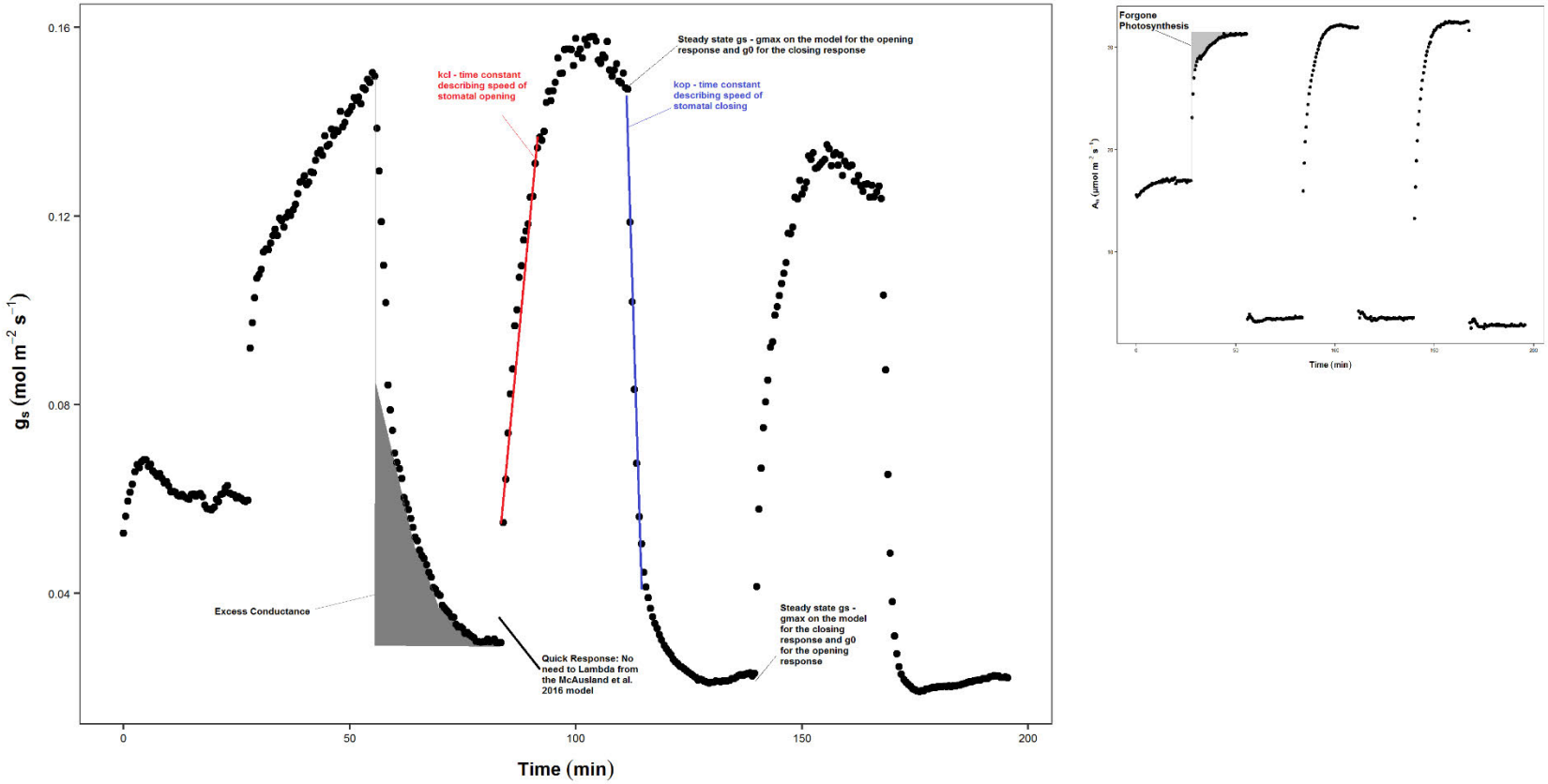

Fig.3.S2 A demonstration of the stomatal and photosynthesis response to synchronized changes in light. The Fig. shows visual representations of calculated parameters (see Materials & Methods) using the models described.

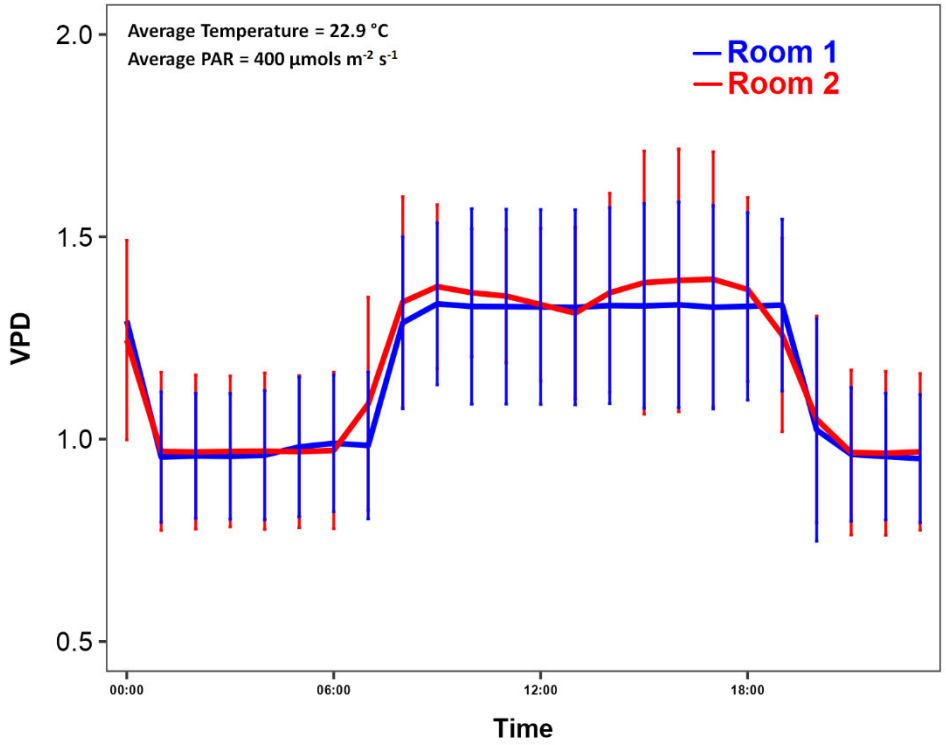

Fig.3.S3 Average changes in vapour pressure deficit in the growth chambers during growth.

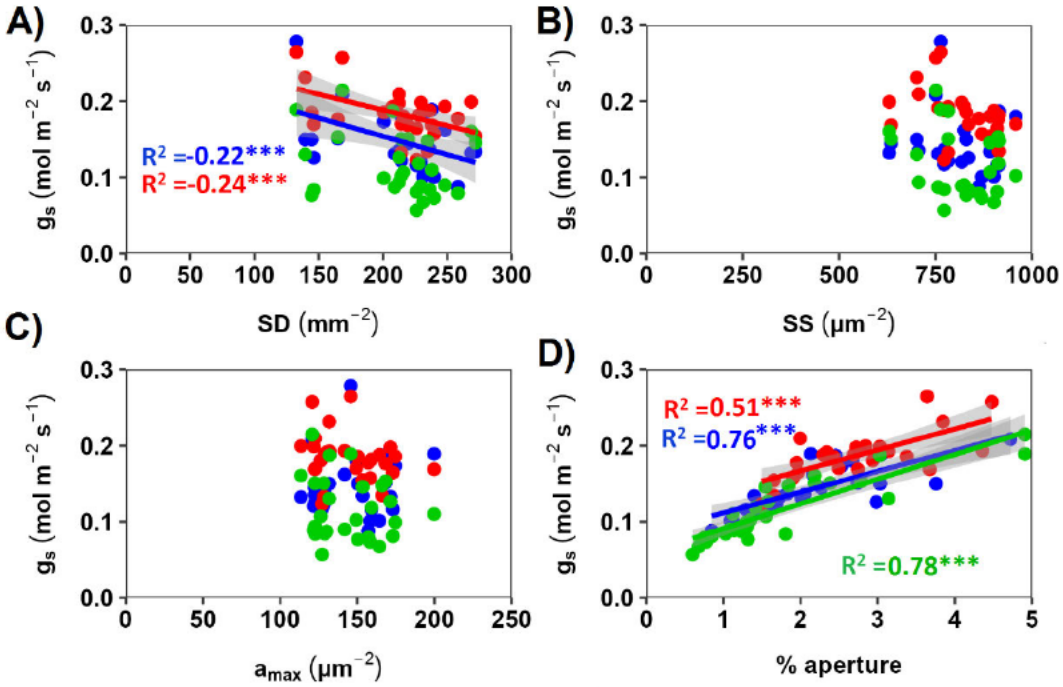

Fig.3.S4 Stomatal conductance (g_s) vs. different anatomical variables. This figure mirrors that of Fig.3.3, but in this instance the replicates are plotted instead of genotype means. This was to prove that the trends shown in Fig.3.3 was not skewed by outliers or the result of non-continuous distribution. A) *SD*: Stomatal density; B) *SS*: Stomatal size, C) a_{max}: maximum stomatal aperture, D) Operational aperture as % of a_{max}.

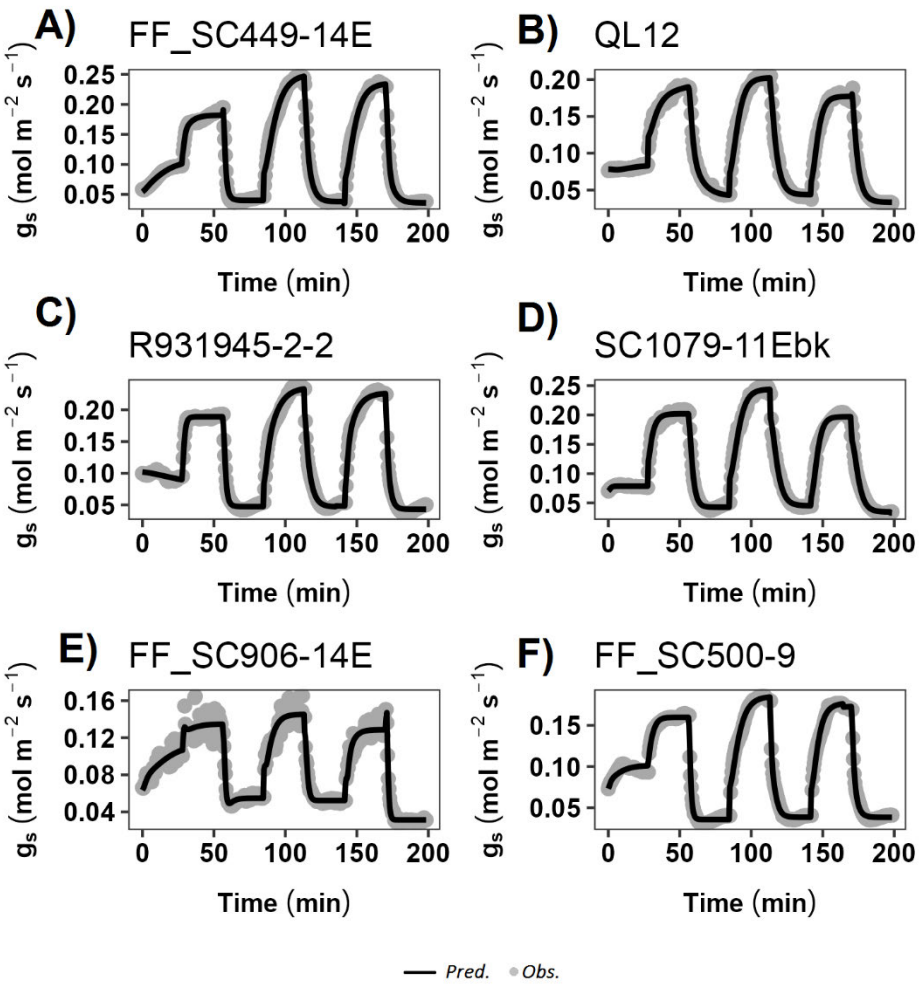

Fig.3.S5 Model fit of equation 3.6 on measured data.

Table 3.S1. Pearson product-moment correlation analysis results for the relationships between the measured variables. The *r* coefficient and the statistical significance were determined using the mean value per genotype for each variable (n=4-5). Statistical significance was judged as: $p<0.001$ (***), $p<0.05$ (**), $p<0.1$ (*), $p>0.1$ (ns).

	A_{mid}	A_{aft}	$g_{s\,mor}$	$g_{s\,mid}$	$g_{s\,aft}$	$iWUE_{mor}$	$iWUE_{mid}$	$iWUE_{aft}$	dA_n	dg_s	$dWUE$	Ψ_{leaf}	k_{cl}	k_{op}	LW	LMA	% N	TS_{mor}	TS_{mid}	TS_{aft}	TS_{total}
A_{mor} (µmol m^{-2} s^{-1})	ns	0.87**	0.93***	ns	0.93***	ns	ns	ns	0.96***	0 95**	ns	0.78*	ns	ns	ns	0.76*	ns	0.86**	ns	ns	0 86**
A_{mid} (µmol m^{-2} s^{-1})	-	ns	ns	ns	ns	ns	ns	ns	ns	ns	ns	ns	ns	ns	ns	ns	-0.83**	ns	ns	ns	ns
A_{aft} (µmol m^{-2} s^{-1})	-	-	ns	ns	0.97***	ns	ns	ns	0.97**	0.77*	ns	0.76*	ns	ns	ns	0.74*	ns	ns	ns	ns	ns
$g_{s\,mor}$ (mol m^{-2} s^{-1})	-	-	-	ns	0.81*	-0.85**	-0.80*	ns	0.81*	0 96**	ns	-0.75*	ns	ns	ns	ns	ns	0.91**	ns	ns	0 85**
$g_{s\,mid}$ (mol m^{-2} s^{-1})	-	-	-	-	ns	ns	-0.92***	ns	ns	0.79*	ns	ns	ns	ns	ns	ns	ns	ns	ns	ns	0 84**
$g_{s\,aft}$ (mol m^{-2} s^{-1})	-	-	-	-	-	ns	ns	ns	0.94***	0 89**	ns	-0.84**	ns	ns	ns	ns	ns	ns	ns	ns	ns
$iWUE_{mor}$	-	-	-	-	-	-	0.74*	ns	ns	ns	0 9**	ns	-0.77*	ns	ns	ns	ns	ns	ns	ns	ns
$iWUE_{mid}$	-	-	-	-	-	-	-	ns	ns	-0.82**	0.86**	ns	-0.80*	ns	ns	ns	ns	-0.79*	ns	-0.87**	-0.76*
$iWUE_{aft}$	-	-	-	-	-	-	-	-	ns	ns	ns	ns	ns	ns	ns	ns	ns	ns	ns	ns	ns
dA_n (µmol m^{-2} s^{-1})	-	-	-	-	-	-	-	-	-	0 88**	ns	0.8*	ns	ns	ns	0.77*	ns	ns	ns	ns	0.76*
dg_s (mol m^{-2} s^{-1})	-	-	-	-	-	-	-	-	-	-	-0.85**	-0.84**	ns	ns	ns	ns	ns	0.87**	ns	0 8*	0 88**
$dWUE$ ($\mu mol\ CO_2\ mol^{-1}\ H_2O$)	-	-	-	-	-	-	-	-	-	-	-	ns	-0.85**	ns	ns	ns	ns	ns	ns	ns	ns
Ψ_{leaf} (-MPa)	-	-	-	-	-	-	-	-	-	-	-	-	ns	ns	ns	ns	ns	ns	0.77*	ns	ns
k_{cl} (min)	-	-	-	-	-	-	-	-	-	-	-	-	-	ns	ns	ns	ns	0.75*	ns	ns	ns
k_{op} (min)	-	-	-	-	-	-	-	-	-	-	-	-	-	-	ns	ns	ns	ns	ns	ns	ns
LW (cm)	-	-	-	-	-	-	-	-	-	-	-	-	-	-	-	ns	ns	ns	ns	ns	ns
LMA (g m^{-2})	-	-	-	-	-	-	-	-	-	-	-	-	-	-	-	-	ns	ns	ns	ns	ns
% N	-	-	-	-	-	-	-	-	-	-	-	-	-	-	-	-	-	ns	ns	ns	ns
$Tot\ Sugar_{mor}$ (g m^{-2})	-	-	-	-	-	-	-	-	-	-	-	-	-	-	-	-	-	-	0.86**	ns	0 95**
$Tot\ Sugar_{mid}$ (g m^{-2})	-	-	-	-	-	-	-	-	-	-	-	-	-	-	-	-	-	-	-	ns	0.79*
$Tot\ Sugar_{aft}$ (g m^{-2})	-	-	-	-	-	-	-	-	-	-	-	-	-	-	-	-	-	-	-	-	0 88**

A_{mor}: carbon assimilation at early morning; A_{mid}: midday carbon assimila ion; A_{aft}: afternoon carbon assimilation; $g_{s\,mor}$: stomatal conductance at early morning; $g_{s\,mid}$: midday stomatal conductance; $g_{s\,aft}$: Afternoon stomatal conductance; iWUE_{mor}: morning intrinsic w ater use efficiency; iWUE_{mid}: midday intrinsic w ater use efficiency; iWUE_{aft}: afternoon intrinsic w ater use efficiency; dA_n: average carbon assimilation rate over the day; dg_s: average stomatal conductance over the day; $dWUE$: average w ater use efficiency over the day; Ψ_{leaf}: midday leaf w ater potential; k_{cl}: closing time constant of the stomatal pore; k_{op}: opening time constant of the stomatal pore; LW: leaf w idth; LMA: leaf mass per area; % N: percentage leaf nitrogen; % C: percentage leaf carbon; TS: Concentra ions of soluble sugars (Glu + Fru + Suc) in he leaf at *mor*: early morning; *mid*: midday; *aft*: afternoon.

Table 3.S1 continued…

	a_{op}	% a	% gs	slope	A_{sat}	$Gluc_{n}$	$Fruc_{n}$	Suc_{n}	$Gluc_{mor}$	$Fruc_{mor}$	Suc_{mor}	$Gluc_{mid}$	$Fruc_{mid}$	Suc_{mid}	$Gluc_{aft}$	$Fruc_{aft}$	Suc_{aft}	TS_{mor}	TS_{mid}	TS_{aft}
R_n (µmol m^{-2} s^{-1})	0.83**	0.88**	ns	ns	ns	ns	ns	ns	ns	ns	ns	ns	ns	0.83**	ns	ns	ns	ns	0.76*	0.75*
A_{mor} (µmol m^{-2} s^{-1})	ns	ns	0.8*	ns	ns	ns	ns	ns	0.73*	ns	ns	ns	ns	ns	ns	ns	ns	0.86**	ns	ns
A_{mid} (µmol m^{-2} s^{-1})	ns	ns	ns	ns	ns	ns	ns	ns	ns	ns	ns	ns	ns	0.78*	ns	ns	ns	ns	ns	ns
A_{aft} (µmol m^{-2} s^{-1})	ns	ns	ns	ns	ns	ns	ns	ns	0.75*	ns	ns	ns	ns	ns	ns	ns	ns	ns	ns	ns
$g_{s\,n}$ (mol m^{-2} s^{-1})	ns	ns	ns	ns	ns	ns	ns	ns	ns	ns	ns	ns	ns	-0.89**	ns	ns	ns	ns	ns	-0.75*
$g_{s\,mor}$ (mol m^{-2} s^{-1})	0.81**	0.75*	0.9**	ns	ns	ns	ns	ns	ns	0.76*	ns	ns	ns	ns	ns	ns	ns	0.91**	ns	ns
$g_{s\,mid}$ (mol m^{-2} s^{-1})	0.87**	0.92***	0.95**	ns	ns	ns	ns	ns	ns	ns	0.83**	ns	ns	0.77*	ns	ns	ns	ns	ns	ns
$g_{s\,aft}$ (mol m^{-2} s^{-1})	ns	ns	0.82**	ns	ns	ns	ns	ns	ns	ns	ns	ns	ns	ns	ns	ns	ns	ns	ns	ns
$iWUE_{mor}$	-0.80*	ns	-0.75*	ns	-0.86**	ns	ns	ns	ns	-0.77*	ns	ns	ns	ns	ns	ns	ns	ns	ns	ns
$iWUE_{mid}$	-0.95***	-0.95***	-0.92**	ns	ns	ns	ns	ns	ns	-0.74*	-0.76*	ns	ns	ns	ns	ns	ns	-0.79*	ns	-0.87**
$iWUE_{aft}$	ns	ns	ns	ns	ns	0.86**	ns	ns	ns	ns	ns	ns	ns	ns	ns	ns	ns	ns	ns	ns
A_{wd} (µmol m^{-2})	ns	ns	ns	ns	ns	ns	ns	ns	ns	ns	ns	ns	ns	ns	ns	ns	ns	0.76*	ns	ns
$g_{s\,wd}$ (mol m^{-2})	0.86**	0.87**	0.92**	ns	ns	ns	ns	ns	ns	ns	0.78*	ns	ns	ns	ns	ns	ns	0.89**	ns	0.93**
$dWUE$	-0.93***	-0.87**	-0.83**	ns	ns	ns	ns	ns	ns	-0.81*	ns	ns	ns	ns	ns	ns	ns	-0.83**	ns	ns
Ψ_{leaf} (-MPa)	ns	ns	ns	ns	ns	ns	ns	ns	ns	ns	ns	ns	ns	ns	ns	ns	ns	ns	0.77*	ns
k_{cl} (min)	0.92**	0.89**	0.79*	ns	0.84**	ns	ns	ns	ns	0.79*	ns	ns	0.76*	ns	ns	ns	ns	0.75*	ns	ns
Excess g_s (mol m^{-2})	0.83**	0.80*	0.81*	ns	0.84**	-0.78*	ns	ns	ns	ns	ns	ns	ns	ns	ns	ns	ns	ns	ns	ns

Table 3.S1 continued…

	a_{op}	% a	% gs	slope	A_{sat}	$Gluc_{n}$	$Fruc_{n}$	Suc_{n}	$Gluc_{mor}$	$Fruc_{mor}$	Suc_{mor}	$Gluc_{mid}$	$Fruc_{mid}$	Suc_{mid}	$Gluc_{aft}$	$Fruc_{aft}$	Suc_{aft}	TS_{mor}	TS_{mid}	TS_{aft}
WUE_{cl}	ns	ns	-0.80*	ns	-0.9**	ns	ns	ns	ns	ns	ns	ns	ns	ns	ns	ns	ns	ns	ns	ns
k_{op} (min)	ns	ns	ns	0.94**	ns	ns	ns	ns	ns	ns	ns	ns	ns	ns	ns	ns	ns	ns	ns	ns
Forgone A (µmol m^{-2})	ns	ns	ns	ns	ns	ns	ns	ns	ns	ns	ns	ns	ns	ns	ns	ns	ns	ns	ns	ns
WUE_{op}	ns	ns	ns	ns	ns	ns	ns	ns	ns	ns	0.89**	ns	ns	ns	ns	ns	0.78*	ns	ns	0.94**
LW (cm)	ns	ns	ns	ns	ns	0.94**	ns	ns	ns	ns	ns	ns	ns	ns	ns	ns	ns	ns	ns	ns
LMA (g m^{-2})	ns	ns	ns	ns	ns	ns	ns	ns	0.74*	ns	ns	ns	ns	ns	ns	ns	ns	ns	ns	ns
% N	ns	ns	ns	ns	ns	ns	ns	ns	ns	ns	ns	ns	ns	-0.87**	ns	ns	ns	ns	ns	ns
% C	ns	ns	ns	ns	ns	ns	ns	ns	ns	ns	ns	ns	ns	ns	ns	ns	ns	ns	ns	ns
SD_{adax} (n° mm^{-2})	-0.78*	-0.76*	-0.79*	ns	ns	ns	ns	ns	ns	ns	-0.93**	ns	ns	ns	ns	ns	-0.77*	-0.96**	ns	-0.85**
SD_{abax} (n° mm^{-2})	-0.98***	-0.97**	-0.92**	ns	ns	ns	ns	ns	ns	-0.86**	-0.75*	ns	-0.82**	ns	ns	-0.76*	ns	-0.86**	ns	-0.81**
SS_{adax} (µm^{2})	ns	ns	ns	ns	ns	ns	ns	ns	ns	ns	ns	ns	ns	-0.76*	ns	ns	ns	ns	ns	-0.78*
SS_{abax} (µm^{2})	ns	-0.75*	ns	ns	ns	ns	ns	ns	ns	ns	ns	ns	-0.78*	-0.79*	ns	-0.76*	ns	ns	-0.8*	ns
g_{smax} (mol m^{-2} s^{-1})	-0.86**	ns	-94**	ns	-0.85**	ns	ns	ns	ns	ns	ns	ns	ns	ns	ns	ns	ns	ns	ns	ns
SI_{adax} (%)	ns	ns	ns	ns	ns	ns	0.92**	ns	ns	0.86**	ns	0.89**	0.88**	ns	0.82**	0.92**	ns	ns	0.89**	ns
SI_{abax} (%)	ns	ns	ns	ns	ns	0.96**	ns	0.79*	0.76*	ns	ns	ns	ns	ns	ns	ns	ns	ns	ns	ns
ES_{adax} (µm^{2})	0.85**	0.84**	0.87*	ns	ns	ns	ns	ns	ns	ns	0.95**	ns	ns	ns	ns	ns	ns	0.96**	ns	0.91**
ES_{abax} (µm^{2})	ns	ns	ns	ns	ns	ns	ns	ns	ns	ns	ns	ns	ns	-0.84**	ns	ns	ns	ns	ns	-0.8*

Table 3.S1 continued…

	% C	SD_{adax}	SD_{abax}	SS_{adax}	SS_{abax}	g_{smax}	SI_{adax}	SI_{abax}	ES_{adax}	ES_{abax}
R_n (µmol m^{-2} s^{-1})	ns	ns	-0.75*	ns	-0.90**	ns	ns	ns	ns	ns
A_{mor} (µmol m^{-2} s^{-1})	-0.79*	-0.77*	ns	ns	ns	-0.78*	ns	ns	0.73*	ns
A_{mid} (µmol m^{-2} s^{-1})	-0.74*	ns	ns	-0.87**	ns	ns	ns	ns	ns	-0.97***
A_{aft} (µmol m^{-2} s^{-1})	-0.88**	ns	ns	ns	ns	ns	ns	ns	ns	ns
$g_{s\,n}$ (mol m^{-2} s^{-1})	0.84**	ns	ns	0.86**	ns	ns	ns	ns	ns	0.84**
$g_{s\,mor}$ (mol m^{-2} s^{-1})	ns	-0.82*	-0.75*	ns	ns	ns	ns	ns	0.81*	ns
$g_{s\,mid}$ (mol m^{-2} s^{-1})	ns	-0.76*	-0.83*	-0.76*	ns	ns	ns	ns	0.84**	-0.79*
$g_{s\,aft}$ (mol m^{-2} s^{-1})	-0.88**	ns	ns	ns	ns	ns	ns	ns	ns	ns
$iWUE_{mor}$	ns	ns	0.77*	ns	ns	ns	ns	ns	ns	ns
$iWUE_{mid}$	ns	0.74*	0.89**	ns	ns	0.85**	ns	ns	-0.82**	ns
$iWUE_{aft}$	ns	ns	ns	ns	ns	ns	ns	0.89**	ns	ns
A_{wd} (µmol m^{-2})	-0.90**	ns	ns	ns	ns	ns	ns	ns	ns	ns
$g_{s\,wd}$ (mol m^{-2})	-0.76*	-0.82**	-0.79*	ns	ns	ns	ns	ns	0.86**	ns
dWUE	ns	0.75*	0.88**	ns	ns	0.77*	ns	ns	-0.78*	ns
Ψ_{leaf} (-MPa)	-0.83**	ns	ns	ns	ns	ns	ns	ns	ns	ns
k_{cl} (min)	ns	-0.74*	-0.97**	ns	ns	-0.75*	ns	ns	0.80*	ns
Excess g_s (mol m^{-2})	ns	ns	-0.86**	ns	ns	ns	ns	ns	ns	ns
WUE_{cl}	ns	ns	ns	ns	ns	0.93**	ns	ns	ns	ns
k_{op} (min)	ns	ns	ns	ns	ns	ns	ns	ns	ns	ns
Forgone A (µmol m^{-2})	0.89**	ns	ns	ns	ns	ns	ns	ns	ns	ns
WUE_{op}	ns	-0.93**	ns	ns	ns	-0.84**	ns	ns	0.79*	-0.81**
LW (cm)	ns	ns	ns	ns	ns	ns	ns	0.90**	ns	ns
LMA (g m^{-2})	ns	ns	ns	ns	ns	ns	ns	ns	ns	ns
% N	0.82**	ns	ns	ns	ns	-0.76*	ns	ns	ns	0.85**
% C	-	ns	ns	ns	ns	ns	ns	ns	ns	0.81*
SD_{adax} (n° mm^{-2})	-	-	0.81**	ns	ns	0.94**	ns	ns	-0.99***	ns
SD_{abax} (n° mm^{-2})	-	-	-	ns	ns	0.87**	ns	ns	-0.87**	ns
SS_{adax} (µm^2)	-	-	-	-	ns	ns	ns	ns	ns	0.83**
SS_{abax} (µm^2)	-	-	-	-	-	ns	ns	ns	ns	ns
g_{smax} (mol m^{-2} s^{-1})	-	-	-	-	-	-	ns	ns	ns	ns
SI_{adax} (%)	-	-	-	-	-	-	-	ns	ns	ns
SI_{abax} (%)	-	-	-	-	-	-	-	-	ns	ns
ES_{adax} (µm^2)	-	-	-	-	-	-	-	-	-	ns
ES_{abax} (µm^2)	-	-	-	-	-	-	-	-	-	-

Chapter 4

The influence of water stress on the relative contribution of photosynthesis and stomatal conductance on intrinsic water use efficiency in a large selection of Sorghum genotypes differing in Aquaporin alleles

4.1 ABSTRACT

Sorghum is the fifth most important cereal crop worldwide, used mainly for food and feed. With increasing temperature and drought, breeding crop varieties that maximize yield from water investment is of paramount importance. At the leaf level, intrinsic water use efficiency (*iWUE*) is defined as the ratio of carbon assimilation rate (A_n) to stomatal conductance (g_s). Breeding for higher *iWUE*, especially in C_4 crops like Sorghum, has been challenging. Furthermore, the relative contributions of A_n and g_s to *iWUE* are underexplored in screening for possible contributions to high *iWUE*. Aquaporins (AQP) are associated with multiple leaf and plant processes, but their role in *iWUE* and drought responses remains to be elucidated. Building on the recent identification of AQP coding genes in Sorghum, I grew a large selection of Sorghum genotypes with different AQP alleles in a greenhouse under well-watered (WW) and water-stress (WS) conditions. There were large variations in leaf gas exchange and water status responses among the genotypes, between and within the two watering treatments. Key parameters such as A_n, g_s and *iWUE* showed high heritability, confirming strong genetic controls on these parameters and moderate water stress lead to significant reduction in g_s and intercellular CO_2 concentration (C_i) of the Sorghum leaves. Variation in *iWUE* mostly depended on g_s, but with exposure to WS the contribution of A_n increased. The genotypic diversity in the relative contribution of these components to *iWUE* creates opportunities to breed Sorghum crop varieties with higher *iWUE* without compromising productivity. These findings extend the data reported on the influence of growth temperature (Chapter 2) and diurnal rhythm (Chapter 3) and give a more complete picture of the physiological drivers of *iWUE* in Sorghum.

4.2 INTRODUCTION

Food security amid water scarcity is one of the key global challenges of the 21st century (UNCTAD, 2011), with rising global populations increasing the demand on agricultural crops. Sorghum (*Sorghum bicolor*) is globally important for fuel, fibre, food (Borrell, van Oosterom, *et al.*, 2014), and importantly in Australia as a rotational crop supplying animal feed (George-Jaeggli *et al.*, 2017). Sorghum, a C_4 species, was first domesticated in Africa, where it remains a key staple crop in the arid and semi-arid areas of sub-Saharan Africa, a region experiencing a rapid rise in population (Dillon *et al.*, 2007; Borrell, Mullet, *et al.*, 2014). Such environments are heavily dependent on rainfall, which is expected to experience more erratic patterns with climate change (Rippke *et al.*, 2016). Selection by farmers in Sorghum (and its wild relatives) has resulted in a repository of drought-adapted and water conserving traits (Dillon *et al.*, 2007). These rich genetic resources, along with small genome size, provides a template for studying the genetic controls of quantitative traits in key crops (Mace *et al.*, 2019).

Given that water scarcity is anticipated to increase, more attention is being paid to the efficiency of crops to produce biomass per unit of transpired water (Passioura, 2006). This characteristic termed transpiration efficiency or water use efficiency (WUE). (Passioura, 1977) incorporated WUE as a key component of higher yield in Wheat (*Triticum aestivum*), along with water use, as follows

$$Y = WU \times pWUE \times HI \qquad (4.1)$$

where Y is yield, WU is water use, $pWUE$ is water use efficiency of the plant, and HI is harvest index. The above expression has been used widely to test for differences in yield and its components (Condon *et al.*, 2004; Hall and Richards, 2013). At crop level, $pWUE$ is estimated by total biomass or grain produced per total amount of water use. At the leaf level, leaf WUE ($lWUE$) is calculated as the ratio of CO_2 assimilation rate to leaf transpiration rate through the stomata. Measuring $pWUE$ at the crop level can be very time consuming and can obscure the impact of possible environmental changes throughout the growth stage on $pWUE$ calculated at the final harvest of biomass or grain (Leakey *et al.*, 2019). Hence, $lWUE$ can provide a short-term physiological alternative to

pWUE. Measured using gas exchange equipment (such as infra-red gas analysers), *lWUE* is expressed as:

$$lWUE = \frac{A_n}{E} \qquad (4.2)$$

where A_n is carbon assimilation rate and E is transpiration rate per unit area. A_n and E can be expressed as follows, based on Fick's Law of diffusion:

$$A_n = g_{CO_2}(C_a - C_i) \qquad (4.3)$$

$$E = g_{H_2O}(W_i - W_a) \qquad (4.4)$$

where g_{CO2} and g_{H2O} are conductances to CO_2 and water vapour respectively; C_a is ambient CO_2 concentration, C_i is CO_2 concentration in the sub-stomatal cavity; W_a is water vapour concentration outside the leaf while W_i represents water vapour concentration inside the leaf. Correcting for the binary diffusivity of water vapour, equations 4.2, 4.3 and 4.4 can be combined as follows to:

$$lWUE = \frac{(C_a - C_i)}{1.6(W_i - W_a)} \qquad (4.5)$$

Equation 4.5 indicates that *lWUE* can be improved by either reducing C_i, or reduction water vapour pressure gradient (W_i-W_a). E is dependent on changes in ambient vapour pressure deficit (VPD) and temperature, leading to environmental variations in *lWUE* that are independent of the genotype (Sinclair, 2012). Therefore, an expression that better reflects genetic determinants is intrinsic *WUE* (*iWUE),* where stomatal conductance (g_s) is used instead of E (Ghannoum, 2016). Stomata are the small pores on leaf surfaces that facilitate CO_2 and water vapour exchange, and the size and number of those is a strong determinant of transpiration and photosynthesis rates (Farquhar and Cowan, 1974; Wong *et al.*, 1979). Also, stomatal features are genetically controlled, including in Sorghum (Liang *et al.*, 1975). Consequently, this study focussed on *iWUE*, defined as:

$$iWUE = \frac{A_n}{g_s} \qquad (4.6)$$

According to equation 4.6, genetic changes in *iWUE* can occur through genetic variation in g_s or A_n (Jackson *et al.*, 2016), with both terms sharing a common link through C_i. In particular, g_s influences C_i through it supply function, whilst A_n is highly responsive to changes in C_i below a certain threshold (Ghannoum, 2016).

Selecting for higher *iWUE* in breeding programs has been challenging for a number of reasons. First, *iWUE* is a complex trait with multiple physiological components contributing to the variation in A_n and g_s (Condon *et al.*, 2004). Secondly, the lack of heritable traits that are easily screened for that correlate with *iWUE*, especially in C_4 crops (Hammer *et al.*, 1997). In C_3 crops, carbon isotope discrimination (Δ) has been used as a proxy for *iWUE* because it relates strongly to C_i and hence *iWUE* (Rebetzke *et al.*, 2002), Additionally, Δ has high heritability (H_b) in Wheat making selection much easier (Condon and Richards, 1992). The estimation of Δ in C_4 plants has proven more complicated (von Caemmerer *et al.*, 2014), even though Δ and *iWUE* have been shown to correlate in some C_4 species (Sorghum, Maize, *Setaria veridis*) with some QTLs mapping to both parameters (Henderson *et al.*, 1998; Ellsworth and Cousins, 2016; Ellsworth *et al.*, 2020). Hence, finding genetic variation in *iWUE* in C_4 crops has mainly depended on gas-exchange parameters (Xin *et al.*, 2009). Consequently, improving *iWUE* in C_4 crops requires a better understanding of the genetic variation in gas exchange mechanisms causing variation in *iWUE* (Jackson *et al.*, 2016).

A key physiological observation is the relationship between A_n and g_s. The A_n-g_s relationship is linear within a range of g_s, but at high values of g_s, the slope of A_n-g_s decreases, exhibiting a curvilinear relationships (Wong *et al.*, 1979; Gilbert *et al.*, 2011). This means that A_n and g_s can contribute different proportions to *iWUE* depending on their position along the curve (Ghannoum, 2016). When comparing different plants, high *iWUE* could be due to higher A_n, or due to lower g_s. Reduced g_s means a lower transpiration rate and most likely water use, which would have a negative impact on yield according (equation 4.1). The operation of the CO_2 concentrating mechanism (CCM) in C_4 leaves leads to the saturation of A_n at low C_i, and hence low g_s, which means that operating with high g_s, may waste water without improving A_n (Ghannoum, 2016). In conclusion, there is a possibility that some crop varieties can sustain high *iWUE* due to higher photosynthetic capacity per given g_s. Finding such variation is agronomically beneficial as it would mean the often-negative relationship between *WUE* and water use might be

alleviated. Exploiting variations in the A_n-g_s relationship is particularly relevant for C_4 crops (Ghannoum, 2016).

Aquaporin channels are proteins embedded in the lipid bilayer that envelopes animal and plant cells. The term "aqua"-porin was attributed to these proteins as they facilitate the rapid and selective transport of water and other nutrients (Chaumont *et al.*, 2001; Reddy *et al.*, 2015). Plant aquaporins (from here on AQPs) can be subdivided into four major families: 1) plasma membrane intrinsic proteins (PIPs); 2) tonoplast intrinsic proteins (TIPs); 3) NOD26-like intrinsic proteins (NIPs); and 4) small basic intrinsic proteins (SIPs). These subdivisions mainly indicate subcellular organ localization (Kaldenhoff *et al.*, 2008). Physiologically, AQPs strongly influence water flow across the leaf, affecting physiological parameters such as hydraulic conductance, especially PIPs (Cochard *et al.*, 2007; Shatil-Cohen *et al.*, 2011; Lopez *et al.*, 2013; Prado and Maurel, 2013; Prado *et al.*, 2013; Caldeira *et al.*, 2014; Sade, Shatil-Cohen, *et al.*, 2014), including in Sorghum (Choudhary *et al.*, 2013). Also, AQP control of leaf hydraulics has been shown to impact stomatal responses. AQP expression is involved in guard cell membrane permeability when guard cells change turgor to open or close (Heinen *et al.*, 2014; Wang *et al.*, 2016). Also, AQPs have been implicated in facilitating abscisic acid (ABA) mediated stomatal responses (Grondin *et al.*, 2015), a key component of crop drought responses (Blum, 2015), with AQPs also involved in plant drought response (Alexandersson *et al.*, 2005). The identification of AQP genes in Sorghum (Groszmann *et al.*, unpublished) paved the way for this experiment to screen for possible impact of different AQP proteins. The physiological impact of AQP proteins on leaf hydraulics, stress response and gas exchange suggest that genetic diversity in AQPs may affect processes involved in determining A_n, g_s and *iWUE*.

The current study focused on studying the responses and drivers of *iWUE* under water deficit, which, as argued above, is agronomically important. In this chapter, I present the results of a screening experiment using 89 genotypes selected based on AQP diversity. The specific objectives were to 1) assess the impact of genetic diversity and the extent of genetic control on *iWUE* and other plant traits in closely related Sorghum genotypes: 2) elucidate the impact of drought stress on leaf gas exchange and hydraulics; 3) partition the photosynthesis and stomatal conductance components of *iWUE*; and 4) determine the impact of water stress on *iWUE* and its underpinning physiological processes.

4.3 MATERIALS & METHODS

Genotype selection

The genotypes used in this study came from a Nested Association Mapping (NAM) population. NAM is a type of selective breeding that allows for statistical robustness while retaining great diversity of parental lines. In general, two methods to identify quantitative trait loci (QTLs) have been used in crop breeding: Linkage Analysis focuses on the construction of large families from two inbred lines, and Association Mapping (such as Genome Wide Association Studies, GWAS) depending on the historical recombination events that occurred throughout crop breeding and domestication. Linkage analysis results in a low number of recombinations and lower diversity due to the limited number of parents. NAM maintains some allelic diversity by breeding recombinant inbred lines (RILs) from multiple parents, with the NAM innovation being the use of a single parent as a reference line (**Fig.4.1**).

The current Sorghum NAM population comprises an elite parental line R937945-2-2 (Recurrent Parent, RP) crossed with >100 exotic lines sourced from unadapted geographical or racial diverse lines (Non-Recurrent Parent, NRP). The F1 progeny were backcrossed with the elite parent to produce BC_1F_1 populations comprising of ~22-25% exotic genome introgressed into the elite parental background. Individual BC_1F_1 populations are genotyped using high density single-nucleotide polymorphism (SNP) markers providing profiles of the exact exotic chromosomal segments. In addition to this resource, whole genome sequencing is available for many of the exotic parental lines and the elite line. With these resources (Jordan *et al.*, 2011), the following steps were conducted:

1. Candidate AQP genes were screened to identify exotic lines carrying non-synonymous SNP alleles to the elite parental line.
2. BC-NAM populations involving these exotic lines were queried to identify individual lines with chromosomal segments harbouring the elite AQP allele or the exotic AQP allele.

3. These were then filtered for populations that contained numerous individuals carrying either the elite or exotic AQP allele. Numerous instances were required for sufficient repetition.
4. The final NAM lines chosen were derived from exotics containing a mix of geographical origins, with specific focus on a mix of dry vs. milder climates with the idea these would have greater extremes in the traits of interest due to necessary adaptations (**Table 4.1**). This is why Table 4.1 shows the background of the exotics based on the different races of Sorghum because the different races indicate the kind of environmental conditions or domestication pressures that influenced the genetic background of the exotic lines.

Plant culture

Ten L capacity cylindrical pots were used to allow ample space for root development before implementation of the water stress treatment. The pots were adjusted to similar weight (1.5 kg) by adding gravel (Lucky stones 100-300mm, Turtle Nursery and Landscape Supplies, South Windsor, NSW), then the same amount of soil was added to all pots. Fly Screen mesh (Cyclone Aluminium Insect Screen) was added to the bottom of the pots minimize soil seeping through pot drainage holes. The potting mix used was a mix of soil, sand and decomposed bark (Turtle Nursery and Landscape Supplies, South Windsor, NSW). It has large particle size for good drainage and root development. Granulated fertiliser (Osmocote Plus Organics All Purpose Fertiliser, Scotts Miracle-Gro Company, Marysville, Ohio) was pre-mixed with the soil, with more fertiliser added in the lower half of the pot where more roots will develop as the plant grows. To each pot, 3.5 kg of soil was added, making the total pot weight 5 kg.

Seeds were directly sown into the soil in October 2019. The plants germinated and grew in a naturally lit, controlled-environment greenhouse (Plexiglas Alltop SDP 16; Evonik Performance Materials, Darmstadt, Germany) at the Hawkesbury Institute for the Environment, Western Sydney University, Richmond, New South Wales, Australia (-33.612032, 150.749098). The ambient temperature was controlled at 30°C during the day period, with night temperatures being 18°C. There was a 2 h period at 24°C between the temperature transitions. The day temperature started at 8 am, and night temperature at 8 pm. CO_2 concentration was kept at ambient levels. Each greenhouse chamber contained both well-watered and water stressed pots, and pots were swapped between the four chambers twice during growth in a randomised fashion. Each glasshouse chamber had 180 pots (two treatments, 89 genotypes, 3 replicates: 89*3*2=534 total pots).

Watering regime & water stress

Pots were fully watered at night and weighed in the morning. This was done a few days in a row to establish pot weight at 100% Field Capacity (FC). All the pots were maintained at FC for the first 6 weeks after germination to ensure good plant growth and root establishment before imposing water stress. The difference between the pot weight at FC

and pot weight before watering (which was 5 kg) represented the amount of water lost due to drainage and transpiration, and that needed to be replaced to maintain FC. Usually, more than this amount was added every evening to compensate for any excess drainage. After 6 weeks of growth, watering was withheld from half of the pots (WS, water stress treatment), while the other half continued to be watered at FC (WW, well-watered treatment). Stomatal conductance was monitored every 2-3 days (along with water addition to WS plants; see below) in WS plants until midday g_s reached around 0.1 mol m^{-2} s^{-1} or less at saturating light, with the plant also showing signs of wilting. Some droughted pots were weighed to check that there was a substantial difference in pot weight compared to FC pots. After the WS plants reached the 0.1 g_s level or started wilting, we added 150 mL of water every three days, at sunset, to the droughted pots, which was estimated to be equivalent to total plant transpiration during the day (50 mL) in the WS treatment. This was sufficient water to maintain plant function whilst imposing a water limitation. This approach does not take into account differences in plant water use due to plant size, but was planned in order to impose a similar soil water content (Volumetric SWC was measured using a sensor – For WW pots at FC it ranged between 15-20%; while for WS pots it was less 5-10%). Plants watered on the previous night were not measured the next day to eliminate any possibility of watering effect from the night before on plant recovery, which is why watering occurred every three days so measurements could occur with plants suffering water deficit 2-3 days after the addition of the 150 mL. The watering regimes were maintained until the end of the experiment. Impact of WS was visible 2 weeks after water withholding for most genotypes (plants were 8 weeks old). There were 3 replicates per genotype and water treatment.

Time of measurements and sampling

Sampling for all plants took place between the 8th and 12th week after germination. Plants had 10–12 fully expanded leaves when sampling occurred. WS plants were measured at least 3 weeks after the onset of the drought treatment. In total, sampling lasted for about a month (mid-December 2019 to mid-January 2020), which represents the peak of the Australian summer.

Midday leaf gas exchange

Midday leaf gas exchange rates were measured between 10 am and 4 pm on sunny days. The photoperiod was 14-15 hours and solar midday was around 1–1:30 pm. A Li-6400XT Infra-red gas analysis (LiCor Biosciences, Lincoln, Nebraska, USA) was used to obtain saturating rates of CO_2 assimilation rate (A_n), stomatal conductance (g_s) and transpiration rate (Tr), cuvette conditions were set at: 30°C block temperature, flow rate of 500 µmol m^{-2} s^{-1}, photosynthetic active radiation (PAR) of 2000 µmol m^{-2} s^{-1}, and ambient CO_2 concentration of 400 ppm. CO_2 concentration in the sub-stomatal cavity (intercellular CO_2, C_i) was also recorded. At the conclusion of photosynthetic measurements, PAR was reduced to 0 in order to measure leaf dark respiration (A_n in the dark, R_{dark}). This is not the same as night respiration but is just a way to estimate leaf metabolism at midday. R_{dark} was measured after a period of 10 minutes under 0 light, after which five logs were taken five seconds apart by the Li6400XT autoprogram. Instantaneous water use efficiency ($iWUE$) was calculated as the ratio of A_n to g_s. All measurements were taken from the middle of the youngest fully expanded leaf (YFEL). Gas exchange was measured once per leaf, per plant (n=3 per treatment). Average relative humidity in the three chambers ranged between 60% to 65%, and this conditions were matched in the Li-6400XT cuvette (RH between 40 – 60 %).

Leaf water potential (Ψ_{leaf}) and hydraulic conductance

A leaf adjacent to the gas exchange leaf was used to measure midday leaf water potential (Ψ_{midday}) using a pressure chamber (Model 1000 and Model 1505D Pressure Chambers, PMS Instrument Company, Albany, Oregon, USA). The leaf below the Ψ_{midday} leaf was covered with cling wrap and tin foil to prevent transpiration and allow the leaf to equilibrate with stem water potential. This leaf was used to estimate midday stem water potential (Ψ_{stem}). Pre-dawn leaf water potential ($\Psi_{pre\text{-}dawn}$) was sampled on different leaves before daybreak. In each case, the leaf was cut at the ligule and placed in a plastic bag that was exhaled into before sealing. The bags were stored on ice, then transported from the greenhouse to the lab where Ψ_{leaf} was measured within 1-2 h of excision. Excision usually occurred at a maximum of 3 hours after excisions, with a maximum of 5 hours between gas exchange measurements and pressure chamber measurements.

Leaf hydraulic conductance and was calculated as shown in Simonin *et al.* (2015):

$$K_{leaf} = \frac{E}{(\Psi_{stem} - \Psi_{midday})} \qquad (4.7)$$

where E refers to the leaf transpiration rate expressed on area basis. While soil-to-leaf hydraulic conductance (referred to as plant hydraulic conductance in this study, K_{plant}) was calculated as shown in Robson *et al.* (2012):

$$K_{plant} = \frac{E}{(\Psi_{predawn} - \Psi_{midday})} \qquad (4.8)$$

Plant and Leaf Morphology

Leaf width (*LW*) was measured at the same leaf area where gas exchange measurements were made. Leaf length (*LL*) was also measured. Leaf thickness (*LT*) was measured using a Photosynq Multispec (Photosynq, East Lansing, Michigan, USA – see Kuhlgert *et al.*, (2016)). At the end of the experiment and before biomass harvest, plant height (*PH*) and number of leaves (*LN*) of each plant were recorded. The area of leaves used for gas exchange and water potential were measured using a LI-3100C Area Meter (LiCor Biosciences, Lincoln, Nebraska, USA). The average area of these three leaves was multiplied by the total number of leaves per plant to obtain total leaf area (*TLA*).

Relative chlorophyll content (*SPAD*)

Relative chlorophyll content was estimated by measuring absorbance at 650 and 940 nm and performing special products analysis division (SPAD). SPAD readings were recorded via the Photosynq Multispec. Measurements were conducted on the same leaf used for gas exchange.

Components of *iWUE*

The relationship between A_n and g_s is often simplified as a linear relationship, but over an wide range of C_i when combining the WW and WS Sorghum plants, the relationship between A_n and g_s is expected to be curvilinear (Ghannoum, 2016). To quantify the relative contribution of A_n and g_s to variations in *iWUE*, the approach of Gilbert *et al.* (2011) was used as modified by (Li *et al.*, 2017). Briefly, variation in *iWUE* ($\Delta iWUE$) attributed to g_s ($\Delta iWUE_{gs}$) was calculated via the equation resulting from applying the line

of best fit to the $iWUE$-g_s relationship. $\Delta iWUE_{gs}$ was expressed as the deviation from the average $iWUE$ of all genotypes (Li *et al.*, 2017).

$$\Delta iWUE = iWUE - iWUE_{mean} \quad (4.9)$$

$$iWUE_{gs} = -29.64 \ln(g_s) + 90.911 \quad (4.10)$$

where $iWUE_{mean}$ is the average $iWUE$ of all genotypes per treatment. g_s is the g_s of the genotype of interest fitted to the relationship of $iWUE$-g_s. $\Delta iWUE_{gs}$ was calculated as:

$$\Delta iWUE_{gs} = iWUE_{gs} - iWUE_{mean} \quad (4.11)$$

Variation in $iWUE$ attributed to photosynthesis ($\Delta iWUE_{pc}$) was calculated for each replicate as the deviation of the observed $iWUE$ from the $iWUE_{gs}$; i.e., if the expected $iWUE$ at the measured g_s is $iWUEg_s$, then the contribution of A_n to observed $iWUE$ is the difference between $iWUE_{gs}$ and $iWUE$ (Li *et al.*, 2017).

$$\Delta iWUE_{pc} = iWUE - iWUE_{gs} \quad (4.12)$$

Genetic variation

Broad-sense heritability was calculated as in Li *et al.* (2017):

$$H_b = \frac{\sigma_g^2}{\sigma_p^2} \quad (4.13)$$

where σ_g^2 and σ_p^2 are the genotypic and phenotypic variances respectively. σ_g^2 was obtained as the sq. of mean from the ANOVA output. σ_p^2 was calculated as:

$$\sigma_p^2 = \sigma_g^2 + \frac{\sigma_{g \times treatment}^2}{number\ of\ treatments} + \frac{\sigma_e^2}{number\ of\ replicates} \quad (4.14)$$

where $\sigma_{g\ x\ treatment}^2$ and σ_e^2 are the genotype * treatment interaction and error variances respectively. $\sigma_{g\ x\ treatment}^2$ was obtained as the mean squared of the genotype * treatment interaction and σ_e^2 was obtained as the sq. of mean residual error. Because the heritability analysis encompasses both treatments, the number of replicates was standardized as 5 (as opposed to 6; 3 WW and 3 WS) to account for genotypes not in both treatments. The

genotypic coefficient of variation (*GCV*) and the phenotypic coefficient of variation (*PCV*) were calculated as:

$$GCV = \frac{\sigma_g}{mean} \times 100 \qquad (4.15)$$

$$PCV = \frac{\sigma_p}{mean} \times 100 \qquad (4.16)$$

where σ_g and σ_p are the genotypic and phenotypic standard deviation. The *mean* refers to the mean of all the measurements across treatments for the variable in question. For the mean value of $iWUE_{gs}$ and $iWUE_{pc}$ where averages are near zero or negative (because these values are expressed as deviations from the average of all observations), the value used for *mean* was that for *iWUE*.

Statistical analyses

Statistical analysis and data visualisation were performed using R software (R Core Team (2020). R: A language and environment for statistical computing. R Foundation for Statistical Computing, Vienna, Austria. URL https://www.R-project.org/). Analysis of variance was carried out using a linear mixed-effects model (packages lme4 and nlme). Variance within groups was performed afterwards using a *post hoc* Tukey test. Regression analysis was carried in R using linear modelling (lm). The model predicted the significance of a linear relationship between the two variables:

$$y = mx + c$$

where *y* (predicted) and *x* (predictor) are the y-axis and x-axis variables respectively, *m* is the slope of the relationship, and *c* is the y-axis intercept. *m* represents the direction of the relationship (negative or positive). A Pearson product moment correlation analysis was performed to test statistical significance of relationships and obtain correlation coefficients.

Note on genetic analysis

Association mapping of *iWUE* phenotypic variation and BC-NAM genetic diversity could not be completed due to extensive delays in lab work and travel restrictions due to the

pandemic outbreak. As international students must adhere to a hard deadline for PhD submission, this analysis will be completed after thesis submission. This process is underway along with additional data relating to biomass and relative water content to be added to analysis.

4.4 RESULTS

Overall variations in physiological parameters

Gas exchange parameters varied among the genotypes under both watering regimes. CO_2 assimilation rate (A_n) experienced a 2.2-fold variation (17.6—39.3 μmol m^{-2} s^{-1}) under WW conditions and 6.1-fold variation (6.8—32.0 μmol m^{-2} s^{-1}) under WS conditions (**Fig.4.2 a,b**). Similarly, stomatal conductance (g_s) experienced 2.9- (0.11 to 0.33 mol m^{-2} s^{-1}) and 6.3-fold variation (0.026 to 0.16 mol m^{-2} s^{-1}) under WW and WS conditions, respectively after removing g_s values below 0.01 and above 0.2 mol m^{-2} s^{-1} (**Fig.4.2 c**,**d**). Sub-stomatal CO_2 concentration (C_i) were similarly variable (**Fig.4.2 g**,**h**). Intrinsic water use efficiency (*iWUE*) experienced less variation, with fold variation of 1.9 and 1.8 under WW (92 to 170 μmol^{-1} CO_2 mol^{-1} H_2O) and WS conditions (121 to 216 μmol^{-1} CO_2 mol^{-1} H_2O), respectively (**Fig.4.2 e,f**). Similar variation was observed for plant height (*PH*; 2.7- and 3.7-fold variation for WW and WS treatments, respectively) and leaf area (*LA*; 6.9- and 4.7-fold variation) (**Fig.4.3 a-d**). Total leaf area (*TLA*) varied much more widely for both treatments (9.0- and 8.5 fold variation for WW and WS treatments, respectively; **Fig.4.3 e,f**). On the other hand, relative chlorophyll content (SPAD) showed much lower variation (1.9- and 3.2-fold variation for WW and WS treatments, respectively; **Fig.4.3 g,h**). Pre-dawn water potential and plant hydraulic conductivity (K_{plant}) also showed significant variation (**Fig.4.4**). Fold-variations are summarised for all parameters in **Table 4.2** and genotype means are shown in **Table S4.2**.

Genetic heritability in physiological parameters

Leaf gas exchange parameters A_n, g_s and *iWUE* had high (≤0.7) broad-sense heritability (H^2_b; **Table 4.2**). However, the phenotypic coefficient of variation (*PCV*) was always slightly higher than the genetic coefficient of variation (*GCV*), with *GCV* for *iWUE* being much lower than A_n or g_s, highlighting a lower degree of variation for *iWUE* as signified by the lower fold-variation observed earlier. *GCV* for A_n and g_s explained almost 50% of variation. Components of *iWUE* ($iWUE_{gs}$ and $iWUE_{pc}$) had lower heritability than the measured gas exchange variables (≈0.5). Hydraulic characteristics exhibited high heritability (0.6-0.7). The highest heritability (≥0.8) observed were for plant morphological features such as PH, leaf width (*LW*), leaf length (*LL*) and *LA* (**Table** 4.**2**).

Effect of water stress on physiological parameters

Leaf gas exchange parameters (A_n, g_s and C_i) significantly (p<0.05) decreased, whilst *iWUE* significantly (p<0.05) increased in response to the WS treatment (**Fig.4.5 a-c**)**.** Leaf size, *LW*, *LL*, leaf thickness (*LT*) and *LA* significantly (p<0.05) decreased under WS (**Fig.4.6 a-c**). Relative chlorophyll content was also significantly lower under WS (**Fig.4.6 h**). On a whole-plant level, *PH* and *TLA* were significantly (p<0.05) lower under WS (**Fig.4.6 e,g**). However, the number of leaves was not affected by WS (**Fig.4.6 f**). Pre-dawn ($\Psi_{pre\text{-}dawn}$), stem (Ψ_{stem}) and midday (Ψ_{midday}) leaf water potentials were significantly (p<0.05) lower under WS, indicating the onset of drought stress in the plants (**Fig.4.7 a-d**). Consequently, K_{plant} (**Fig.4.7 d**) and leaf hydraulic conductivity (K_{leaf}; **Fig.4.7 e**) were significantly lower under WS. There was a positive relationship between K_{plant} and K_{leaf} (r=0.66, p<0.001), with these two variables tracking each other across treatments (**Fig.4.7 f**).

Relationships between leaf gas exchange parameters

There was a strong positive curvilinear correlation between A_n and g_s when including all replicates (**Fig.4.8 a**; Table S4.1 for regression statistics). This resulted in high *iWUE* values at very low g_s (due to either WS or genotypes with low g_s), yielding another curvilinear relationship between *iWUE* and g_s, when including all replicates (**Fig.4.8 c**; Table S4.1). The relationship between A_n and *iWUE* was best fit by a linear regression (**Fig.4.8 b**; r=-0.7, p<0.001), and the data was more scattered compared to the A_n/g_s and $iWUE/g_s$ curves. Within treatments, An and iWUE were significantly correlated under WS (r=-0.58, p<0.001), but at WW the relationship was not significant (r=0.16) but still a negative trend can be observed. There was a positive linear relationship between C_i and both A_n and g_s (**Fig.4.8 d,e**; r=0.53, p<0.001 and r=0.64, p<0.001 respectively), but A_n vs C_i relationship does weaken significantly within treatments, but is statistically significant under WS (r=0.23, p<0.05). A strong negative linear correlation was observed between *iWUE* and C_i (r=-0.8, p<0.001; **Fig.4.8 f**).

Relationships between leaf gas exchange and plant hydraulics

The sharp decrease in Ψ_{leaf} under WS led to mostly exponential relationships with A_n, g_s, *iWUE* (**Fig.4.9**). In particular, there were strong positive (exponential) associations

between g_s and $\Psi_{pre\text{-}dawn}$ & Ψ_{midday} (**Fig.4.9 a,b**; r=0.68 and r=0.69, respectively, p<0.001), and between A_n and $\Psi_{pre\text{-}dawn}$ & Ψ_{midday} (**Fig.4.9 d,e**; r=0.68 and r=0.7, respectively, p<0.001). Within treatments, g_s was correlated with $\Psi_{pre\text{-}dawn}$ & Ψ_{midday} at WS only (r=0.45 and 0.47 respectively, p<0.001). It was similar for A_n (r=0.39 and 0.41 for $\Psi_{pre\text{-}dawn}$ & Ψ_{midday} respectively, p<0.001). Both parameters (A_n and g_s) rapidly collapsed below a $\Psi_{pre\text{-}dawn}$-of -0.5 MPa. Moreover, A_n and g_s increased in a mostly linear fashion with increasing K_{plant} (**Fig.4.9 c,f**; r=0.76 and r=0.75, respectively, p<0.001). In contrast, *iWUE* increased exponentially with increasing Ψ_{leaf} (**Fig.4.9 g**)., and mostly linearly with increasing Ψ_{midday} and K_{plant} (**Fig.4.9 h,i**; p<0.001). Within treatments, *iWUE* was mostly correlated at WS with Ψ (r=-0.42 and -0.50 for $\Psi_{pre\text{-}dawn}$ & Ψ_{midday} respectively, p<0.001) but persisted under both treatments for K_{plant}.

Components of *iWUE*

Variation in *iWUE* (*ΔiWUE*) due to variations in g_s(*ΔiWUE*$_{gs}$) and A_n (*ΔiWUE*$_{pc}$), relative to the respective averages of all genotypes in the WW and WS treatments, were calculated (**Fig.4.10**) according to the framework developed by (Gilbert *et al.*, 2011) and modified by (Li *et al.*, 2017). Under WW conditions, genotypes that exhibited the highest relative-to-average *ΔiWUE* also had higher than average *ΔiWUE*$_{pc}$ (genotypes R05012-64, R05012-90 and R04044-132 among others; **Fig.4.10 a**). Under WS condition, genotypes with low Δ*iWUE* also had the lowest *ΔiWUE*$_{pc}$ (**Fig.4.10 b**). There was a much stronger positive correlation between Δ*iWUE* and *ΔiWUE*$_{pc}$ (r=0.47, p<0.001) than between Δ*iWUE* and *ΔiWUE*$_{gs}$ (r=0.14; p<0.1) (**Table S4.1**). *ΔiWUE*$_{pc}$ and *ΔiWUE*$_{gs}$ were not correlated (**Fig.4.11 a**). Treatment effect on mean *ΔiWUEpc* was statistically significant (p<0.05) with *ΔiWUEpc* higher under WS (**Fig.4.11 b**). WS caused a significant (p<0.05) decrease in *ΔiWUEgs* (**Fig.4.11 c**).

4.5 DISCUSSION

This study was conducted to screen for variation in leaf gas exchange between Sorghum genotypes that are the progeny of parents that have different Aquaporin (AQP) alleles. A water stress (WS) treatment was implemented to test how gas exchange parameters vary under stressful conditions and its impact on intrinsic water use efficiency (*iWUE*). The nested association mapping (NAM) strategy used to generate those genotypes (see Materials & Methods) means that the genotypes share most of their genetic composition but differ in key genes passed on from the exotic parental line. This potential diversity was used to screen for genetic diversity in the key gas exchange parameters as well as other leaf and plant characteristics. Finally, the range of gas exchange values provided due to the WS treatment allowed for the exploration of how CO_2 assimilation (A_n) and stomatal conductance (g_s) separately influenced *iWUE*.

Genetic diversity of *iWUE* in Sorghum

In this study, we found that mean A_n, g_s, *iWUE* and C_i vary greatly between the genotypes under both WW and WS conditions (**Fig.4.2**), with all four variables displaying high broad-sense heritability (H_b, **Table 4.2**). A previous screen of *iWUE* in 48 field grown Sorghum genotypes (Pan *et al.*, 2021) recorded higher maximal A_n and *iWUE*, with some genotypes having A_n of >40 µmol m^{-2} s^{-1} and *iWUE* of >170 µmol CO_2 mol^{-1} H_2O, which is similar to the average *iWUE* recorded under WS in the current study (**Table 4.S2**). However, the field site used by Pan *et al.* was experiencing lower than expected soil moisture. On the other hand, another screen of 25 selected Sorghum accessions showed overall g_s and C_i lower than this study, but similar A_n range (Xin *et al.*, 2009). Overall, the leaf gas exchange values reported here were within those expected for Sorghum and similar to measurements in previous chapters of this thesis.

The high H_b of *iWUE* (and more specifically g_s) bodes well with previous findings in this thesis that showed strong dependence of *iWUE* on leaf width (*LW*) and stomatal characteristics. *LW* also showed high H_b in this study but it did not correlate with *iWUE* (**Table 4.S1**), likely because the range of *LW* measured in this study was narrower relative to Chapter 2 (2–8 cm in chapter 2; 3-6 cm in this chapter). While stomatal anatomical characters were not measured in this study, early work on Sorghum leaves

showed that *LW* and stomatal features have high H_b, and hence also have high genetic control (Liang *et al.*, 1973, 1975). Furthermore, the ratio of sub-stomatal to ambient CO_2 concentration (C_i:C_a), which is considered a more robust parameter than C_i as accounts for variations in C_a (Ghannoum, 2016) also showed strong H_b (0.56; **Table 4.2**). Despite high H_b, the variation in the phenotypic coefficient of variation (*PCV*, **Table 4.2**) meant that WS treatment (*i.e.*, environmental factors) played an important role in determining variation for the gas exchange and hydraulic parameters, especially as the statistical analyses presented in **Table 4.2** combined the WW and WS treatments. A solution for reducing *PCV* is more replication per genotype (up to 16 according to Li *et al.*, 2017), which was beyond the capacity of this study. Nevertheless, high H_b under environmental variation is a significant finding considering the genotypes shared about 75% of their genetic material due to the backcrossing step included in the NAM to produce the progeny. Also, the high number of genotypes screened here (89) exceeds that of other *WUE* screens in Sorghum (49 in Hammer *et al.*, (1997), which found little genetic variation) and might partially compensate for low replication. Considering that previous key improvements in Sorghum, such as the stay-green trait, were achieved via breeding with significant contribution from wild Sorghum relatives (Ochieng *et al.*, 2021), finding room for genetic improvements within inbred genotypes is highly desirable, especially in an important trait such as *iWUE*. While **Figs 4.2-4.4** presented color-coded genotypes based on their exotic parent, there was no discernible pattern observed that was consistent among the main variables. Delving into the possible mechanisms determining the genetic material of progeny based on the parents is a future goal of this research.

Reduction in A_n and g_s under WS

The WS treatment elicited trade-offs in plant and leaf function which highlighted genotypic variance without completely stopping plant growth and leaf generation. The average g_s under WS was 0.093 (**Table 4.S2**), which is within the operational conductance range for grasses, including C_4 grasses (Ghannoum *et al.*, 2003; Taylor *et al.*, 2014; Ocheltree *et al.*, 2016). Guard cells are very sensitive to changes in leaf water status, as control of stomatal aperture depends on changes in guard cell turgor pressure and on hydraulic signals from epidermal cells (Buckley, 2005), along with other drought sensing mechanisms such as ABA-induced stomatal closure (Pou *et al.*, 2008; McAdam *et al.*, 2016). During transpiration, water in the xylem comes under physical tension as low

(negative) water potential in the leaf (Ψ_{leaf}) pulls water from the soil to the leaf (Brodribb *et al.*, 2003). Under high tensions, air bubbles could form in pit membranes of the xylem resulting in cavitation (Brodribb *et al.*, 2003). Under soil water deficit, this tension in the xylem is exacerbated and can lead to cavitation as well as loss of cell turgor. The loss of turgor causes stomatal closure, but because embolised vessels can be refilled when water is abundant, species have developed a mechanism to reduce tension under drought stress by closing the stomata at higher (less negative) water potentials (isohydric). This is compared to other species that maintain high transpiration rates even with more negative Ψ_{leaf} (anisohydry). Ψ_{leaf} decreased significantly under WS (**Fig.4.7 a,b,c**), leading to a reduction in hydraulic conductivity (K; **Fig.4.7 d,e**; **Table 4.S1**). The formation of emboli and disruption of the hydraulic supply to the sub-stomatal cavity, causing partial stomatal closure is one possible cause for reduction in K. Xylem embolism is related to irreversible damage (Johnson *et al.*, 2018), however, with our WS treatment more likely causing limitation than permanent damage (even though some genotypes responded in that fashion). More likely, damage to the photosynthetic apparatus was more likely the cause of reduced A_n, g_s and K (as shown by reduction in SPAD in **Fig.4.6 h**), plus cellular mechanical deformation and plasmolysis induced by declining turgor (Yang *et al.*, 2017).

The reduction in A_n under WS can be mainly attributed to reduced C_i due to low g_s. Under optimum conditions, A_n is saturated in C_4 leaves when C_i reaches 100-150 ppm (Ghannoum *et al.*, 2003). In this experiment, C_i was at those levels under WW (**Fig.4.5 d**), while the average C_i under WS (91 ppm) was significantly lower (**Fig.4.5 d**; **Table 4.S2**), albeit at the higher end of the linear part of a typical C_4 A_n-C_i curve (Ghannoum, 2009). The A_n-C_i curves performed for Chapter 3 of this thesis also showed similar C_i range for Sorghum (**Fig.4.S2**), but with saturation starting at C_i higher than 150 and close to 200 ppm. Indeed, while within treatment relationships between A_n and C_i were weaker than the global one, under WS there relationship is still statistically significant, highlighting that low g_s conditions constrain C_4 photosynthesis to C_i. To sum up, stomatal limitation played the main role in curtailing A_n under WS. Notably, there were variations in genotypic response to WS for all variables. In some genotypes, WS reduced photosynthesis primarily as a result of stomatal (diffusional) limited, while others might have experienced biochemical damage to the photosynthetic apparatus, such as reduced

enzyme activity (Ghannoum *et al.*, 2003; Ghannoum, 2009; Yan *et al.*, 2017), or reduced chlorophyll as observed in **Fig.4.6 h** and **Fig.4.S1 g**.

Significant decrease in leaf and plant size due to WS (**Fig. 4.6**) is observed routinely in Sorghum studies (Borrell, Mullet, *et al.*, 2014; Borrell, van Oosterom, *et al.*, 2014; Sutka *et al.*, 2016). Like reduced g_s, reduced leaf size under WS minimises transpiration potential by reducing total surface area and promotes soil water conservation for latter stages of development such as grain filling. Nearly all the plants in this experiment flowered and produced seeds by the end of the experiment, further highlighting that the WS treatment was not extreme. Furthermore, reducing total leaf area under WS (**Fig. 4.6 g**) reduced the total area for light intercept, and can reduce the heat load which would otherwise lead to leaf overheating and positive feedback on transpirational cooling.

Hydraulic safety vs efficiency vs water use efficiency

Hydraulic conductivity (whether leaf-specific, K_{leaf}, or soil-to-leaf, K_{plant}) has been consistently shown to correlate with higher A_n and g_s (Sack and Holbrook, 2006; Scoffoni *et al.*, 2016). This relationship was confirmed in this study (**Fig.4.9 c,f**). Limiting K_{leaf} has been hypothesised as a trait that could enhance drought tolerance via allowing soil moisture conservation in rainfed Sorghum (Sinclair *et al.*, 2005). The relationship between g_s and different estimates of Ψ_{leaf} was exponential (**Fig.4.9 a,b**), indicating that g_s suffered a rapid decrease below a certain threshold of leaf water content. This was especially true under WS, where this relationship persisted, probably due to the larger range of Ψ *values.* Usually, this threshold is determined by hydraulic techniques that measure the loss of K_{leaf} as the leaf dries while simultaneously monitoring g_s (Brodribb and Holbrook, 2003). Because only a "spot" measurement was made after the onset of WS in this study, it cannot be concluded from the data presented here what was that threshold, especially considering the wide diversity of the drought responses exhibited from the genotypes. Still, having higher K_{leaf} (or K_{plant}) can lead to a more drought sensitive plant in Sorghum (Choudhary and Sinclair, 2014). This was also shown in a study of nine C_4 grasses (Ocheltree *et al.*, 2016), where the species with higher K_{leaf} lost more of their hydraulic function at more positive water potentials. Furthermore, Henry *et al.* (2019) found that tree species with higher g_s at WW conditions were more sensitive to WS and closed their stomata at higher water potentials. Interestingly, there seems to be a

diversity in response within cultivated Sorghum genotypes in whether maintaining high K_{leaf} to match transpiration demand (hydraulic efficiency, high g_s, anisohydric) or a moisture conservation strategy (low K_{leaf} and early stomatal closure; hydraulic safety, isohydric) when encountering WS (Gholipoor *et al.*, 2012; Choudhary *et al.*, 2013).

Consequently, higher $K_{leaf/plant}$ (and hence g_s) correlates with lower *iWUE*, as observed in this experiment (**Fig.4.9 i**; **Table 4.S1**), highlighting the possible trade-off between *iWUE* and yield under water limitation in the following ways: 1) Drought resistant (low K_{plant}) genotypes can reduce gas exchange (and hence assimilation of carbon and water use, while raising *iWUE*) at high soil water content, foregoing a high proportion of water that can be used for assimilation and would constitute a loss if water limitation was alleviated later on, which is a likely scenario in rainfed crop systems such as Sorghum's (Choudhary *et al.*, 2013; Choudhary and Sinclair, 2014). 2) As highlighted above, K_{plant} correlated positively with A_n and g_s, which is important as maintaining hydraulic supply is key to maintaining leaf integrity and low K_{plant} under, for example, high temperatures, can impede evaporative cooling and damage the leaf. 3) Higher *iWUE* under WS due to low g_s means that the plant is experiencing stress and has a lower plant water status (Blum, 2009), as observed here with higher *iWUE* in more stressed (negative Ψ_{leaf}) plants (**Fig.4.9 g,h**), and is further confirmed with the negative *iWUE* vs Ψ relationship at WS, showing that lower Ψ (more negative) leading to higher *iWUE.* To sum up, selecting for high *iWUE* (due to low K_{leaf} and low transpiration) on the assumption that it confers drought tolerance does not necessarily lead to more productivity under WS (Holloway-Phillips and Brodribb, 2011a), and reminds us that looking at *iWUE* alone as a predictor of yield under adverse conditions is counterproductive as it can compromise water use (Ghannoum, 2016).

Contribution of components of *iWUE* under WS

Because *iWUE* is calculated as a ratio of A_n to g_s, it is not always obvious what influences changes in *iWUE*. *iWUE* increases because A_n increased, g_s decreased, or both. The extent of A_n increase or g_s decrease are highly dependent on environmental variation such as humidity or [CO_2]. Usually, changes in *iWUE* are due to changes in A_n and g_s but at different magnitudes. Hence, there is a possibility that there is genetic variation in the magnitude of changes in A_n and g_s that lead to changes in *iWUE*. This can be important because high

iWUE can mean a reduction in water use or productivity, and low g_s may mean low A_n. But if a plant can reduce g_s more than A_n in response to an environmental variable, such as drought, this can be beneficial for productivity. Overall, g_s (-2.5×) decreased more than A_n (-1.9×) in response to WS (**Fig.4.5 a,b**).

More importantly, the exposure of plants in this experiment to WS expanded the range of g_s value measured and resulted in the curvilinear relationship between A_n and g_s (**Fig.4.8 a**), which then led to a curvilinear relationship between *iWUE* and g_s (**Fig.4.8 c**). This type of relationship indicates that the level of influence exerted by g_s on A_n on *iWUE* changes along the curve. To partition *iWUE* into effects caused by A_n and g_s, the methods introduced by Gilbert *et al.* (2011) and adapted by Li *et al.* (2017) were used to calculate variation in *iWUE* ($\Delta iWUE$) due to changes in A_n ($\Delta iWUE_{pc}$) and g_s ($\Delta iWUE_{gs}$). Both components varied differently among genotypes (**Fig.4.10**) under both treatments, with a general trend that increases in the components led to an increase in $\Delta iWUE$, as also shown in **Table 4.S1**, with $\Delta iWUE_{pc}$ showing a much stronger positive relationship with *iWUE* than $\Delta iWUE_{gs}$. This finding highlights the complexity of *iWUE* as a trait, the importance of accounting for the range of g_s measured when screening for *iWUE* variation, and the possibility of finding varieties that attain higher *iWUE* due to photosynthetic gains rather than reduced g_s (and hence transpiration) that might impair productivity (Blum, 2009), especially as the data demonstrate that $\Delta iWUE_{pc}$ and $\Delta iWUE_{gs}$ varied independently (**Fig.4.11 a**).

Under plentiful water availability, plants can increase g_s to maximize CO_2 uptake without risking hydraulic failure. These high g_s values lead to the 'saturated' part of the A_n-g_s curve (**Fig.4.8 a**), where the impact of increase in g_s is marginal for A_n. Under WW conditions, any genotype showing a lower g_s would have a higher *iWUE*, resulting in the strong dependence of *iWUE* on g_s observed in previous studies on C_4 plants (Jackson *et al.*, 2016; Cano *et al.*, 2019; Pan *et al.*, 2021; previous chapters of this thesis). Under WS conditions, the low values of g_s impose a diffusional limitation on *iWUE* caused by low C_i, and hence higher photosynthetic capacity has the potential to overcome some of this limitation and maintain high *iWUE*. This diffusional limitation was observed with the negative A_n-*iWUE* relationship under WS (**Fig.4.8 b**), which was not observed under WW. Also, the independence of $\Delta iWUE_{pc}$ and $\Delta iWUE_{gs}$ suggests that along the g_s-*iWUE* relationship, the

impact of g_s changes from a limitation on water loss (H_2O contribution) to a limitation more on CO_2 uptake (CO_2 contribution) as well as H_2O. Hence, under WS, *iWUE* is influenced by the early linear part of A_n-g_s relationship, where the genotype that maximizes A_n per given g_s achieves higher *iWUE*. **Fig.4.11 b,c** illustrate that under WS, $\Delta iWUE_{pc}$ increases while $\Delta iWUE_{gs}$ decreases (and becoming more negative compared to mean *iWUE*), further confirming that under low g_s, *iWUE* is strongly influenced by photosynthetic variation. This is confirmed by looking back at **Fig.4.10 b**, where the genotypes with the lowest $\Delta iWUE$ at WS have a much lower $\Delta iWUE_{pc}$ compared to $\Delta iWUE_{gs}$.

Finally, while this is encouraging, the genotype*treatment variance for $\Delta iWUE_{pc}$ was large compared to genotypic variation (**Table 4.2**), suggesting that genotype ranking will change depending on water availability. While this should be taken into consideration, it is part and parcel of measuring *iWUE* (or at a larger scale, whole plant *WUE*), as environmental factors such as changes in VPD or temperature will always play a role in determining physiological responses that impact *iWUE* (Sinclair *et al.*, 2008; Gholipoor *et al.*, 2010; Gilbert *et al.*, 2011). Also, while the shape of the A_n-g_s relationship promotes an increase in $\Delta iWUE_{pc}$ under WS, a good thing in the context of climate change and increasing drought, it might be as important to have high $\Delta iWUE_{pc}$ under WW conditions, where $\Delta iWUE_{gs}$ is highest. I discussed earlier how limiting g_s (and transpiration) leads to a reduction in water use and hence yield (as per equation 4.1), and yet it is under WW conditions where water use needs to be at its maximum along with *iWUE* to maximize yield under growing worldwide demand. Synthesizing these ideas and applying them is a challenge for breeders and scientists alike and highlight the complex physiological nature of *iWUE*.

Possible AQP impact on observed responses

The variation in the observed responses is encouraging for later identification of AQP function and impact on sorghum leaf physiology. AQPs regulate water flux between cells and consequently can influence membrane permeability (Sade, Shatil-Cohen, *et al.*, 2014) as well as impact K (Cochard *et al.*, 2007; Shatil-Cohen *et al.*, 2011; Lopez *et al.*, 2013; Prado *et al.*, 2013), with changes in Kleaf linked to changes in PIP AQP expression in Maize (Caldeira *et al.*, 2014). This means that AQP expression would very likely have influence

the drought responses observed here. Further, AQP expression in guard cells can also influence stomatal response as it facilitates ABA or pressure-gradient mediated responses (Heinen *et al.*, 2014; Grondin *et al.*, 2015). The impact of AQPs, especially PIPs, on mesophyll conductance and CO2 membrane permeability (Flexas *et al.*, 2008; Kaldenhoff *et al.*, 2014; Sade, Gallé, *et al.*, 2014; Ding *et al.*, 2016) would likely have contributed to the photosynthetic diversity and response to drought observed in sorghum here.

Conclusion

This study was conducted to screen for variation in *iWUE* in Sorghum genotypes that were the result of a nested association mapping of eight aquaporin genes identified in *Sorghum bicolor*. Large variations in gas exchange and hydraulic responses were found among the genotypes, with key parameters such as A_n, g_s and *iWUE* showing high heritability. This can indicate the possible role different aquaporin proteins can play in determining leaf gas exchange rates and paves the way for further screening of those genotypes to identify the genetic and molecular mechanisms of aquaporin influence while also providing a genetic breeding target. The study showed that moderate WS leads to significant reduction in g_s, and hence A_n, likely due to decreased K_{leaf} and to conserve soil water. I also discussed possible trade-offs between drought tolerance and *iWUE* in the context of maintaining productivity. Ultimately, the extension of the A_n-g_s relationship into a curvilinear shape due to low g_s under WS allowed for exploration of *iWUE* in relation to its components, A_n and g_s. I found that photosynthetic capacity becomes crucial to high *iWUE* as g_s decreases, providing a fresh avenue to explore variation in *iWUE* in Sorghum. Considering the location of g_s along the A_n-g_s curve can be an important tool in selection for higher *iWUE* without sacrificing yield in Sorghum.

Table 4.1. Genotype profiling of the six exotic parental lines included in this study and their racial composition.

ID	LIMS	Origin	Caudatum	Guinea	Kafir	Asian Durra	East African Durra	Description
SC35-14E	S1001734H1	Ethiopia	0.0515476	0.0497845	0.0851101	0.638718	0.174839	Used in breeding programs for drought tolerance traits.
SC103-14E	S1001734H2	South Africa	0.805411	0.0300111	0.1033	0.0373942	0.0238837	Originates from hot, dry regions of Ethiopia and Sudan.
Ai4	S1001735B2	China breeding program	0.134933	0.0383872	0.0728902	0.656071	0.097719	Breeding variety not known for drought resistance.
FF_RTx7000	S1001735C2	USA breeding program	0.0426457	0.0347866	0.626611	0.272332	0.023625	High yielding line that uses a lot of water and grows very well; drought sensitive.
QL12	S1001735D6	Australia breeding program	1.00E-04	0.506423	0.43325	0.0396663	0.0205605	Australian breeding variety known for drought tolerance
IS9710	S1001735E3	Sudan	0.0326895	0.177449	0.229347	0.560414	1.00E-04	Known for high transpiration efficiency; originated in dry regions.

Table 4.2. Statistical summary of measured outputs along with the calculated heritability and genetic variation information. The analysis of variance was conducted using a linear mixed effects model (see Materials & Methods). The analysis incorporated both WW and WS measurements (both *n*=3), but to correct for genotypes that did not experience both treatments and for the odd *n*=2 genotype/treatment, *n* was taken to be 5 for the calculations of Phenotypic Variance. Detailed summary of mean (±SE) are in Table 4.S2.

	Mean	Fold Change WW (%)	Fold Change WS (%)	Genotypic Variance	Treatment Variance	G * T Interaction	Residual Error	Phenotypic Variance	H_b	GCV (%)	PCV (%)
A_n (μmol m^{-2} s^{-1})	23.2	2.23	6.05	127.2	14436.1	61.6	61.49	170.3	0.75	48.61	56.25
R_{dark} (μmol m^{-2} s^{-1})	-1.33	0.42	5.3	0.33	19.81	0.2	0.16	0.46	0.71	43.19	51.11
g_s (mol m^{-2} s^{-1})	0.17	2.89	6.35	0.01	1.22	0	0.01	0.01	0.71	58.82	69.6
iWUE	148.35	1.86	1.78	963	102434	570	643.17	1376.63	0.7	20.92	25.01
$\Delta iWUE_{pc}$	-1.4	-	-	694.67	90	910	714.5	1292.57	0.54	17.77	24.24
$\Delta iWUE_{gs}$	0.19	-	-	293.3	2770.6	304.5	289	503.35	0.58	11.54	15.12
C_i (ppm)	111.14	2.83	6.31	2214	91498	2170	2011.93	3701.39	0.6	42.34	54.74
$C_i : C_a$	0.28	2.83	6.31	0.01	0.57	0.01	0.01	0.02	0.57	35.71	47.38
$\Psi_{pre\text{-}dawn}$ (-MPa)	-0.41	14.28	14.62	0.34	40.87	0.31	0.23	0.54	0.63	141.38	178.73
Ψ_{stem} (-MPa)	-0.74	3.14	10.3	0.32	59.4	0.19	0.21	0.46	0.7	76.92	91.85
Ψ_{midday} (-MPa)	-1.26	2.25	2.57	0.25	46.64	0.16	0.17	0.36	0.69	39.76	47.82
K_{plant} (mmol m^{-2} s^{-1} MPa^{-1})	5.6	4.32	11.1	18.26	756.1	13.11	11.95	27.21	0.67	76.31	93.14
K_{leaf} (mmol m^{-2} s^{-1} MPa^{-1})	9.11	3.96	10.03	27.87	847.68	26.84	27.35	46.76	0.6	57.95	75.06
Leaf Width (cm)	4.54	2.35	2.3	2.16	4	1.01	1.41	2.95	0.73	32.37	37.81
Leaf Length (cm)	62.1	2.9	2.48	484.39	797.31	126.64	135.04	574.72	0.84	35.44	38.6
Leaf Thickness (mm)	0.54	5.41	5.01	0.14	0.56	0.11	0.1	0.22	0.65	69.29	85.87
Leaf Area (cm^2)	175	6.85	4.73	10097	113348	3507	5509.3	12952.36	0.78	57.42	65.03
Plant Height (cm)	56.98	2.7	3.74	863.3	7632.2	132	140.77	957.45	0.9	51.57	54.3
Number of Leaves	12.97	1.7	1.57	7.1	5.21	1.04	1.2	7.86	0.9	20.54	21.61
Total Leaf Area (cm^2)	2126	8.98	8.53	2300053	66973672	1532072	1311009	3328290.8	0.69	71.34	85.81
SPAD	39.48	1.92	3.21	177.8	5760.2	134.4	78.63	260.73	0.68	33.77	40.9

A_n: Carbon assimilation rate; R_{dark}: Dark respiration rate; g_s: Stomatal conductance; *iWUE*: Instantaneous water use efficiency; $\Delta iWUE_{pc}$: relative change in *iWUE* attributed to variation in A_n; $\Delta iWUE_{gs}$: relative change in *iWUE* attributed to variation in g_s; C_i: Sub-stomatal carbon dioxide concentration; $C_i : C_a$: Ra io of C_i to ambient carbon dioxide concentration; $\Psi_{pre\text{-}dawn}$ and Ψ_{midday}: leaf water potenial; Ψ_{stem}: Stem water poten ial at midday; K_{plant}: Plant hydraulic conductivity; K_{leaf}: Leaf hydraulic conductivity; *SPAD*: Relative Chlorophyll content bvased on special products analysis division; H_b: Broad-sense heritability; *GCV*: Genetic coefficient of variation; *PCV*: Phenotypic coefficient of varia ion.

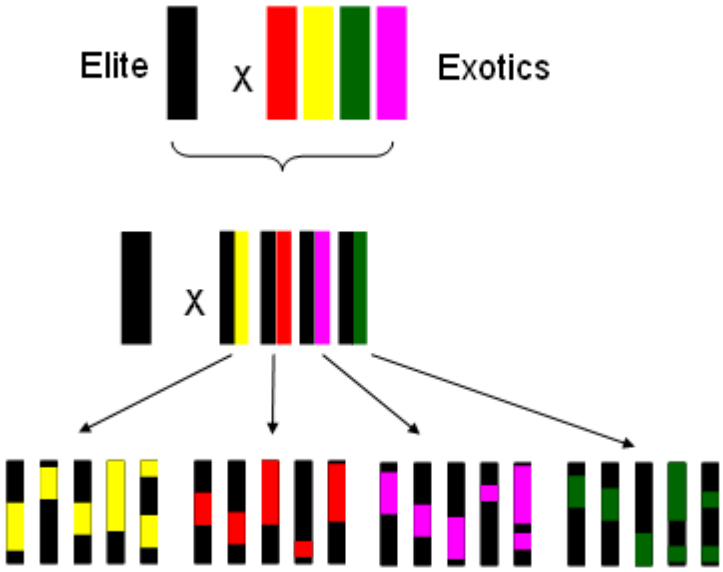

Fig.4.1 A simplified illustration of how recombinant inbred lines (RILs) are produced using nested association mapping (NAM).

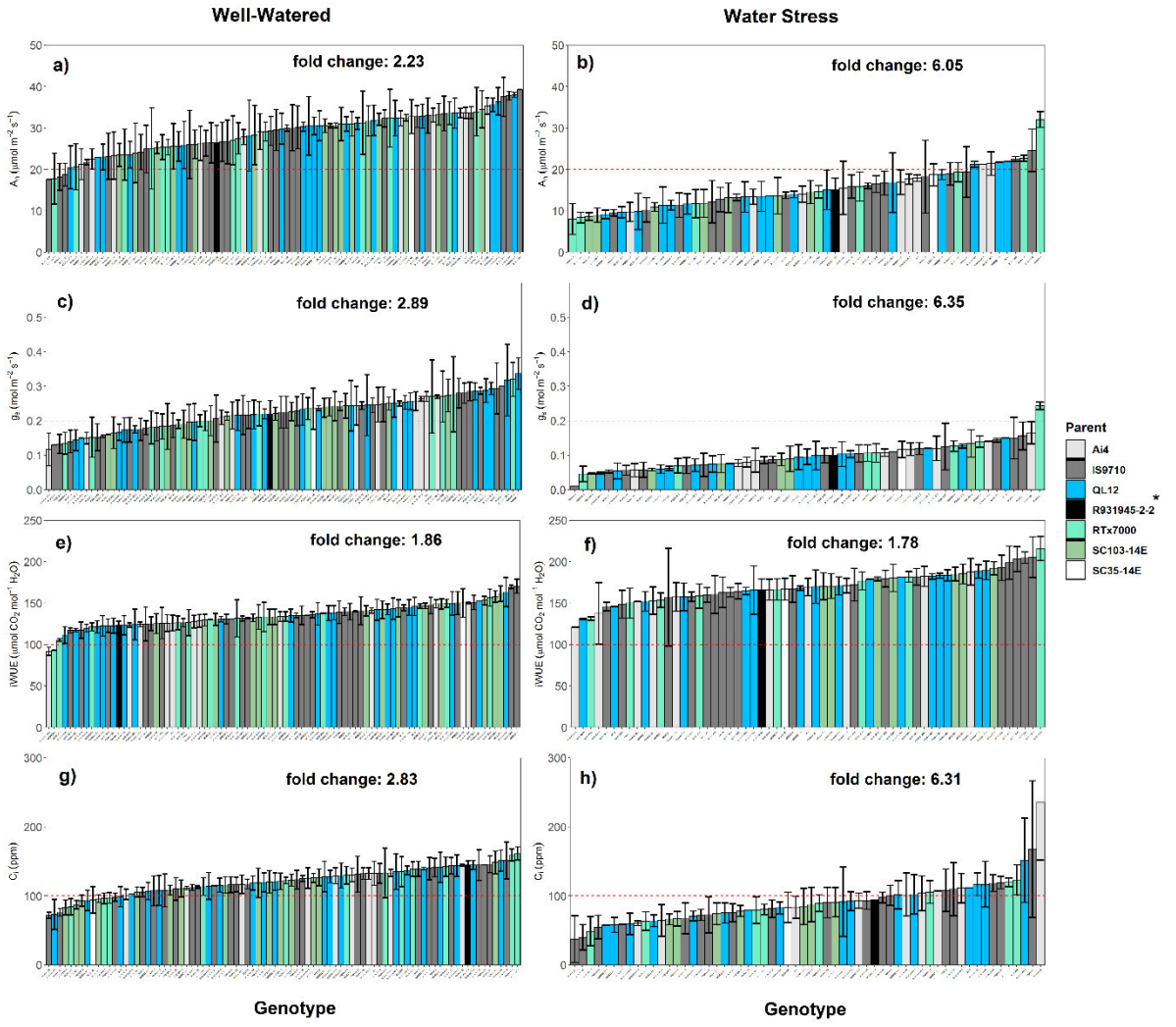

Fig.4.2 Bar chart highlighting the genotypic diversity in gas exchange derived parameters from the Sorghum genotypes for both watering treatments. Each bar's value represents the mean for each genotype (n=3), with error bars representing standard error (SE). The colors of the bars represent the exotic (non-recurrent) parental line that the specific genotype represents. The recurrent parent R931945-2-2 is represented with an * in the legend. **(a)** & **(b)**Net carbon assimilation rate (A_n); **(c)** & **(d)** Stomatal conductance (g_s); **(e)** & **(f)** Intrinsic water use efficiency ($iWUE$); **(g)** & **(h)** Sub-stomatal carbon dioxide concentration (C_i). For **Fig.4.2 g**, the bar for genotype R04047-116-1 as the it would have made the presentation of the Fig. much harder because its error scale margins are to large for the bar plot. Value is presented in **Table 4.S2**.

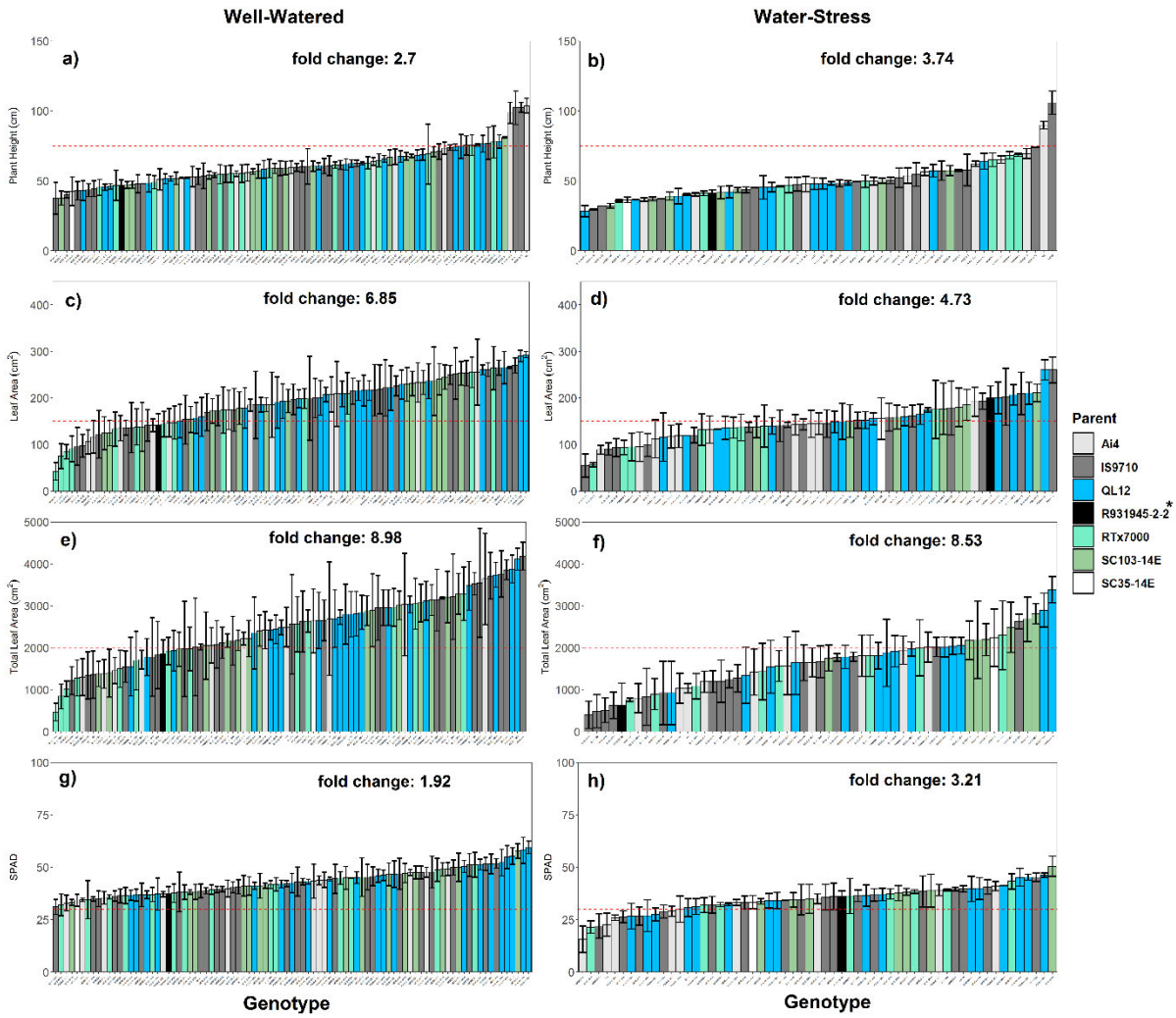

Fig.4.3 Bar chart highlighting the genotypic diversity in morphological and compositional parameters from the Sorghum genotypes for both watering treatments. Each bar's value represents the mean for each genotype (n=3), with error bars representing standard error (SE). The colors of the bars represent the exotic (non-recurrent) parental line that the specific genotype represents. The recurrent parent R931945-2-2 is represented with an * in the legend. **(a)** & **(b)**Plant Height; **(c)** & **(d)** Leaf Area; **(e)** & **(f)** Total Leaf Area; **(g)** & **(h)** Relative Chlorophyll Content as calculated by Special Products Analysis Division (SPAD).

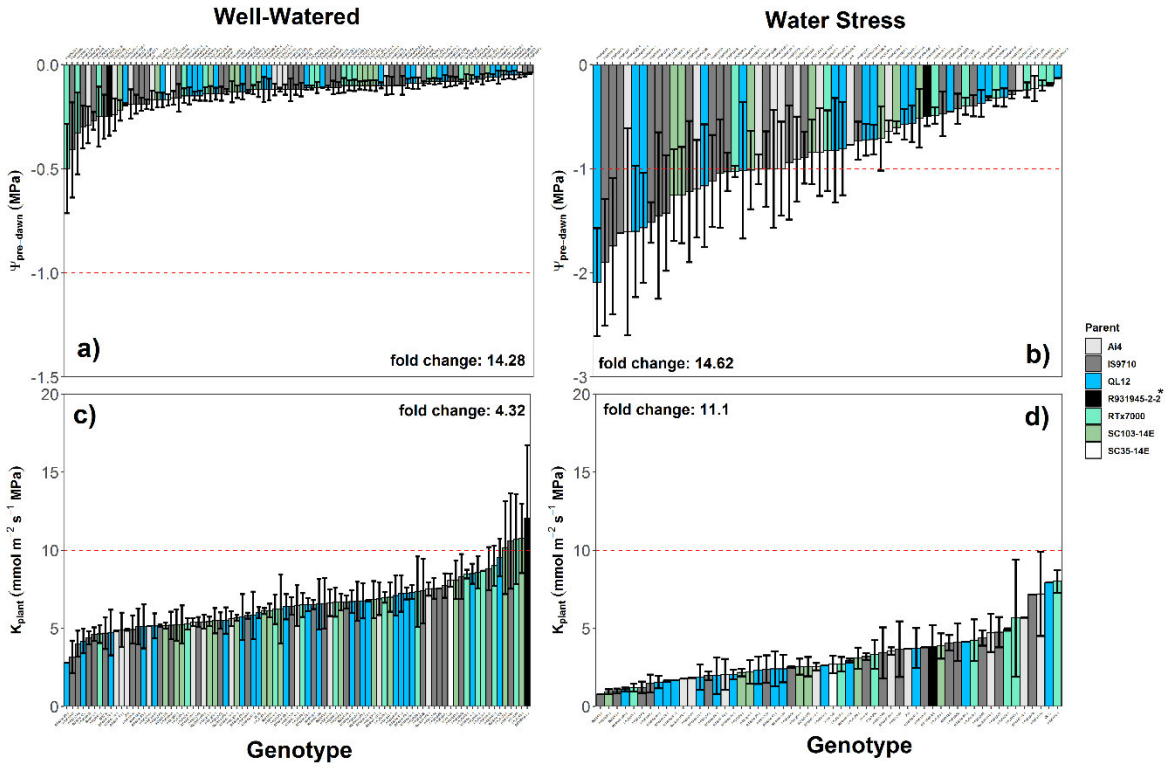

Fig.4.4 Bar chart highlighting the genotypic diversity in plant hydraulic parameters from the Sorghum genotypes for both watering treatments. Each bar's value represents the mean for each genotype (n=3), with error bars representing standard error (SE). The colors of the bars represent the exotic (non-recurrent) parental line that the specific genotype represents. The recurrent parent R931945-2-2 is represented with an * in the legend. **(a)** & **(b)** Pre-Dawn leaf water potential ($\Psi_{pre\text{-}dawn}$); **(c)** & **(d)** Plant hydraulic conductivity (K_{plant}).

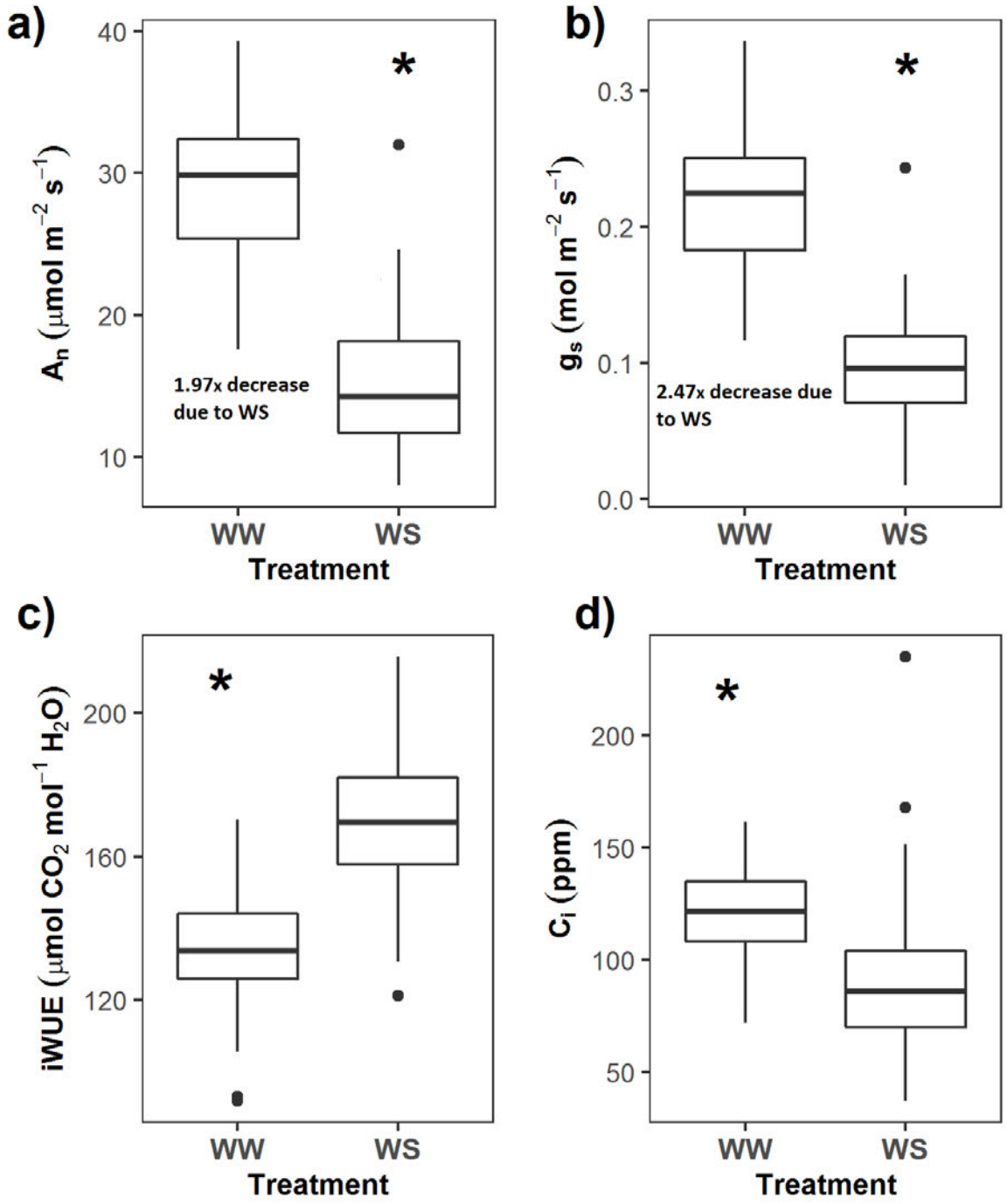

Fig.4.5 The distribution of gas exchange values within the two watering treatments. The distribution is summarized by boxplots for each treatment. The values in each distribution compromise the mean of every genotype (n=3) per treatment, yielding *n=89* for Well-Watered treatment and *n=60* for Water Stress treatment. Each box encompasses the 25th and 75th percentiles, with whiskers extending to show the extremes. Statistically significant difference is represented at the top of each boxplot with * indication to highlight a *p*-value of 0.05 or lower. **(a)** Net carbon assimilation rate (A_n); **(b)** Stomatal conductance (g_s); **(c)** Intrinsic water use efficiency (*iWUE*); **(d)** Sub-stomatal carbon dioxide concentration (C_i).

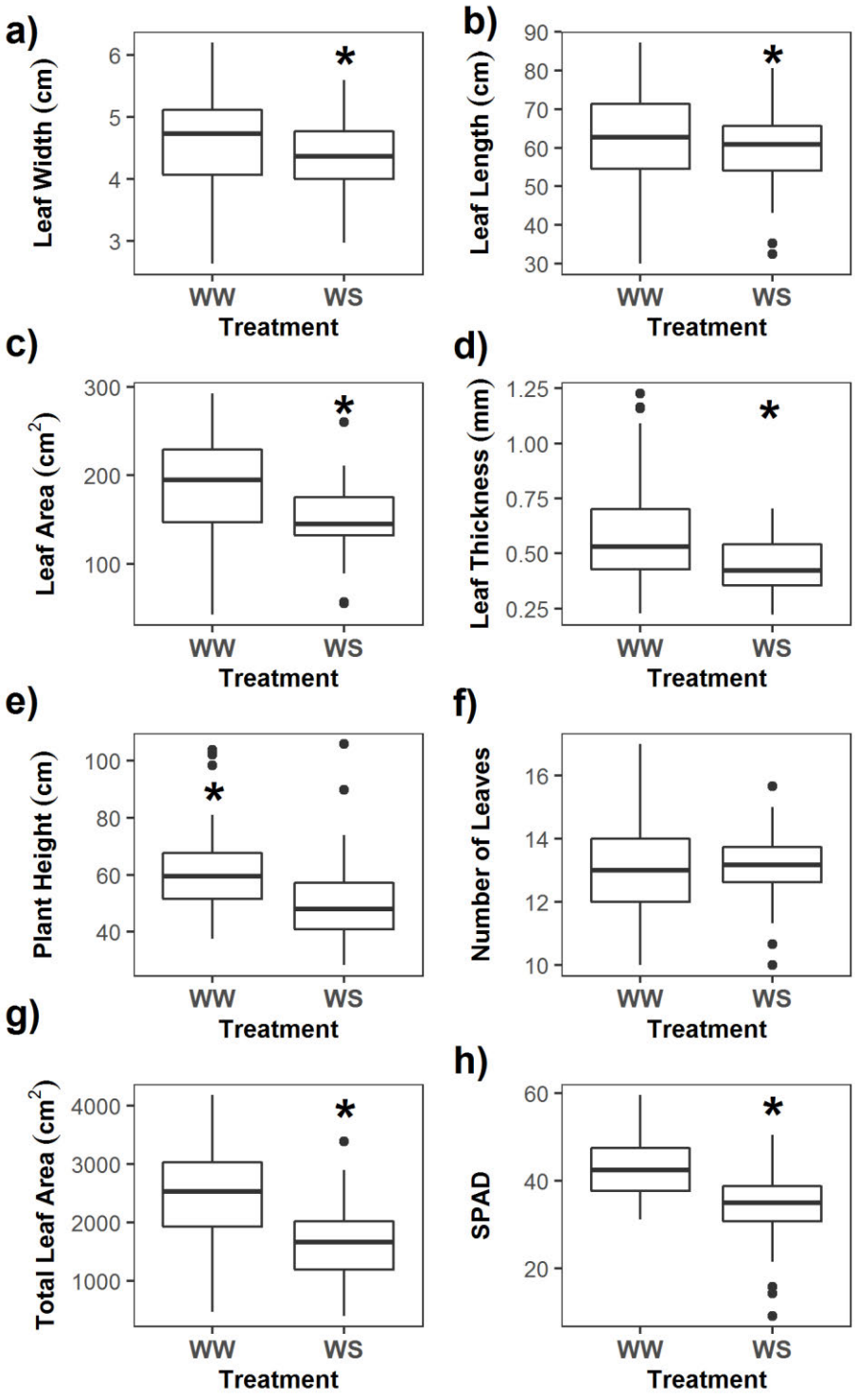

Fig.4.6 The distribution of leaf morphological and compositional characteristics within the two watering treatments. The distribution is summarized by boxplots for each treatment. The values in each distribution compromise the mean of every genotype (n=3) per treatment, yielding *n=89* for Well-Watered treatment and *n=60* for Water Stress treatment. Each box encompasses the 25th and 75th percentiles, with whiskers extending to show the extremes. Statistically significant difference is represented at the top of each boxplot with * indication to highlight a *p*-value of 0.05 or lower. **(a)** Leaf Width; **(b)** Leaf Length; **(c)** Leaf Area; **(d)** Leaf Thickness; **(e)** Plant Height; **(f)** Number of Leaves; **(g)** Total Leaf Area; **(h)** Relative Chlorophyll Content as calculated by Special Products Analysis Division (SPAD).

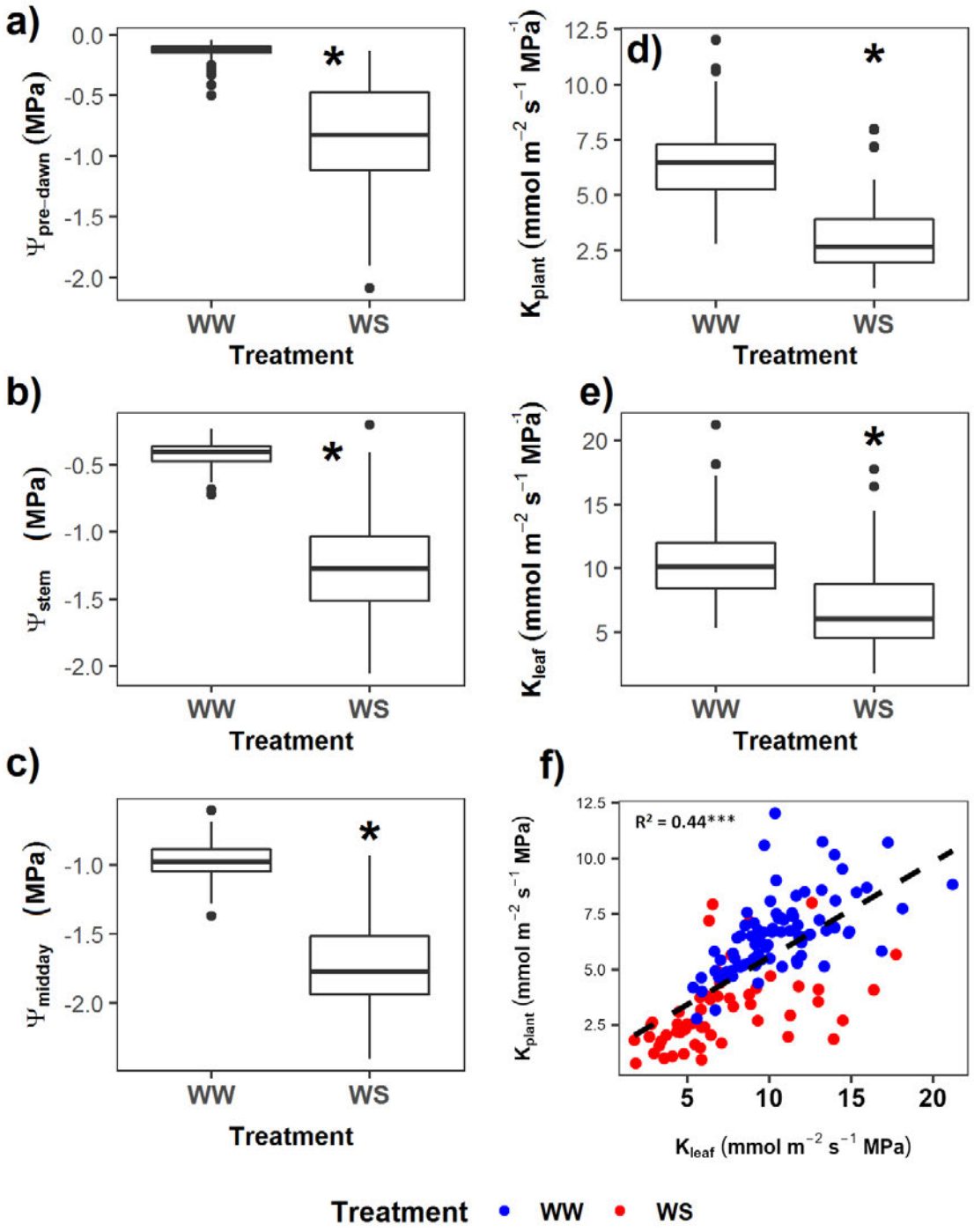

Fig.4.7 The distribution of leaf and plant hydraulic characteristics within the two watering treatments. The distribution is summarized by boxplots for each treatment. The values in each distribution compromise the mean of every genotype (n=3) per treatment, yielding *n=89* for Well-Watered treatment and *n=60* for Water Stress treatment. Each box encompasses the 25th and 75th percentiles, with whiskers extending to show the extremes. Statistically significant difference is represented at the top of each boxplot with * indication to highlight a *p*-value of 0.05 or lower. **(a)** Pre-Dawn leaf water potential ($\Psi_{pre\text{-}dawn}$); **(b)** Midday stem water potential (Ψ_{stem}); **(c)** Midday leaf water potential (Ψ_{midday}); **(d)** Plant hydraulic conductivity (K_{plant}); **(e)** Leaf-specific hydraulic conductivity (K_{leaf}). **Fig.4** (**f**) shows the relationship between K_{leaf} and $K_{plant,}$ with the line of best fit shown and the R^2 regression coefficient shown based on a Pearson product-moments correlation analysis (Table 4.S1). Different watering treatments are represented by the different fill colour of the scatter points: blue=Well-Watered, red=Water Stress. Each point in the scatter plot represents the mean value of the variable per species, per treatment (n=3). Standard error bars were removed to ensure clearer presentation (Table 4.S2).

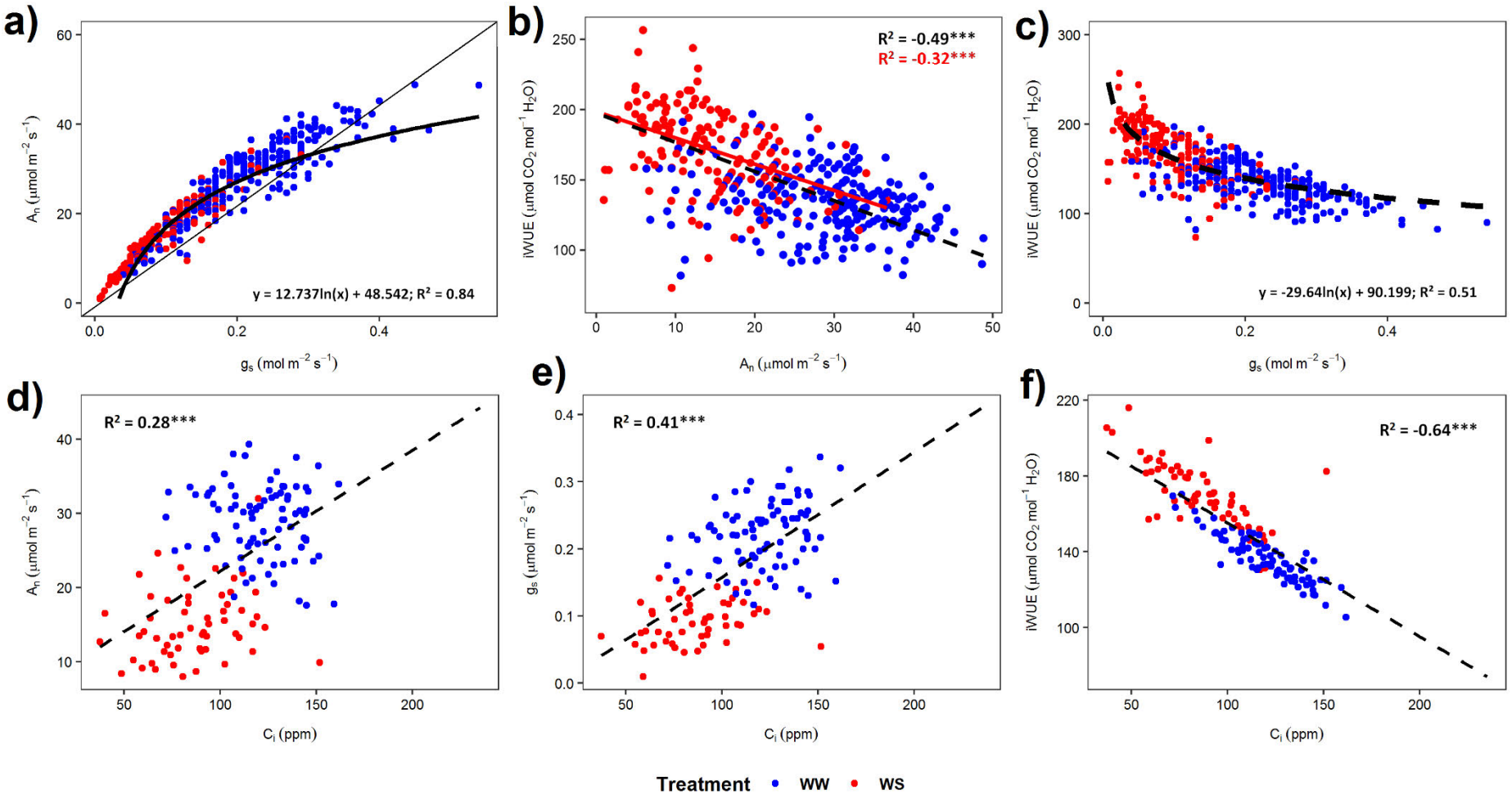

Fig.4.8 Relationship between gas exchange parameters. Data was collected on the youngest fully expanded leaf and measured at corresponding growth temperature and saturating light levels (see Materials & Methods). Each point in scatter plots **(a)**, **(b)** and **(c)** represent individual replicates, while in scatter plots **(d)**, **(e)** and **(f)** each point represents the genotype mean (n=3). Standard error bars were removed to ensure clearer presentation (Table 4.S2). The black line represents the line of best fit for the data, with the corresponding R^2 value represented that is deduced from a Pearson product-moment correlation analysis (Table 4.S1). The equation of the curve and the corresponding R^2 value for plots **(a)** and **(c)** were extracted from Excel after plotting the line of best fit. Different watering treatments are represented by the different fill colour of the scatter points: blue=Well-Watered, red=Water Stress. Degrees of statistical significance are represented as: $p<0.001$ (***), $p<0.05$ (**), $p<0.1$ (*). **(a)** Net carbon assimilation rate (A_n) vs. Stomatal conductance (g_s); **(b)** Intrinsic water use efficiency ($iWUE$) vs. Net carbon assimilation rate (A_n) vs. **(c)** $iWUE$ vs g_s; **(d)** A_n vs. Sub-stomatal carbon dioxide concentration (C_i) **(e)** g_s vs. C_i; **(f)** $iWUE$ vs C_i.

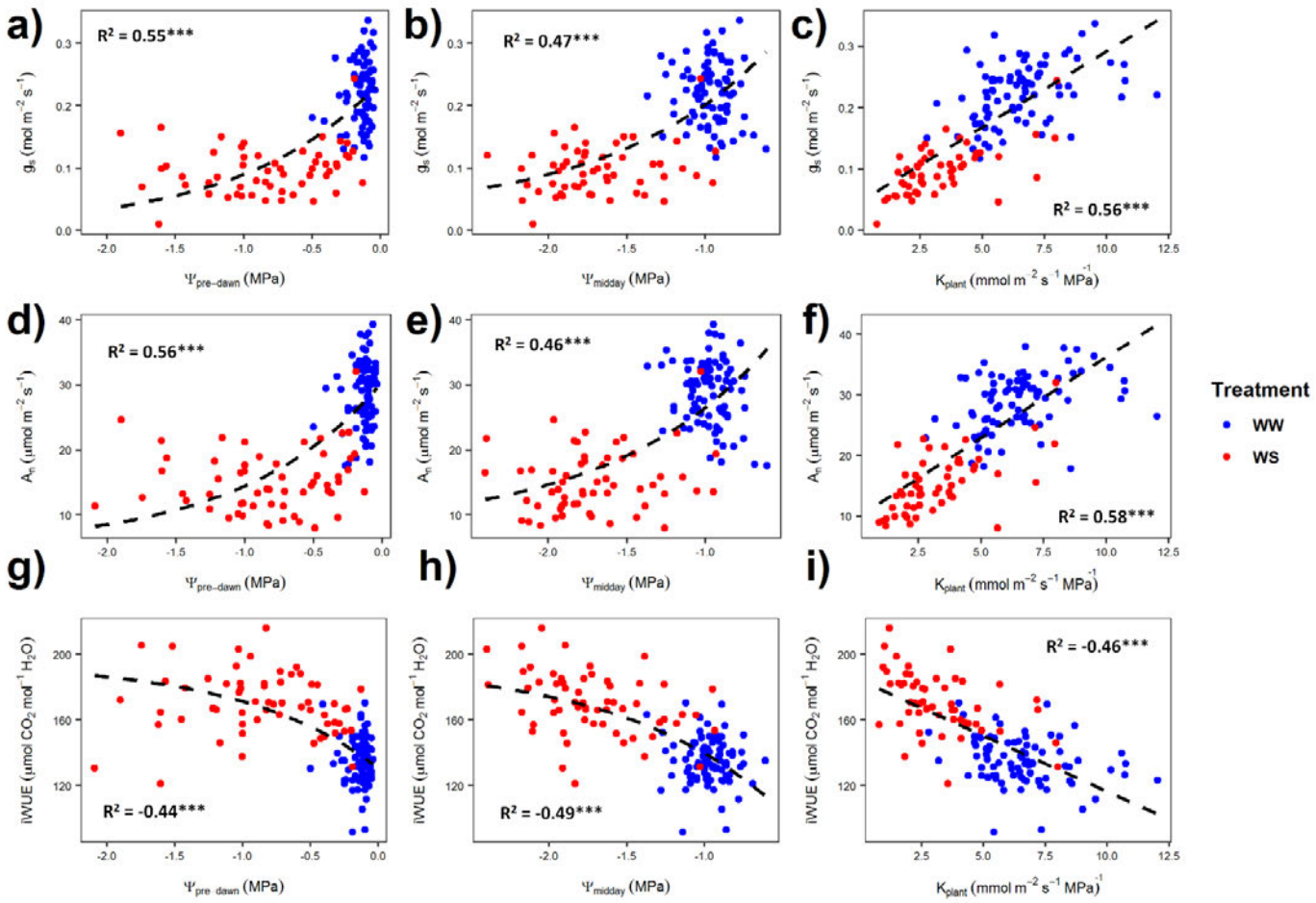

Fig.4.9 Relationship between gas exchange and hydraulic parameters. Gas exchange data was collected on the youngest fully expanded leaf and measured at corresponding growth temperature and saturating light levels (see Materials & Methods). Each point in the scatter plots represents the genotype mean (n=3). Standard error bars were removed to ensure clearer presentation (Table 4.S2). The black line represents the line of best fit for the data, with the corresponding R^2 value represented that is deduced from a Pearson product-moment linear correlation analysis (Table 4.S1). Different watering treatments are represented by the different fill colour of the scatter points: blue=Well-Watered, red=Water Stress. Degrees of statistical significance are represented as: $p<0.001$ (***), $p<0.05$ (**), $p<0.1$ (*). Stomatal conductance (g_s) vs. **(a)** Pre-Dawn leaf water potential ($\Psi_{pre\text{-}dawn}$); **(b)** Midday leaf water potential (Ψ_{midday}); **(c)** Plant hydraulic conductivity (K_{plant}). Net carbon assimilation rate (A_n) vs. **(d)** Pre-Dawn leaf water potential ($\Psi_{pre\text{-}dawn}$); **(e)** Midday leaf water potential (Ψ_{midday}); **(f)** Plant hydraulic conductivity (K_{plant}). Intrinsic water use efficiency ($iWUE$) vs. **(g)** Pre-Dawn leaf water potential ($\Psi_{pre\text{-}dawn}$); **(h)** Midday leaf water potential (Ψ_{midday}); **(i)** Plant hydraulic conductivity (K_{plant}).

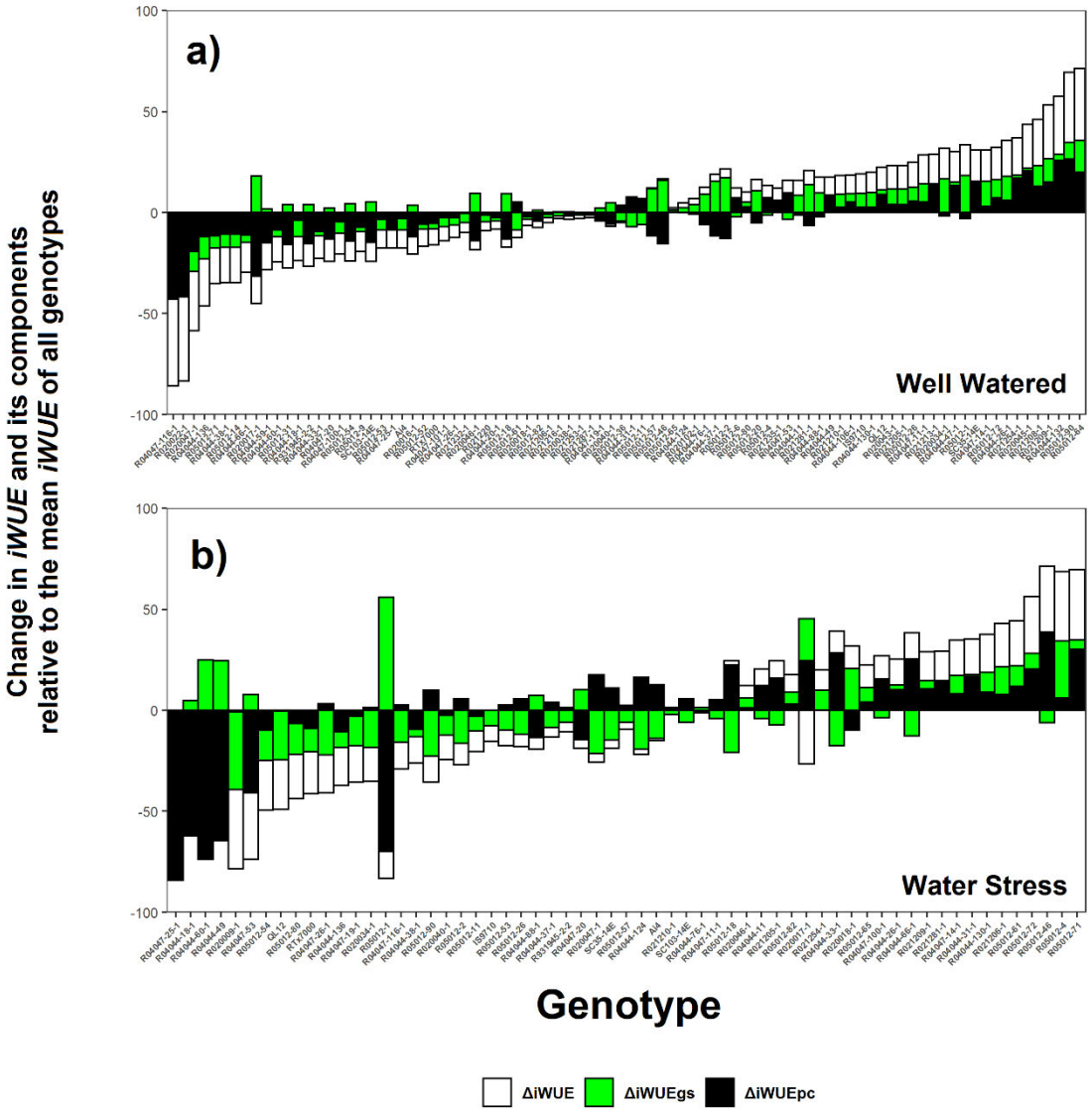

Fig.4.10 Bar chart representing the diversity in intrinsic water use efficiency (*iWUE*) response with its calculated components. Gas exchange data was collected on the youngest fully expanded leaf and measured at corresponding growth temperature and saturating light levels, with *iWUE* and its components calculated as described in Materials & Methods ($\Delta iWUE_{gs}$ (green bars): Change in *iWUE* based on changes in stomatal conductance relative to genotype average; $\Delta iWUE_{pc}$ (black bars): Change in *iWUE* based on changes in carbon assimilation rate relative to genotype average. $\Delta iWUE$ (clear bars) is the deviation of genotype *iWUE* from the mean *iWUE* of all genotypes per treatment). The bar charts represent the change in *iWUE* and its components as a deviation from the average *iWUE* of all genotypes per treatment. The value of each bar is the mean cumulative value of *iWUE* and its components (*n=3*) with standard error (SE) bars removed to enable clearer presentation (Table 4.S2).

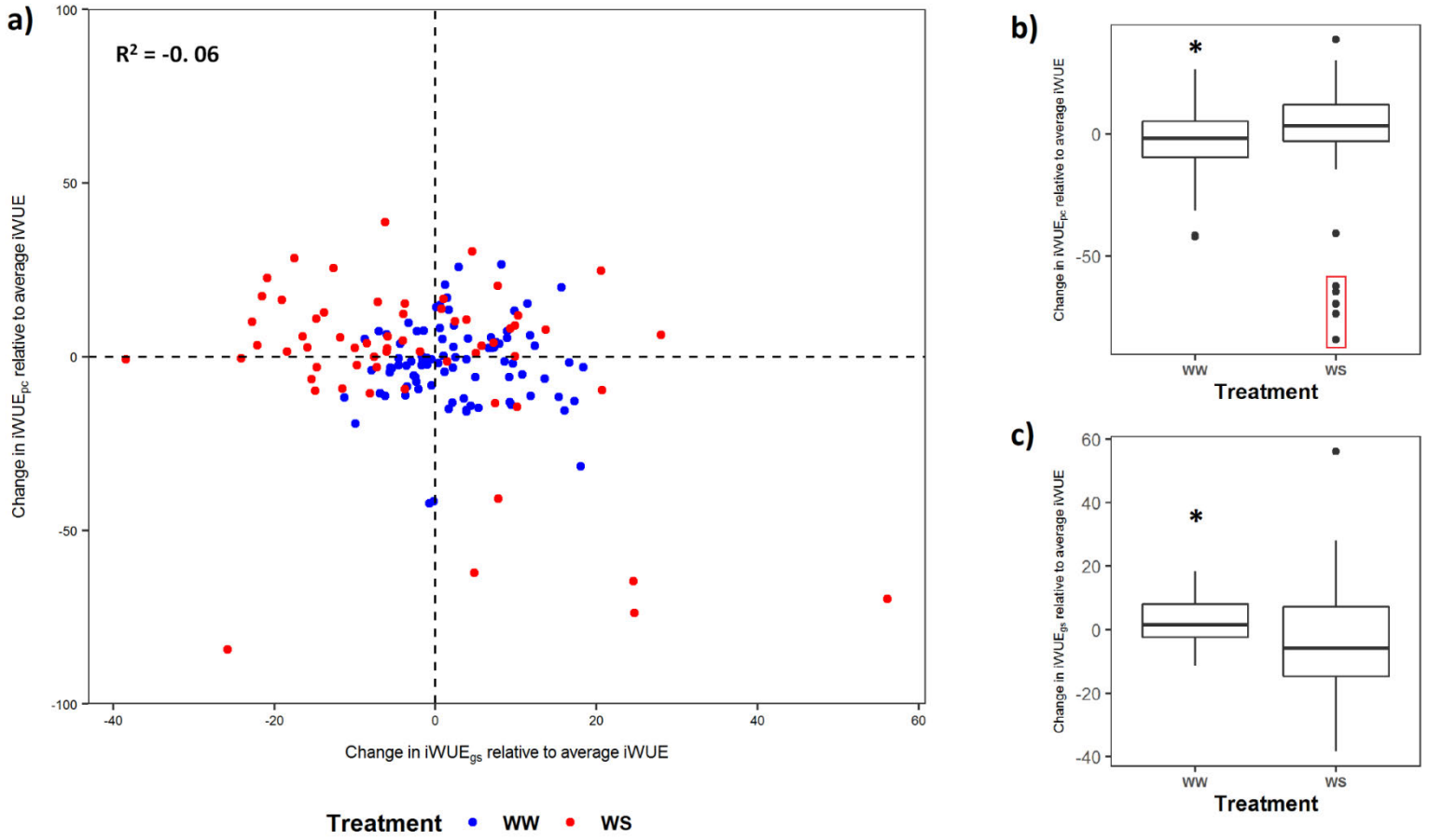

Fig.4.11 (a) The relationship between the two components of intrinsic water use efficiency (*iWUE*). Change in iWUE due to stomatal conductance (*ΔiWUEgs*) and change in *iWUE* due to carbon assimilation rate (*ΔiWUEpc*) were calculated as deviations from the genotype mean *iWUE* per treatment as explained in Materials & Methods. Each point in the scatter plots represents the genotype mean (n=3). Standard error bars were removed to ensure clearer presentation (Table S2). Different watering treatments are represented by the different fill colour of the scatter points: blue=Well-Watered, red=Water Stress. The distribution of *ΔiWUEpc* **(b)** & *ΔiWUEgs* **(c)** within the two watering treatments is also shown. The distribution is summarized by boxplots for each treatment. The values in each distribution compromise the mean of every genotype (n=3) per treatment, yielding n=89 for Well-Watered treatment and n=60 for Water Stress treatment. Each box encompasses the 25th and 75th percentiles, with whiskers extending to show the extremes. Statistically significant difference is represented at the top of each boxplot with * indication to highlight a p-value of 0.05 or lower. The red box indicates a group of significant outliers that skewed the results of the ANOVA test and were removed when testing for statistical significance.

4.6 SUPPLEMENTARY

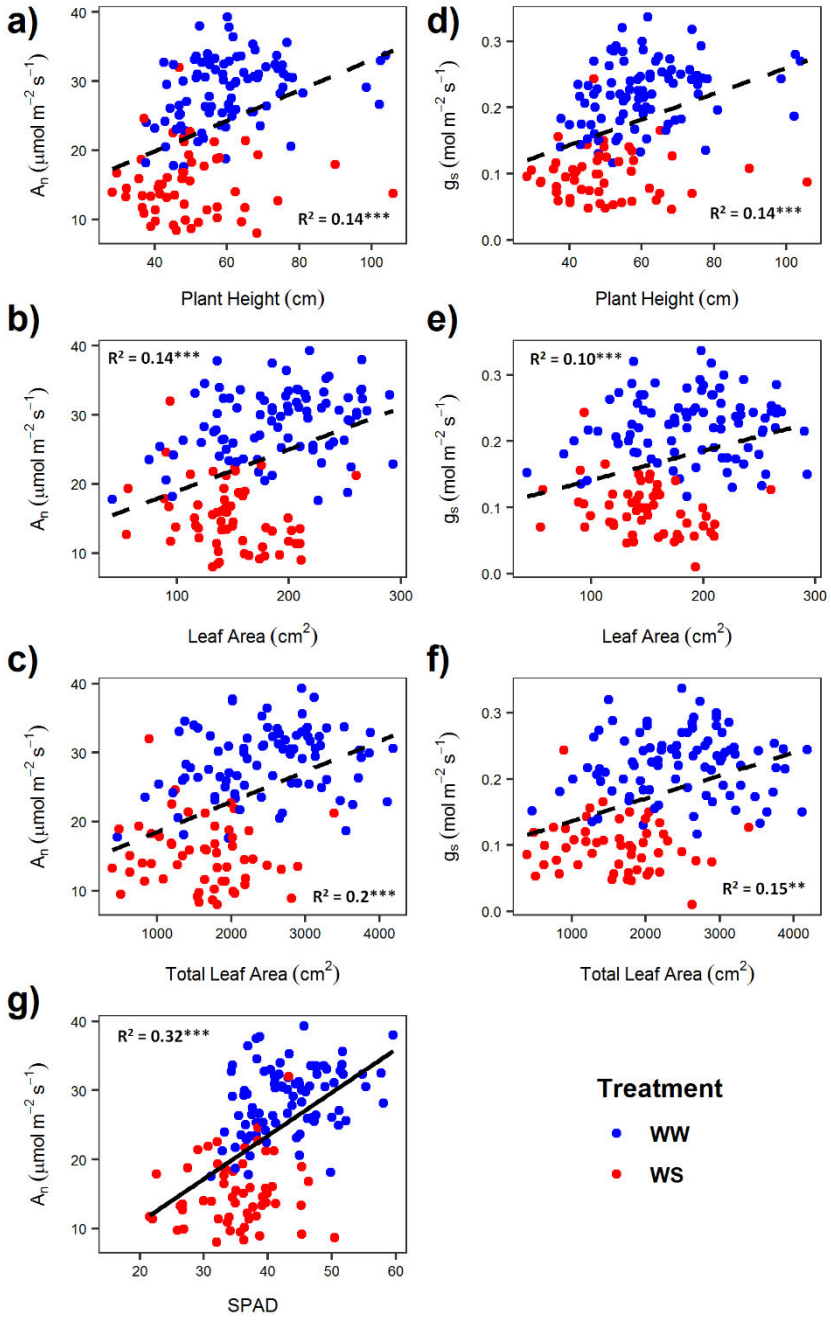

Fig.4.S1 Relationship between gas exchange with leaf and plant characteristics. Data was collected on the youngest fully expanded leaf and measured at corresponding growth temperature and saturating light levels (see Materials & Methods). Each point in the scatter plot represents the mean value of the variable per species, per treatment (n=3). Standard error bars were removed to ensure clearer presentation (Table 4.S2). The black line represents the line of best fit for the data, with the corresponding R^2 value represented that is deduced from a Pearson product-moment correlation analysis (Table 4.S1). Different watering treatments are represented by the different fill colour of the scatter points: blue=Well-Watered, red=Water Stress. Degrees of statistical significance are represented as: $p<0.001$ (***), $p<0.05$ (**), $p<0.1$ (*). Net carbon assimilation rate (A_n) vs. **(a)** Plant Height; **(b)** Leaf Area; **(c)** Total Leaf Area; **(g)** Relative Chlorophyll Content calculated by Special Products Analysis Division (*SPAD*). Stomatal conductance (g_s) vs. **(d)** Plant Height; **(e)** Leaf Area; **(f)** Total Leaf Area. (n=3).

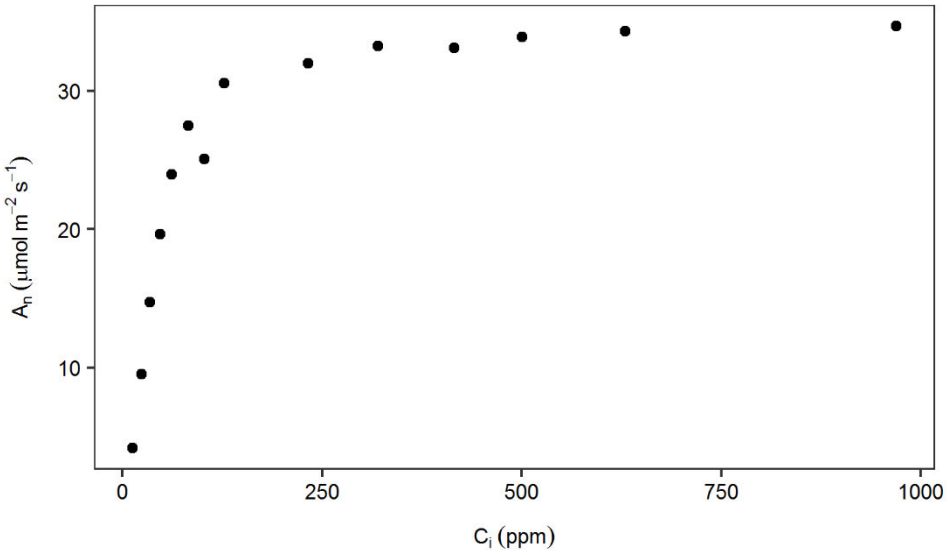

Fig.4.S2 Net carbon assimilation (A_n) response to intercellular CO_2 (C_i). This data is reproduced from chapter 3 as a reference. Each point on the plot represents the average of the six genotypes in chapter 3. See section 3.3 of this thesis for details on experimental procedure that resulted in this data.

Table 4.S1. Pearson product-moment correlation analysis results for the relationships between the measured variables. The *r* coefficient and the statistical significance were determined using the mean value per genotype per treatment (*n*=2-3). Statistical significance was judged as: p<0.001 (***), *p*<0.05 (**), *p*<0.1 (*), *p*>0.1 (ns).

	R_{dark}	g_s	*iWUE*	$iWUE_{pc}$	$iWUE_{gs}$	C_i	$C_i : C_a$	$\Psi_{pre\text{-}dawn}$	Ψ_{stem}	Ψ_{midday}	K_{plant}	K_{leaf}
A_n (µmol m^{-2} s^{-1})	-0.83***	0.96***	-0.70***	ns	-0.19**	0.53***	0.57***	0.678***	0.75***	0.702***	0.76***	0.58***
R_{dark} (µmol m^{-2} s^{-1})	-	-0.75***	0.48***	-0.23**	0.26**	-0.24**	-0.41***	-0.58***	-0.64***	-0.57***	-0.56***	-0.40***
g_s (mol m^{-2} s^{-1})	-	-	-0.84***	ns	-0.19**	0.64***	0.68***	0.68***	0.73***	0.69***	0.75***	0.55***
iWUE	-	-	-	0.47***	0.14*	-0.80***	-0.84***	-0.61***	-0.66***	-0.65***	-0.68***	-0.49***
$iWUE_{pc}$	-	-	-	-	-0.25**	-0.57***	-0.55***	ns	ns	ns	ns	ns
$iWUE_{gs}$	-	-	-	-	-	ns	ns	ns	ns	ns	-0.16*	-0.25**
C_i *(ppm)*	-	-	-	-	-	-	N/A	0.35***	0.48***	0.51***	0.45***	0.31***
$C_i : C_a$	-	-	-	-	-	-	-	0.57***	0.66***	0.69***	0.62***	0.46***
$\Psi_{pre\text{-}dawn}$ (-MPa)	-	-	-	-	-	-	-	-	0.78***	0.76***	0.51***	0.44***
Ψ_{stem} (-MPa)	-	-	-	-	-	-	-	-	-	0.95***	0.7***	0.35***
Ψ_{midday} (-MPa)	-	-	-	-	-	-	-	-	-	-	0.74***	0.48***
K_{plant} (mmol m^{-2} s^{-1} MPa^{-1})	-	-	-	-	-	-	-	-	-	-	-	0.66***
K_{leaf} (mmol m^{-2} s^{-1} MPa^{-1})	-	-	-	-	-	-	-	-	-	-	-	-
Leaf Width (cm)	-	-	-	-	-	-	-	-	-	-	-	-
Leaf Length (cm)	-	-	-	-	-	-	-	-	-	-	-	-
Leaf Thickness (mm)	-	-	-	-	-	-	-	-	-	-	-	-
Leaf Area (cm^2)	-	-	-	-	-	-	-	-	-	-	-	-
Plant Height (cm)	-	-	-	-	-	-	-	-	-	-	-	-
Number of Leaves	-	-	-	-	-	-	-	-	-	-	-	-
Total Leaf Area (cm^2)	-	-	-	-	-	-	-	-	-	-	-	-

Table 4.S1 continued

	LW	*LL*	*LT*	*LA*	*PH*	*LN*	*TLA*	*SPAD*
A_n (µmol m^{-2} s^{-1})	0.29***	0.14*	0.23**	0.38***	0.38***	-0.18**	0.45***	0.57***
R_{dark} (µmol m^{-2} s^{-1})	-0.41***	-0.18**	-0.14*	-0.42***	-0.29***	ns	-0.5**	-0.49***
g_s (mol m^{-2} s^{-1})	0.25**	ns	0.24**	0.31***	0.38***	-0.18**	0.39**	0.52***
iWUE	ns	ns	-0.18**	ns	-0.25**	ns	-0.22**	-0.36***
$iWUE_{pc}$	0.26**	ns	ns	0.2**	ns	ns	ns	0.16*
$iWUE_{gs}$	ns	ns	ns	0.15*	ns	ns	0.16*	ns
C_i *(ppm)*	-0.17**	-0.14*	ns	ns	0.24**	ns	ns	ns
$C_i : C_a$	ns	ns	0.22**	ns	0.27**	ns	ns	0.24**
$\Psi_{pre\text{-}dawn}$ (-MPa)	ns	ns	0.22**	ns	0.25**	ns	0.4***	0.49***
Ψ_{stem} (-MPa)	ns	ns	0.28***	0.24**	0.34***	ns	0.36***	0.45***
Ψ_{midday} (-MPa)	ns	ns	0.27***	0.21**	0.32***	ns	0.32***	0.43***
K_{plant} (mmol m^{-2} s^{-1} MPa^{-1},	ns	ns	0.27**	ns	0.27**	ns	0.25**	0.35***
K_{leaf} (mmol m^{-2} s^{-1} MPa^{-1})	ns	ns	ns	ns	0.15*	-0.18*	ns	0.34***
Leaf Width (cm)	-	0.57***	0.14*	0.72***	0.23**	0.25**	0.68***	0.25**
Leaf Length (cm)	-	-	0.16*	0.62***	ns	0.41***	0.63***	0.15*
Leaf Thickness (mm)	-	-	-	ns	ns	ns	ns	0.19**
Leaf Area (cm^2)	-	-	-	-	ns	0.2**	0.84***	0.31***
Plant Height (cm)	-	-	-	-	-	-0.24**	0.18**	0.19**
Number of Leaves	-	-	-	-	-	-	0.35***	ns
Total Leaf Area (cm^2)	-	-	-	-	-	-	-	0.36***

A_n: Carbon assimilation rate; R_{dark}: Dark respira ion rate; g_s: Stomatal conductance; *iWUE* : Instantaneous water use efficiency; $iWUE_{pc}$: *iWUE* attributed to variation in A_n; $iWUE_{gs}$: *iWUE* attributed to variation in g_s; C_i: Sub-stomatal carbon dioxide concentration; $C_i : C_a$: Ratio of C_i to ambient carbon dioxide concentration; $\Psi_{pre\text{-}dawn}$ and Ψ_{midday}: leaf water potenial; Ψ_{stem}: Stem water potential at midday; K_{plant}: Plant hydraulic conductivity; K_{leaf}: Leaf hydraulic conductivity; *LW*: Leaf width; *LL* : Leaf length; *LT* : Leaf thickness; *LA* : Average leaf area; *PH* : Plant height; *LN* : Number of leaves; *TLA* : Total leaf area; *SPAD* : Relative Chlorophyll content bvased on special products analysis division.

Table 4.S2. Summary of the mean (±SE) for all the measured variables under the two watering treatments for each genotype. The table also shows in the specific genotype code of each offspring belonging to each specific exotic (Non-recurrent) parental line. The recurrent parent is marked with a * in the last row of the table.

Exotic Parent and Genotype Progeny	Well Watered																		
	PH	*LN*	*TLA*	$\Psi_{pre\text{-}dawn}$	Ψ_{stem}	Ψ_{midday}	K_{leaf}	K_{plant}	*LW*	*LL*	*LT*	*LA*	*SPAD*	A_n	g_s	R_{dark}	*iWUE*	$iWUE_{gs}$	$iWUE_{pc}$	C_i
RTx7000	55.17 (6.31)	0 (0.94)	2561.89 (657.27)	-0.08 (0.01)	-0.32 (0.04)	-0.84 (0.2)	17.25 (5.2)	10.72 (2.88)	3.6 (0.54)	64.17 (7.83)	0.5 (0.12)	147 (35.46)	41.72 (1.88)	32.36 (6.98)	0.27 (0.07)	-1.35 (0.28)	119.84 (15.74)	-2.66 (7.44)	-5.41 (13.12)	135.11 (21.78)
R020038-1	64.67 (4.65)	13.33 (0.72)	2635.78 (266.17)	-0.33 (0.2)	-0.4 (0.09)	-0.75 (0.1)	9.65 (0.01)	6.68 (0.94)	4.4 (0.37)	74.75 (0.88)	0.48 (0.03)	198.78 (21.24)	44.85 (2.99)	31.26 (7.63)	0.28 (0.11)	-1.15 (0.22)	113 (17.69)	0.38 (11.38)	-1.8 (8.47)	96.43 (7.68)
R020040-1	55 (6.14)	14.67 (0.27)	3047.78 (604.58)	-0.14 (0.03)	-0.27 (0.04)	-0.86 (0.06)	8.53 (0.22)	6.98 (0.35)	4.93 (0.53)	68 (6.01)	1.09 (0.38)	209.89 (44.77)	38.18 (3.43)	25.39 (1.85)	0.19 (0.01)	-1.32 (0.07)	133.61 (5.8)	4.95 (1.89)	-5.84 (5.81)	129.81 (12.71)
R020043-1	48.88 (4.64)	11.75 (0.41)	1969.67 (517.58)	-0.11 (0.03)	-0.41 (0.03)	-1.07 (0.09)	6.92 (1.28)	4.64 (0.58)	4.58 (0.79)	52.25 (8.34)	0.54 (0.22)	174 (49.58)	51.19 (5.86)	27.04 (5.9)	0.18 (0.04)	-1.55 (0.23)	147.51 (2.9)	7.53 (5.74)	4.1 (8.03)	97.12 (7.84)
R020045-1	62.83 (4.36)	12.33 (0.27)	3287.11 (635.68)	-0.1 (0.02)	-0.38 (0.05)	-0.87 (0.05)	15.95 (0)	8.68 (0)	5.35 (0.67)	53.9 (1.91)	0.41 (0.12)	264.11 (46.46)	48.76 (5.47)	33.55 (2.76)	0.22 (0.04)	-1.8 (0)	152.48 (10.29)	1.2 (3.96)	20.66 (6.33)	84.26 (11.76)
R020046-1	69.17 (21.42)	11 (0.47)	841 (297.83)	-0.5 (0.21)	-0.46 (0.12)	-0.93 (0.17)	12.87 (4.22)	19.65 (5.42)	3.07 (0.43)	42.5 (5.21)	0.75 (0.08)	75.44 (26.85)	35.84 (1.06)	23.55 (6.2)	0.18 (0.05)	-1.26 (0.2)	130.37 (0.47)	9.45 (8.02)	-13.91 (8.31)	138.6 (10.59)
R020047-1	54.67 (6.84)	10.67 (0.27)	1496.44 (439.39)	-0.12 (0.02)	-0.36 (0.09)	-0.89 (0.03)	10.42 (1.06)	9.01 (1.29)	4.17 (0.79)	58.33 (5.21)	0.53 (0.19)	138 (38.69)	41.89 (3.24)	33.94 (5.87)	0.32 (0.05)	-1.53 (0.18)	106.05 (1.67)	-9.96 (3.8)	-19.28 (5.48)	161.58 (9.5)
R020102-1	61.25 (2.3)	14.5 (0.35)	1695.67 (700.58)	-0.1 (0.03)	-0.42 (0.04)	-1.01 (0.07)	11.81 (0.09)	6.49 (0.76)	3.93 (0.58)	57 (7.21)	0.63 (0.14)	133.22 (36.54)	37.61 (4.39)	27.52 (3.78)	0.2 (0.03)	-1.46 (0.23)	137.6 (0.46)	3.85 (3.47)	-0.75 (3.01)	122.27 (4.77)
R020009-1	45 (0)	10 (0)	0 (0)	-0.12 (0)	-0.23 (0)	-0.78 (0)	0 (0)	0 (0)	3.9 (0)	57 (0)	0.26 (0.02)	0 (0)	32.07 (5.22)	0 (0)	0 (0)	0 (0)	0 (0)	0 (0)	0 (0)	0 (0)
R020016-1	58.67 (6.59)	12 (0)	1018 (186.9)	-0.11 (0.01)	-0.35 (0.02)	-0.86 (0.13)	11.96 (4.25)	6.21 (0.93)	3.17 (0.28)	47.5 (8.69)	0.41 (0.06)	84.83 (15.57)	39.26 (2.23)	25.39 (3.01)	0.2 (0.02)	-1.19 (0.21)	126.93 (8.24)	3.55 (2.46)	-12.05 (9.5)	142.27 (13.8)
R020017-1	45.17 (5.71)	0 (0.27)	466 (211.22)	-0.25 (0.14)	-0.4 (0.09)	-0.69 (0.1)	13.2 (3.17)	8.58 (1.03)	2.63 (0.28)	30.03 (3.77)	0.41 (0.11)	42.72 (19.01)	36.98 (3.33)	17.78 (6.12)	0.15 (0.06)	-1.02 (0.21)	116.95 (4.81)	18.06 (11.55)	-31.59 (9.37)	159.23 (8.57)
R020018-1	75.5 (7.42)	11.5 (0.35)	2962.83 (451.01)	-0.15 (0.04)	-0.43 (0.03)	-0.77 (0.02)	15.33 (0.3)	8.47 (0.27)	4.95 (0.04)	77.75 (1.24)	0.77 (0.25)	255.17 (32.81)	34.49 (9.04)	29.14 (2.29)	0.24 (0.03)	-1.61 (0.16)	123.98 (22.48)	-0.98 (3.32)	-2.24 (19.16)	133.14 (35.73)
R020022-1	46.75 (10.78)	13.5 (0.35)	1920.5 (324.76)	-0.1 (0.04)	-0.35 (0)	-0.86 (0)	10.65 (2.82)	7.34 (2.25)	4.1 (0.64)	60.25 (5.13)	0.46 (0.11)	144 (27.14)	36.54 (3.89)	25.04 (9.8)	0.27 (0.11)	-1.29 (0.25)	92.74 (0.16)	-0.18 (10.72)	-41.58 (10.56)	0 (12.59)
R020034-1	77.67 (11.45)	13.67 (0.54)	1279 (428.61)	-0.08 (0.01)	-0.47 (0.14)	-0.89 (0.17)	11.71 (1.13)	5.28 (0.37)	3.4 (0.46)	49.9 (10.38)	0.35 (0)	90.78 (27.51)	44.92 (0)	20.6 (5.59)	0.14 (0.03)	-0.97 (0.28)	152.56 (5)	16.64 (5.93)	-1.63 (10.93)	113.37 (13.22)
SC103-14E	47.17 (2.52)	14 (0)	2406.44 (370.24)	-0.08 (0.03)	-0.41 (0.01)	-0.98 (0.04)	8.11 (0.39)	5.16 (0.2)	4.43 (0.29)	66.1 (1.97)	0.28 (0.03)	171.89 (26.45)	38.2 (1.02)	23.5 (2.76)	0.2 (0.04)	-1.23 (0.14)	117.52 (12.01)	5.32 (6.42)	-14.8 (6.15)	148.37 (16.74)
R021232-1	67.83 (1.16)	11 (0)	1372.56 (301.46)	-0.22 (0.05)	-0.45 (0.06)	-0.89 (0.09)	13.99 (1.8)	10.16 (2.97)	3.97 (0.32)	47.5 (4.95)	0.56 (0.1)	124.78 (27.41)	38.29 (3.57)	34.53 (4.45)	0.27 (0.05)	-1.74 (0.05)	126.34 (7.03)	-4.55 (5.51)	-0.48 (3.71)	126.02 (6.28)
R021235-1	54 (2.69)	11.75 (0.41)	2166.92 (158.32)	-0.1 (0.02)	-0.3 (0.04)	-0.82 (0.15)	14.04 (3.35)	8.1 (1.23)	4.65 (0.27)	66.88 (2.35)	0.47 (0.13)	185.42 (14.6)	48.96 (3.14)	30.56 (1.67)	0.22 (0.02)	-1.6 (0.03)	138.76 (6.1)	0.87 (2.75)	5.14 (3.81)	105.6 (7.2)
R021253-1	51.75 (4.42)	13.75 (0.41)	3206.33 (611.66)	-0.07 (0.02)	-0.41 (0.05)	-0.97 (0.11)	11.74 (1.75)	6.99 (0.93)	5.08 (0.48)	77.13 (2.26)	0.82 (0.32)	229.08 (36.08)	41.08 (4.32)	30.97 (2.94)	0.24 (0.03)	-1.63 (0.12)	130.41 (9.25)	-1.02 (3.52)	-0.35 (7.18)	120.28 (16.27)
R021254-1	59.17 (4.77)	11.33 (0.27)	2883.22 (354.69)	-0.1 (0.02)	-0.43 (0.07)	-1.03 (0.1)	10.16 (0.72)	6.68 (0.54)	5.33 (0.27)	62 (3.86)	0.46 (0.15)	252.78 (25.26)	57.72 (3.46)	32.49 (0.77)	0.21 (0.01)	-1.58 (0.07)	152.3 (5.14)	1.47 (1.64)	17.01 (3.58)	87.14 (6.14)
R021281-1	37.67 (5.04)	14.33 (0.54)	2050.56 (798.62)	-0.12 (0.04)	-0.4 (0.03)	-1.01 (0.22)	8.47 (1.36)	5.21 (1)	3.47 (0.5)	55 (10.62)	0.46 (0.1)	138.11 (52.28)	33.24 (1.37)	23.99 (7.19)	0.18 (0.07)	-1.06 (0.23)	130.85 (10.72)	13.6 (13.38)	-6.3 (7.03)	110.75 (12.14)
R021287-1	58.85 (3.63)	12.5 (0.56)	1963.42 (404.16)	-0.1 (0.03)	-0.43 (0.06)	-1.01 (0.17)	9.91 (1.01)	6.1 (0.19)	3.5 (0.16)	55.5 (2.86)	0.58 (0.14)	153.67 (28.14)	44.91 (5.51)	30.96 (3.99)	0.24 (0.04)	-1.5 (0.1)	127.66 (9.39)	-0.47 (5.62)	-0.82 (4.86)	120.91 (11.96)
R021205-1	81 (0.71)	12.5 (0.35)	1392.56 (568.54)	-0.1 (0.02)	-0.45 (0.1)	-0.95 (0.06)	9.44 (2.1)	6.25 (2.21)	3.63 (0.6)	50.5 (9.33)	0.43 (0.12)	124.22 (35.3)	45.26 (9.17)	28.3 (7.16)	0.2 (0.05)	-1.6 (0.28)	144.37 (3.34)	7.93 (9.67)	3.76 (7.11)	108.35 (6.79)
R021206-1	56.83 (5.07)	13 (0.47)	3068.22 (448.82)	-0.06 (0.02)	-0.32 (0.02)	-0.86 (0.05)	10.21 (1.45)	6.84 (1.18)	5.43 (0.5)	80.83 (2.41)	0.65 (0.11)	233.44 (25.83)	41.15 (5.89)	31.68 (3.65)	0.24 (0.03)	-1.6 (0.26)	132 (4.57)	-1.59 (3.41)	-0.87 (5.16)	122.7 (8.54)
R021208-1	47 (2.46)	11.33 (0.27)	2175.22 (243.74)	-0.08 (0.02)	-0.39 (0.02)	-0.98 (0.13)	9.33 (1.01)	5.68 (0.19)	4.8 (0.16)	66.87 (1.98)	1.16 (0.34)	193.33 (24.86)	41.23 (1.31)	25.23 (1.37)	0.16 (0)	-1.43 (0.16)	157.69 (7)	9.86 (0)	13.17 (7)	93.06 (8.15)
R021209-1	66.67 (5.38)	12.33 (0.27)	2897.78 (867.56)	-0.13 (0.05)	-0.36 (0.06)	-1.03 (0.11)	9.05 (1.42)	5.49 (0.81)	5.07 (0.96)	75.5 (6.33)	0.44 (0.07)	236.11 (73.22)	47.24 (4.59)	25.55 (5.48)	0.17 (0.05)	-1.71 (0.36)	154.82 (9.56)	11.44 (7.13)	15.24 (2.43)	83.09 (10.75)
R021210-1	60.5 (3.7)	13.67 (0.27)	3285.89 (483.89)	-0.17 (0.04)	-0.52 (0.05)	-1.08 (0.11)	8.74 (1.92)	5.25 (1.21)	5.63 (0.6)	77.83 (3.74)	0.67 (0.09)	240.11 (33.58)	49.98 (6.72)	26.07 (3.41)	0.19 (0.04)	-1.86 (0.16)	137.19 (10.49)	6.62 (5.87)	2.55 (4.86)	115.78 (11.87)
R021213-1	56.67 (1.96)	13 (0)	3007.33 (339.96)	-0.05 (0.02)	-0.46 (0.01)	-1.02 (0.04)	9.51 (0.91)	5.43 (0.3)	4.87 (0.11)	67.37 (6.08)	0.43 (0.07)	231.33 (26.15)	47.51 (3.13)	33.32 (2.62)	0.23 (0.03)	-1.85 (0.09)	146.99 (6.1)	0.13 (3.4)	14.24 (2.98)	95.96 (5.52)
R021216-1	67.5 (2.63)	12.75 (0.22)	3134.83 (368.42)	-0.14 (0.04)	-0.37 (0.06)	-0.87 (0.09)	13.25 (2.01)	10.75 (2.21)	5.63 (0.74)	65.93 (1.9)	0.71 (0.28)	244.83 (26.37)	46.56 (5.44)	30.63 (0.56)	0.24 (0.04)	-1.8 (0.1)	125.89 (14.85)	-1.68 (3.56)	0.24 (11.39)	118.7 (21.13)
R021220	70.75 (3.45)	12.5 (0.25)	2218 (431.73)	-0.13 (0.03)	-0.39 (0.04)	-1 (0.07)	9.15 (1.05)	6.13 (0.45)	4.25 (0.37)	58.9 (6.87)	0.52 (0.2)	178 (35.14)	41.06 (4.92)	32.09 (1.43)	0.25 (0.02)	-1.8 (0.14)	128.36 (7.08)	-3.01 (2.37)	-1.43 (5.17)	126.7 (12.26)
SC35-14E	42.5 (10.25)	14.5 (1.06)	2637.33 (762.1)	-0.17 (0.03)	-0.31 (0.06)	-0.91 (0.04)	10.07 (0.24)	8.08 (0.42)	4.1 (1.2)	79.5 (6.72)	0.6 (0.24)	174.33 (42.15)	34.26 (2.89)	32.73 (4.07)	0.24 (0.06)	-1.16 (0.01)	139.28 (17.21)	0.54 (6.48)	14.86 (10.73)	93.98 (19.15)
QL12	51.4 (3.55)	12.67 (0.72)	2800.78 (540.81)	-0.11 (0.01)	-0.72 (0.11)	-1.06 (0.15)	9.8 (0.44)	6 (0.36)	4.4 (0.29)	69.33 (1.78)	0.83 (0.22)	215.89 (33.39)	55.34 (3.96)	30.51 (3.59)	0.22 (0.04)	-1.45 (0.22)	139.97 (10.97)	2.31 (5.66)	8.91 (6.4)	98.95 (14.71)
R04044-106-1	74 (2.26)	13.25 (0.22)	2733.5 (170.34)	-0.05 (0.02)	-0.45 (0.03)	-0.99 (0.08)	10.04 (2.21)	5.5 (0.84)	5.03 (0.34)	62.78 (3.38)	0.75 (0.32)	207.17 (15.35)	43.2 (1.11)	31.85 (3.67)	0.32 (0.1)	-1.67 (0.1)	100.32 (18.47)	4.09 (3.46)	5.17 (4.67)	135.02 (25.76)
R04044-132	60.5 (2.46)	13.33 (0.72)	3881.11 (332.34)	-0.13 (0.04)	-0.38 (0.03)	-1.37 (0.01)	5.35 (1.16)	4.18 (0.79)	5.9 (0.53)	64.17 (5.71)	0.52 (0.21)	290.11 (12.36)	51.34 (2.56)	32.86 (2.9)	0.22 (0.04)	-2.17 (0.13)	152.62 (17.49)	2.88 (5.94)	25.88 (11.57)	72.92 (21.94)
R04044-136	61.67 (3.95)	12.67 (0.54)	2485.11 (179.21)	-0.09 (0.03)	-0.33 (0.02)	-0.78 (0.02)	14.47 (1.59)	9.53 (1.21)	3.93 (0.27)	87.17 (2.24)	0.97 (0.37)	197.89 (19.09)	36.87 (1.88)	36.41 (3.29)	0.34 (0.05)	-1.63 (0.17)	108.16 (10.04)	-11.28 (4.37)	-11.76 (6.99)	150.99 (15.29)
R04044-18-1	76.5 (6.02)	12.67 (0.98)	2957.11 (426.72)	-0.14 (0.03)	-0.4 (0.1)	-0.98 (0.09)	12.16 (0.87)	8.5 (0.64)	5.5 (0.33)	75.17 (3.18)	0.88 (0.22)	236 (37.38)	51.65 (4.67)	35.61 (1.6)	0.29 (0.02)	-1.68 (0.15)	121.4 (9.13)	-7.94 (1.88)	-3.92 (7.63)	129.45 (17.93)
R04044-20-1	68.75 (3.95)	13 (0.35)	2421.5 (236.19)	-0.06 (0.02)	-0.33 (0.06)	-0.92 (0.05)	9.32 (0.73)	6.38 (0.81)	4.75 (0.34)	65.78 (1.98)	0.73 (0.29)	185.25 (15.34)	44.35 (0.85)	30.96 (1.75)	0.24 (0.01)	-1.5 (0.04)	130.82 (3.14)	-1.7 (0.79)	-2.43 (3.85)	115.4 (10.17)
R04044-26-1	48.17 (6.25)	13.33 (0.72)	4110.83 (259.33)	-0.12 (0.06)	-0.62 (0.06)	-1.27 (0.09)	5.57 (0)	2.79 (0)	5.25 (0.18)	76 (9.19)	0.25 (0.04)	292.83 (6.45)	36.71 (2.82)	22.88 (0)	0.15 (0)	-2.29 (0)	152.53 (0)	11.77 (0)	6.1 (0)	102.67 (0)
R04044-31-1	52.33 (0.36)	11.67 (0.27)	3121.89 (462.53)	-0.1 (0.01)	-0.37 (0.02)	-0.98 (0.14)	9.32 (0.1)	6.77 (0.06)	5.4 (0.26)	80.67 (1.96)	0.48 (0.13)	265.22 (34.48)	59.55 (2.97)	38 (0.64)	0.29 (0.02)	-2.21 (0.02)	133.33 (7.75)	-7.03 (2.11)	7.35 (5.64)	106.79 (12.43)
R04044-33-1	62.33 (2.73)	14 (0.94)	2800 (713.97)	-0.19 (0.01)	-0.54 (0.11)	-0.96 (0.16)	13.06 (2.02)	7.23 (1.16)	4.73 (0.63)	67.33 (4.25)	0.66 (0.24)	193 (36.79)	45.94 (3.11)	29.79 (3.71)	0.25 (0.04)	-1.56 (0.17)	119.17 (11.44)	-2.09 (5.15)	-9.29 (7.93)	143.63 (15.64)
R04044-37-1	43 (7)	14.67 (0.27)	2650.56 (668.07)	-0.12 (0.05)	-0.48 (0.11)	-0.82 (0.04)	16.86 (8.43)	5.82 (1.52)	4.67 (0.84)	69.33 (4.77)	0.37 (0.09)	178.56 (43.17)	37.2 (7.7)	20.51 (5.2)	0.14 (0.03)	-1.38 (0.28)	143.09 (8.38)	15.34 (6.77)	-11.65 (14.92)	127.81 (22.01)
R04044-38-1	51.5 (1.77)	12 (0.71)	1551.89 (702.71)	-0.15 (0.04)	-0.43 (0.06)	-1.12 (0.09)	8.91 (0.18)	6.51 (0.41)	3.83 (0.69)	62.67 (5.54)	0.55 (0.09)	157 (32.88)	46.69 (6.29)	33.59 (3.63)	0.29 (0.03)	-1.57 (0.14)	116.78 (1.97)	-6.86 (3.69)	-10.51 (2.78)	139.44 (1.91)
R04044-47-1	45.25 (2.18)	14.25 (0.54)	3034.25 (201.54)	-0.15 (0.02)	-0.49 (0.11)	-1.02 (0.1)	14.9 (6.22)	6.71 (0.73)	5.07 (0.23)	53.8 (1.79)	0.99 (0.22)	215.58 (21.12)	54.8 (5.48)	32.36 (4.29)	0.23 (0.05)	-1.76 (0.1)	139.19 (14.14)	1.65 (6.93)	13.49 (7.31)	93.35 (14.82)
R04044-49	75.63 (0.85)	11.67 (0.27)	2440.44 (340.14)	-0.15 (0.02)	-0.4 (0.04)	-1 (0.09)	9.07 (1.24)	7.09 (1.28)	5.1 (0.36)	69.5 (2.78)	0.67 (0.13)	209 (27.54)	50.36 (2.82)	31.1 (1.43)	0.22 (0.01)	-1.42 (0.14)	141.38 (12.84)	0.54 (1.56)	8.2 (11.28)	107.72 (21.76)
R04044-59-1	74.67 (8.6)	11.67 (0.98)	2348.78 (857.29)	-0.11 (0)	-0.39 (0.03)	-1.09 (0.07)	7.79 (1.8)	5.73 (1.46)	4.8 (0.68)	54.5 (3.52)	0.95 (0.36)	190.22 (54.74)	58.03 (6.24)	28.17 (8.56)	0.25 (0.09)	-1.42 (0.24)	114.98 (7.24)	1.7 (9.63)	-14.98 (2.39)	136.74 (6.39)
R04044-60-1	65.67 (2.33)	14.33 (0.98)	3736.78 (297.16)	-0.08 (0.01)	-0.34 (0.08)	-0.84 (0.06)	10.89 (0.59)	7.24 (0.39)	5.7 (0.25)	62.03 (4.01)	0.83 (0.2)	260.67 (10.57)	41.09 (1.69)	30.32 (1.09)	0.25 (0.02)	-1.6 (0.03)	119.68 (12.25)	-3.51 (2.24)	-8.65 (10.05)	141.22 (22.08)
R04044-66-1	68.33 (3.79)	13 (0.94)	2842.56 (403.04)	-0.07 (0.01)	-0.35 (0.04)	-0.98 (0.12)	10.56 (0.83)	7.31 (0.45)	5.47 (0.6)	73.17 (1.3)	0.34 (0.07)	215.89 (20.85)	42.05 (1.86)	30.48 (2.13)	0.26 (0.02)	-1.48 (0.16)	118.77 (4.58)	-3.73 (2.94)	-11.12 (2.94)	144.57 (6.52)
R04044-76-1	46 (1.87)	15 (0.47)	3476.67 (582.59)	-0.08 (0.03)	-0.37 (0.05)	-0.91 (0.02)	7.1 (2.2)	4.73 (1.45)	5.07 (0.6)	75.7 (1.58)	0.4 (0.04)	229 (31.27)	36.64 (2.34)	23.02 (3.11)	0.17 (0.04)	-1.36 (0.12)	132.79 (9.06)	9.16 (5.59)	-5.94 (4.51)	127.91 (8.84)
R04044-88-1	58.17 (6.37)	11.33 (0.27)	1777.22 (442.95)	-0.06 (0.03)	-0.54 (0.05)	-0.98 (0.03)	10.79 (0.75)	5.12 (1.4)	4.13 (0.52)	59 (2.87)	0.61 (0.14)	159.22 (41.78)	45.06 (2.83)	23.58 (3.19)	0.17 (0.02)	-1.46 (0.17)	141.5 (6.38)	9.66 (4.63)	-1.94 (6.64)	120.79 (12.68)
R04044-11	62.5 (1.08)	12.67 (0.27)	1931.56 (485.15)	-0.05 (0.02)	-0.37 (0.07)	-0.9 (0.12)	8.24 (0.89)	5.16 (0.79)	4.33 (0.39)	55.5 (4.03)	0.61 (0.14)	150.33 (35.98)	46.2 (2.46)	25.89 (5.73)	0.2 (0.05)	-1.82 (0.54)	131.66 (12.82)	8.56 (10.66)	-1.32 (4.4)	119.45 (13.67)
R04044-124	78.17 (4.76)	13 (0.94)	2696.78 (688.43)	-0.17 (0.04)	-0.43 (0.1)	-1 (0.02)	12.43 (5.43)	6.56 (1.62)	5.73 (1.55)	72 (6.33)	1.23 (0.24)	200.11 (37.12)	42.42 (4.65)	30.48 (7.08)	0.24 (0.07)	-1.37 (0.35)	125.25 (13.37)	2.48 (10.59)	-0.19 (2.82)	118.63 (10.39)
R04044-130-1	67.3 (4.13)	13 (0.47)	2814 (531.27)	-0.09 (0.02)	-0.48 (0.12)	-0.88 (0.17)	13.48 (1.05)	6.75 (1.13)	4.73 (0.73)	77.83 (3.34)	0.76 (0.07)	221.56 (47.77)	52.23 (6.32)	25.56 (3.56)	0.18 (0.01)	-1.23 (0.39)	146.03 (9.45)	7.31 (1.47)	2.66 (10.92)	114.33 (19.57)

Table 4.S2 continued

Ai4	103.83 (5.27)	12 (0.47)	2489.56 (468.98)	-0.17 (0.05)	-0.51 (0.1)	-1.21 (0.1)	7.69 (0.49)	4.92 (0.07)	6.1 (0.24)	49.57 (5.31)	0.36 (0.1)	207.44 (37.74)	34.48 (0.83)	33.68 (1.35)	0.27 (0.01)	-1.8 (0.04)	124.72 (9.48)	-5.57 (1.27)	-3.15 (8.21)	132.52 (17.52)
R04047-100-1	63.83 (2.79)	13.33 (1.19)	3030.56 (1223.35	-0.16 (0.03)	-0.37 (0.05)	-0.98 (0.04)	10.43 (1.07)	7.51 (0.43)	4.87 (0.88)	59.5 (2.86)	0.52 (0.18)	208.67 (69.84)	47.4 (1.43)	33.6 (1.13)	0.27 (0)	-1.87 (0.17)	124.46 (2.9)	-5.64 (0.52)	-4.61 (3.09)	133.22 (5.17)
R04047-53	67.17 (5.6)	10.33 (0.27)	2417.33 (444)	-0.12 (0.02)	-0.63 (0.12)	-1.25 (0)	13.36 (0)	5.14 (0)	5.1 (0.64)	53.25 (1.24)	0.47 (0.04)	233.17 (42.27)	43.35 (8.13)	35.31 (1.99)	0.25 (0.01)	-1.47 (0.11)	141.24 (3.23)	-3.35 (0.68)	9.7 (3.92)	102.13 (7.6)
R04047-101-1	51.08 (7.58)	10.75 (0.41)	1299.25 (442.36)	-0.12 (0.03)	-0.46 (0.01)	-1 (0.05)	14 (3.19)	6.89 (1.04)	3.63 (0.54)	47.38 (5.32)	0.6 (0.08)	116.29 (35.12)	49.19 (3.01)	33.09 (1.67)	0.26 (0.01)	-1.62 (0.13)	125.67 (7.44)	-4.57 (2.29)	-2.45 (5.42)	125.55 (14.8)
R04047-11-1	52 (0.35)	15 (1.41)	2691.22 (1353.04	-0.12 (0.01)	-0.39 (0.01)	-0.93 (0.04)	7.38 (1.47)	4.89 (1.11)	0 (0.57)	53 (14.85)	1.16 (0.13)	185.44 (70.1)	32.92 (3.75)	21.25 (3.71)	0.12 (0.05)	-1.2 (0.26)	182.11 (4.89)	8.9 (4.1)	5.34 (0.79)	116.56 (13.45)
R04047-116-1	59.67 (4.58)	14 (0)	2056.44 (424.47)	-0.19 (0.07)	-0.4 (0.06)	-1.14 (0.09)	7.03 (0.45)	5.42 (0.46)	4.7 (0.46)	59.67 (6.74)	0.55 (0.06)	146.89 (30.32)	37.22 (1.25)	23.34 (5.71)	0.25 (0.05)	-1.19 (0.1)	94.61 (4.79)	-0.71 (7.01)	-42.19 (11.64)	0 (17.73)
R04047-14-1	53 (7.31)	14 (1.25)	3638.67 (1088.41	-0.29 (0.09)	-0.45 (0.04)	-0.94 (0.03)	7.48 (0.05)	4.83 (0.02)	5.17 (0.78)	62.83 (9.74)	0.38 (0.09)	255.56 (70.95)	39.83 (4.06)	22.49 (2.45)	0.15 (0.02)	-1.68 (0.27)	149.91 (0.93)	12.32 (3.27)	3.11 (2.88)	111.43 (2.49)
R04047-19-1	55 (2.05)	10.67 (0.27)	1453.56 (314.08)	-0.09 (0.03)	-0.57 (0.05)	-1.04 (0.07)	11.95 (1.76)	5.62 (0.48)	3.73 (0.32)	49.33 (1.3)	0.6 (0.17)	135 (27.06)	43.76 (2.04)	27.8 (1.84)	0.21 (0.02)	-1.51 (0.19)	132.4 (5.8)	2.2 (2.77)	-3.17 (4.17)	130.31 (9.79)
R04047-20	55.75 (5.92)	13 (0)	1373.67 (340.25)	-0.24 (0.08)	-0.68 (0.02)	-1.05 (0.12)	14.84 (2.3)	6.64 (0.86)	3.5 (0.92)	47.5 (8.49)	0.38 (0.03)	105.67 (26.17)	35.45 (2.99)	26.31 (4.09)	0.22 (0.04)	-1.13 (0.05)	122.37 (2.7)	2.1 (4.48)	-13.19 (1.77)	144.51 (1.08)
R04047-25-1	98.5 (7.6)	12 (0)	2214.67 (151.51)	-0.1 (0.04)	-0.47 (0.1)	-1.08 (0.07)	9.33 (1.73)	5.39 (0.25)	4.8 (0.07)	59.25 (3.71)	0.44 (0.09)	184.56 (12.63)	43.99 (3.61)	29.12 (4.31)	0.24 (0.06)	-1.52 (0.21)	119.66 (10.06)	-0.45 (6.27)	-8.32 (5.07)	132.32 (8.34)
R04047-26-1	73.33 (4.15)	12 (0.47)	1715.22 (219.97)	-0.05 (0.01)	-0.47 (0.02)	-1.11 (0.13)	12.04 (3.6)	6.46 (1.32)	3.97 (0.29)	61.2 (5.04)	0.33 (0.05)	141.56 (13.99)	47.68 (2.32)	32.36 (1.85)	0.26 (0.03)	-1.43 (0.2)	126.09 (7.76)	-3.59 (3.41)	-2.56 (4.47)	128.98 (11.37)
IS9710	102.2 (11.98)	12.33 (0.54)	2561.44 (1185.54	-0.13 (0.01)	-0.59 (0.08)	-1.2 (0.11)	7.76 (1.06)	4.69 (1.02)	4.93 (1.42)	59.17 (13.5)	0.52 (0.05)	199.22 (89.92)	38.66 (3.28)	26.64 (4.71)	0.19 (0.04)	-1.31 (0.15)	142.71 (3.4)	7.06 (6.08)	2.52 (3.62)	117.16 (6.88)
R05012-1	59.67 (2.83)	15.67 (0.71)	3547.33 (1300.25	-0.19 (0.05)	-0.33 (0.04)	-0.97 (0.14)	5.85 (1.01)	4.63 (0.44)	4.6 (0.63)	84.78 (3.77)	0.58 (0.13)	252.33 (55.34)	34.95 (3.73)	18.72 (2.71)	0.13 (0.03)	-1.02 (0.12)	141.28 (13.75)	18.36 (6.84)	-3.11 (10.79)	107.2 (21.51)
R05012-4	75.33 (6.87)	12.33 (0.27)	3190 (21.94)	-0.1 (0)	-0.53 (0.07)	-0.97 (0.1)	12.5 (2.46)	6.58 (1.62)	5.7 (0.14)	57.75 (0.88)	0.43 (0.04)	265.83 (1.83)	51.77 (2.22)	32.33 (2.06)	0.25 (0.05)	-1.97 (0.14)	130.36 (16.85)	-1.43 (5.68)	7.41 (11.2)	107.92 (23.74)
R05012-46	48 (0)	15 (0)	1967.5 (1135.94)	-0.27 (0.04)	-0.24 (0.01)	-0.61 (0.05)	11.38 (0)	11.03 (0)	4.8 (0.21)	77.1 (0.07)	0.7 (0.16)	226 (20.98)	31.07 (3.55)	17.58 (0)	0.13 (0)	-1.37 (0)	135.23 (0)	16.01 (0)	-15.44 (0)	144.85 (0)
R05012-52	76.8 (11.46)	15.4 (0.36)	4182.67 (329.71)	-0.12 (0.02)	-0.41 (0.03)	-1.09 (0.06)	7.89 (0.88)	5.49 (0.52)	5.9 (0.22)	81.5 (1.59)	0.49 (0.03)	269.87 (16.32)	42.17 (1.48)	30.57 (0.51)	0.24 (0.01)	-1.7 (0.1)	125.29 (4.82)	-2.51 (1.31)	-5.86 (3.63)	132.22 (8.4)
R05012-53	53 (5.67)	13.33 (0.27)	2650.89 (487.11)	-0.05 (0.01)	-0.34 (0.02)	-0.98 (0.05)	9.32 (2.72)	4.38 (0.41)	5.7 (0.31)	68.07 (5.12)	0.61 (0.13)	197.11 (32.61)	39.44 (1.47)	32.74 (2.64)	0.29 (0.07)	-1.68 (0.07)	111.63 (19.02)	-5.39 (7.23)	-3.38 (11.8)	131.36 (25.99)
R05012-54	42.83 (6.55)	12.33 (0.27)	1216.78 (331.7)	-0.13 (0.01)	-0.5 (0.06)	-1.05 (0.05)	9.17 (2.13)	5.2 (0.87)	3.3 (0.43)	48 (6.8)	0.48 (0.02)	97.11 (24.25)	39.59 (1.31)	24.19 (4.24)	0.22 (0.06)	-1.19 (0.17)	111.65 (20.38)	4.37 (8.61)	-14.22 (13.07)	151.29 (26.8)
R05012-57	44.33 (5.66)	11 (0)	1340.78 (560.32)	-0.25 (0.11)	-0.5 (0.08)	-1.2 (0.05)	6.71 (2.17)	3.17 (1.03)	3.53 (0.63)	50.67 (7.15)	0.32 (0.03)	121.89 (50.94)	46.88 (7.48)	26.02 (8.24)	0.21 (0.07)	-1.6 (0.49)	125.92 (11.21)	11.8 (15.98)	-11.32 (9.1)	123.5 (13.45)
R05012-6	73.75 (1.91)	13.25 (0.22)	3524.92 (266.02)	-0.11 (0.03)	-0.47 (0.04)	-1.09 (0.04)	10.72 (1.13)	6.69 (0.41)	6.2 (0.3)	78.13 (1.62)	0.29 (0.06)	265.17 (15.96)	51.58 (3.11)	33.71 (1.44)	0.24 (0.01)	-1.75 (0.07)	139.01 (4.62)	-2.3 (1.57)	7.26 (3.81)	105.62 (6.83)
R05012-61	60.17 (4.15)	13.33 (0.54)	2951.78 (775.5)	-0.07 (0.02)	-0.33 (0.02)	-0.95 (0.1)	11.33 (0)	0 (0)	5.33 (0.63)	69.6 (3.65)	0.47 (0.11)	218.44 (52.27)	45.68 (4.46)	39.29 (0)	0.3 (0)	-1.82 (0)	130.97 (0)	-8.78 (0)	5.08 (0)	114.88 (0)
R05012-64	61.33 (3.18)	14 (0.82)	3218.78 (1019.89	-0.1 (0.04)	-0.44 (0.04)	-1.12 (0.12)	5.89 (1.85)	4.01 (0.83)	4.53 (0.75)	56.67 (8.68)	0.23 (0.02)	221.44 (60.26)	51.09 (5.33)	24.94 (5.74)	0.15 (0.04)	-1.32 (0.27)	163.74 (8.65)	15.64 (10.13)	19.99 (2.07)	76.25 (5.62)
R05012-65	59 (5.3)	12 (1.41)	1822.67 (804.06)	-0.04 (0)	-0.36 (0.06)	-1.12 (0.17)	8.18 (1.42)	5.16 (0.08)	3.95 (1.38)	53.25 (11.14)	0.67 (0.17)	136.33 (53.89)	43.12 (6.97)	30.15 (5.2)	0.23 (0.05)	-1.41 (0.3)	134 (3.81)	1.04 (5.09)	0.2 (1.28)	112.09 (4.24)
R05012-11	0 (12.09)	12 (0.71)	2017.17 (1164.61	-0.12 (0.05)	-0.56 (0.05)	-0.9 (0.04)	21.19 (2.56)	8.82 (1.38)	4.95 (1.45)	64.5 (15.2)	0.37 (0.11)	185.17 (72.27)	38.18 (9.41)	37.52 (4.71)	0.28 (0.04)	-1.87 (0.27)	133.98 (2.97)	-6.03 (3.72)	6.46 (0.76)	139.64 (16.24)
R05012-71	102.5 (3.47)	13.67 (0.27)	2953.67 (425.54)	-0.19 (0.02)	-0.35 (0.02)	-1.28 (0.06)	6.65 (0.19)	5.81 (0.19)	5.4 (0.57)	71.33 (3.67)	0.64 (0.27)	214.56 (27.61)	40.41 (2.63)	32.98 (4.23)	0.28 (0.03)	-1.9 (0.21)	117.77 (3.08)	-6.26 (3.02)	-11.34 (5.62)	145.62 (12.08)
R05012-72	70.97 (5.41)	11 (0)	1548.56 (373.26)	-0.12 (0.03)	-0.48 (0.07)	-0.75 (0.14)	18.14 (0.15)	7.74 (0.78)	4.77 (0.6)	53 (4.92)	0.42 (0.14)	140.78 (33.93)	47.54 (3.01)	26.42 (4.86)	0.18 (0.04)	-1.38 (0.15)	145.18 (8.55)	8.89 (8)	7.3 (0.65)	98.17 (6.1)
R05012-80	60.83 (7.07)	14.67 (0.54)	3757.56 (551.87)	-0.3 (0.1)	-0.32 (0.04)	-0.84 (0.02)	9.7 (1.23)	10.59 (3.06)	5.4 (0.65)	79.17 (3.13)	0.3 (0.08)	253.22 (27.17)	36.24 (2.46)	29.31 (3.49)	0.22 (0.04)	-1.53 (0.12)	135.26 (9.82)	2.26 (5.17)	2.76 (6.63)	116.55 (10.7)
R05012-82	47.83 (6.37)	12.33 (0.27)	2167.56 (578.73)	-0.08 (0.02)	-0.57 (0.09)	-1.05 (0.15)	11.68 (1.52)	5.4 (0.32)	4.67 (0.72)	50.37 (4.07)	0.58 (0.15)	174.5 (45.96)	45.3 (6.06)	30.04 (5.54)	0.23 (0.04)	-1.65 (0.31)	131.75 (2.99)	1.16 (6.22)	-4.32 (7.51)	116.11 (11.43)
R05012-9	62.4 (2.22)	14.8 (0.33)	3859.83 (234.85)	-0.11 (0.03)	-0.37 (0.06)	-1.09 (0.11)	8.26 (0.41)	6.52 (0.29)	5.08 (0.17)	69.1 (7.51)	0.56 (0.16)	260.77 (14.7)	36.35 (3.34)	29.95 (0.79)	0.25 (0.02)	-1.58 (0.11)	122.24 (8.27)	-2.33 (2.3)	-7.28 (5.19)	139.08 (10.81)
R05012-90	43.33 (4.58)	14.67 (0.27)	3137.44 (735.72)	-0.41 (0.23)	-0.32 (0.04)	-0.89 (0.01)	8.65 (1.06)	7.57 (0)	4.63 (0.64)	66.83 (4.63)	0.4 (0.1)	216.89 (55.13)	36.82 (5.57)	29.49 (4.95)	0.18 (0.03)	-1.69 (0.19)	168.49 (2.04)	8.21 (4.5)	26.52 (2.46)	71.69 (4.3)
R05012-14	54.83 (5.92)	12.67 (0.98)	2622.33 (728.51)	-0.1 (0.04)	-0.36 (0.03)	-0.94 (0.1)	11.4 (0.19)	7.55 (0.65)	4.23 (0.55)	64 (3.01)	0.49 (0.1)	200 (41.96)	47.72 (7.57)	33.48 (4.19)	0.28 (0.03)	-1.84 (0.11)	117.61 (9.94)	-6.84 (2.69)	-10.51 (10.64)	144.6 (22.19)
R05012-18	40 (2.12)	13.5 (0.35)	1779 (935.7)	-0.11 (0.01)	-0.37 (0.06)	-1.1 (0.07)	6.7 (1.25)	4.93 (0.9)	4.23 (1.08)	59.7 (6.85)	0.37 (0.04)	153.56 (52.37)	44.5 (6.91)	23.15 (5.6)	0.17 (0.04)	-1.56 (0.33)	133.58 (5.85)	9.22 (5.72)	-13.12 (11.02)	132.62 (14.08)
R05012-2	37.5 (11.38)	14.33 (0.72)	1356 (562.98)	-0.09 (0.01)	-0.38 (0.03)	-0.9 (0.09)	8.23 (2.15)	5.12 (1.14)	3.63 (0.61)	46.7 (9.66)	0.85 (0.15)	96.22 (40.58)	49.85 (3.54)	18.15 (3.26)	0.14 (0.03)	-1.36 (0.42)	129.64 (13.58)	17.25 (8.88)	-12.82 (4.9)	141.07 (13.4)
R05012-20	53.5 (9.19)	12.33 (0.27)	2118.89 (369.37)	-0.14 (0.03)	-0.35 (0.05)	-0.76 (0.08)	11.47 (2.57)	7.39 (2.07)	4.53 (0.35)	72.43 (3.84)	0.7 (0.34)	173.22 (32.52)	34.89 (1.09)	21.75 (0.61)	0.16 (0)	-1.22 (0.1)	140.32 (0.59)	10.81 (0.55)	-5.18 (1.14)	124.96 (4.31)
R05012-26	54 (1.7)	14.67 (0.98)	3717.56 (555.21)	-0.19 (0.03)	-0.33 (0.03)	-0.91 (0.08)	8.04 (0.65)	6.42 (0.56)	6 (0.43)	75.03 (1.78)	0.5 (0.14)	249.44 (20.21)	40.75 (3.41)	26.35 (3.11)	0.18 (0.02)	-2.08 (0.53)	146.39 (9.8)	6.91 (3.22)	5.46 (9.64)	110.05 (16.54)
R05012-31	60.38 (12.6)	11.75 (0.65)	2082.58 (563.99)	-0.08 (0.02)	-0.39 (0.04)	-0.88 (0.15)	11.26 (1.59)	6.74 (1.24)	4.25 (0.5)	57 (3.39)	0.76 (0.14)	169.42 (39.59)	43.12 (1.5)	26.66 (5.28)	0.23 (0.05)	-1.53 (0.17)	118.49 (8.16)	3.89 (8.86)	-15.74 (6.85)	143.54 (11.98)
R05012-36	60.5 (5.33)	15.33 (1.44)	2021.11 (71.4)	-0.16 (0.07)	-0.42 (0.02)	-0.94 (0.02)	11.64 (0.51)	8.31 (1.43)	5 (0.25)	54.5 (2.46)	0.87 (0.15)	136.33 (16.21)	38.77 (1.47)	37.78 (1.01)	0.29 (0.01)	-2.14 (0.07)	131.8 (0.97)	-4.34 (2.73)	3.69 (0.81)	112.9 (2.03)
R931945-2-2*	46.75 (3.91)	12.67 (0.56)	1845.44 (342.79)	-0.25 (0.09)	-0.32 (0.02)	-0.89 (0.05)	10.35 (1.67)	12.04 (4.67)	3.7 (0.38)	57.12 (4.52)	0.72 (0.09)	142.11 (24.24)	37.49 (3.28)	0 (4.13)	0 (0.04)	-1.41 (0.14)	120.35 (4.88)	3.88 (6.35)	-15.31 (5.9)	144.54 (6.25)
Mean	60.24 (1.47)	12.94 (0.15)	2468.2 (84.28)	-0.13 (0.01)	-0.42 (0.01)	-0.97 (0.01)	10.54 (0.31)	6.72 (0.24)	4.62 (0.08)	63.01 (1.17)	0.58 (0.02)	189.74 (5.64)	43.01 (0.67)	28.79 (0.52)	0.22 (0.01)	-1.54 (0.03)	134.99 (1.49)	2.65 (0.74)	-2.07 (1.26)	122.72 (2.4)

A_n Carbon assimilation rate (μmol m^{-2} s^{-1}); R_{dark} Dark respiration rate (μmol m^{-2} s^{-1}); g_s Stomatal conductance (mol m^{-2} s^{-1}); *iWUE* Instantaneous water use efficiency (μmol CO_2 mol^{-1} H_2O); $iWUE_{pc}$ *iWUE* attributed to variation in A_n (%); $iWUE_{gs}$ *iWUE* attributed to variation in g_s (%); C_i Sub-stomatal carbon dioxide concentration (ppm); $\Psi_{pre\text{-}dawn}$ and Ψ_{midday} leaf water potenial (MPa); Ψ_{stem} Stem water potential at midday (MPa); *LW* Leaf width (cm); *LL* Leaf length (cm); *LT* Leaf thickness (mm); *PH* Plant height (cm); *LN* Number of leaves; *SPAD* Relative Chlorophyll content based on special products analysis division; *TLA* Total leaf area (cm^2); *LA* Average leaf area (cm^2); K_{plant} Plant hydraulic conductivty (mmol m^{-2} s^{-1} MPa^{-1}); K_{leaf} Leaf hydraulic conductivty (mmol m^{-2} s^{-1} MPa^{-1}).

Table 4.S2 continued

Exotic Parent and Genotype Progeny	Water Stress																		
	PH	*LN*	*TLA*	$\Psi_{pre\text{-}dawn}$	Ψ_{stem}	Ψ_{midday}	K_{leaf}	K_{plant}	*LW*	*LL*	*LT*	*LA*	*SPAD*	A_n	g_s	R_{dark}	*iWUE*	$iWUE_{gs}$	$iWUE_{pc}$	C_i
RTx7000	41 (1.7)	15.67 (1.09)	2296.44 (818.79)	-0.4 (0.08)	-0.97 (0.27)	-1.33 (0.23)	7.8 (1.09)	3.33 (0.92)	3.37 (0.61)	66 (0.13)	0.43 (7.32)	139.56 (45.39)	39.22 (0.49)	14.6 (1.52)	0.11 (0.02)	-0.86 (0.05)	137.7 (18.09)	-11.52 (6.85)	-9.17 (11.33)	123.24 (21.66)
R020038-1																				
R020040-1	35.67 (0.89)	14.5 (0.35)	1432.44 (674.11)	-0.32 (0.08)	-0.93 (0.34)	-1.29 (0.23)	11.79 (1.85)	4.24 (1.33)	3.77 (0.14)	64.44 (0.02)	0.31 (3.27)	136.33 (22.39)	37.27 (2.51)	15.87 (3.55)	0.11 (0.03)	-1.03 (0.15)	148.75 (14.69)	-9.72 (10.11)	-2.46 (7.96)	63.52 (13.39)
R020043-1																				
R020045-1																				
R020046-1	65 (4.87)	11.67 (0.54)	1082.5 (302.24)	-1.03 (0.05)	-1.35 (0.39)	-1.81 (0.38)	4.76 (2.18)	11.13 (7.48)	3.87 (0.35)	52.83 (0.14)	0.41 (7.8)	94.5 (29.73)	21.5 (2.98)	11.72 (3.36)	0.07 (0.02)	-1.04 (0.01)	167.48 (10.76)	5.04 (12.66)	1.08 (3.32)	89.43 (12.37)
R020047-1	49.67 (4.35)	11.67 (0.27)	1998.33 (667.38)	-0.24 (0.07)	-1.35 (0.32)	-1.76 (0.24)	14.49 (5.93)	2.7 (0.46)	4.93 (0.93)	63.17 (0.02)	0.33 (6.69)	175.39 (62.36)	38.45 (0.92)	22.69 (0.75)	0.14 (0.02)	-1.56 (0.28)	162.05 (12.95)	-21.53 (3.27)	17.45 (9.76)	79.37 (19.38)
R020102-1																				
R020009-1	46.83 (5.46)	12 (0)	892 (369.92)	-0.19 (0.01)	-0.47 (0.16)	-1.03 (0.1)	12.61 (2.43)	8 (0.72)	0 (0.32)	49.83 (0.08)	0.38 (2.38)	93.89 (15.37)	43.29 (3.68)	32.02 (1.9)	0.24 (0.01)	-1.65 (0.09)	131.58 (1.98)	-38.39 (1.29)	-0.84 (3.19)	119.64 (6.47)
R020016-1																				
R020017-1	46 (0.47)	11.33 (0.72)	1565.33 (367.57)	-0.83 (0.39)	-1.75 (0.38)	-2.05 (0.34)	4.78 (0.51)	1.19 (0.26)	4.2 (0.61)	50.33 (0.06)	0.47 (3.57)	136.78 (28.67)	36.24 (8.37)	8.37 (1.27)	0 (0.15)	-0.37 (0.05)	0 (14.47)	20.59 (7.02)	24.7 (7.44)	48.63 (21.09)
R020018-1	68.25 (2.65)	13.5 (0.35)	1809 (494.02)	-0.49 (0.08)	-0.87 (0.15)	-1.26 (0.33)	7.68 (4.9)	5.65 (3.74)	3.85 (0.18)	58.25 (0.17)	0.57 (2.65)	131.83 (33.77)	31.96 (3.59)	8 (3.74)	0.05 (0.02)	-0.61 (0.06)	173.8 (6.49)	20.7 (14.7)	-9.65 (8.21)	80.43 (7.62)
R020022-1																				
R020034-1	68.5 (1.03)	13.33 (0.27)	753.89 (42.98)	-0.2 (0.05)	-0.41 (0.02)	-0.93 (0.03)	6.82 (0.26)	4.92 (0.08)	3.07 (0.21)	46 (0.14)	0.46 (3.59)	56.78 (4.19)	32.16 (1.01)	19.34 (2.31)	0.13 (0.02)	-1.07 (0.07)	152.71 (8.68)	-18.41 (3.87)	1.49 (8.5)	105.45 (16.42)
SC103-14E	32.17 (1.57)	14.67 (0.27)	2176.44 (463.49)	-0.52 (0.28)	-1.03 (0.27)	-1.58 (0.34)	5.24 (1.41)	2.54 (0.61)	3.5 (0)	50 (0.05)	0.25 (6.36)	150.33 (35.13)	34.45 (3.51)	14.52 (2.79)	0.09 (0.02)	-1.37 (0.18)	165 (14.86)	-5.89 (7.39)	5.87 (11.9)	84.58 (26.13)
R021232-1																				
R021235-1																				
R021253-1																				
R021254-1	50 (1.93)	12.67 (0.27)	1751.89 (308.25)	-0.84 (0.31)	-1.79 (0.68)	-1.61 (0.25)	4.57 (1.8)	2.17 (0.25)	4.63 (0.38)	60.17 (0.05)	0.49 (4.45)	137.89 (22.86)	50.44 (4.85)	8.63 (0.91)	0.05 (0)	-0.62 (0.08)	181.12 (16.53)	9.86 (0.6)	0.11 (16.87)	87.41 (25.12)
R021281-1	43.33 (1.66)	14.33 (0.54)	2677 (529.94)	-1.25 (0.46)	-1.4 (0.44)	-1.78 (0.4)	8.77 (3.15)	3.87 (0.81)	4.97 (0.5)	59.57 (0.2)	0 (3.04)	185.44 (32.91)	37.63 (3.62)	13.14 (3.55)	0.08 (0.03)	-1.15 (0.21)	172.89 (11.94)	0.78 (9.34)	13.84 (2.68)	66.85 (10.34)
R021287-1																				
R021205-1	57.33 (3.54)	13.67 (0.27)	2190.11 (381.41)	-1.01 (0.38)	-1.46 (0.35)	-1.9 (0.32)	4.39 (0.72)	2.54 (0.51)	4.5 (0.49)	66.4 (0.28)	0.68 (5.08)	158.89 (25.43)	38.2 (1.62)	11.79 (3.37)	0.13 (0.04)	-0.98 (0.15)	0 (43.61)	-7.13 (3.22)	15.8 (5.59)	78.14 (7.73)
R021206-1	39 (2.86)	13.33 (0.27)	2810.78 (240.47)	-0.6 (0.06)	-2.06 (0.18)	-2.12 (0.05)	5.87 (1.66)	0.94 (0.16)	5.6 (0)	80.6 (0.09)	0.37 (1.84)	211 (18.73)	38.77 (7.85)	8.94 (1.74)	0 (0.12)	-0.79 (0.17)	0 (47.7)	13.71 (8.81)	7.81 (1.01)	66.12 (7.92)
R021208-1																				
R021209-1	37 (1.41)	13.5 (0.35)	2187.56 (924.62)	-1.25 (0.44)	-1.44 (0.39)	-1.92 (0.34)	4.49 (1.08)	3.08 (0.67)	4.3 (0.84)	68.43 (0.13)	0.56 (8.39)	176.67 (55.03)	33.67 (1.33)	10.9 (1.05)	0.06 (0)	-0.72 (0.19)	185.8 (8.21)	3.88 (1.97)	10.62 (9.22)	74.12 (15.84)
R021210-1	41.5 (4.49)	13.67 (0.27)	2487.22 (598.45)	-0.71 (0.31)	-1.18 (0.34)	-1.78 (0.21)	4.36 (0.92)	2.2 (0.76)	4.57 (0.78)	68.67 (0.08)	0.36 (5.66)	179.89 (41.18)	34.9 (6.95)	13.64 (4.37)	0.09 (0.04)	-1.51 (0.03)	152.16 (16.35)	-1.87 (11.35)	1.48 (7.52)	90.75 (21.13)
R021213-1																				
R021216-1																				
R021220																				
SC35-14E	36.33 (1.91)	14 (0.47)	2239.56 (688.72)	-0.23 (0.12)	-1.11 (0.35)	-1.53 (0.28)	9.3 (1.88)	2.69 (0.57)	4.43 (0.75)	77.77 (0.05)	0.38 (4.37)	155.56 (44.81)	33.34 (3.13)	18.7 (2.66)	0.12 (0.02)	-0.9 (0.05)	160.29 (13.23)	-14.78 (6.2)	10.94 (9.8)	83.32 (21.75)
QL12	48 (4.24)	13.5 (0.35)	2042.83 (204.09)	-1.17 (0.59)	-0.94 (0.5)	-1.52 (0.51)	6.54 (0)	7.94 (0)	4.05 (0.46)	64 (0.18)	0 (9.19)	152.5 (18.38)	30.69 (4.25)	21.9 (0)	0.15 (0)	-1.26 (0)	146 (0)	-24.14 (0)	-0.43 (0)	111.72 (0)
R04044-106-1																				
R04044-132																				
R04044-136	42 (4.24)	12.5 (0.35)	1341.22 (670.3)	-0.32 (0.09)	-1.4 (0.57)	-1.91 (0.44)	6.04 (1.16)	2.41 (0.87)	3.03 (0.68)	64.23 (0.12)	0.66 (8.18)	116 (51.79)	39.9 (5.23)	15.05 (4.74)	0.1 (0.04)	-0.95 (0.33)	145.61 (11.74)	-8.09 (9.7)	-10.48 (9.55)	116.75 (16.25)
R04044-18-1	64 (5.67)	12.67 (0.54)	2049.56 (198.31)	-0.32 (0.02)	-1.09 (0.19)	-1.44 (0.21)	5.86 (1.81)	2.41 (1.12)	3.67 (0.5)	60.37 (0.14)	0.64 (4.34)	164.56 (21.55)	34.13 (3.89)	9.64 (1.34)	0.06 (0.01)	-0.57 (0.11)	160.72 (16.51)	4.82 (5.85)	-62.23 (51.86)	102.32 (28.31)
R04044-20-1																				
R04044-26-1	40.25 (0.53)	15 (0)	1878.33 (800.52)	-0.72 (0.14)	-1.6 (0.42)	-2.06 (0.38)	4.87 (0.64)	2.31 (0.88)	5.23 (0.46)	75.17 (0.1)	0.69 (5.55)	206.67 (21.71)	37.04 (2.93)	11.37 (1.16)	0.06 (0.01)	-0.7 (0.12)	183.33 (2.86)	2.45 (2.83)	10.12 (4.37)	70.9 (7.08)
R04044-31-1	45.5 (3.47)	13.67 (0.54)	2895.22 (402.57)	-0.57 (0.15)	-1.61 (0.22)	-1.97 (0.34)	13.93 (9.01)	1.87 (0.82)	4.6 (0.45)	69.83 (0.03)	0.22 (4.25)	210.11 (23.55)	26.68 (6.11)	13.49 (3.64)	0.07 (0.02)	-0.54 (0.06)	180.67 (8.03)	0.99 (9.41)	16.65 (2.35)	57.88 (10.99)
R04044-33-1	0 (0)	0 (0)	0 (0)	-0.45 (0)	-1.93 (0)	-2.39 (0)	7.09 (0)	1.68 (0)	4.6 (0)	80.5 (0.05)	0 (0)	132.67 (0)	36.43 (5.09)	21.77 (0)	0.12 (0)	-1.96 (0)	181.42 (0)	-17.53 (0)	28.37 (0)	57.73 (0)
R04044-37-1	28.33 (3.93)	15 (0)	921.67 (752.54)	-0.82 (0.5)	-1.43 (0.44)	-1.94 (0.31)	5.78 (0.91)	3.74 (1.27)	4.83 (1.04)	65.5 (0.1)	0.45 (5.31)	149.67 (38.81)	31.24 (3.71)	13.92 (0.76)	0.1 (0.02)	-1.07 (0.3)	145.47 (29.22)	-8.5 (6.62)	3.81 (22.85)	91.28 (50.25)
R04044-38-1	39 (5.44)	12.67 (0.72)	1812 (316.78)	-0.37 (0.13)	-1.27 (0.22)	-1.71 (0.35)	5.47 (1.65)	1.62 (0.07)	4.13 (0.31)	61 (0.18)	0.54 (2.86)	140.11 (17.45)	45.2 (4.28)	13.34 (3.66)	0.09 (0.04)	-0.78 (0.29)	140.88 (16.76)	-3.75 (11.68)	-9.29 (11.02)	75.23 (14.66)
R04044-47-1																				
R04044-49	0 (3.62)	14 (0.47)	1917 (372.82)	-2.09 (0.52)	-1.61 (0.43)	-1.91 (0.37)	5.44 (1.68)	13.88 (0)	0 (0.5)	62 (0.09)	0.41 (6.91)	135.44 (24.67)	32.26 (0.71)	11.36 (4.37)	0 (0.19)	-0.67 (0.12)	0 (0.67)	24.59 (26.95)	-64.64 (26.28)	116.91 (32.96)
R04044-59-1																				
R04044-60-1	48.5 (1.55)	12.67 (0.27)	2021.44 (240.69)	-1.02 (0.65)	-1.43 (0.52)	-1.91 (0.43)	3.28 (1.43)	1.56 (0.4)	4.53 (0.24)	64.17 (0.14)	0.6 (2.19)	160.22 (20.1)	26.83 (7.53)	9.87 (4.39)	0.05 (0.02)	-0.78 (0.17)	180.55 (35.44)	24.73 (24.17)	-73.74 (73.8)	151.58 (61.14)
R04044-66-1	57.17 (4.41)	12.67 (0.27)	1968 (167.78)	-1.57 (0.53)	-1.25 (0.35)	-1.62 (0.3)	9.21 (2.02)	4.16 (0)	4.93 (0.59)	61.33 (0.11)	0.68 (6.47)	155.44 (12.78)	27.44 (3.14)	18.76 (1.21)	0.1 (0.01)	-1.35 (0.06)	181.58 (6.88)	-12.66 (2.98)	25.51 (4.28)	63.82 (8.33)
R04044-76-1	36.5 (0.35)	14.5 (0.35)	1640.67 (754.98)	-0.81 (0.45)	-1.51 (0.31)	-1.83 (0.23)	6.44 (1.44)	2.04 (0.32)	4.87 (0.58)	69.1 (0.09)	0.32 (5)	200.11 (33.67)	33.96 (3.5)	11.66 (2.44)	0.07 (0.02)	-0.86 (0.03)	163.46 (10.94)	1.44 (8.77)	-1.4 (7.3)	92.34 (13.58)
R04044-88-1	48 (3.97)	12 (0)	1780 (276.56)	-1.6 (0.63)	-1.8 (0.25)	-2.17 (0.29)	11.15 (7.09)	1.97 (1.17)	4.23 (0.59)	54.33 (0.04)	0.27 (8.98)	148.33 (23.05)	46.35 (1.03)	16.79 (7.17)	0.1 (0.04)	-0.96 (0.27)	169.6 (4.36)	7.4 (24.45)	-13.4 (28.02)	101.75 (20.44)
R04044-11	0 (0)	0 (0)	0 (0)	-0.13 (0)	-0.2 (0)	-0.95 (0)	2.87 (0)	2.62 (0)	4.2 (0)	51 (0)	0.36 (0)	119.33 (0)	41.26 (0)	13.59 (0)	0.08 (0)	-1.38 (0)	178.82 (0)	-3.99 (0)	12.23 (0)	79.25 (0)
R04044-124	48.17 (1.3)	13 (0.47)	3387.44 (314.08)	-0.57 (0.18)	-1.36 (0.23)	-1.81 (0.13)	11.28 (4.22)	2.93 (0.11)	0 (0.55)	80.47 (0.1)	0.37 (1.62)	260.22 (21.52)	39.74 (6.05)	21.22 (0.67)	0.13 (0.01)	-1.67 (0.27)	167.55 (2.55)	-19.05 (1.24)	16.29 (1.74)	82.5 (8.5)
R04044-130-1	45.25 (8.31)	13 (0.71)	1544 (631.83)	-0.72 (0.15)	-1.6 (0.32)	-2.17 (0.34)	4.09 (1.55)	1.08 (0.12)	4.53 (0.15)	61.83 (0.1)	0.5 (2.79)	174.11 (4.87)	45.26 (1.48)	9.13 (1)	0.05 (0)	-0.86 (0.22)	190.21 (11.04)	9.87 (2.18)	8.96 (11.9)	59.36 (15.27)

Table 4.S2 continued

Ai4	89.83 (2.71)	11.67 (0.27)	1033.11 (106.24)	-0.77 (0)	-1.26 (0.11)	-1.79 (0)	7.58 (1.86)	3.71 (0)	4.97 (0.55)	35.27 (0.04)	0.33 (1.8)	88.89 (9.75)	22.62 (5.41)	17.89 (0.81)	0.11 (0.01)	-1.12 (0.09)	166.19 (10.55)	-13.82 (3.17)	12.68 (7.4)	83.34 (15.85)
R04047-100-1	62.25 (1.94)	13.5 (0.35)	797.33 (347.82)	-0.84 (0.42)	-0.88 (0.16)	-1.42 (0.17)	3.4 (0.11)	1.78 (0)	4 (0.42)	56.83 (0.03)	0.66 (4.51)	116.78 (24.68)	30 (6.23)	14.01 (1.92)	0.08 (0.01)	-1.12 (0.06)	181.12 (12.15)	-3.75 (3.81)	15.33 (11.72)	60.34 (3.33)
R04047-53	69.5 (3.57)	10.67 (0.27)	1032.78 (354.03)	-1.01 (0.14)	-0.9 (0.22)	-1.39 (0.14)	1.77 (0)	1.82 (0)	3.37 (0.34)	43.17 (0.07)	0.38 (5.81)	95.22 (31.45)	15.72 (6.29)	0 (1.93)	0 (0.04)	-0.82 (0.21)	0 (37.19)	7.84 (16.02)	-40.83 (21.18)	235.05 (83.11)
R04047-101-1																				
R04047-11-1	36.5 (1.31)	13.33 (0.27)	1941.89 (338.02)	-0.91 (0.41)	-0.93 (0.25)	-1.62 (0.11)	4.98 (1.6)	2.55 (0.23)	4.4 (0.57)	61.17 (0.13)	0.42 (3.58)	144.67 (23.21)	39.11 (2.72)	13.39 (1.84)	0.08 (0.01)	-0.92 (0.16)	167.33 (8.77)	-4.01 (5.54)	4.56 (5.94)	92.92 (10.91)
R04047-116-1	53.67 (5.5)	14 (0.47)	2013.67 (359.32)	-1 (0.57)	-1.26 (0.27)	-1.65 (0.24)	10.08 (0.49)	4.7 (1.22)	4.63 (0.27)	54.67 (0.08)	0.41 (2.73)	142.67 (21.93)	33.15 (1.4)	17.68 (1.23)	0.12 (0.02)	-1.14 (0.06)	150.25 (17.06)	-15.87 (4.6)	2.66 (12.93)	103.56 (25.27)
R04047-14-1	40.25 (1.24)	14.5 (0.35)	1568.89 (693.37)	-0.64 (0.11)	-1.23 (0.21)	-1.72 (0.21)	3.71 (1.3)	2.04 (0.99)	5.17 (0.57)	60.73 (0.07)	0.63 (7.74)	191.78 (30.99)	25.89 (1.25)	9.74 (2.31)	0.06 (0.02)	-0.74 (0.16)	171.88 (15.99)	9.3 (9.22)	8.08 (6.83)	64.49 (22.97)
R04047-19-1	47.75 (5.48)	10 (0)	1188.33 (253.07)	-0.25 (0)	-1.85 (0.94)	-2.11 (0.82)	17.74 (6.02)	5.67 (0)	3.75 (0.18)	47.75 (0.05)	0.45 (4.07)	118.83 (25.31)	9.14 (1.64)	16.91 (2.97)	0.12 (0.04)	-0.99 (0)	140.92 (16.57)	-14.7 (7.59)	-3 (8.98)	111.12 (21.2)
R04047-20	49.67 (2.81)	13.33 (0.72)	1806.67 (491.34)	-1.19 (0.47)	-1.27 (0.31)	-1.63 (0.26)	6.33 (2.5)	7.2 (2.69)	4.13 (0.5)	60.1 (0.02)	0.32 (2.71)	131.89 (29.25)	35.01 (2.31)	15.52 (6.42)	0.09 (0.03)	-0.94 (0.25)	181.13 (12.65)	10.15 (23.26)	-14.52 (35.9)	102.17 (31.29)
R04047-25-1	65.17 (2.6)	12.33 (0.27)	1418.78 (549.55)	-1.61 (0.99)	-1.56 (0.49)	-1.83 (0.43)	12.99 (2.72)	3.55 (0.23)	4 (0.87)	44.67 (0.04)	0.29 (9.23)	112.33 (41)	29.05 (2.42)	21.4 (2.84)	0.17 (0.03)	-1.05 (0.11)	129.7 (6.9)	-25.82 (4.79)	-84.25 (39.72)	0 (41.42)
R04047-26-1	56.5 (2.66)	11.33 (0.27)	1648.11 (346.22)	-1 (0.45)	-1.16 (0.27)	-1.57 (0.25)	8.41 (0)	8.8 (0)	4.07 (0.44)	59.5 (0.1)	0.43 (6.54)	144.44 (29.19)	40.98 (2.14)	21.24 (0)	0.14 (0)	-1.13 (0)	151.71 (0)	-22.1 (0)	3.24 (0)	107.25 (0)
IS9710	105.83 (8.35)	12.67 (0.27)	1274.22 (326.88)	-0.4 (0.1)	-0.69 (0.02)	-1.06 (0.07)	5.83 (0.64)	3.19 (0.22)	3.57 (0.44)	45.23 (0.03)	0.25 (4.79)	99.11 (24.3)	39.68 (1.46)	13.73 (0.74)	0.09 (0.01)	-0.99 (0.25)	157.25 (18.43)	-7.58 (3.2)	-0.1 (15.61)	108.16 (30.76)
R05012-1	0 (0)	0 (0)	2625.33 (179.13)	-1.62 (0)	-1.9 (0)	-2.1 (0)	#VALUE!	#VALUE!	5 (0)	80 (0)	0.33 (0)	193.11 (17.25)	34.16 (0)	0 (0)	0.01 (0)	-0.37 (0)	0 (58.93)	56.13 (0)	-69.7 (0)	58.93 (0)
R05012-4	57.33 (0.72)	13.67 (0.27)	0 (0)	-1.52 (0.2)	-1.84 (0.45)	-2.17 (0.38)	3.59 (1.58)	1 (0.15)	4.77 (0.11)	62.33 (0.13)	0.52 (5.66)	260.33 (27.84)	28.91 (3.14)	0 (0.22)	0 (0)	-0.48 (0.04)	0 (6.76)	28 (1.98)	6.24 (4.78)	167.66 (99.06)
R05012-46	0 (0)	0 (0)	2019.33 (229.29)	-1.03 (0.18)	-1.52 (0.27)	-2.4 (0.28)	6.4 (1.99)	3.66 (1.78)	0 (0.99)	0 (0.04)	0 (1.58)	143.11 (11.46)	33.15 (3.12)	16.48 (2.02)	0 (0.22)	-0.77 (0.17)	0 (15.14)	-6.23 (6.52)	38.72 (8.62)	39.99 (18.32)
R05012-52																				
R05012-53	47.5 (4.92)	14 (0.47)	1664.44 (383.33)	-0.73 (0.18)	-0.6 (0.04)	-1.14 (0.04)	5.32 (1.05)	13.65 (5.56)	4.37 (0.14)	52 (0.12)	0.44 (0.47)	144.78 (29.61)	39.59 (0.93)	15.86 (2.84)	0.1 (0.02)	-0.99 (0.2)	160.17 (5.71)	-9.97 (5.92)	2.57 (3.79)	93.29 (12.63)
R05012-54	43.5 (2.01)	11.33 (0.27)	1643 (427.82)	-0.47 (0.21)	-0.7 (0.31)	-1.88 (0.38)	2.79 (0.08)	2.52 (0.05)	4.3 (0.34)	59.83 (0.3)	0 (5.2)	140.33 (33.68)	40.67 (3.43)	16.04 (0.7)	0.11 (0)	-1.08 (0.04)	145.77 (5.17)	-14.95 (0)	-9.85 (5.17)	119.11 (8.79)
R05012-57	50.25 (2.3)	11.5 (0.35)	920 (751.18)	-1.22 (0.68)	-1.42 (0.61)	-1.77 (0.48)	7.51 (1.53)	4.75 (0.98)	4.25 (0.88)	57.5 (0.06)	0.39 (11.67)	158.78 (30.03)	34.55 (7.29)	18.25 (8.77)	0.13 (0.07)	-1.04 (0.26)	145.96 (15.98)	-5.96 (17.05)	2.39 (1.07)	72.5 (26.19)
R05012-6																				
R05012-61	57.25 (6.89)	15 (0)	1769.33 (90.65)	-1.05 (0.52)	-1.07 (0.21)	-1.74 (0.16)	2.69 (0.6)	1.97 (0.29)	4.43 (0.52)	60.17 (0.08)	0.68 (4.02)	137 (10.61)	36.34 (2.75)	10.19 (2.94)	0.06 (0.02)	-0.62 (0.06)	175.69 (15.28)	10.27 (11.06)	11.85 (5.7)	54.78 (16.95)
R05012-64																				
R05012-65	52.17 (6.9)	13 (0.47)	509.17 (293.97)	-1.12 (0.44)	-1.33 (0.13)	-1.95 (0.13)	2.96 (0.74)	1.22 (0.36)	4.73 (0.19)	64.17 (0.2)	0.7 (1.57)	178.67 (57.93)	35.71 (6.15)	9.52 (0.78)	0.05 (0)	-0.86 (0.21)	180.76 (9.88)	7.22 (2.64)	4.04 (9.14)	75.59 (12.95)
R05012-11	32 (0)	13 (0)	397.22 (324.33)	-1.45 (0.8)	-0.88 (0.22)	-1.26 (0.14)	6.86 (0.81)	3.78 (0)	4.2 (1.06)	71.25 (0.02)	0.5 (8.31)	202.61 (61.29)	26.35 (2.87)	13.24 (0.82)	0.09 (0.01)	-1.08 (0.1)	153.9 (22.82)	-7.25 (2.81)	-2.99 (20.01)	109.7 (38.54)
R05012-71	74 (0)	13 (0)	627.33 (312.18)	-1.74 (0.66)	-1.26 (0.34)	-1.9 (0.3)	3.46 (0.73)	8.53 (3.34)	5.1 (0.88)	70 (0.13)	0.59 (6.94)	55 (24.9)	26.68 (4.41)	12.69 (2.96)	0.07 (0.02)	-1.32 (0.23)	181.29 (24.55)	4.55 (11.71)	30.24 (13.27)	37.27 (33.93)
R05012-72	54.5 (8.44)	10.67 (0.54)	829.11 (676.97)	-0.94 (0.55)	-1.11 (0.17)	-1.39 (0.07)	5.79 (0.2)	1.47 (0.56)	2.97 (0.63)	32.5 (0.08)	0.35 (7.22)	209.89 (45.65)	21.99 (5.83)	11.39 (2.95)	0.06 (0.01)	-0.94 (0.05)	202.13 (20.11)	7.77 (7.6)	20.34 (23.98)	90.22 (22.14)
R05012-80	49.5 (0)	13 (0)	1783.67 (106.04)	-0.43 (0.15)	-1.11 (0.22)	-1.46 (0.18)	13.01 (5.23)	4.1 (1.2)	5.13 (0.89)	71.4 (0.06)	0.31 (2.38)	142.33 (5.2)	36.1 (6.23)	19.35 (6.1)	0.15 (0.06)	-1.22 (0.06)	129 (16.96)	-15.39 (13.87)	-6.54 (3.09)	118.34 (12.06)
R05012-82	48.17 (2.33)	12.67 (0.27)	0 (0)	-1.43 (0.56)	-1.89 (0.75)	-2.14 (0.65)	8.86 (0.38)	3.43 (1.63)	5.05 (0.39)	58 (0.17)	0.53 (1.77)	120.06 (16.33)	36.77 (3)	12.19 (5.14)	0.07 (0.03)	-1.05 (0.18)	168.07 (10.02)	5.72 (13.42)	3.15 (3.4)	72.38 (8.17)
R05012-9																				
R05012-90	45 (0)	0 (0)	1200.78 (507.69)	-0.29 (0.04)	-0.59 (0.15)	-1.18 (0.09)	6.99 (1.29)	4.38 (0.49)	3.43 (0.19)	64.17 (0.17)	0.54 (4.46)	152 (17.34)	32.08 (4.02)	22.54 (0.53)	0.14 (0.01)	-1.22 (0.01)	157.28 (5.82)	-22.73 (1.15)	9.98 (4.91)	97.49 (7.55)
R05012-14																				
R05012-18	37 (0)	13.5 (0.35)	1246.78 (200.28)	-1.9 (0.61)	-1.45 (0.38)	-1.96 (0.33)	8.78 (0.83)	7.16 (0)	5.13 (0.58)	62.83 (0.06)	0.41 (3.08)	90.44 (13.18)	38.47 (7.36)	24.6 (5.11)	0.16 (0.04)	-1.4 (0.34)	157.71 (19.7)	-20.87 (10.21)	22.59 (10.14)	67.44 (22.38)
R05012-2	57.83 (11.27)	13.67 (0.27)	488.44 (398.81)	-0.89 (0.25)	-1.5 (0.46)	-1.77 (0.38)	16.38 (3.99)	4.08 (0.5)	4.03 (0.21)	49.33 (0.06)	0.49 (5.3)	161.11 (23.22)	45.27 (1.98)	18.94 (2.69)	0.12 (0.02)	-0.9 (0.07)	158.72 (8.84)	-16.44 (4.22)	5.8 (8.2)	100.76 (14.35)
R05012-20																				
R05012-26	29.5 (0.29)	14 (0)	1194.44 (259.83)	-1 (0.36)	-1.44 (0.3)	-1.97 (0.25)	4.87 (0.11)	2.39 (0.87)	4.57 (0.4)	53.43 (0.05)	0.35 (7.27)	93.22 (19.02)	14.23 (3.52)	16.69 (2.87)	0.11 (0.02)	-1.18 (0.4)	158.9 (9.26)	-11.82 (5.93)	5.5 (3.33)	81.41 (12.48)
R05012-31																				
R05012-36																				
R931945-2-2*	41.3 (2.19)	13 (0.35)	634.67 (518.2)	-0.5 (0.09)	-1.1 (0.29)	-1.69 (0.24)	6.15 (1.63)	3.82 (1.39)	4.33 (0.69)	56.5 (0.06)	0.38 (6.62)	199.56 (26.29)	36.15 (2.62)	15.06 (2.82)	0.1 (0.02)	-1.07 (0.1)	152.12 (13.24)	-6.03 (7.9)	1.45 (9.72)	94.06 (18.68)
Mean	49.97 (1.8)	13.08 (0.15)	1628.54 (82.87)	-0.84 (0.06)	-1.27 (0.05)	-1.72 (0.04)	6.95 (0.45)	3.82 (0.36)	4.38 (0.09)	60.64 (1.33)	0.49 (0.02)	149.43 (5.29)	34.75 (0.84)	14.66 (0.66)	0.09 (0)	-1 (0.04)	169.89 (2.4)	-2.86 (2)	-0.74 (3.12)	91.51 (4.28)

A_n Carbon assimilation rate (μmol m^{-2} s^{-1}); R_{dark} Dark respiration rate (μmol m^{-2} s^{-1}); g_s Stomatal conductance (mol m^{-2} s^{-1}); *iWUE* Instantaneous water use efficiency (μmol CO_2 mol^{-1} H_2O); $iWUE_{pc}$ *iWUE* attributed to variation in A_n (%); $iWUE_{gs}$ *iWUE* attributed to variation in g_s (%); C_i Sub-stomatal carbon dioxide concentration (ppm); $\Psi_{pre\text{-}dawn}$ and Ψ_{midday} leaf water potenial (MPa); Ψ_{stem} Stem water potential at midday (MPa); *LW* Leaf width (cm); *LL* Leaf length (cm); *LT* Leaf thickness (mm); *PH* Plant height (cm); *LN* Number of leaves; *SPAD* Relative Chlorophyll content based on special products analysis division; *TLA* Total leaf area (cm^2); *LA* Average leaf area (cm^2); K_{plant} Plant hydraulic conductivity (mmol m^{-2} s^{-1} MPa^{-1}); K_{leaf} Leaf hydraulic conductivity (mmol m^{-2} s^{-1} MPa^{-1}).

Chapter 5

GENERAL DISCUSSION

5.1 BACKGROUND AND AIMS

Rising global population combined with global climate change pose serious challenges on agricultural production worldwide. Most of future increases in the world population will occur in tropical and sub-tropical regions, especially in Africa (Borrell, Mullet, *et al.*, 2014). These regions will likely experience the most erratic and unpredictable weather extremes, such as droughts, high temperatures and changing rainfall patterns, fuelled by anthropogenic climate change, leading to agricultural losses (Rippke *et al.*, 2016). Nonetheless, C_4 crops were domesticated and are widely cultivated in these mid-latitude regions where they are expected to have higher advantages over C_3 cereals (Lobell *et al.*, 2008; Battisti and Naylor, 2009).

For generations, crop breeding has been centred around increasing yield and productivity (Boyer, 1982; Duvick, 2005), which may compromise crop resilience to abiotic stresses (Claeys and Inzé, 2013; Dolferus, 2014). One of the key targets to increase crop production is to find varieties with better water conservation traits that maximize the use of available water (Sinclair, 2018). Water use efficiency (*WUE*) describes the efficiency of biomass production per unit water transpired. At the leaf level, *WUE* is expressed as the ratio of CO_2 assimilation (A_n) to transpiration rates. This term, depends on the leaf-to-air vapour pressure deficit (VPD), which in turn, depends on temperature and relative humidity. A more appropriate term, that is independent of the environment and more connected to genotypic variation, is intrinsic *WUE* (*iWUE*), which is calculated as the ratio of A_n to stomatal conductance to water vapour (g_s). Breeding for high *iWUE* has been challenging because it is a physiologically complex trait with potential trade-offs, and in many cases, pleiotropic effects, which may cancel out some of the expected benefits of improved *iWUE* (Flexas, 2016). Furthermore, not many easily measured, heritable traits that determine *iWUE* have been identified, especially in C_4 crops, such as Sorghum. Sorghum is a key crop in the tropical and sub-tropical areas likely to experience marked climate change. C_4 crops already have high *iWUE* because of their carbon concentrating mechanism (CCM), and mechanisms to increase their *iWUE* are even more restricted.

This thesis builds on the recent discovery that leaf width has a close association with g_s and *iWUE* in C_4 grasses (Cano *et al.*, 2019). The aim of the first experimental chapter

(Chapter 2) was to elucidate the anatomical arrangements of narrow and wide leaves, and how that equips them to regulate *iWUE*. These mechanisms were explored in Sorghum genotypes presenting a large range of leaf width and growing under different temperatures. Chapter 3 aimed to build on findings reported in the previous chapter and explore the effects of diurnal and transient variations in light intensity. Crops experience changes in light levels during the day (diurnal, sun flecks) that can determine photosynthesis and transpiration levels, and hence impact *iWUE* and whole plant *WUE*. The last experimental chapter 4 was part of a larger study aimed at exploring the effect of Aquaporin protein diversity on leaf conductances (hydraulic, stomatal, mesophyll) and *iWUE* from a Nested Association Mapping (NAM) Sorghum population under well-watered and water stress conditions. Due to time constraints and delays caused by the pandemic outbreak, only the initial screen for gas exchange variables and relationships with plant hydraulics were reported in Chapter 4. Even so, the large data set allowed me to determine the level of genetic variation and heritability of some key crop traits under different watering regimes. The overall hypotheses of my thesis included:

1) Narrow leaves will have higher *iWUE* due to the coordination between stomatal and vascular anatomical traits;
2) Stomatal anatomical features will influence how diurnal and short-term variations in light intensity control *iWUE*; and
3) Water stress will impact the trade-offs between A_n, g_s and *iWUE*.

Here, I synthesise the general findings of my thesis and discuss them in relation to different environmental and agronomic conditions, I also suggest possible paths to carry this line of research forward.

5.2 LEAF WATER USE EFFICIENCY: SOURCES OF VARIABILITY

Leaf water use efficiency is estimated as the ratio of CO_2 assimilation per transpiration rate. To eliminate the environmental factors that control transpiration and to elucidate genetic determinants of *WUE*, the term *iWUE* is used here, where g_s is taken to represent the rate of water loss from the leaf (Osmond *et al.*, 1980). Hence, the relationship between A_n and g_s, is key in determining *iWUE*. CO_2 diffuses into the leaf through the stomatal pore, and the resistance to diffusion through the stomatal pore is one of the key determinants of sub-stomatal CO_2 concentration, also called intercellular CO_2 concentration (C_i), which is lower than ambient [CO_2] because of this resistance (Farquhar and Sharkey, 1982). The C_i pool is ultimately what is available for the mesophyll to drawdown and sustain photosynthesis. In C_3 plants, A_n is mostly Rubisco-limited at low C_i, and by the rate of RuBP regeneration at higher C_i (Farquhar *et al.*, 1980). In C_4 photosynthesis, the limiting factors are more complex due to the CO_2 concentrating mechanism (CCM) that operates in between two parenchyma cells. The first carboxylation by PEPC in the mesophyll cells constitutes the main limitation of the initial A_n-C_i slope at low C_i, while the CO_2-saturated photosynthesis rate depends on Rubisco activity, RuBP or PEP regeneration (von Caemmerer, 2021). Hence, there is a tight link between g_s and A_n that is partly mediated by C_i. At low C_i, increased g_s strongly stimulates A_n, but when approaching the CO_2 saturated phase, the advantage of higher g_s is diminished in terms of carbon gain, resulting in the often observed curvilinear and asymptotic relationship between A_n and g_s when comparing different species or growth condition (Ghannoum, 2009).

Since *iWUE* is the ratio of A_n to g_s, it reflects changes in both A_n and g_s depending on where the operational A_n and g_s are located along the A_n-C_i curve (Ghannoum, 2016). When A_n is close to CO_2-saturation, reducing g_s results in higher *iWUE,* although at the expense of slight reduction in A_n (moving from point 1 (G1) to 2 (G2) in **Fig.5.1**). However, by increasing photosynthetic capacity of the leaf for the same g_s, *iWUE* would be improved and the operating C_i would be lower (comparing G1 and G3). The combination of both strategies would maximize *iWUE* without penalising A_n (compare point 4 with 1). In other words, under optimum conditions, the genotype situated around the inflexion point of the A_n-C_i curve would have the best balance between A_n and *iWUE*. Another way of looking at *iWUE* is as a ratio between the two controls on C_i (C_i supply, g_s, and C_i utilisation, A_n), positioning the operational C_i as one of the most physiologically grounded parameters

available that can be related to *iWUE* (Ghannoum, 2016). The question then becomes how do we separate the different controls of A_n and g_s on C_i and *iWUE*?

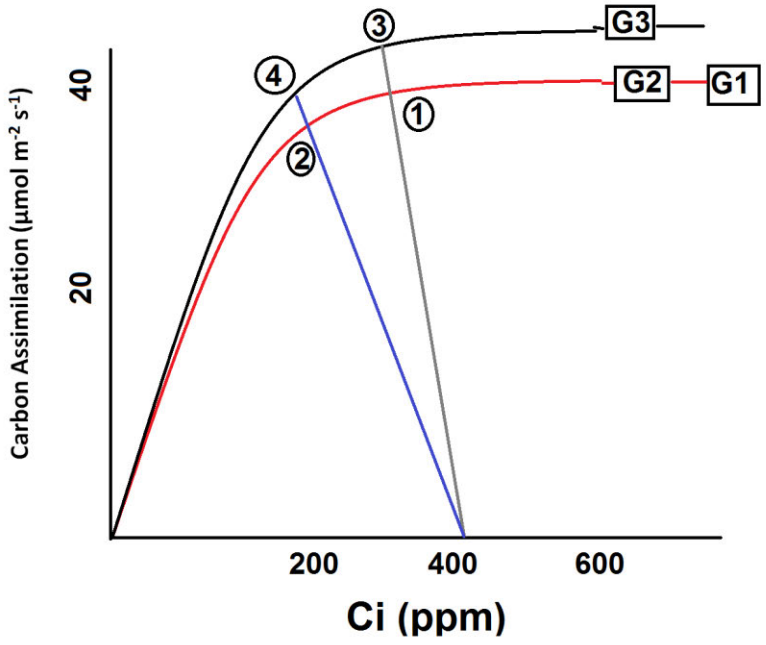

Fig.5.1 A_n-C_i curves for three hypothetical genotypes (G1-G3) and two situations well-watered (g_s^W) or drought (g_s^D) (Ghannoum, 2016).

When operational C_i is not limiting, genotypic differences in *iWUE* most likely reflect different controls on water loss through the stomatal pore that result in high *iWUE*. Chapters 2 and 3 investigated the stomatal features which impart the greatest control on g_s and *iWUE* in Sorghum. Water deficit may induce additional stomatal closure to save water and avoid leaf desiccation, which may affect the roles of A_n and g_s on *iWUE*. For genotypes with high *iWUE* and low operational C_i, that hover close to the inflexion point, water stress will reduce A_n more than in genotypes with high operational C_i and low *iWUE* under well-watered conditions. This is indeed one of the conclusions of Chapter 4, where obtaining a range of g_s values as a result of the water stress (WS) treatment changed the dependence of *iWUE* from mainly on g_s (Chapters 2 and 3) to a co-dependence on A_n and g_s mediated through C_i (moving from the plateau part of the A_n-g_s curve under well-watered (WW) conditions to the linear part under WS; see **Fig.4.8**, **Fig.4.10** and **Fig.4.11**). These observations highlight the important contribution of environmental

conditions in determining *iWUE*. The results also showed that changes in C_i (under mild to moderate WS) in C_4 plants were due to stomatal closure (Ghannoum, 2009). and that g_s was the main determinant of A_n as both C_i and A_n decreased with reduced g_s (Farquhar and Sharkey, 1982).

The overall dominance of g_s control on *iWUE* observed in this thesis aligns with previous studies on C_4 grasses under WW conditions (Cano *et al.*, 2019). Since chapters 2 and 3 were more concerned with anatomical and mechanistic controls on *iWUE*, I combined the gas exchange data from chapters 2 and 3 to contextualize the findings of this thesis (**Fig.5.2**). How do Sorghum genotypes regulate *iWUE* under WW conditions? Mainly through changing g_s. The combination of different conditions for these measurements (growth temperatures, diurnal, genotypes) yielded a similar range of g_s and A_n values as reported in chapter 4, again showing a curvilinear relationship (**Fig.5.2 a**). Interestingly, the *iWUE*-g_s relationship (**Fig.5.2 c**), showed a different slope for the two datasets, probably due to the different light intensities used during measurements, but the *iWUE*-C_i (**Fig.5.2 d**) relationship was common for the two datasets (both were measured at ambient [CO_2]).

This confirms what was mentioned earlier about C_i being a robust predictor of *iWUE* when leaves are exposed to similar CO_2 concentrations, as it integrates the contributions of A_n and g_s. While the performance of *iWUE* partitioning analysis (Gilbert *et al.*, 2011; Li *et al.*, 2017) is feasible for this combined data set, it was not within the aims (and time limits) of those specific chapters and is a possible future goal. Nevertheless, the combined data clearly show the strong stomatal influence on A_n, C_i and *iWUE* (**Fig.5.2 a**). But what determines g_s?

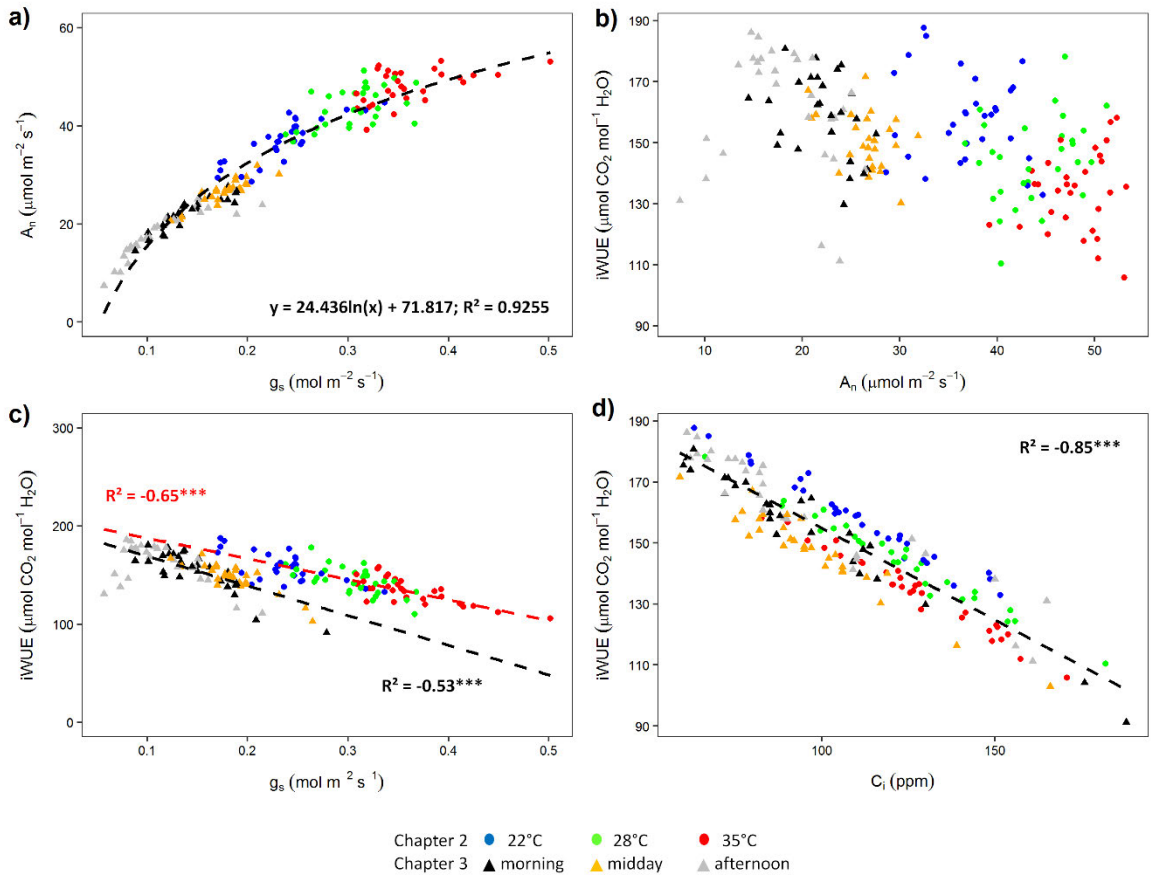

Fig.5.2 The relationship between leaf gas exchange parameters for the combined data sets of chapters 2 and 3 of this thesis. Data points represent individual replicates. Measurements were obtained from the youngest fully expanded leaf under maximum growth irradiance (2000 µmols m^{-2} s^{-1} for chapter 2 data and 1000 µmols m^{-2} s^{-1} for chapter 3 data). The lines of best fit are presented and the R^2 values are those obtained from Pearson product-moment correlation analyses (except for plot **(a)** where the equation of best bit was reproduced from Microsoft Excel). **(a)** Net carbon assimilation rate (A_n) vs. stomatal conductance (g_s); **(b)** Intrinsic water use efficiency (*iWUE*) vs. A_n; **(c)** *iWUE* vs g_s; **(d)** *iWUE* vs. Sub-stomatal carbon dioxide concentration (C_i).

5.3 STOMATAL CONDUCTANCE AND STOMATAL ANATOMY

Stomatal conductance per area basis (g_s) is determined by the size (*SS*) and number (stomatal density, *SD*) of stomata and its pore aperture (Franks and Beerling, 2009). As described in previous chapters, several studies have shown that manipulating *SS* and *SD* affects g_s and *iWUE* (Doheny-Adams *et al.*, 2012; Franks *et al.*, 2015; Bertolino *et al.*, 2019; Caine *et al.*, 2019; among others). In chapter 2, I found a strong dependence of g_s on *SS*, especially at elevated temperatures (**Fig.2.4**). In chapter 3, this control was much weaker (**Fig.3.3 c, d**), replaced instead by a negative dependence of g_s on *SD* at morning and midday (**Fig.3.3 a,b**). What g_s in both data sets showed is a consistent dependence on the operational aperture (a_{op}) and the percentage of the maximum aperture (a_{max}) that a_{op} represents (*% aperture*) (see **Fig.2.4** and **Fig.3.4**). In a previous study of 48 Sorghum genotypes measured for gas exchange and leaf anatomy under field conditions field (Pan *et al.*, 2021), we found *SD* and *SS* do not co-vary with g_s, but it was *% aperture* and a_{op} that were the main determinants. However, in this study there was some incipient mild water stress and air temperatures were above 40 ºC (Pan *et al.*, 2021). If the ultimate regulation of g_s was due to *% aperture*, it is likely that under irrigation better correlation with its anatomical determinants would be found as seen in chapter 2. Sorghum is a C_4 graminoid species, with dumbbell shaped guard cells and adjacent subsidiary cells. Franks and Farquhar (2007) described how that type of stomata functions with the osmotic pressure in subsidiary cells decreasing and allowing the guard cells to "swell" and displace the subsidiary cell, opening the pore. This mechanism leads to fast stomatal response by C_4 graminoid grasses as the high volume to surface area ratio of the guard-cell-subsidiary-cell complex allows for quick exchange of solutes that change guard cell turgor and hence open or close the pore (Lawson and Matthews, 2020). This mechanical control on the stomatal pore could also enable grasses to have stronger control on g_s opening especially since, in C_4 grasses especially, high A_n does not require relatively large g_s (Malone *et al.*, 1993).

In section 5.2, we established that at high A_n, the impact of g_s on A_n is low, but its impact on *iWUE* is high such that it is the main determinant of *iWUE* variation. Going back to the large dataset from chapter 4 (**Fig.4.8 a**), A_n starts to plateau when g_s reaches somewhere in the range of 0.24-0.26 mol m^{-2} s^{-1}. This means that genotypes that increase g_s further are doing so at a water cost without A_n gain. Stomatal opening after maximizing CO_2

diffusion has no photosynthetic advantage and hence it follows that some genotypes (or species in general) would develop to minimize excess transpiration through the stomata after A_n starts to plateau, which constitutes the basis for the optimality theory of carbon assimilation by unit of water loss (Cowan and Farquhar, 1977). Indeed, looking at **Fig.5.2**, the maximum A_n values are achieved during the two high temperature treatments, when g_s exceeds 0.25 mol m^{-2} s^{-1}, where the demand for transpiration was larger (**Fig.5.4 a**). To explore this further some of the anatomical data of chapters 2 and 3 were combined (**Fig.5.3**). Under limited evaporative demand (and with water availability), it is likely that *SS* does not confer an advantage to speedy graminoid stomata, at least within Sorghum genotypes. Indeed, in **Fig.5.4**, leaf-to-air vapour pressure deficit (VPD_L; based on leaf temperature measured using the thermocouples touching the transpiring leaf in the LI-6400XT chamber) was plotted against g_s (**Fig.5.4 a**), showing the positive association between g_s and VPD_L. What **Fig.5.3 b** shows is the line of best fit between *SS* and g_s for VPD_L higher than 2 kPa, where it is significantly positive (r=0.46, p<0.001). Higher g_s at higher VPD can be explained by the role of leaf transpiration as an effective way to regulate leaf temperature (Gates, 1968; Jarvis and McNaughton, 1986). There is a possibility that higher g_s at higher temperatures can be a mechanism to supply CO_2 for the higher rate of C_4 photosynthesis stimulated under high temperature. However, the key point here is that *LW* and g_s are related, while *LW* and A_n are not. Variation in *LW* drives higher g_s because of the boundary layer effects and both g_s and *LW* respond to temperature. Hence, at high VPD, due to temperature, changes in g_s and A_n are not necessarily related, especially since g_s already is operating at maximum (see **Fig.5.2 a**). Increase in g_s to thermoregulate and offset BL effect due to *LW* does lead to higher A_n (via higher CO_2 supply) but ultimately *iWUE* still decreases because g_s increases beyond any level required for maximum A_n under those conditions.

I also need to highlight that the g_s response to VPD can be a temporary due to g_s dependence on leaf water status, as often seen in stomatal response to humidity (Buckley, 2005). This "Iwanoff" effect, shows wrong-way response by g_s when humidity decreases (high VPD), but also can be imposed with perturbation in leaf or plant water status, as Comstock and Mencuccini (1998) show. Most studies measure g_s under constant conditions and with standardized humidity, which means that 1) these perturbations are

not captured in the data but 2) that measured g_s can be attributed to other factors like we do here, as the purpose of those measurements is to capture steady-state g_s.

While the close association of the subsidiary-guard cell complex in graminoid species leads to a more active control on the stomatal pore, the large size of the complex compared to other angiosperms means that guard cells need greater displacement of subsidiary cells to open the stomata (Franks and Farquhar, 2007). In this thesis and in the study of Pan *et al.*, Sorghum *% aperture* was, among most genotypes, around 10%, highlighting the substantial physiological constraint on large pore apertures (compared to *SS*). This percentage of operational pore (and with it lower operational g_s) was much lower than that of other angiosperm species (Franks *et al.*, 2014). Ultimately, species like Sorghum have struck a balance between g_s just high enough to sustain photosynthesis, and fast kinetic responses (see below).

Two final points on the variation in stomatal anatomy discussed above: 1) As chapter 2, and references within, highlighted, changes in stomatal anatomy are linked to changes in other anatomical features (e.g., vascular), and I will touch on that when discussing leaf width below. Those anatomical changes work to facilitate more efficient gas exchange through the stomatal pore. 2) Finding stomatal traits that are linked to higher *iWUE* in Sorghum is promising as stomatal traits have been shown to be highly heritable (Liang *et al.*, 1975), and because scientists have been struggling to find significant variation in *WUE* or traits that benefit higher *WUE* in Sorghum (see Section 5.7). Because of the high photosynthetic capacity of Sorghum, manipulating g_s to achieve high *iWUE* is an achievable goal, especially with the wealth of genetic stomatal targets already elucidated that have been shown to increase *iWUE* (see Table 1 in Leakey *et al.* (2019)).

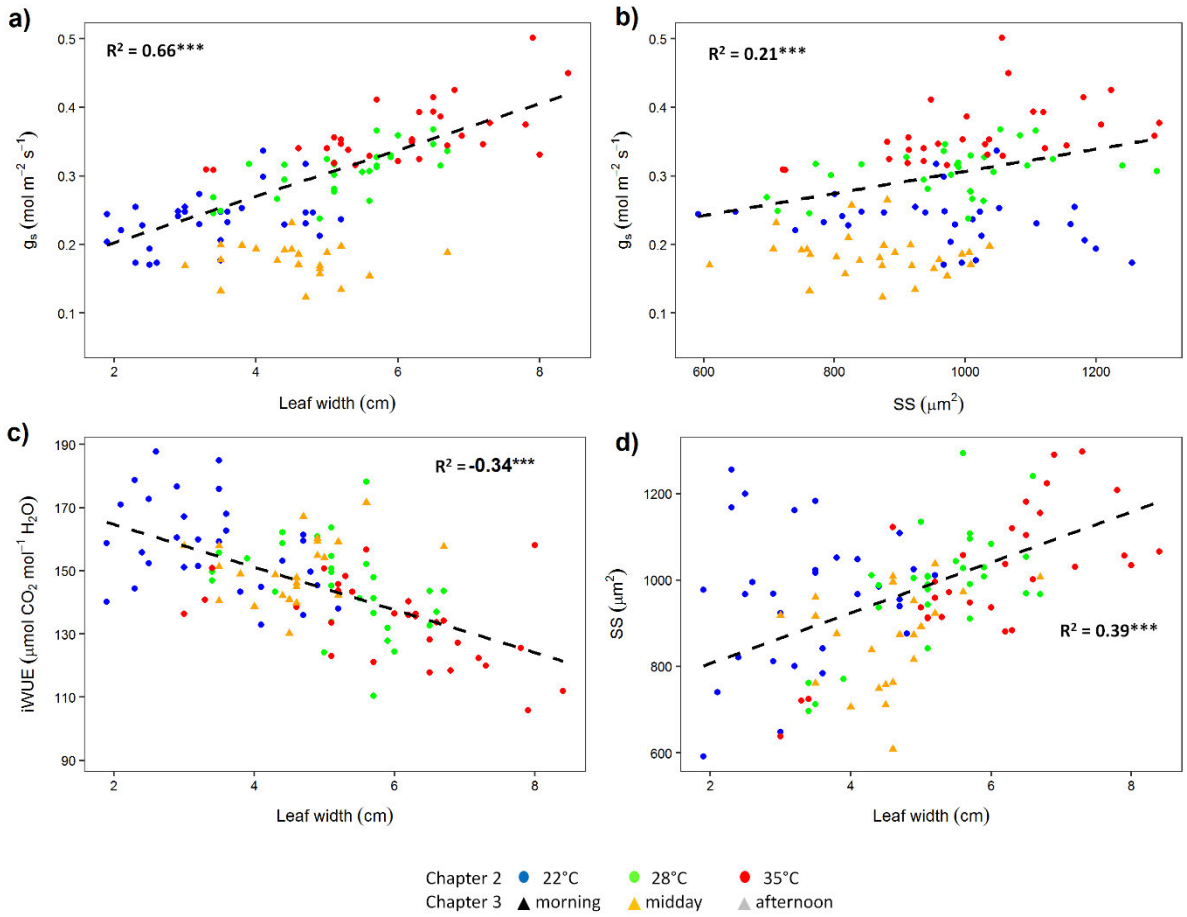

Fig.5.3 The relationship between stomatal conductance (g_s) and some of its anatomical determinants for the combined data sets of chapters 2 and 3 of this thesis. Data points represent individual replicates. Gas exchange measurements were obtained from the youngest fully expanded leaf under maximum growth irradiance (2000 µmols m^{-2} s^{-1} for chapter 2 data and 1000 µmols m^{-2} s^{-1} for chapter 3 data). Leaf width and stomatal anatomy measurements were taken from the same leaf and from the same location on the leaf as where gas exchange was measured (middle of the leaf). The lines of best fit are presented and the R^2 values are those obtained from Pearson product-moment correlation analyses. The lines of best fit represented only considered values under leaf level VPD (VPD_L) of high than 2 kPA for plots (b) and (d). **(a)** g_s vs Leaf width; **(b)** g_s vs. Stomatal size *(SS)*; **(c)** intrinsic water use efficiency vs. Leaf width **(d)** *SS* vs Leaf width. (NB: only midday g_s data is included from chapter 3 as it was midday leaves that were sampled for stomatal anatomy and there was g_s vs *SS* relationship observed there).

5.4 LEAF WIDTH AND LEAF ANATOMY

In C_4 monocots, signals during vein development determine stomatal production to files alongside the veins (McKown and Bergmann, 2018). Hence, determination of SS and SD is ultimately linked to leaf development. In chapter 2, increasing growth temperature stimulated an increase in cell expansion and cell size. This allowed us to discover the associations between different anatomical determinants of C_4 photosynthesis. Genotypes with narrow leaves (smaller leaf size and less cell expansion), had smaller stomata, mesophyll and bundle sheath cells, and were thinner, with smaller sub-stomatal airspaces and shorter path lengths for gaseous exchange, while wider leaves had the opposite arrangement. The densely packed arrangement of narrow leaves is thought to enable capture of CO_2 leaking from the bundle sheath and hence maintaining high A_n at lower g_s than in wider leaves (Dengler *et al.*, 1994). Increased A_n in chapter 2 was most likely associated with increasing temperature, but the anatomical arrangement of narrow leaves enabled those leaves to reduce g_s and transpiration, and combined with the possible improvement in capturing leaked CO_2 means that narrow leaves would achieve high *iWUE* (**Fig.5.3 c**) by reducing g_s (**Fig.5.3 a**) without sacrificing A_n. Interestingly, in **Fig.5.2 d**, the combined data of chapters 2 and 3 regarding *LW* and *SS* showed a positive association for VPD_L higher than 2 kPa. This highlights that these anatomical controls were more important during periods of high evaporative demand (midday) or in environments that elicit high evaporative demand (higher growth temperatures). This shows that the stomatal anatomical control on g_s explained in section 5.3, relied upon a coordinated anatomical arrangement that equips the leaf to control transpiration rates under high VPD (**Fig.5.4 b**).

Most C_4 grasses, including Sorghum ancestor, dominate grasslands and savannahs in the warm and dry climates close to the equator (Edwards *et al.*, 2010). Furthermore, weather conditions have strongly influenced leaf width (*LW*) in those C_4 species (Liu *et al.*, 2012). Ancient selection for sorghum varieties during early domestication involved selection for smaller plants that are better at combatting drought, and varieties with larger leaves when water was not limited and air evaporative demand low (Dillon *et al.*, 2007). Leaf width (and leaf area) are strong genetic determinants in Sorghum, as confirmed with high heritability estimated by Liang *et al.* (1973). Also, *LW* can be easily screened for. Ultimately, this means that there is the possibility of breeding for *LW* that could enable

us to achieve higher *iWUE*. Furthermore, narrower leaves would allow more light to penetrate through the canopy possibly increasing radiation use efficiency as more leaves would be exposed to light (Cano *et al.*, 2019). Narrow (and thin) leaves would also have thinner boundary layers, enabling faster gas and heat exchange with the environment, and hence wide leaves would require a higher stomatal aperture to maintain leaf temperature under safe values, especially when radiation is high and wind speed low, reducing *iWUE* (Gates, 1968; Jarvis and McNaughton, 1986; Pan *et al.*, 2021). Over a canopy, having narrow leaves can increase plant and field level *WUE*. On the other hand, Blum (2009) suggested that less canopy shading (for example, due to smaller total leaf area because of narrow leaves) would expose the soil to radiation and increase soil evaporation, reducing the amount of available water. However, given that narrow leaves are usually shorter, an increase in plant density would shade soil and reduce soil evaporation and control of weeds.

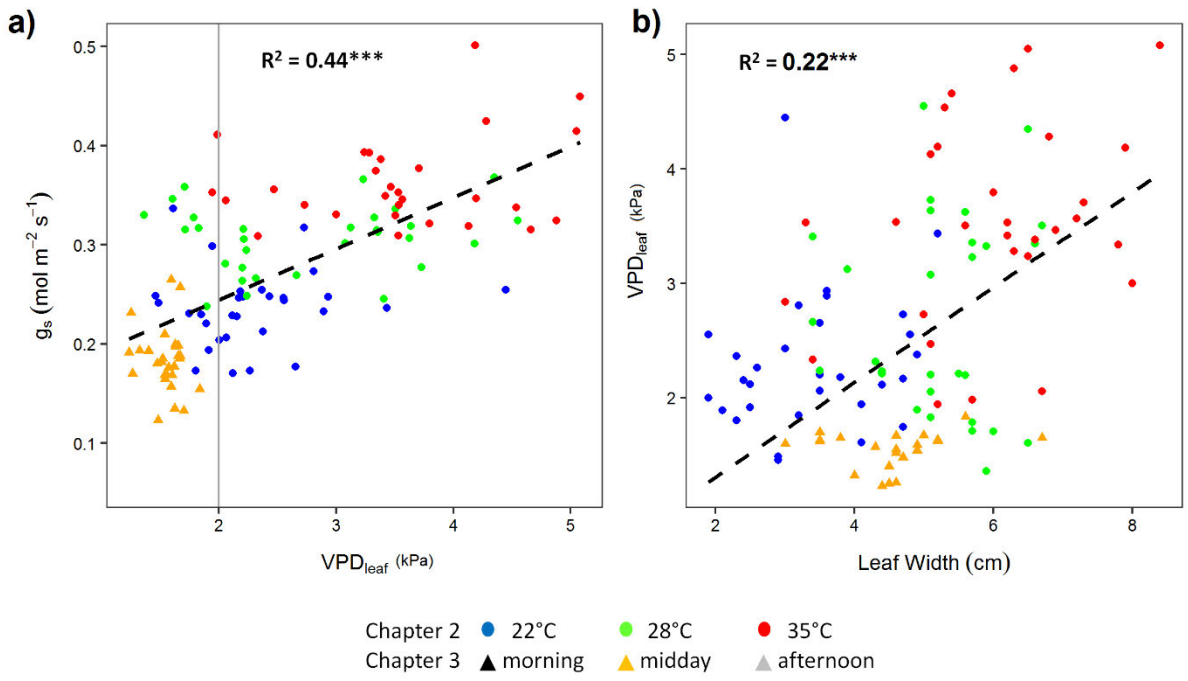

Fig.5.4 The relationship between stomatal conductance (g_s) and leaf width with leaf level vapour pressure deficit (VPD_L). VPD_L was estimated from leaf temperature data measured via the thermocouple touching the leaf abaxial side inside the LI-6400XT (LiCor Biosciences, Lincoln, Nebraska) chamber. Data points represent individual replicates. (a) g_s vs VPD_L; (b) VPD_L vs leaf width. (NB: only midday data is included from chapter 3 as it was midday leaves that were sampled for leaf width).

5.5 TEMPORAL VARIATION IN *iWUE*: DYNAMIC *iWUE*?

Leaves independently regulate transpiration (and photosynthesis) in response to environmental changes (Matthews *et al.*, 2017). Over the day, there is significant change in climatic conditions, whether transient such as passing clouds or changing wind speed, or more predictable such as photoperiod and diurnal VPD fluctuations. Changes in A_n and g_s across the day are strongly influenced by those changes, especially light (Pearcy and Way, 2012), and with Sorghum domestication involving significant selection for photoperiod (Dillon *et al.*, 2007), it is likely that circadian regulation is very strong in determining gas exchange patterns and hence *iWUE* (Resco de Dios and Gessler, 2018). "Single" measurements of gas exchange would only represent a time specific representation of *iWUE*. What stimulated the design of chapter 3 further is the recent surge in research highlighting the importance of stomatal kinetic response to changes in light, and the possibility of those responses scaling up to determine stomatal diurnal response (Vialet-Chabrand *et al.*, 2013, 2016; Moualeu-Ngangue *et al.*, 2016; Matthews *et al.*, 2017). This is important for the aims of this thesis in two ways. First, stomatal responses to change in light are orders of magnitude slower than those of the photosynthetic apparatus (Lawson and Blatt, 2014). Hence, slow stomatal opening can impede full photosynthetic gain when radiation increases because of stomatal limit on CO_2 diffusion. Conversely, when light changes from high to low, slow stomatal closing can cause excess transpiration (as coined by Deans *et al.* (2019)) without any gain as photosynthesis is immediately reduced. This weak synchronization between A_n and g_s determines the rate of carbon gain for water loss over the day, mirroring the ratio of A_n to g_s that determines instantaneous *iWUE*. *WUE* in Sorghum has been generally measured at the whole-plant level (Hammer *et al.*, 1997; Balota *et al.*, 2008; Vadez, 2019), yielding limited genetic variability (Vadez, 2019 and references within). Hence, it is of interest to find possible indicators that can be scaled to longer timescales or are at least linked to integrated *WUE*, such as the differential correlation between morning and afternoon g_s in determining diurnal *WUE* (*dWUE*) (**Fig.3.2 b** and **Table 3.S1**). Furthermore, a link between a faster rate of stomatal closure (k_{cl}) and higher *dWUE* was also found in chapter 3 (**Table 3.S1**), directly associating efficient water conservation over a transient change in light with diurnally integrated *iWUE*. At least for morning and midday measurements

(see **Fig.3.2**, **Fig.3.4** and **Fig.3.5**), there is an association between lower g_s, faster stomatal closing and high *iWUE* at different scales.

The second reason why this research is important is that a number of recent studies reported a close association between smaller stomata and faster stomatal response to light (Drake *et al.*, 2013; McAusland *et al.*, 2016; Faralli *et al.*, 2019). This could pave the way for finding genetic determinants that are associated with *iWUE* not just at steady state levels, but during transient environmental changes. In chapter 3, a_{op} and *% aperture* were the main determinants of g_s and k_{cl}. This means that genotypes that maintained a smaller stomatal pore relative to the maximum anatomical pore, i.e. displaying a low transpiration and high water conservation strategy, were more likely to exhibit faster stomatal closing when conditions became unfavourable, restricting unnecessary water loss. This coincides with my earlier discussion regarding aperture kinetics being the determinant of g_s under low g_s or mild evaporative conditions, such as the ones applied during the experiment for chapter 3. However, there was an influence observed on k_{cl} by *SD* (**Fig.3.6 a**). This was slightly surprising as *SS* is thought to influence stomatal kinetics more than *SD* (see section **3.5**). However, it does indicate a possible anatomical and genetic link between all those gas exchange related variables (there was a negative association between g_{smax} and k_{cl}, further indicating a possible anatomical control on k_{cl} beyond *SS*, as g_{smax} incorporates *SD* as well as pore depth and maximum aperture).

I attempted to relate diurnal variation in gas exchange with changes in sugar content in chapter 3. This is because soluble sugar concentrations are linked to stomatal function (Flütsch and Santelia, 2021), and sugars being a key photo-assimilate of photosynthesis that has been theorized to have a diurnal and feedback influence on A_n (Henry *et al.*, 2020). Nothing conclusive was found, but the author aims to carry analysis of starch content on samples from chapter 3 to further investigate this link, as starch has been more closely linked with stomatal function (Lawson and Matthews, 2020). Several possible avenues of research can be investigated here that might shed light on diurnal variation in gas exchange rates and *iWUE*, including aquaporin expression at different diurnal time periods (Groszmann *et al.*, 2017), hydraulic changes (Mencuccini *et al.*, 2000; Bucci *et al.*, 2003) or clock related mechanisms (Haydon *et al.*, 2013; Resco de Dios, 2017).

5.6 WATER STRESS & OTHER ENVIRONMENTAL FACTORS: IS *iWUE* EVEN GOOD?

Above I discussed *iWUE* in Sorghum at different temporal scales and in response to transient changes in the environment. Under field conditions, growth conditions are usually variable on annual basis and along the growing season, and with the impact of climate change this variability will likely be more extreme (Challinor *et al.*, 2014). It is not advisable to select for traits that only maximise *iWUE*. Whether a decrease in g_s, where A_n might be sacrificed and hence productivity, or through a combined increase of A_n and g_s which requires high soil water availability. As discussed in chapter 2, while having low g_s under high growth temperatures improves *iWUE*, this is because of several anatomical adaptations that enable it to thermo-regulate more effectively. Under temperatures higher than 35°C (the hot treatment in chapter 2), which Sorghum does experience in the field, will the anatomical constrain on low g_s in the high *iWUE* genotypes enable them to achieve evaporative cooling effectively? For the plants grown in chapter 3 that exhibit smaller aperture and quick closing response, would that rapidity help under extreme heat if g_s decreases quickly when a cloud passes reducing transpirative cooling?

In chapter 2, the availability of water allowed genotypes with bigger *SS* and higher g_s to maintain A_n via high transpiration rates. This brings up several issues. Under higher temperatures, there is a risk of an increased transpiration irrespective of changes in g_s as the VPD_L increases. This can complicate selection for determinants of g_s. For example, when selecting for higher *iWUE*, this advantage might be lost under a certain VPD threshold. Additionally, selecting for a trait that is beneficial under a certain set of conditions ignores temporal change in environmental conditions, and the importance of genotypic characteristics under different environments. To follow the example from chapter 2, small *SS* is beneficial for high *iWUE* under increasing temperatures (and VPD). But if conditions change to mild temperatures, would restricting *SS* lead to a constraint on A_n and productivity due to a decrease in C_i? Or would an onset of water stress cause small *SS* genotypes to restrict g_s even further, sacrificing potential yield and productivity? For rainfed crops like Sorghum, is a genotype with low *SS* best suited to make use of a rainfall event that increases soil moisture and reduces temperatures and VPD? A genotype with "medium-range" *SS*, that regulates g_s mainly through a_{op} and *% aperture* (as discussed above), might be more beneficial for different conditions.

In the context of *iWUE*, this interaction between the genetic and phenotypic traits and environmental conditions is probably most pronounced under water limitation. Sorghum, as well as other crops, has been bred under drought conditions based on grain yield (Dillon *et al.*, 2007; Tardieu *et al.*, 2018). Sorghum is a grain crop, and hence the main target for producing water efficient Sorghum is to combine a crop that is fit by the stage of grain filling, combined with soil water availability at that stage to facilitate production of sugars and efficient grain filling and production. Even under WW conditions, the importance of *iWUE* has been questioned (Condon *et al.*, 2004; Blum, 2009), as reduced transpiration and water use, as expressed in the Passioura (1977) formulation, can lead to reductions in yield. However, as discussed earlier, this discount seasonal changes in water availability and weather conditions. One of the arguments for selecting for high *iWUE* under drought is the need for new mechanisms of water conservation (Sinclair, 2018) to make sure those grain yielding traits remain and are functional (as selection for higher yield has already been accomplished in Sorghum) (George-Jaeggli *et al.*, 2017). Because guard cells (in angiosperms at least) are regulated by changes in their osmotic pressure in relation to leaf water status (Buckley, 2005), changes in soil moisture, and hence along the soil-to-leaf hydraulic track, are sensed by the stomata. The nature of guard cell signalling mechanism in terms of water status are still debated (see Buckley (2019) for a recent review) and are beyond the focus of this chapter. What matters in terms of *iWUE* is that the stomatal pore is reduced in response to a decrease in soil moisture to reduce transpiration, as observed in Sorghum as well (Gholipoor *et al.*, 2010, 2012; Tingting *et al.*, 2010; Sutka *et al.*, 2016). This is indeed what was observed in chapter 4 (**Fig.4.5 b**). Our study in chapter 4 measured g_s (and A_n and *iWUE*) after the onset of moderate drought and plant acclimation to it. While genotypes that reduced g_s had higher *iWUE*, this came at the expense of reduced A_n due to reduced C_i (**Fig.4.7**). Also, genotypes with higher *iWUE* under drought also had more negative water potentials, signalling a more stressed leaf. So, is breeding for high *iWUE* under drought useful?

We must remind ourselves that the main driver for all this research is the maintenance and increase of crop production. And high transpiration rates / water use are a key component of maintaining production via accumulating biomass (Blum, 2009; Sinclair, 2018). Some of the mechanisms suggested to combat water stress irrespective of WUE

and controls on transpiration include reducing leaf permeability (the smaller fluxes between the leaf and atmosphere are usually ignored in gas exchange calculation, although small in Sorghum because of its thick cuticle), synchronizing growth stages with water availability, selecting for genotypes that senesce older unproductive leaves and to minimise soil evaporation (Blum, 2009). However, climate change and erratic weather makes synchronizing growth stages harder. Also, maintaining young transpiring leaves or minimising soil evaporation assumes that even during drought events, crops are in deep soils that allow deep root development and access to extra soil moisture, but what if the soil is shallow or the crop does not have the capacity for deep rooting? In such a case, controlling transpiration might be imperative for plant survival, but with a yield penalty.

Sinclair (2018) raises another issue. Genotypes with high *iWUE* due to low g_s and hydraulic conductance (as shown in **Fig.4.9**) would likely forego more soil moisture as their stomata start closing at higher soil moisture content (a mechanism seen in some Sorghum genotypes (Gholipoor *et al.*, 2012)). However, this water conservation strategy would lead to more available water during the reproductive stage, which is the key one for Sorghum (Sinclair, 2018). Of course, this is dependent on soil ability to keep water and not lose it to drainage, and this important aspect of field management would ultimately hover over all the physiological mechanisms described here. Ultimately, water stress results from the supply of water failing to meet crop demand (Tardieu *et al.*, 2018; Leakey *et al.*, 2019), but success of Sorghum under drought conditions is linked to water availability during grain-filling, facilitated mainly by pre-anthesis reduction in water use (Vadez, 2019), so Sorghum's demand might be met by water conservation until reproduction. The key question becomes, is the gain in soil water conservation (through high *iWUE*) more beneficial than loss of productivity early in the season (Sinclair, 2018)? Stay-green Sorghum genotypes, that fill grains for longer periods, were found to minimize water use during the vegetative stage via reducing leaf size and reduced tillering, leading to more grain yield (Borrell, Mullet, *et al.*, 2014; Borrell, van Oosterom, *et al.*, 2014). These traits are associated with higher *iWUE*, and highlight the importance of taking *iWUE* (and associated physiology) as a key crop trait, especially in Sorghum.

5.7 BREEDING FOR *iWUE* IN SORGHUM

Selection based on physiological traits has had little contribution to crop breeding under different conditions (Tardieu *et al.*, 2018). Indeed, as elaborated above, most physiological traits that are positive in a given environment, would have an undesired impact in a different environment (Tardieu *et al.*, 2018). Hence, success in breeding for high *iWUE* is hugely dependent on the understanding of *iWUE* dynamics under the target environment and predicting the effect of high *iWUE* on other adaptive traits of that environment. Higher *iWUE* must not come at the expense of reduced water use because higher *iWUE* means reduced transpiration and water uptake. Of course, reduced water use would mean a lessened ability to assimilate and/or partition carbon into consumable sugars during seed formation, so "water use" in this context is a proxy for plant productive capacity, as lesser water use means lesser productivity. Benefits of reduced water loss can be crop-specific, as in the case of Sorghum reducing water use until grain filling can be beneficial. But this needs to account for environmental variability. For example, Sorghum is mainly cultivated in dry and warm environments, and any breeding for *iWUE* will have to consider the trade-offs with these types of environments. Combining field trials (with environment specific conditions), simulation modelling and several different alleles at once during screening trials is a daunting task, but it is the most straightforward way to highlight possible trade-offs and how to reconcile them (Tardieu *et al.*, 2018).

Within the findings of this thesis, the high heritability of *LW* (**Table 4.2**) and stomatal features (Liang *et al.*, 1975) means that they could be used in breeding programs. Other key parameters explored in this thesis that are beneficial could be high vein density (*VD*) and faster k_{cl}. We established how narrow leaves achieve high *iWUE*. What was also found in chapter 2 is that *VD* and *LW* are negatively linked (**Fig.2.5 a**). This can suggest a higher hydraulic conductance for narrow leaves, but higher hydraulic conductance is linked to higher transpiration in Sorghum (Choudhary *et al.*, 2013; Choudhary and Sinclair, 2014; Chapter 4), the opposite of what narrow leaves are associated with. However, what high *VD* could be providing is not just high conductivity values, which are ultimately linked to transpirational flux (Sack and Holbrook, 2006), but in concert with stomata, maintain a constant homeostasis by efficiently reaching all the sub-stomatal cavities and maintaining effective supply of water to the stomata (Fiorin *et al.*, 2016). The other

anatomical features of narrow leaves explained in chapter 2 (lower airspace cavity size, smaller cell sizes) could help in constraining transpiration rate as a whole, while the high *VD* helps maintain a constant transpiration rate to keep photosynthesis functional, and together yielding higher *iWUE*. This phenotype would be very beneficial under high VPD or temperature to maintain leaf cooling. Also, smaller leaves with high *VD* have been shown to be less vulnerable to hydraulic failure during drought (Scoffoni *et al.*, 2011; Nardini *et al.*, 2012). Faster stomatal closure in response to low irradiance suggests a water conserving leaf, which under drought might lead to excessive stomatal closure. While this can increase *iWUE*, it can have repercussions for productivity and maintain growth. But as mentioned, high *VD* can enable drought tolerance and hence prevent excessive stomatal closure. On the other hand, because of the link between k_{cl} and stomatal pore features, it is possible to find a genotype that maintains moderate levels of g_s to extract maximum productivity (close to inflexion of A_n-C_i curve), but also able to close its stomata quickly under photosynthetically unfavourable conditions, hence maximizing its temporally *integrated iWUE* under water deficit conditions. This is especially feasible in graminoid species that control their stomatal pore due to the shape and architecture of their guard cells and association with subsidiary cells as opposed to strictly the size of the stomatal complex (Franks and Farquhar, 2007). Hence, it might be possible to breed for a high g_s and fast k_{cl} genotype, but again, this is environment dependant. The key point here is that such a stomatal phenotype could be one located around the inflexion point of the A_n-g_s curve, where *SS* and a_{op} are still on the smaller side, but still with g_s values high enough to bring A_n close to saturation. It is exactly this kind of delicate balancing of traits that determine A_n and g_s that can bring the most benefit out of high *iWUE* varieties.

To sum up (within the set of traits measured in this thesis and typical Sorghum cultivation environments (dry, warm, erratic rainfall)), a hypothetical successful genotype will have: 1) structural features that enable it to reduce excess transpiration while avoiding heat stress under high radiation and temperature (narrow, thin leaf), resist hydraulic failure (high *VD*, smaller vascular bundles) 2) stomata that respond quickly to changes in light (smaller operational pore) but also less dependent on quick hydraulic signals that might cause it to close and give up soil moisture that could be used for productivity. This could mean a genotype that takes hydraulic risks by maintaining an open stomata, but this kind

of behaviour has been observed in grasses to increase *WUE* (Holloway-Phillips and Brodribb, 2011b). Similarly, such a genotype would need to be located on the A_n-g_s curve in a position where the minimum g_s is attained for the maximum A_n.

To take these findings further, the aim of future research should be to strengthen the link between *LW* and associated anatomical features as a determinant of *iWUE*, especially because *LW* is an easily measured trait that can be screened quickly. Also, elucidating the links between instantaneous measures of *iWUE* and linking them to temporal variation especially during day and under field conditions, to gain a fuller perspective of how beneficial *iWUE* is to whole plant function. Along similar lines, attempts to find variation in the rate of stomatal response across large range of diverse genotypes and linking it to integrated measures of soil water conservation. This is to establish the degree of gain from having kinetically fast stomata and whether it can combine the benefits of water consumption during periods of water availability and high irradiance with water conservation and reduced transpiration under photosynthetically unfavourable conditions. Finally, and following on from the discussion in this section of chapter 5, attempt large scale screening trials that combine multiple traits to properly test trade-offs and possible combinations that increase *iWUE* without sacrificing yield.

5.8 CLOSING SUMMARY

This thesis attempted to find sources of variation in intrinsic water use efficiency (*iWUE*) in a key C_4 crop. Diverse Sorghum genotypes were selected to test the extent of the influence of leaf anatomical features on *iWUE* under different growth and diurnal environments. There was large variation in *iWUE* within Sorghum genotypes, and in the contribution of photosynthetic capacity and stomatal conductance (g_s) to that variation. High *iWUE* was generally achieved via low (g_s), regulated mainly by reduced pore size. Under higher evaporative demands, the size of the guard cell complex in determining g_s was more prominent as tighter control on transpiration and water loss was needed. Narrow leaves were associated with smaller stomatal pores, achieving higher *iWUE* through lower g_s. Narrow leaves were also characterised by smaller cell size and increased vein density that likely allowed for better thermoregulation. Stomatal aperture anatomy was linked to the speed of stomatal response to irradiance and to different *iWUE* levels across the day, linking Instantaneous measures of *iWUE* in the morning and midday with temporally integrated, and hence more representative, measures of water use efficiency. The trade-offs that these traits exhibit under different environmental scenarios were discussed and possible future areas of concentration are suggested.

REFERENCE LIST

Aasamaa, K., Niinemets, Ü. and Sõber, A. (2005) Leaf hydraulic conductance in relation to anatomical and functional traits during *Populus tremula* leaf ontogeny, *Tree Physiology*, **25**(**11**), p 1409–1418.

Aasamaa, K., Sõber, A. and Rahi, M. (2001) Leaf anatomical characteristics associated with shoot hydraulic conductance, stomatal conductance and stomatal sensitivity to changes of leaf water status in temperate deciduous trees, *Australian Journal of Plant Physiology*, **28**(**8**), p 765–774.

Alexander, L. V, Zhang, X., Peterson, T. C., Caesar, J., Gleason, B., Klein Tank, A. M. G., Haylock, M., Collins, D., Trewin, B., Rahimzadeh, F., Tagipour, A., Rupa Kumar, K., Revadekar, J., Griffiths, G., Vincent, L., Stephenson, D. B., Burn, J., Aguilar, E., Brunet, M., Taylor, M., New, M., Zhai, P., Rusticucci, M. and Vazquez-Aguirre, J. L. (2006) Global observed changes in daily climate extremes of temperature and precipitation, *Journal of Geophysical Research Atmospheres*, **111**(**5**), p 1–22.

Alexandersson, E., Fraysse, L., Sjövall-Larsen, S., Gustavsson, S., Fellert, M., Karlsson, M., Johanson, U. and Kjellbom, P. (2005) Whole gene family expression and drought stress regulation of aquaporins, *Plant Molecular Biology*, **59**(**3**), p 469–484.

Apple, M. E., Olszyk, D. M., Ormrod, D. P., Lewis, J., Southworth, D. and Tingey, D. T. (2000) Morphology and stomatal function of Douglas fir needles exposed to climate change: Elevated CO_2 and temperature, *International Journal of Plant Sciences*, **161**(**1**), p 127–132.

Assouline, S., Narkis, K. and Or, D. (2010) Evaporation from partially covered water surfaces, *Water Resources Research*, **46**(**10**), p 1–12.

Baldocchi, D. D., Verma, S. B., Rosenberg, N. J., Blad, B. L. and Specht, J. E. (1985) Microclimate-plant architectural interactions: Influence of leaf width on the mass and energy exchange of a Soybean canopy, *Agricultural and Forest Meteorology*, **35**(**1–4**), p 1–20.

Balota, M., Payne, W. A., Rooney, W. and Rosenow, D. (2008) Gas exchange and transpiration ratio in Sorghum, *Crop Science*, **48**(**6**), p 2361–2371.

Bathellier, C., Tcherkez, G., Lorimer, G. H. and Farquhar, G. D. (2018) Rubisco is not really so bad, *Plant Cell and Environment*, **41**(**4**), p 705–716.

Battisti, D. S. and Naylor, R. L. (2009) Historical warnings of future food insecurity with unprecedented seasonal heat, *Science*, **323**(**January**), p 240–244.

Ben-Haj-Salah, H. and Tardieu, F. (1995) Temperature affects expansion rate of Maize leaves without change in spatial distribution of cell length, *Plant Physiology*, **109**(**3**), p 861–870.

Bergmann, D. C. (2004) Integrating signals in stomatal development, *Current Opinion in Plant Biology*, **7**(**1**), p 26–32.

Bertolino, L. T., Caine, R. S. and Gray, J. E. (2019) Impact of stomatal density and morphology on water-use efficiency in a changing world, *Frontiers in Plant Science*, **10**(**March**), p 225.

Betti, M., Bauwe, H., Busch, F. A., Fernie, A. R., Keech, O., Levey, M., Ort, D. R., Parry, M. A. J., Sage, R., Timm, S., Walker, B. and Weber, A. P. M. (2016) Manipulating photorespiration to increase plant productivity: Recent advances and perspectives for crop improvement, *Journal of Experimental Botany*, **67**(**10**), p 2977–2988.

Bläsing, O. E., Gibon, Y., Günther, M., Höhne, M., Morcuende, R., Osuna, D., Thimm, O., Usadel, B., Scheible, W. R. and Stitt, M. (2005) Sugars and circadian regulation make major contributions to the global regulation of diurnal gene expression in *Arabidopsis*, *Plant Cell*, **17**(**12**), p 3257–3281.

Blum, A. (2009) Effective use of water (EUW) and not water-use efficiency (WUE) is the target of crop yield improvement under drought stress, *Field Crops Research*, **112**(**2–3**), p 119–123.

Blum, A. (2015) Towards a conceptual ABA ideotype in plant breeding for water limited environments, *Functional Plant Biology*, **42**, p 502–513.

Borrell, A. K., Mullet, J. E., George-Jaeggli, B., Van Oosterom, E. J., Hammer, G. L., Klein, P. E. and Jordan, D. R. (2014) Drought adaptation of stay-green Sorghum is associated with canopy development, leaf anatomy, root growth, and water uptake, *Journal of Experimental Botany*, **65**(**21**), p 6251–6263.

Borrell, A. K., van Oosterom, E. J., Mullet, J. E., George-Jaeggli, B., Jordan, D. R., Klein, P. E. and Hammer, G. L. (2014) Stay-green alleles individually enhance grain yield in Sorghum under drought by modifying canopy development and water uptake patterns, *New Phytologist*, **203**(**3**), p 817–830.

Boyce, C. K., Brodribb, T. J., Feild, T. S. and Zwieniecki, M. A. (2009) Angiosperm leaf vein evolution was physiologically and environmentally transformative, *Proceedings of the Royal Society B: Biological Sciences*, **276**(**1663**), p 1771–1776.

Boyer, J. S. (1982) Plant productivity and environment, *Science*, **218**(**4571**), p 443–448.

Brodribb, T. J. and Feild, T. S. (2010) Leaf hydraulic evolution led a surge in leaf photosynthetic capacity during early angiosperm diversification, *Ecology Letters*, **13**(**2**), p 175–183.

Brodribb, T. J. and Holbrook, N. M. (2003) Stomatal closure during leaf dehydration, correlation with other leaf physiological traits, *Plant Physiology*, **132**(**4**), p 2166–2173.

Brodribb, T. J. and Holbrook, N. M. (2004) Stomatal protection against hydraulic failure: A comparison of coexisting ferns and angiosperms, *New Phytologist*, **162**(**3**), p 663–670.

Brodribb, T. J., Holbrook, N. M., Edwards, E. J. and Gutiérrez, M. V (2003) Relations between stomatal closure, leaf turgor and xylem vulnerability in eight tropical dry forest trees, *Plant, Cell and Environment*, **26**(**3**), p 443–450.

Brodribb, T. J., Jordan, G. J. and Carpenter, R. J. (2013) Unified changes in cell size permit coordinated leaf evolution, *New Phytologist*, **199**(**2**), p 559–570.

Brodribb, T. J., McAdam, S. A. M. and Carins Murphy, M. R. (2017) Xylem and stomata, coordinated through time and space, *Plant, Cell & Environment*, **40**(**6**), p 872–880.

Brown, R. H. (1999) Agronomic implications of C_4 photosynthesis, in Sage, R. F. and Monson, R. K. (eds) *C4 Plant Biology*. UK: Academic Press, p 473–507.

Brown, R. H. and Hattersley, P. W. (1989) Leaf anatomy of C3-C4 species as related to evolution of C4 photosynthesis, *Plant physiology*, **91**(**4**), p 1543–1550.

Bucci, S. J., Scholz, F. G., Goldstein, G., Meinzer, F. C. and Sternberg, L. D. S. L. (2003) Dynamic changes in hydraulic conductivity in petioles of two savanna tree species: Factors and mechanisms contributing to the refilling of embolized vessels, *Plant, Cell & Environment*, **26**(**10**), p 1633–1645.

Buckley, T. N. (2005) The control of stomata by water balance, *New Phytologist*, **168**(**2**), p 275–292.

Buckley, T. N. (2019) How do stomata respond to water status?, *New Phytologist*.

Buckley, T. N., John, G. P., Scoffoni, C. and Sack, L. (2017) The sites of evaporation within leaves, *Plant Physiology*, **173**(**3**), p 1763–1782.

Buckley, T. N., Mott, K. A. and Farquhar, G. D. (2003) A hydromechanical and biochemical model of stomatal conductance, *Plant, Cell and Environment*, **26**(**10**), p 1767–1785.

von Caemmerer, S. (2021) *Updating the steady state model of C_4 photosynthesis*, *bioRxiv*.

von Caemmerer, S., Ghannoum, O., Pengelly, J. J. L. and Cousins, A. B. (2014) Carbon isotope discrimination as a tool to explore C_4 photosynthesis, *Journal of Experimental Botany*, **65**(**13**), p 3459–3470.

von Caemmerer, S., Lawson, T., Oxborough, K., Baker, N. R., Andrews, T. J. and Raines, C. A. (2004) Stomatal conductance does not correlate with photosynthetic capacity in transgenic tobacco with reduced amounts of Rubisco, *Journal of Experimental Botany*, **55**(**400**), p 1157–1166.

Cai, S., Papanatsiou, M., Blatt, M. R. and Chen, Z. H. (2017) Speedy grass stomata: Emerging molecular and evolutionary features, *Molecular Plant*, **10**(**7**), p 912–914.

Caine, R. S., Yin, X., Sloan, J., Harrison, E. L., Mohammed, U., Fulton, T., Biswal, A. K., Dionora, J., Chater, C. C., Coe, R. A., Bandyopadhyay, A., Murchie, E. H., Swarup, R., Quick, W. P. and Gray, J. E. (2019) Rice with reduced stomatal density conserves water and has improved drought tolerance under future climate conditions, *New Phytologist*, (**July**).

Caldeira, C. F., Jeanguenin, L., Chaumont, F. and Tardieu, F. (2014) Circadian rhythms of hydraulic conductance and growth are enhanced by drought and improve plant performance, *Nature Communications*, **5**, p 5365.

Cano, F. J., Sharwood, R. E., Cousins, A. B. and Ghannoum, O. (2019) The role of leaf width and conductances to CO_2 in determining water use efficiency in C_4 grasses, *New Phytologist*, **223**(**3**), p 1280–1295.

Carins Murphy, M. R., Jordan, G. J. and Brodribb, T. J. (2012) Differential leaf expansion can enable hydraulic acclimation to sun and shade, *Plant, Cell and Environment*, **35**(**8**), p 1407–1418.

Carins Murphy, M. R., Jordan, G. J. and Brodribb, T. J. (2016) Cell expansion not cell differentiation predominantly co-ordinates veins and stomata within and among herbs and woody angiosperms grown under sun and shade, *Annals of Botany*, **118**(**6**), p 1127–1138.

Challinor, A. J., Watson, J., Lobell, D. B., Howden, S. M., Smith, D. R. and Chhetri, N. (2014) A meta-analysis of crop yield under climate change and adaptation, *Nature Climate Change*, **4**(**4**), p 287–291.

Chaumont, F., Barrieu, F., Wojcik, E., Chrispeels, M. J. and Jung, R. (2001) Aquaporins constitute a large and highly divergent protein family in Maize, *Plant Physiology*, **125**(**3**), p 1206–1215.

Chaves, M. M., Costa, J. M., Zarrouk, O., Pinheiro, C., Lopes, C. M. and Pereira, J. S. (2016) Controlling stomatal aperture in semi-arid regions—The dilemma of saving water or being cool?, *Plant Science*, **251**, p 54–64.

Choudhary, S. and Sinclair, T. R. (2014) Hydraulic conductance differences among sorghum genotypes to explain variation in restricted transpiration rates, *Functional Plant Biology*, **41**(**3**), p 270–275.

Choudhary, S., Sinclair, T. R. and Prasad, P. V. V. (2013) Hydraulic conductance of intact plants of two contrasting sorghum lines, SC15 and SC1205, *Functional Plant Biology*, **40**(**7**), p 730–738.

Christin, P. A., Boxall, S. F., Gregory, R., Edwards, E. J., Hartwell, J. and Osborne, C. P. (2013) Parallel recruitment of multiple genes into C_4 photosynthesis, *Genome Biology and Evolution*, **5**(**11**), p 2174–2187.

Christin, P. A. and Osborne, C. P. (2013) The recurrent assembly of C_4 photosynthesis, an evolutionary tale, *Photosynthesis Research*, **117**(**1**–**3**), p 163–175.

Ciampitti, Ignacio A, Prasad, P. V. V, Schlegel, A. J., Haag, L., Schnell, R. W., Arnall, B. and Lofton, J. (2019) Genotype × environment × management interactions: US Sorghum cropping systems, in Ciampitti, I A and Prasad, P. V. V (eds) *Sorghum: State of the Art and Future Prespectives*. Madison, WI: ASA and CSSA, p 277–296.

Claeys, H. and Inzé, D. (2013) The agony of choice: How plants balance growth and survival under water-limiting conditions, *Plant Physiology*, **162**(**4**), p 1768–1779.

Cochard, H., Venisse, J.-S., Barigah, T. S., Brunel, N., Herbette, S., Guilliot, A., Tyree, M. T. and Sakr, S. (2007) Putative role of aquaporins in variable hydraulic conductance of leaves in response to light, *Plant Physiology*, **143**(**1**), p 122–133.

Colbert, J. T. and Evert, R. F. (1982) Leaf vasculature in sugarcane (*Saccharum officinarum* L.), *Planta*, **156**, p 136–151.

Comstock, J. and Mencuccini, M. (1998) Control of stomatal conductance by leaf water potential in *Hymenoclea salsola* (T. & G.), a desert subshrub, *Plant, Cell & Environment*, **21**(**10**), p 1029–1038.

Condon, A. G. and Richards, R. A. (1992) Broad sense heritability and genotype × environment interaction for carbon isotope discrimination in field-grown Wheat, *Australian Journal of Agricultural Research*, **43**(**5**), p 921–934.

Condon, A. G., Richards, R. A., Rebetzke, G. J. and Farquhar, G. D. (2004) Breeding for high water-use efficiency, *Journal of Experimental Botany*, **55**(**407**), p 2447–2460.

Cowan, I. R. (1978) Stomatal behaviour and environment, in Preston, R. D. and Woolhouse, H. W. B. T.-A. (eds) *Advances in Botanical Research*. Academic Press, p 117–228.

Cowan, I. R. and Farquhar, G. D. (1977) Stomatal function in relation to leaf metabolism and environment., *Symposia of the Society for Experimental Biology*, **31**, p 471–505.

Deans, R. M., Brodribb, T. J., Busch, F. A. and Farquhar, G. D. (2019) Plant water-use strategy mediates stomatal effects on the light induction of photosynthesis, *New Phytologist*, **222**(**1**), p 382–395.

Dengler, N. G., Dengler, R. E., Donnelly, P. M. and Hattersley, P. W. (1994) Quantitative leaf anatomy of C_3 and C_4 grasses (*Poaceae*): Bundle sheath and mesophyll surface area relationships, *Annals of Botany*, **73**, p 241–255.

Dengler, N. G., Dengler, R. E. and Hattersley, P. W. (1985) Differing ontogenetic origins of PCR ('Kranz') sheaths in leaf blades of C_4 grasses (*Poaceae*), *American Journal of Botany*, **72**(**2**), p 284–302.

Dengler, N. G., Dengler, R. E. and Hattersley, P. W. (1986) Comparative bundle sheath and mesophyll differentiation in the leaves of the C_4 grasses *Panicum effusum* and *P.bulbosum*, *American Journal of Botany*,

73(**10**), p 1431–1442.

Dengler, N. G. and Nelson, T. (1999) Leaf structure and development in C4 Plants, in Sage, R. F. and Monson, R. K. (eds) *C4 Plant Biology*. UK: Academic Press, p 133–172.

Dillon, S. L., Shapter, F. M., Henry, R. J., Cordeiro, G., Izquierdo, L. and Lee, L. S. (2007) Domestication to crop improvement: Genetic resources for *Sorghum* and *Saccharum* (Andropogoneae), *Annals of Botany*, **100**(**5**), p 975–989.

Ding, L., Gao, L., Liu, W., Wang, M., Gu, M., Ren, B., Xu, G., Shen, Q. and Guo, S. (2016) Aquaporin plays an important role in mediating chloroplastic CO_2 concentration under high-N supply in rice (*Oryza sativa*) plants, *Physiologia Plantarum*, **156**(**2**), p 215–226.

de Dios, V. R., Loik, M. E., Smith, R., Aspinwall, M. J. and Tissue, D. T. (2016) Genetic variation in circadian regulation of nocturnal stomatal conductance enhances carbon assimilation and growth, *Plant Cell and Environment*, **39**(**1**), p 3–11.

Dittberner, H., Korte, A., Mettler-Altmann, T., Weber, A. P. M., Monroe, G. and de Meaux, J. (2018) Natural variation in stomata size contributes to the local adaptation of water-use efficiency in *Arabidopsis thaliana*, *Molecular Ecology*, **27**(**20**), p 4052–4065.

Djanaguiraman, M., Prasad, P. V. V, Boyle, D. L. and Schapaugh, W. T. (2011) High-temperature stress and Soybean leaves: Leaf anatomy and photosynthesis, *Crop Science*, **51**(**5**), p 2125–2131.

Doheny-Adams, T., Hunt, L., Franks, P. J., Beerling, D. J. and Gray, J. E. (2012) Genetic manipulation of stomatal density influences stomatal size, plant growth and tolerance to restricted water supply across a growth carbon dioxide gradient, *Philosophical Transactions of the Royal Society B: Biological Sciences*, **367**(**1588**), p 547–555.

Dolferus, R. (2014) To grow or not to grow: A stressful decision for plants, *Plant Science*, **229**, p 247–261.

Dow, G. J., Berry, J. A. and Bergmann, D. C. (2014) The physiological importance of developmental mechanisms that enforce proper stomatal spacing in Arabidopsis thaliana, *New Phytologist*, **201**(**4**), p 1205–1217.

Dow, G. J., Berry, J. A. and Bergmann, D. C. (2017) Disruption of stomatal lineage signaling or transcriptional regulators has differential effects on mesophyll development, but maintains coordination of gas exchange, *New Phytologist*, **216**(**1**), p 69–75.

Drake, J. E., Tjoelker, M. G., Vårhammar, A., Medlyn, B. E., Reich, P. B., Leigh, A., Pfautsch, S., Blackman, C. J., López, R., Aspinwall, M. J., Crous, K. Y., Duursma, R. A., Kumarathunge, D., De Kauwe, M. G., Jiang, M., Nicotra, A. B., Tissue, D. T., Choat, B., Atkin, O. K. and Barton, C. V. M. (2018) Trees tolerate an extreme heatwave via sustained transpirational cooling and increased leaf thermal tolerance, *Global Change Biology*, **24**(**6**), p 2390–2402.

Drake, P. L., Froend, R. H. and Franks, P. J. (2013) Smaller, faster stomata: Scaling of stomatal size, rate of response, and stomatal conductance, *Journal of Experimental Botany*, **64**(**2**), p 495–505.

Dunn, J., Hunt, L., Afsharinafar, M., Meselmani, M. Al, Mitchell, A., Howells, R., Wallington, E., Fleming, A. J. and Gray, J. E. (2019) Reduced stomatal density in bread wheat leads to increased water-use efficiency, *Journal of Experimental Botany*, **70**(**18**), p 4737–4747.

Duvick, D. N. (2005) The contribution of breeding to yield advances in Maize (*Zea mays* L.), *Advances in Agronomy*, **86**, p 83–145.

Edwards, E. J., Osborne, C. P., Stromberg, C. A. E., Smith, S. A. and Consortium, C. G. (2010) The origins of C_4 grasslands: integrating evolutionary and ecosystem science, *Science*, **328**(**April**), p 587–59. Available at: https://science.sciencemag.org/content/328/5978/587.abstract?casa_token=fKTPqJE-ggUAAAAA:47ezSF84Pr6ZbnkWPhpnaj059FfroX-gW5qraQMCN_9D9DfDdbwE0LG8oAiiCRw8eBpWnWaKboXKpQ.

Ehleringer, J. R., Cerling, T. E. and Helliker, B. R. (1997) C_4 photosynthesis, atmospheric CO_2, and climate, *Oecologia*, **112**(**3**), p 285–299.

Elliott-Kingston, C., Haworth, M., Yearsley, J. M., Batke, S. P., Lawson, T. and McElwain, J. C. (2016) Does size matter? Atmospheric CO_2 may be a stronger driver of stomatal closing rate than stomatal size in taxa that diversified under low CO_2, *Frontiers in Plant Science*, **7**(**August**), p 1253.

Elliott, J., Deryng, D., Müller, C., Frieler, K., Konzmann, M., Gerten, D., Glotter, M., Flörke, M., Wada, Y., Best,

N., Eisner, S., Fekete, B. M., Folberth, C., Foster, I., Gosling, S. N., Haddeland, I., Khabarov, N., Ludwig, F., Masaki, Y., Olin, S., Rosenzweig, C., Ruane, A. C., Satoh, Y., Schmid, E., Stacke, T., Tang, Q. and Wisser, D. (2014) Constraints and potentials of future irrigation water availability on agricultural production under climate change, *Proceedings Of The National Academy Of Sciences Of The United States Of America*, **111**(**9**), p 3239–3244.

Ellsworth, P. Z. and Cousins, A. B. (2016) Carbon isotopes and water use efficiency in C_4 plants, *Current Opinion in Plant Biology*, **31**(**6**), p 155–161.

Ellsworth, P. Z., Feldman, M. J., Baxter, I. and Cousins, A. B. (2020) A genetic link between leaf carbon isotope composition and whole-plant water use efficiency in the C_4 grass *Setaria*, *Plant Journal*, **102**(**6**), p 1234–1248.

Evans, J. R. (2020) Mesophyll conductance: walls, membranes and spatial complexity, *New Phytologist*.

Faralli, M., Cockram, J., Ober, E., Wall, S., Galle, A., Van Rie, J., Raines, C. and Lawson, T. (2019) Genotypic, developmental and environmental effects on the rapidity of gs in Wheat: Impacts on carbon gain and water-use efficiency, *Frontiers in Plant Science*, **10**(**April**), p 492.

Farquhar, G. D., von Caemmerer, S. and Berry, J. A. (1980) A biochemical model of photosynthetic CO_2 assimilation in leaves of C_3 species, *Planta*, **149**, p 78–90.

Farquhar, G. D. and Cowan, I. R. (1974) Oscillations in stomatal conductance, *Plant Physiology*, **54**(**5**), p 769–772.

Farquhar, G. D. and Richards, R. A. (1984) Isotopic composition of plant carbon correlates water-use efficiency of wheat genotypes, *Australian Journal of Plant Physiology*, **11**, p 539–552.

Farquhar, G. D. and Sharkey, T. D. (1982) Stomatal conductance and photosynthesis, *Annual Review of Plant Physiology*, **33**(**1**), p 317–345.

Feldman, A. B., Leung, H., Baraoidan, M., Elmido-Mabilangan, A., Canicosa, I., Quick, W. P., Sheehy, J. and Murchie, E. H. (2017) Increasing leaf vein density via mutagenesis in Rice results in an enhanced rate of photosynthesis, smaller cell sizes and can reduce interveinal mesophyll cell number, *Frontiers in Plant Science*, **8**, p 1883.

Feldman, A. B., Murchie, E. H., Leung, H., Baraoidan, M., Coe, R., Yu, S. M., Lo, S. F. and Quick, W. P. (2014) Increasing leaf vein density by mutagenesis: Laying the foundations for C4 rice, *PLoS ONE*, **9**(**4**), p e94947.

Feldman, M. J., Ellsworth, P. Z., Fahlgren, N., Gehan, M. A., Cousins, A. B. and Baxter, I. R. (2018) Components of water use efficiency have unique genetic signatures in the model C_4 grass Setaria, *Plant Physiology*, **178**(**2**), p pp.00146.2018.

Ferris, R., Nijs, I., Behaeghe, T. and Impens, I. (1996) Elevated CO_2 and temperature have different effects on leaf anatomy of perennial Ryegrass in spring and summer, *Annals of Botany*, **78**(**4**), p 489–497.

Fiorin, L., Brodribb, T. J. and Anfodillo, T. (2016) Transport efficiency through uniformity: Organization of veins and stomata in angiosperm leaves, *New Phytologist*, **209**(**1**), p 216–227.

Flexas, J. (2016) Genetic improvement of leaf photosynthesis and intrinsic water use efficiency in C_3 plants: Why so much little success?, *Plant Science*, **251**, p 155–161.

Flexas, J., Ribas-Carbó, M., Diaz-Espejo, A., Galmés, J. and Medrano, H. (2008) Mesophyll conductance to CO_2: Current knowledge and future prospects, *Plant, Cell and Environment*, **31**(**5**), p 602–621.

Flütsch, S. and Santelia, D. (2021) Mesophyll-derived sugars are positive regulators of light-driven stomatal opening, *New Phytologist*, **accepted**.

Foley, J. A., Ramankutty, N., Brauman, K. A., Cassidy, E. S., Gerber, J. S., Johnston, M., Mueller, N. D., O'Connell, C., Ray, D. K., West, P. C., Balzer, C., Bennett, E. M., Carpenter, S. R., Hill, J., Monfreda, C., Polasky, S., Rockström, J., Sheehan, J., Siebert, S., Tilman, D. and Zaks, D. P. M. (2011) Solutions for a cultivated planet, *Nature*, **478**(**7369**), p 337–342.

Franks, P. J. (2006) Higher rates of leaf gas exchange are associated with higher leaf hydrodynamic pressure gradients, *Plant, Cell and Environment*, **29**(**4**), p 584–592.

Franks, P. J. and Beerling, D. J. (2009) Maximum leaf conductance driven by CO_2 effects on stomatal size and density over geologic time, *Proceedings of the National Academy of Sciences of the United States of America*, **106**(**25**), p 10343–10347.

Franks, P. J. and Casson, S. (2014) Connecting stomatal development and physiology, *New Phytologist*, **201**(**4**), p 1079–1082.

Franks, P. J., Doheny-Adams, T., Britton-Harper, Z. J. and Gray, J. E. (2015) Increasing water-use efficiency directly through genetic manipulation of stomatal density, *New Phytologist*, **207**(**1**), p 188–195.

Franks, P. J., Drake, P. L. and Beerling, D. J. (2009) Plasticity in maximum stomatal conductance constrained by negative correlation between stomatal size and density: An analysis using *Eucalyptus globulus*, *Plant, Cell and Environment*, **32**(**12**), p 1737–1748.

Franks, P. J. and Farquhar, G. D. (2001) The effect of exogenous abscisic acid on stomatal development, stomatal mechanics, and leaf gas exchange in Tradescantia virginiana, *Plant Physiology*, **125**(**February**), p 935–942.

Franks, P. J. and Farquhar, G. D. (2007) The mechanical diversity of stomata and its significance in gas-exchange control, *Plant Physiology*, **143**(**1**), p 78–87.

Franks, P. J., Royer, D. L., Beerling, D. J., Van de Water, P. K., Cantrill, D. J., Barbour, M. M. and Berry, J. A. (2014) New constraints on atmospheric CO_2 concentration for the Phanerozoic, *Geophysical Research Letters*, **41**(**13**), p 4685–4694.

Gates, D. M. (1968) Transpiration and leaf temperature, *Annual Review of Plant Physiology*, **19**(**1**), p 211–238.

George-Jaeggli, B., Mortlock, M. Y. and Borrell, A. K. (2017) Bigger is not always better: Reducing leaf area helps stay-green sorghum use soil water more slowly, *Environmental and Experimental Botany*, **138**, p 119–129.

Ghannoum, O. (2009) C4 photosynthesis and water stress, *Annals of Botany*, **103**(**4**), p 635–644.

Ghannoum, O. (2016) How can we breed for more water use-efficient sugarcane?, *Journal of Experimental Botany*, **67**(**3**), p 555–557.

Ghannoum, O., von Caemmerer, S. and Conroy, J. P. (2001) Plant water use efficiency of 17 Australian NAD-ME and NADP-ME C_4 grasses at ambient and elevated CO_2 partial pressure, *Australian Journal of Plant Physiology*, **28**(**12**), p 1207–1217.

Ghannoum, O., von Caemmerer, S. and Conroy, J. P. (2002) The effect of drought on plant water use efficiency of nine NAD-ME and nine NADP-ME Australian C_4 grasses, *Functional Plant Biology*, **29**(**11**), p 1337–1348.

Ghannoum, O., Von Caemmerer, S., Taylor, N. and Millar, A. H. (2017) Carbon dioxide assimilation and respiration, in *Plants in Action*, p 1–75.

Ghannoum, O., Conroy, J. P., Driscoll, S. P., Paul, M. J., Foyer, C. H. and Lawlor, D. W. (2003) Nonstomatal limitations are responsible for drought-induced photosynthetic inhibition in four C_4 grasses, *New Phytologist*, **159**(**3**), p 599–608.

Ghannoum, O., Evans, J. R. and von Caemmerer, S. (2011) Nitrogen and water use efficiency of C_4 plants, in Raghavendra, A. S. and Sage, R. F. (eds) *C4 photosynthesis and related CO2 concentrating mechanisms*. Dordrecht, p 162-129–146.

Gholipoor, M., Prasad, P. V. V., Mutava, R. N. and Sinclair, T. R. (2010) Genetic variability of transpiration response to vapor pressure deficit among sorghum genotypes, *Field Crops Research*, **119**(**1**), p 85–90.

Gholipoor, M., Sinclair, T. R. and Prasad, P. V. V. (2012) Genotypic variation within sorghum for transpiration response to drying soil, *Plant and Soil*, **357**(**1**), p 35–40.

Gilbert, M. E., Zwieniecki, M. A. and Holbrook, N. M. (2011) Independent variation in photosynthetic capacity and stomatal conductance leads to differences in intrinsic water use efficiency in 11 Soybean genotypes before and during mild drought, *Journal of Experimental Botany*, **62**(**8**), p 2875–2887.

Granier, C. and Tardieu, F. (1998) Is thermal time adequate for expressing the effects of temperature on sunflower leaf development?, *Plant, Cell and Environment*, **21**(**7**), p 695–703.

Grondin, A., Rodrigues, O., Verdoucq, L., Merlot, S., Leonhardt, N. and Maurel, C. (2015) Aquaporins contribute to ABA-triggered stomatal closure through OST1-mediated phosphorylation, *The Plant Cell*, **27**(**7**), p 1945–1954.

Groszmann, M., Osborn, H. L. and Evans, J. R. (2017) Carbon dioxide and water transport through plant

aquaporins, *Plant, Cell & Environment*, **40**(**6**), p 938–961.

Hall, A. J. and Richards, R. A. (2013) Prognosis for genetic improvement of yield potential and water-limited yield of major grain crops, *Field Crops Research*, **143**, p 18–33.

Hammer, G. L., Farquhar, G. D. and Broad, I. J. (1997) On the extent of genetic variation for transpiration efficiency in sorghum, *Australian Journal of Agricultural Research*, **48**, p 649–655.

Hammer, G., McLean, G., Doherty, A., van Oosterom, E. and Chapman, S. (2016) Sorghum crop modeling and its utility in agronomy and breeding, in Ciampitti, I. A. and Prasad, P. V. V (eds) *Sorghum: State of the Art and Future Prespectives*. Madison, WI: ASA and CSSA, p 215–239.

Hanba, Y. T., Shibasaka, M., Hayashi, Y., Hayakawa, T., Kasamo, K., Terashima, I. and Katsuhara, M. (2004) Overexpression of the barley aquaporin HvPIP2;1 increases internal CO_2 conductance and CO_2 assimilation in the leaves of transgenic rice plants, *Plant and Cell Physiology*, **45**(**5**), p 521–529. Available at: https://www.ncbi.nlm.nih.gov/pubmed/15169933.

Harrison, E. L., Arce Cubas, L., Gray, J. E. and Hepworth, C. (2020) The influence of stomatal morphology and distribution on photosynthetic gas exchange, *The Plant Journal*, **101**(**4**), p 768–779.

Hatch, M. D. (1987) C_4 photosynthesis: a unique blend of modified biochemistry, anatomy and ultrastructure, *Biochimica et Biophysica Acta*, **895**, p 81–106.

Haydon, M. J., Mielczarek, O., Robertson, F. C., Hubbard, K. E. and Webb, A. A. R. (2013) Photosynthetic entrainment of the *Arabidopsis thaliana* circadian clock, *Nature*, **502**, p 689–692.

Heinen, R. B., Bienert, G. P., Cohen, D., Chevalier, A. S., Uehlein, N., Hachez, C., Kaldenhoff, R., Le Thiec, D. and Chaumont, F. (2014) Expression and characterization of plasma membrane aquaporins in stomatal complexes of *Zea mays*, *Plant Molecular Biology*, **86**(**3**), p 335–350.

Henderson, S. A., von Caemmerer, S. and Farquhar, G. D. (1992) Short-term measurements of carbon isotope discrimination in several C4 species, *Australian Journal of Plant Physiology*, **19**(**1976**), p 263–85.

Henderson, S. A., von Caemmerer, S., Farquhar, G. D., Wade, L. and Hammer, G. (1998) Correlation between carbon isotope discrimination and transpiration efficiency in lines of the C_4 species *Sorghum bicolor* in the glasshouse and the field, *Australian Journal of Plant Physiology*, **25**, p 111–123.

Henry, C., John, G. P., Pan, R., Bartlett, M. K., Fletcher, L. R., Scoffoni, C. and Sack, L. (2019) A stomatal safety-efficiency trade-off constrains responses to leaf dehydration, *Nature Communications*, **10**(**1**), p 3398.

Henry, C., Watson-Lazowski, A., Oszvald, M., Griffiths, C., Paul, M. J., Furbank, R. T. and Ghannoum, O. (2020) Sugar sensing responses to low and high light in leaves of the C_4 model grass *Setaria viridis*, *Journal of Experimental Botany*, **71**(**3**), p 1039–1052.

Hentschel, R., Hommel, R., Poschenrieder, W., Grote, R., Holst, J., Biernath, C., Gessler, A. and Priesack, E. (2016) Stomatal conductance and intrinsic water use efficiency in the drought year 2003: a case study of European beech, *Trees*, **30**(**1**), p 153–174.

Hepworth, C., Caine, R. S., Harrison, E. L., Sloan, J. and Gray, J. E. (2018) Stomatal development: focusing on the grasses, *Current Opinion in Plant Biology*, **41**, p 1–7.

Hetherington, A. M. and Woodward, F. I. (2003) The role of stomata in sensing and driving environmental change, *Nature*, **424**(**6951**), p 901–908.

Hirasawa, T. and Hsiao, T. C. (1999) Some characteristics of reduced leaf photosynthesis at midday in Maize growing in the field, *Field Crops Research*, **62**(**1**), p 53–62.

Holloway-Phillips, M. M. and Brodribb, T. J. (2011a) Contrasting hydraulic regulation in closely related forage grasses: Implications for plant water use, *Functional Plant Biology*, **38**(**7**), p 594–605.

Holloway-Phillips, M. M. and Brodribb, T. J. (2011b) Minimum hydraulic safety leads to maximum water-use efficiency in a forage grass, *Plant, Cell and Environment*, **34**(**2**), p 302–313.

Hughes, J., Hepworth, C., Dutton, C., Dunn, J. A., Hunt, L., Stephens, J., Waugh, R., Cameron, D. D. and Gray, J. E. (2017) Reducing stomatal density in Barley improves drought tolerance without impacting on yield, *Plant Physiology*, **174**(**2**), p 776–787.

Huxman, T. E. and Monson, R. K. (2003) Stomatal responses of C_3, C_3-C_4 and C_4 *Flaveria* species to light and intercellular CO_2 concentration: Implications for the evolution of stomatal behaviour, *Plant, Cell and Environment*, **26**(**2**), p 313–322.

Israel, W. K. (2020) *Carbon isotope discrimination and stomatal function in C4 grasses*. Western Sydney University.

Jackson, P., Basnayake, J., Inman-Bamber, G., Lakshmanan, P., Natarajan, S. and Stokes, C. (2016) Genetic variation in transpiration efficiency and relationships between whole plant and leaf gas exchange measurements in *Saccharum* spp. and related germplasm, *Journal of Experimental Botany*, **67**(**3**), p 861–871.

Jarvis, P. G. and McNaughton, K. G. (1986) Stomatal Control of Transpiration: Scaling Up from Leaf to Region, *Advances in Ecological Research*, **15**, p 1–49.

Jezek, M. and Blatt, M. R. (2017) The membrane transport system of the guard cell and its integration for stomatal dynamics, *Plant Physiology*, **174**(**2**), p 487–519.

Johnson, K. M., Jordan, G. J. and Brodribb, T. J. (2018) Wheat leaves embolised by water stress do not recover function upon rewatering, *Plant, Cell & Environment*, **41**, p 2704–2714.

Jones, H. G. (2013) *Plants and Microclimate: A Quantitative Approach to Environmental Plant Physiology*. 3rd ed. Cambridge: Cambridge University Press.

Jordan, D. B. and Ogren, W. L. (1984) The CO_2/O_2 specificity of ribulose 1,5-bisphosphate carboxylase/oxygenase - Dependence on ribulosebisphosphate concentration, pH and temperature, *Planta*, **161**(**4**), p 308–313.

Jordan, D. R., Mace, E. S., Cruickshank, A. W., Hunt, C. H. and Henzell, R. G. (2011) Exploring and exploiting genetic variation from unadapted sorghum germplasm in a breeding program, *Crop Science*, **51**(**4**), p 1444–1457.

Kaldenhoff, R., Kai, L. and Uehlein, N. (2014) Aquaporins and membrane diffusion of CO_2 in living organisms, *Biochimica et Biophysica Acta*, **1840**(**5**), p 1592–1595.

Kaldenhoff, R., Ribas-Carbo, M., Flexas Sans, J., Lovisolo, C., Heckwolf, M. and Uehlein, N. (2008) Aquaporins and plant water balance, *Plant, Cell and Environment*, **31**(**5**), p 658–666.

Kelly, G., Moshelion, M., David-Schwartz, R., Halperin, O., Wallach, R., Attia, Z., Belausov, E. and Granot, D. (2013) Hexokinase mediates stomatal closure, *Plant Journal*, **75**(**6**), p 977–988.

Kemp, P. R. and Cunningham, G. L. (1981) Light, temperature and salinity effects on growth, leaf anatomy and photosynthesis of *Distichlis spicata* (L.) Greene, *American Journal of Botany*, **68**(**4**), p 507–516.

Kim, S.-H., Gitz, D. C., Sicher, R. C., Baker, J. T., Timlin, D. J. and Reddy, V. R. (2007) Temperature dependence of growth, development, and photosynthesis in Maize under elevated CO_2, *Environmental and Experimental Botany*, **61**(**3**), p 224–236.

Kirschbaum, M. U. F., Gross, L. J. and Pearcy, R. W. (1988) Observed and modelled stomatal responses to dynamic light environments in the shade plant Alocasia macrorrhiza, *Plant, Cell & Environment*, **11**(**2**), p 111–121.

Knapp, A. K. (1993) Gas exchange dynamics in C_3 and C_4 grasses: Consequence of differences in stomatal conductance, *Ecology*, **74**(**1**), p 113–123.

Kuhlgert, S., Austic, G., Zegarac, R., Osei-Bonsu, I., Hoh, D., Chilvers, M. I., Roth, M. G., Bi, K., TerAvest, D., Weebadde, P. and Kramer, D. M. (2016) MultispeQ Beta: A tool for large-scale plant phenotyping connected to the open photosynQ network, *Royal Society Open Science*, **3**(**10**), p 160592.

Lafarge, T., De Raïssac, M. and Tardieu, F. (1998) Elongation rate of Sorghum leaves has a common response to meristem temperature in diverse African and European environmental conditions, *Field Crops Research*, **58**(**1**), p 69–79.

Langdale, J. A., Lane, B., Freeling, M. and Nelson, T. (1989) Cell lineage analysis of Maize bundle sheath and mesophyll cells, *Developmental Biology*, **133**(**1**), p 128–139.

Lange, O. L., Lösch, R., Schulze, E. D. and Kappen, L. (1971) Responses of stomata to changes in humidity, *Planta*, **100**, p 76–86.

Lawson, T. and Blatt, M. R. (2014) Stomatal size, speed, and responsiveness impact on photosynthesis and water use efficiency, *Plant Physiology*, **164**(**4**), p 1556–1570.

Lawson, T. and Matthews, J. (2020) Guard cell metabolism and stomatal function, *Annual Review of Plant Biology*, p 273–302.

Lawson, T. and Vialet-Chabrand, S. (2018) Speedy stomata, photosynthesis and plant water use efficiency, *New Phytologist*, **221**(**1**), p 93–98.

Le, S., Josse, J. and Husson, F. (2008) FactoMineR: An R package for multivariate analysis, *Journal of Statistical Software*, **25**(**1**), p 1–18.

Leakey, A. D. B. (2009) Rising atmospheric carbon dioxide concentration and the future of C4 crops for food and fuel, *Proceedings of the Royal Society B: Biological Sciences*, **276**(**1666**), p 2333–2343.

Leakey, A. D. B., Ferguson, J. N., Pignon, C. P., Wu, A., Jin, Z., Hammer, G. L. and Lobell, D. B. (2019) Water use efficiency as a constraint and target for improving the tesilience and productivity of C3 and C4 crops, *Annual Review of Plant Biology*, **70**, p 781–808.

Leegood, R. C. and Walker, R. P. (1999) Regulation of the C_4 Pathway, in Sage, R. F. and Monson, R. K. (eds) *C4 Plant Biology*. UK: Academic Press, p 89–131.

Lehmeier, C., Pajor, R., Lundgren, M. R., Mathers, A., Sloan, J., Bauch, M., Mitchell, A., Bellasio, C., Green, A., Bouyer, D., Schnittger, A., Sturrock, C., Osborne, C. P., Rolfe, S., Mooney, S. and Fleming, A. J. (2017) Cell density and airspace patterning in the leaf can be manipulated to increase leaf photosynthetic capacity, *The Plant Journal*, **92**(**6**), p 981–994.

Leigh, A., Sevanto, S., Close, J. D. and Nicotra, A. B. (2017) The influence of leaf size and shape on leaf thermal dynamics: does theory hold up under natural conditions?, *Plant Cell and Environment*, **40**(**2**), p 237–248.

Lever, J., Krzywinski, M. and Altman, N. (2017) Points of Significance: Principal component analysis, *Nature Methods*, **14**(**7**), p 641–642.

Li, C., Jackson, P., Lu, X., Xu, C., Cai, Q., Basnayake, J., Lakshmanan, P., Ghannoum, O. and Fan, Y. (2017) Genotypic variation in transpiration efficiency due to differences in photosynthetic capacity among sugarcane-related clones, *Journal of Experimental Botany*, **68**(**9**), p 2377–2385.

Liang, G. H., Chu, C. C., Reddi, N. S., Lin, S. S. and Dayton, A. D. (1973) Leaf blade areas of grain Sorghum varieties and hybrids, *Agronomy Journal*, **65**(**3**), p 456–459. Available at: https://acsess.onlinelibrary.wiley.com/doi/abs/10.2134/agronj1973.00021962006500030030x.

Liang, G. H., Dayton, A. D., Chu, C. C. and Casady, A. J. (1975) Heritability of stomatal density and distribution on leaves of grain Sorghum, *Crop Science*, **15**, p 567–570.

Liu, H., Edwards, E. J., Freckleton, R. P. and Osborne, C. P. (2012) Phylogenetic niche conservatism in C_4 grasses, *Oecologia*, **170**(**3**), p 835–845.

Lobell, D. B., Burke, M. B., Tebaldi, C., Mastrandrea, M. D., Falcon, W. P. and Naylor, R. L. (2008) Prioritizing climate change adaptation needs for food security in 2030, *Science*, **319**(**February**), p 607–610.

Long, S. P. (1999) Environmental Responses, in Sage, R. F. and Monson, R. K. (eds) *C4 Plant Biology*. UK: Academic Press, p 215–249.

Long, S. P., Marshall-Colon, A. and Zhu, X.-G. (2015) Meeting the global food demand of the future by engineering crop photosynthesis and yield potential, *Cell*, **161**(**1**), p 56–66.

Lopez, D., Venisse, J. S., Fumanal, B., Chaumont, F., Guillot, E., Daniels, M. J., Cochard, H., Julien, J. L. and Gousset-Dupont, A. (2013) Aquaporins and leaf hydraulics: Poplar sheds new light, *Plant and Cell Physiology*, **54**(**12**), p 1963–1975.

Lundgren, M. R., Mathers, A., Baillie, A. L., Dunn, J., Wilson, M. J., Hunt, L., Pajor, R., Fradera-Soler, M., Rolfe, S., Osborne, C. P., Sturrock, C. J., Gray, J. E., Mooney, S. J. and Fleming, A. J. (2019) Mesophyll porosity is modulated by the presence of functional stomata, *Nature Communications*, **10**(**1**), p 2825.

Luomala, E. M., Laitinen, K., Sutinen, S., Kellomäki, S. and Vapaavuori, E. (2005) Stomatal density, anatomy and nutrient concentrations of Scots pine needles are affected by elevated CO_2 and temperature, *Plant, Cell and Environment*, **28**(**6**), p 733–749.

Mace, E., Innes, D., Hunt, C., Wang, X., Tao, Y., Baxter, J., Hassall, M., Hathorn, A. and Jordan, D. (2019) The Sorghum QTL Atlas: a powerful tool for trait dissection, comparative genomics and crop improvement, *Theoretical and Applied Genetics*, **132**(**3**), p 751–766.

Malone, S. R., Mayeux, H. S., Johnson, H. B. and Polley, H. W. (1993) Stomatal density and aperture length in four plant species grown across a subambient CO_2 gradient, *American Journal of Botany*, **80**(**12**), p 1413–1418. Available at: https://www.jstor.org/stable/2445670.

Marrero, T. R. and Mason, E. A. (1972) Gaseous diffusion coefficients, *Journal of Physical and Chemical Reference Data*, **1**(**1**), p 3–118.

Masle, J., Gilmore, S. R. and Farquhar, G. D. (2005) The <i>ERECTA<i/> gene regulates plant transpiration efficiency in *Arabidopsis*, *Nature*, **436**, p 866–870.

Matthews, J. S. A., Vialet-Chabrand, S. R. M. and Lawson, T. (2017) Diurnal variation in gas exchange: The balance between carbon fixation and water loss, *Plant Physiology*, **174**(**2**), p 614–623.

Matthews, J. S. A., Vialet-Chabrand, S. R. M. and Lawson, T. (2018) Acclimation to fluctuating light impacts the rapidity and diurnal rhythm of stomatal conductance, *Plant Physiology*, **176**(**March**), p 1939–1951.

McAdam, S. A. M. and Brodribb, T. J. (2014) Separating active and passive influences on stomatal control of transpiration, *Plant Physiology*, **164**(**4**), p 1578–1586.

McAdam, S. A. M. and Brodribb, T. J. (2016) Linking turgor with ABA biosynthesis: Implications for stomatal responses to vapor pressure deficit across land plants, *Plant Physiology*, **171**(**3**), p 2008–2016.

McAdam, S. A. M., Sussmilch, F. C. and Brodribb, T. J. (2016) Stomatal responses to vapour pressure deficit are regulated by high speed gene expression in angiosperms, *Plant, Cell and Environment*, **39**(**3**), p 485–491.

McAusland, L., Vialet-Chabrand, S., Davey, P., Baker, N. R., Brendel, O. and Lawson, T. (2016) Effects of kinetics of light-induced stomatal responses on photosynthesis and water-use efficiency, *New Phytologist*, **211**(**4**), p 1209–1220.

Mckown, A. D. and Dengler, N. G. (2007) Key innovations in the evolution of Kranz anatomy and C4 vein pattern in Flaveria (Asteraceae), *American Journal of Botany*, **94**(**3**), p 382–399.

McKown, A. D. and Dengler, N. G. (2009) Shifts in leaf vein density through accelerated vein formation in C_4 *Flaveria* (*Asteraceae*), *Annals of Botany*, **104**(**6**), p 1085–1098.

McKown, K. H. and Bergmann, D. C. (2018) Grass stomata, *Current Biology*, **28**(**15**), p R814–R816.

Medrano, H., Pou, A., Tomás, M., Martorell, S., Gulias, J., Flexas, J. and Escalona, J. M. (2012) Average daily light interception determines leaf water use efficiency among different canopy locations in grapevine, *Agricultural Water Management*, **114**, p 4–10.

Medrano, H., Tomás, M., Martorell, S., Flexas, J., Hernández, E., Rosselló, J., Pou, A., Escalona, J. M. and Bota, J. (2015) From leaf to whole-plant water use efficiency (WUE) in complex canopies: Limitations of leaf WUE as a selection target, *Crop Journal*, **3**(**3**), p 220–228.

Meinzer, F. C., Goldstein, G., Jackson, P., Holbrook, N. M., Gutiérrez, M. V and Cavelier, J. (1995) Environmental and physiological regulation of transpiration in tropical forest gap species: the influence of boundary layer and hydraulic properties, *Oecologia*, **101**(**4**), p 514–522.

Meinzer, F. C. and Grantz, D. A. (1990) Stomatal and hydraulic conductance in growing sugarcane: stomatal adjustment to water transport capacity, *Plant, Cell & Environment*, **13**(**4**), p 383–388.

Mencuccini, M., Mambelli, S. and Comstock, J. (2000) Stomatal responsiveness to leaf water status in common bean (*Phaseolus vulgaris* L.) is a function of time of day, *Plant, Cell and Environment*, **23**(**10**), p 1109–1118.

Miller-Rushing, A. J., Primack, R. B., Templer, P. H., Rathbone, S. and Mukunda, S. (2009) Long-term relationships among atmospheric CO_2, stomata, and intrinsic water use efficiency in individual trees, *American Journal of Botany*, **96**(**10**), p 1779–1786.

Miranda, V., Baker, N. R. and Long, S. P. (1981) Anatomical variation along the length of *Zea mays* in relation to photosynthesis, *New Phytologist*, **88**(**4**), p 595–605.

Monda, K., Araki, H., Kuhara, S., Ishigaki, G., Akashi, R., Negi, J., Kojima, M., Sakakibara, H., Takahashi, S., Hashimoto-Sugimoto, M., Goto, N. and Iba, K. (2016) Enhanced stomatal conductance by a spontaneous *Arabidopsis* tetraploid, Me-0, results from increased stomatal size and greater stomatal aperture, *Plant Physiology*, **170**(**3**), p 1435–1444.

Morison, J. I. L., Baker, N. R., Mullineaux, P. M. and Davies, W. J. (2008) Improving water use in crop production, *Philosophical Transactions of the Royal Society B: Biological Sciences*, **363**(**1491**), p 639–658.

Mott, K. A. (1988) Do stomata respond to CO_2 concentrations other than intercellular?, *Plant Physiology*, **86**(**1**), p 200–203.

Mott, K. A., Denne, F. and Powell, J. (1997) Interactions among stomata in response to perturbations in humidity, *Plant, Cell & Environment*, **20**(**9**), p 1098–1107.

Mott, K. A. and Franks, P. J. (2001) The role of epidermal turgor in stomatal interactions following a local perturbation in humidity, *Plant, Cell and Environment*, **24**(**6**), p 657–662.

Mott, K. A. and Parkhurst, D. F. (1991) Stomatal responses to humidity in air and helox, *Plant, Cell & Environment*, **14**(**5**), p 509–515.

Mott, K. A. and Peak, D. (2010) Stomatal responses to humidity and temperature in darkness, *Plant, Cell and Environment*, **33**(**7**), p 1084–1090.

Mott, K. A., Sibbernsen, E. D. and Shope, J. C. (2008) The role of the mesophyll in stomatal responses to light and CO_2, *Plant, Cell and Environment*, **31**(**9**), p 1299–1306.

Moualeu-Ngangue, D. P., Chen, T.-W. and Stützel, H. (2016) A modeling approach to quantify the effects of stomatal behavior and mesophyll conductance on leaf water use efficiency, *Frontiers in Plant Science*, **7**(**June**), p 1–15.

Mueller, N. D., Butler, E. E., Mckinnon, K. A., Rhines, A., Tingley, M., Holbrook, N. M. and Huybers, P. (2016) Cooling of US Midwest summer temperature extremes from cropland intensification, *Nature Climate Change*, **6**(**3**), p 317–322.

Murchie, E. H., Kefauver, S., Araus, J. L., Muller, O., Rascher, U., Flood, P. J. and Lawson, T. (2018) Measuring the dynamic photosynthome, *Annals of Botany*, **122**(**2**), p 207–220.

Murray, M., Soh, W. K., Yiotis, C., Spicer, R. A., Lawson, T. and McElwain, J. C. (2020) Consistent relationship between field-measured stomatal conductance and theoretical maximum stomatal conductance in C_3 woody angiosperms in four major biomes, *International Journal of Plant Sciences*, **181**(**1**), p 142–154.

Nardini, A., Pedà, G. and Rocca, N. La (2012) Trade-offs between leaf hydraulic capacity and drought vulnerability: Morpho-anatomical bases, carbon costs and ecological consequences, *New Phytologist*, **196**(**3**), p 788–798.

Ocheltree, T. W., Nippert, J. B. and Prasad, P. V. V. (2016) A safety vs efficiency trade-off identified in the hydraulic pathway of grass leaves is decoupled from photosynthesis, stomatal conductance and precipitation, *New Phytologist*, **210**(**1**), p 97–107.

Ochieng, G., Ngugi, K., Wamalwa, L. N., Manyasa, E., Muchira, N., Nyamongo, D. and Odeny, D. A. (2021) Novel sources of drought tolerance from landraces and wild Sorghum relatives, *Crop Science*, **61**(**1**), p 104–118.

OECD (2017) Sorghum (Sorghum bicolor), in *Safety assessment of transgenic orgaisms in the environment*. Paris: OECD Publishing.

Ogle, K. (2003) Implications of interveinal distance for quantum yield in C4 grasses: A modeling and meta-analysis, *Oecologia*, **136**(**4**), p 532–542.

Ohsumi, A., Kanemura, T., Homma, K., Horie, T. and Shiraiwa, T. (2007) Genotypic variation of stomatal conductance in relation to stomatal density and length in rice (*Oryza sativa* L.), *Plant Production Science*, **10**(**3**), p 322–328.

Osborne, C. P. and Sack, L. (2012) Evolution of C_4 plants: a new hypothesis for an interaction of CO_2 and water relations mediated by plant hydraulics, *Philosophical Transactions of the Royal Society B: Biological Sciences*, **367**(**1588**), p 583–600.

Osmond, C. B., Bjorkman, O. and Anderson, D. J. (1980) *Physiological processes in plant ecology: Towards a synthesis with Atriplex*. Springer Berlin Heidelberg.

Outlaw, W. H. (2003) Integration of cellular and physiological functions of guard cells, *Critical Reviews in Plant Sciences*, **22**(**6**), p 503–529.

Ouyang, W., Struik, P. C., Yin, X. and Yang, J. (2017) Stomatal conductance, mesophyll conductance, and trans piration efficiency in relation to leaf anatomy in rice and wheat genotypes under drought, *Journal of Experimental Botany*, **68**(**18**), p 5191–5205.

Pan, L., George-Jaeggli, B., Borrell, A., Jordan, D., Koller, F., Al-Salman, Y., Ghannoum, O., Cano, F.J. (2021) Coordinatoin of stomata and vein patterns with leaf width underpins water-use efficiency in a C4 crop. *Plant, Cell & Environment*, accepted.

Parkhurst, D. F. (1994) Diffusion of CO_2 and other gases inside leaves., *New Phytologist*, **126**(**65**), p 449–

479.

Passioura, J. (2006) Increasing crop productivity when water is scarce - From breeding to field management, *Agricultural Water Management*, **80**(**1-3 SPEC. ISS.**), p 176–196.

Passioura, J. B. (1977) Grain yield, harvest index, and water use of Wheat, *The Journal of the Australian Institute of Agricultural Science*, **43**(**3**–**4**), p 177–120.

Pathare, V. S., Koteyeva, N. K. and Cousins, A. B. (2020) Increased adaxial stomatal density is associated with greater mesophyll surface area exposed to intercellular air spaces and mesophyll conductance in diverse C_4 grasses, *New Phytologist*, **225**(**January**), p 169–182.

Paul, M. J. and Foyer, C. H. (2001) Sink regulation of photosynthesis, *Journal of Experimental Botany*, **52**(**360**), p 1383–1400.

Paul, M. J. and Pellny, T. K. (2003) Carbon metabolite feedback regulation of leaf photosynthesis and development, *Journal of Experimental Botany*, **54**(**382**), p 539–547.

Pearcy, R. W. and Way, D. A. (2012) Two decades of sunfleck research: Looking back to move forward, *Tree Physiology*, **32**(**9**), p 1059–1061.

Peng, Y., Li, C. and Fritschi, F. B. (2014) Diurnal dynamics of Maize leaf photosynthesis and carbohydrate concentrations in response to differential N availability, *Environmental and Experimental Botany*, **99**, p 18–27.

Pieruschka, R., Huber, G. and Berry, J. A. (2010) The control of transpiration by absorbed radiation, *Proceedings Of The National Academy Of Sciences Of The United States Of America*, **107**(**30**), p 13372–13377.

Pinto, H., Powell, J. R., Sharwood, R. E., Tissue, D. T. and Ghannoum, O. (2016) Variations in nitrogen use efficiency reflect the biochemical subtype while variations in water use efficiency reflect the evolutionary lineage of C_4 grasses at inter-glacial CO_2, *Plant, Cell and Environment*, **39**(**3**), p 514–526.

Pinto, H., Sharwood, R. E., Tissue, D. T. and Ghannoum, O. (2014) Photosynthesis of C_3, C_3-C_4, and C_4 grasses at glacial CO_2, *Journal of Experimental Botany*, **65**(**13**), p 3669–3681.

Postel, S. L., Daily, G. C. and Ehrlich, P. R. (1996) Human appropriation of renewable fresh water, *Science*, **271**, p 785–788.

Pou, A., Flexas, J., Alsina, M. D. M., Bota, J., Carambula, C., De Herralde, F., Galmés, J., Lovisolo, C., Jiménez, M., Ribas-Carbó, M., Rusjan, D., Secchi, F., Tomàs, M., Zsófi, Z. and Medrano, H. (2008) Adjustments of water use efficiency by stomatal regulation during drought and recovery in the drought-adapted *Vitis* hybrid Richter-110 (*V. berlandieri* x *V. rupestris*), *Physiologia Plantarum*, **134**(**2**), p 313–323.

Prado, K., Boursiac, Y., Tournaire-Roux, C., Monneuse, J.-M., Postaire, O., Da Ines, O., Schaffner, A. R., Hem, S., Santoni, V. and Maurel, C. (2013) Regulation of Arabidopsis leaf hydraulics involves light-Dependent Phosphorylation of Aquaporins in Veins, *The Plant Cell*, **25**(**3**), p 1029–1039.

Prado, K. and Maurel, C. (2013) Regulation of leaf hydraulics: from molecular to whole plant levels, *Frontiers in Plant Science*, **4**, p 255.

Raissig, M. T., Matos, J. L., Ximena, M., Gil, A., Kornfeld, A., Bettadapur, A., Abrash, E., Allison, H. R., Badgley, G., Vogel, J. P., Berry, J. A. and Bergmann, D. C. (2017) Mobile MUTE specifies subsidiary cells to build physiologically improved grass stomata, *Science*, **355**(**March**), p 1215.

Raven, J. A. (2014) Speedy small stomata?, *Journal of Experimental Botany*, **65**(**6**), p 1415–1424.

Ray, D. K., Mueller, N. D., West, P. C. and Foley, J. A. (2013) Yield trends are insufficient to double global crop production by 2050, *PLoS ONE*, **8**(**6**), p e66428.

Rebetzke, G. J., Condon, A. G., Richards, R. A. and Farquhar, G. D. (2002) Selection for reduced carbon isotope discrimination increases aerial biomass and grain yield of rainfed bread wheat, *Crop Science*, **42**, p 739–745.

Reddy, K. R., Robana, R. R., Hodges, H. F., Liu, X. J. and McKinion, J. M. (1998) Interactions of CO_2 enrichment and temperature on cotton growth and leaf characteristics, *Environmental and Experimental Botany*, **39**(**2**), p 117–129.

Reddy, P. S., Rao, T. S. R. B., Sharma, K. K. and Vadez, V. (2015) Genome-wide identification and characterization of the aquaporin gene family in *Sorghum bicolor* (L.), *Plant Gene*, **1**, p 18–28.

Reeves, G., Singh, P., Rossberg, T. A., Sogbohossou, E. O. D., Schranz, M. E. and Hibberd, J. M. (2018) Natural

variation within a species for traits underpinning C4 photosynthesis, *Plant Physiology*, **177**(**2**), p 504–512.

Resco de Dios, V. (2017) Circadian regulation and diurnal variation in gas exchange, *Plant Physiology*, **175**(**September**), p 3–4.

Resco de Dios, V., Anderegg, W. R. L., Li, X., Tissue, D. T., Bahn, M., Landais, D., Milcu, A., Yao, Y., Nolan, R. H., Roy, J. and Gessler, A. (2020) Circadian regulation does not optimize stomatal behaviour, *Plants*, **9**(**9**), p 1–10.

Resco de Dios, V. and Gessler, A. (2018) Circadian regulation of photosynthesis and transpiration from genes to ecosystems, *Environmental and Experimental Botany*, **152**(**July 2017**), p 37–48.

Resco de Dios, V., Gessler, A., Ferrio, J. P., Alday, J., Bahn, M., del Castillo, J., Devidal, S., García-Muñoz, S., Kayler, Z., Landais, D., Martín-Gómez, P., Milcu, A., Piel, C., Pirhofer-Walzl, K., Ravel, O., Salekin, S., Tissue, D., Tjoelker, M., Voltas, J. and Roy, J. (2017) Circadian rhythms regulate the environmental responses of net CO_2 exchange in bean and cotton canopies, *Agricultural and Forest Meteorology*, **239**, p 185–191.

Reymond, M., Muller, B., Leonardi, A., Charcosset, A. and Tardieu, F. (2003) Combining quantitative trait loci analysis and an ecophysiological model to analyze the genetic variability of the responses of Maize leaf growth to temperature and water deficit, *Plant Physiology*, **131**(**2**), p 664–675.

Richards, R. A. (2006) Physiological traits used in the breeding of new cultivars for water-scarce environments, *Agricultural Water Management*, **80**, p 197–211.

Rippke, U., Ramirez-Villegas, J., Jarvis, A., Vermeulen, S. J., Parker, L., Mer, F., Diekkrüger, B., Challinor, A. J. and Howden, M. (2016) Timescales of transformational climate change adaptation in sub-Saharan African agriculture, *Nature Climate Change*, **6**(**6**), p 605–609.

Rizal, G., Thakur, V., Dionora, J., Karki, S., Wanchana, S., Acebron, K., Larazo, N., Garcia, R., Mabilangan, A., Montecillo, F., Danila, F., Mogul, R., Pablico, P., Leung, H., Langdale, J. A., Sheehy, J., Kelly, S. and Quick, W. P. (2015) Two forward genetic screens for vein density mutants in sorghum converge on a cytochrome P450 gene in the brassinosteroid pathway, *The Plant Journal*, **84**(**2**), p 257–266.

Robson, T. M., Sánchez-Gómez, D., Cano, F. J. and Aranda, I. (2012) Variation in functional leaf traits among beech provenances during a Spanish summer reflects the differences in their origin, *Tree Genetics and Genomes*, **8**(**5**), p 1111–1121.

Rockwell, F. E., Holbrook, N. M. and Stroock, A. D. (2014) The competition between liquid and vapor transport in transpiring leaves, *Plant Physiology*, **164**(**4**), p 1741–1758.

Rosenzweig, C. and Parry, M. L. (1994) Potential impact of climate change on world food supply, *Nature*, **367**, p 133–138.

Rudall, P. J., Chen, E. D. and Cullen, E. (2017) Evolution and development of monocot stomata, *American Journal of Botany*, **104**(**8**), p 1122–1141.

Russell, S. H. and Evert, R. F. (1985) Leaf vasculature in *Zea mays* L., *Planta*, **164**, p 448–458.

Sack, L. and Buckley, T. N. (2016) The developmental basis of stomatal density and flux, *Plant Physiology*, **171**, p 2358–2363.

Sack, L. and Frole, K. (2006) Leaf structural diversity is related to hydraulic capacity in tropical rain forest trees, *Ecology*, **87**(**2**), p 483–491.

Sack, L. and Holbrook, N. M. (2006) Leaf hydraulics, *Annual Review of Plant Biology*, **57**, p 361–381.

Sack, L., Scoffoni, C., McKown, A. D., Frole, K., Rawls, M., Havran, J. C., Tran, H. and Tran, T. (2012) Developmentally based scaling of leaf venation architecture explains global ecological patterns, *Nature Communications*, **3**(**May**), p 810–837.

Sade, N., Gallé, A., Flexas, J., Lerner, S., Peleg, G., Yaaran, A. and Moshelion, M. (2014) Differential tissue-specific expression of NtAQP1 in *Arabidopsis thaliana* reveals a role for this protein in stomatal and mesophyll conductance of CO_2 under standard and salt-stress conditions, *Planta*, **239**(**2**), p 357–366.

Sade, N., Shatil-Cohen, A., Attia, Z., Maurel, C., Boursiac, Y., Kelly, G., Granot, D., Yaaran, A., Lerner, S. and Moshelion, M. (2014) The role of plasma membrane aquaporins in regulating the bundle sheath-mesophyll continuum and leaf hydraulics, *Plant Physiology*, **166**(**3**), p 1609–1620.

Sadras, V. O., Montoro, A., Moran, M. A. and Aphalo, P. J. (2012) Elevated temperature altered the reaction norms of stomatal conductance in field-grown grapevine, *Agricultural and Forest Meteorology*, **165**, p 35–

42.

Sage, R. F. (2001) Environmental and evolutionary preconditions for the origin and diversification of the C_4 photosynthetic Syndrome, *Plant Biology*, **3**(**3**), p 202–213.

Sage, R. F. (2002) Variation in the k_{cat} of Rubisco in C_3 and C_4 plants and some implications for photosynthetic performance at high and low temperature, *Journal of Experimental Botany*, **53**(**369**), p 609–620.

Sage, R. F. (2004) The evolution of C_4 photosynthesis, *New Phytologist*, **161**(**2**), p 341–370.

Sage, R. F., Christin, P. A. and Edwards, E. J. (2011) The C_4 plant lineages of planet Earth, *Journal of Experimental Botany*, **62**(**9**), p 3155–3169.

Sage, R. F. and McKown, A. D. (2006) Is C_4 photosynthesis less phenotypically plastic than C_3 photosynthesis?, *Journal of Experimental Botany*, **57**(**2**), p 303–317.

Salisbury, E. J. (1928) On the causes and ecological significance of stomatal frequency, with special reference to the woodland flora, *Philosophical Transactions of the Royal Society B: Biological Sciences*, **216**, p 1–65.

Schneider, C. A., Rasband, W. S. and Eliceiri, K. W. (2012) NIH Image to ImageJ: 25 years of image analysis, *Nature Methods*, **9**(**7**), p 671–675.

Schneider, J. V, Habersetzer, J., Rabenstein, R., Wesenberg, J., Wesche, K. and Zizka, G. (2017) Water supply and demand remain coordinated during breakdown of the global scaling relationship between leaf size and major vein density, *New Phytologist*, **214**(**1**), p 473–486.

Schuepp, P. H. (1993) Leaf boundary layers, *New Phytologist*, **125**(**3**), p 477–507.

Schuler, M. L., Sedelnikova, O. V, Walker, B. J., Westhoff, P. and Langdale, J. A. (2018) SHORTROOT-mediated increase in stomatal density has no impact on photosynthetic efficiency, *Plant Physiology*, **176**(**1**), p 757–772.

Scoffoni, C., Chatelet, D. S., Pasquet-kok, J., Rawls, M., Donoghue, M. J., Edwards, E. J. and Sack, L. (2016) Hydraulic basis for the evolution of photosynthetic productivity, *Nature Plants*, **2**, p 16072.

Scoffoni, C., Rawls, M., McKown, A. D., Cochard, H. and Sack, L. (2011) Decline of leaf hydraulic conductance with dehydration: Relationship to leaf size and venation architecture, *Plant Physiology*, **156**(**2**), p 832–843.

Sharwood, R. E., Ghannoum, O. and Whitney, S. M. (2016) Prospects for improving CO_2 fixation in C_3-crops through understanding C_4-Rubisco biogenesis and catalytic diversity, *Current Opinion in Plant Biology*, **31**, p 135–142.

Shatil-Cohen, A., Attia, Z. and Moshelion, M. (2011) Bundle-sheath cell regulation of xylem-mesophyll water transport via aquaporins under drought stress: A target of xylem-borne ABA?, *The Plant Journal*, **67**(**1**), p 72–80.

Sheen, J. (1990) Metabolic repression of transcription in higher plants, *Plant Cell*, **2**(**10**), p 1027–1038.

Shope, J. C., Peak, D. and Mott, K. A. (2008) Stomatal responses to humidity in isolated epidermes, *Plant, Cell and Environment*, **31**(**9**), p 1290–1298.

Simonin, K. A., Burns, E., Choat, B., Barbour, M. M., Dawson, T. E. and Franks, P. J. (2015) Increasing leaf hydraulic conductance with transpiration rate minimizes the water potential drawdown from stem to leaf, *Journal of Experimental Botany*, **66**(**5**), p 1303–1315.

Sinclair, T. R. (2012) Is transpiration efficiency a viable plant trait in breeding for crop improvement?, *Functional Plant Biology*, **39**(**5**), p 359–365.

Sinclair, T. R. (2018) Effective water use required for improving crop growth rather than transpiration efficiency, *Frontiers in Plant Science*, **9**(**September**), p 1–8.

Sinclair, T. R., Hammer, G. L. and Van Oosterom, E. J. (2005) Potential yield and water-use efficiency benefits in sorghum from limited maximum transpiration rate, *Functional Plant Biology*, **32**(**10**), p 945–952.

Sinclair, T. R., Zwieniecki, M. A. and Holbrook, N. M. (2008) Low leaf hydraulic conductance associated with drought tolerance in soybean, *Physiologia Plantarum*, **132**(**4**), p 446–451.

Sonawane, B. V, Sharwood, R. E., von Caemmerer, S., Whitney, S. M. and Ghannoum, O. (2017) Short-term thermal photosynthetic responses of C4 grasses are independent of the biochemical subtype, *Journal of Experimental Botany*, **68**, p 5583–5597.

Stamp, P., Thiraporn, R. and Geisler, G. (1985) Anatomy of chlorenchyma cells in Maize lines developed at different latitudes and grown at sub- and supraoptimal temperatures, *Physiologia Plantarum*, **63**(**2**), p 159–162.

Steduto, P., Katerji, N., Puertos-Molina, H., Ünlü, M., Mastrorilli, M. and Rana, G. (1997) Water-use efficiency of sweet Sorghum under water stress conditions gas-exchange investigations at leaf and canopy scales, *Field Crops Research*, **54**(**2**–**3**), p 221–234.

Sutka, M. R., Manzur, M. E., Vitali, V. A., Micheletto, S. and Amodeo, G. (2016) Evidence for the involvement of hydraulic root or shoot adjustments as mechanisms underlying water deficit tolerance in two *Sorghum bicolor* genotypes, *Journal of Plant Physiology*, **192**, p 13–20.

Tanaka, Y., Sugano, S. S., Shimada, T. and Hara-Nishimura, I. (2013) Enhancement of leaf photosynthetic capacity through increased stomatal density in *Arabidopsis*, *New Phytologist*, **198**(**3**), p 757–764.

Tardieu, F., Reymond, M., Hamard, P., Granier, C. and Muller, B. (2000) Spatial distributions of expansion rate, cell division rate and cell size in Maize leaves: A synthesis of the effects of soil water status, evaporative demand and temperature, *Journal of Experimental Botany*, **51**(**350**), p 1505–1514.

Tardieu, F., Simonneau, T. and Muller, B. (2018) The physiological basis of drought tolerance in crop plants: a scenario-dependent probablistic approach, *Annual Review of Plant Biology*, **69**(**1**), p 733–759.

Taylor, S. H., Franks, P. J., Hulme, S. P., Spriggs, E., Christin, P.-A., Edwards, E. J., Woodward, F. I. and Osborne, C. P. (2012) Photosynthetic pathway and ecological adaptation explain stomatal trait diversity amongst grasses, *New Phytologist*, **193**(**2**), p 387–396.

Taylor, S. H., Hulme, S. P., Rees, M., Ripley, B. S., Woodward, F. I. and Osborne, C. P. (2010) Ecophysiological traits in C_3 and C_4 grasses: a phylogenetically controlled screening experiment, *New Phytologist*, **185**(**3**), p 780–791.

Taylor, S. H., Ripley, B. S., Martin, T., De-Wet, L.-A., Woodward, F. I. and Osborne, C. P. (2014) Physiological advantages of C_4 grasses in the field: A comparative experiment demonstrating the importance of drought, *Global Change Biology*, **20**(**6**), p 1992–2003.

Taylor, S. H., Ripley, B. S., Woodward, F. I. and Osborne, C. P. (2011) Drought limitation of photosynthesis differs between C_3 and C_4 grass species in a comparative experiment, *Plant, Cell and Environment*, **34**(**1**), p 65–75.

Teuling, A. J. (2018) A hot future for European droughts, *Nature Climate Change*, **8**(**5**), p 364–365.

Thalmann, M., Pazmino, D., Seung, D., Horrer, D., Nigro, A., Meier, T., Kölling, K., Pfeifhofer, H. W., Zeeman, S. C. and Santelia, D. (2016) Regulation of leaf starch degradation by abscisic acid is important for osmotic stress tolerance in plants, *The Plant Cell*, **28**(**8**), p 1860–1878.

Thalmann, M. and Santelia, D. (2017) Starch as a determinant of plant fitness under abiotic stress, *New Phytologist*, **214**(**3**), p 943–951.

Thompson, M., Gamage, D., Hirotsu, N., Martin, A. and Seneweera, S. (2017) Effects of elevated carbon dioxide on photosynthesis and carbon partitioning: A perspective on root sugar sensing and hormonal crosstalk, *Frontiers in Physiology*, **8**(**AUG**), p 1–13.

Tingting, X., Peixi, S. and Lishan, S. (2010) Photosynthetic characteristics and water use efficiency of sweet Sorghum under different watering regimes, *Pakistani Journal of Botany*, **42**(**6**), p 3981–3994. Available at: https://www.cabdirect.org/cabdirect/abstract/20113034418.

Tinoco-Ojanguren, C. and Pearcy, R. W. (1993a) Stomatal dynamics and its importance to carbon gain in two rainforest Piper species, *Oecologia*, **94**(**3**), p 388–394.

Tinoco-Ojanguren, C. and Pearcy, R. W. (1993b) Stomatal dynamics and its importance to carbon gain in two rainforest Piper species .I. VPD effects on the transient stomatal response to lightflecks, *Oecologia*, **94**(**3**), p 388–394.

Ueno, O., Kawano, Y., Wakayama, M. and Takeda, T. (2006) Leaf vascular systems in C_3 and C_4 grasses: A two-dimensional analysis, *Annals of Botany*, **97**(**4**), p 611–621.

UNCTAD (2011) Water for food: Innovative water management technologies for foodsecurity andpoverty alleviation. New York, Geneva: United Nations, p 39.

Vadez, V. (2019) Water-use efficiency, in Ciampitti, I. and Prasad, P. V. V (eds) *Sorghum: State of the Art and Future Prespectives*. Madison, WI: ASA and CSSA, p 267–276.

Vadez, V., Kholova, J., Medina, S., Kakkera, A. and Anderberg, H. (2014) Transpiration efficiency: New insights into an old story, *Journal of Experimental Botany*, **65**(**21**), p 6141–6153.

Valin, H., Sands, R. D., van der Mensbrugghe, D., Nelson, G. C., Ahammad, H., Blanc, E., Bodirsky, B., Fujimori, S., Hasegawa, T., Havlik, P., Heyhoe, E., Kyle, P., Mason-D'Croz, D., Paltsev, S., Rolinski, S., Tabeau, A., van Meijl, H., von Lampe, M. and Willenbockel, D. (2014) The future of food demand: Understanding differences in global economic models, *Agricultural Economics*, **45**(**1**), p 51–67.

Vialet-Chabrand, S., Dreyer, E. and Brendel, O. (2013) Performance of a new dynamic model for predicting diurnal time courses of stomatal conductance at the leaf level, *Plant, Cell and Environment*, **36**(**8**), p 1529–1546.

Vialet-Chabrand, S., Matthews, J. S. A., Brendel, O., Blatt, M. R., Wang, Y., Hills, A., Griffiths, H., Rogers, S. and Lawson, T. (2016) Modelling water use efficiency in a dynamic environment: An example using *Arabidopsis thaliana*, *Plant Science*, **251**, p 65–74.

Vialet-Chabrand, S. R. M., Matthews, J. S. A., McAusland, L., Blatt, M. R., Griffiths, H. and Lawson, T. (2017) Temporal dynamics of stomatal behavior: Modeling and implications for photosynthesis and water use, *Plant Physiology*, **174**(**2**), p 603–613.

Vico, G., Manzoni, S., Palmroth, S. and Katul, G. (2011) Effects of stomatal delays on the economics of leaf gas exchange under intermittent light regimes, *New Phytologist*, **192**(**3**), p 640–652.

Virmani, S. M. and Sivakumar, M. V. K. (eds) (1984) *Agrometeorology of Sorghum and Millet in the semi-arid tropics*. Patancheru: ICRISAT. Available at: http://oar.icrisat.org/802/.

Vogan, P. J. and Sage, R. F. (2011) Water-use efficiency and nitrogen-use efficiency of C_3-C_4 intermediate species of *Flaveria* Juss. (*Asteraceae*), *Plant, Cell and Environment*, **34**(**9**), p 1415–1430.

Wand, S. J. E., Midgley, G. F., Jones, M. H. and Curtis, P. S. (1999) Responses of wild C_4 and C_3 grass (*Poaceae*) species to elevated atmospheric CO_2 concentration: a meta-analytic test of current theories and perceptions, *Global Change Biology*, **5**, p 723–741.

Wang, C., Hu, H., Qin, X., Zeise, B., Xu, D., Rappel, W. J., Boron, W. F. and Schroeder, J. I. (2016) Reconstitution of CO_2 regulation of SLAC1 anion channel and function of CO_2-permeable PIP2;1 aquaporin as CARBONIC ANHYDRASE4 interactor, *Plant Cell*, **28**(**2**), p 568–582.

Wang, Y., Bräutigam, A., Weber, A. P. M. and Zhu, X. G. (2014) Three distinct biochemical subtypes of C_4 photosynthesis? A modelling analysis, *Journal of Experimental Botany*, **65**(**13**), p 3567–3578.

Ward, J. K., Tissue, D. T., Thomas, R. B. and Strain, B. R. (1999) Comparative responses of model C_3 and C_4 plants to drought in low and elevated CO_2, *Global Change Biology*, **5**(**8**), p 857–867.

Watson-Lazowski, A., Papanicolaou, A., Sharwood, R. and Ghannoum, O. (2018) Investigating the NAD-ME biochemical pathway within C_4 grasses using transcript and amino acid variation in C_4 photosynthetic genes, *Photosynthesis Research*, **138**(**2**), p 233–248.

Way, D. A. (2012) What lies between: The evolution of stomatal traits on the road to C_4 photosynthesis, *New Phytologist*, **193**(**2**), p 291–293.

Way, D. A., Katul, G. G., Manzoni, S. and Vico, G. (2014) Increasing water use efficiency along the C_3 to C_4 evolutionary pathway: A stomatal optimization perspective, *Journal of Experimental Botany*, **65**(**13**), p 3683–3693.

Weissmann, S., Ma, F., Furuyama, K., Gierse, J., Berg, H., Shao, Y., Taniguchi, M., Allen, D. K. and Brutnell, T. P. (2015) Interactions of C_4 subtype metabolic activities and transport in Maize are revealed through the characterization of DCT2 mutants, *Plant Cell*, **28**(**2**), p 466–484.

Whitehead, D. (1998) Regulation of stomatal conductance and transpiration in forest canopies, *Tree physiology*, **18**, p 633–644.

Wong, S. C., Cowan, I. R. and Farquhar, G. D. (1979) Stomatal conductance correlates with photosynthetic capacity, *Nature*, **282**(**5737**), p 424–426.

Xin, Z., Aiken, R. and Burke, J. (2009) Genetic diversity of transpiration efficiency in Sorghum, *Field Crops Research*, **111**(**1–2**), p 74–80.

Xiong, D., Flexas, J., Yu, T., Peng, S. and Huang, J. (2017) Leaf anatomy mediates coordination of leaf hydraulic conductance and mesophyll conductance to CO_2 in *Oryza*, *New Phytologist*, **213**(**2**), p 572–583.

Yan, H., Wu, L., Filardo, F., Yang, X., Zhao, X. and Fu, D. (2017) Chemical and hydraulic signals regulate stomatal behavior and photosynthetic activity in maize during progressive drought, *Acta Physiologiae Plantarum*, **39**(**6**), p 125.

Yang, D., Pan, S., Ding, Y. and Tyree, M. T. (2017) Experimental evidence for negative turgor pressure in small leaf cells of *Robinia pseudoacacia* L versus large cells of *Metasequoia glyptostroboides* Hu et W.C.Cheng. 1. Evidence from pressure-volume curve analysis of dead tissue., *Plant Cell and Environment*, **40**, p 351–363.

Yin, X. and Struik, P. C. (2021) Exploiting differences in the energy budget among C_4 subtypes to improve crop productivity, *New Phytologist*, **229**(**5**), p 2400–2409.

Zhang, F. P., Carins Murphy, M. R., Cardoso, A. A., Jordan, G. J. and Brodribb, T. J. (2018) Similar geometric rules govern the distribution of veins and stomata in petals, sepals and leaves, *New Phytologist*, **219**(**4**), p 1224–1234.

Zhang, S. B., Guan, Z. J., Sun, M., Zhang, J. J., Cao, K. F. and Hu, H. (2012) Evolutionary association of Stomatal traits with leaf vein density in *Paphiopedilum*, *Orchidaceae*, *PLoS ONE*, **7**(**6**), p e40080.

Zhao, W., Sun, Y., Kjelgren, R. and Liu, X. (2015) Response of stomatal density and bound gas exchange in leaves of maize to soil water deficit, *Acta Physiologiae Plantarum*, **37**(**1**), p 1704.

Zhou, X., Ge, Z. M., Kellomäki, S., Wang, K. Y., Peltola, H. and Martikainen, P. (2011) Effects of elevated CO_2 and temperature on leaf characteristics, photosynthesis and carbon storage in aboveground biomass of a boreal bioenergy crop (*Phalaris arundinacea* L.) under varying water regimes, *GCB Bioenergy*, **3**(**3**), p 223–234.

Zur, B. and Jones, J. W. (1984) Diurnal changes in the instantaneous water use efficiency of a soybean crop, *Agricultural and Forest Meteorology*, **33**(**1**), p 41–51.

Zwieniecki, M. A. and Holbrook, N. M. (1998) Diurnal variation in xylem hydraulic conductivity in white ash (*Fraxinus americana* L.), red maple (*Acer rubrum* L.) and red spruce (*Picea rubens* Sarg.), *Plant, Cell & Environment*, **21**, p 1173–1180.